INFORMATION TO USERS

This material was produced from a microfilm copy of the original document. While the most advanced technological means to photograph and reproduce this document have been used, the quality is heavily dependent upon the quality of the original submitted.

The following explanation of techniques is provided to help you understand markings or patterns which may appear on this reproduction.

1. The sign or "target" for pages apparently lacking from the document photographed is "Missing Page(s)". If it was possible to obtain the missing page(s) or section, they are spliced into the film along with adjacent pages. This may have necessitated cutting thru an image and duplicating adjacent pages to insure you complete continuity.

2. When an image on the film is obliterated with a large round black mark, it is an indication that the photographer suspected that the copy may have moved during exposure and thus cause a blurred image. You will find a good image of the page in the adjacent frame.

3. When a map, drawing or chart, etc., was part of the material being photographed the photographer followed a definite method in "sectioning" the material. It is customary to begin photoing at the upper left hand corner of a large sheet and to continue photoing from left to right in equal sections with a small overlap. If necessary, sectioning is continued again — beginning below the first row and continuing on until complete.

4. The majority of users indicate that the textual content is of greatest value, however, a somewhat higher quality reproduction could be made from "photographs" if essential to the understanding of the dissertation. Silver prints of "photographs" may be ordered at additional charge by writing the Order Department, giving the catalog number, title, author and specific pages you wish reproduced.

5. PLEASE NOTE: Some pages may have indistinct print. Filmed as received.

Xerox University Microfilms
300 North Zeeb Road
Ann Arbor, Michigan 48106

74-3579

BECVAR, James Edgar, 1942-
STUDIES ON THE BINDING OF FLAVINS TO THE RIBOFLAVIN BINDING PROTEIN FROM LEGHORN EGG WHITE.

The University of Michigan, Ph.D., 1973
Biophysics, general

University Microfilms, A XEROX Company, Ann Arbor, Michigan

THIS DISSERTATION HAS BEEN MICROFILMED EXACTLY AS RECEIVED.

STUDIES ON THE BINDING OF FLAVINS TO THE RIBOFLAVIN BINDING PROTEIN FROM LEGHORN EGG WHITE

by

James Edgar Becvar

A dissertation submitted in partial fulfillment
of the requirements for the degree of
Doctor of Philosophy
(Biophysics)
in The University of Michigan
1973

Doctoral Committee:

Professor Graham Palmer, Chairman
Professor Vincent Massey
Professor J. Lawrence Oncley
Professor Richard H. Sands
Associate Professor Charles H. Williams, Jr.

ACKNOWLEDGMENTS

I am indebted to Dr. Graham Palmer for his direction of my thesis research and for his extensive review and critical evaluation of the dissertation. I wish to express my appreciation to Dr. Vincent Massey, Dr. J. Lawrence Oncley, Dr. Richard H. Sands, and Dr. Charles H. Williams, Jr., for their suggestions during the course of my research and with regard to the dissertation. I am grateful to Dr. Margaret J. Hunter for her helpful review of parts of the dissertation. I can not adequately thank Dr. David Ballou for his untiring help and copious suggestions with regard to the design and construction of the fluorimeter described in this thesis. Many of his excellent ideas are integrated into the apparatus. I wish to thank Dr. Franz Muller, Dr. Vincent Massey, Dr. Sandro Ghisla, and Dr. Dale Edmondson for their gifts of flavin analogs which allowed my investigations to be made. My warmest appreciation goes to the students and postdoctoral fellows in the Biophysics Research Division and especially in Dr. Palmer's laboratory, for their helpful discussions. I gratefully acknowledge the traineeship support of the National Institutes of Health through Training Grant GM 1355, made to the Biophysics Research Division and through Research Grant GM 12176 for assistance related to the equipment used during the course of my studies. I thank Mrs. Peggy Rogers for her unending patience and beautiful craftsmanship in the typing of the thesis. I thank Mr. Leo Evans for the concern and guidance given me during the writing of the dissertation.

I am most grateful of all to my wife, Betty Ann, who somehow managed to stand by me during all the moments of this experience.

TABLE OF CONTENTS

	Page
ACKNOWLEDGMENTS	ii
LIST OF TABLES	viii
LIST OF FIGURES	ix
LIST OF APPENDICES	xiii
LIST OF ABBREVIATIONS	xiv
CHAPTER 1. INTRODUCTION	1
SOME ASPECTS OF FLAVIN CHEMISTRY	3
Nomenclature and Structure of Flavins	3
Some Important Chemical Properties of Flavins	3
SOME COMMENTS ABOUT FLAVIN BINDING	8
HISTORICAL BACKGROUND OF FLAVIN BINDING	12
Old Yellow Enzyme (OYE)	12
Cytochrome b_5 Reductase	16
D-Amino Acid Oxidase (DAAO)	19
Lipoamide Dehydrogenase	23
Glucose Oxidase	25
Flavodoxins	28
Riboflavin Binding Protein (RBP)	39
RESEARCH OBJECTIVE	45
CHAPTER 2. A FLUORIMETER CAPABLE OF BOTH STATIC AND STOPPED-FLOW OPERATION	47
FLUORIMETER CONSTRUCTION AND ASSEMBLY	47

TABLE OF CONTENTS (Cont.)

	Page
Group I Components: Excitation	47
Group II Components: Fluorescence Emission	52
Group III Components: Detection	74
FLUORIMETER PERFORMANCE	78
1) Overall System Stability	78
2) Linearity of Signal Magnitude with Sample Concentration	79
3) Sample Temperature Measurement	79
4) Sensitivity	82
5) Dead Time	85
6) Response Time	93
7) Reproducibility	93
8) Mechanical Performance	95
CHAPTER 3. EXPERIMENTAL METHODS	97
CHEMICAL METHODS	97
Preparation of RBP	97
Preparation of ApoRBP	98
Disc Gel Electrophoresis	99
Sodium Dodecyl Sulfate (SDS) Gel Electrophoresis	102
Gel Electrofocusing	103
Riboflavin Purification	104
FMN Purification	104

TABLE OF CONTENTS (Cont.)

	Page
Flavin Purification by Chromatography	105
Thin Layer Chromatography (TLC)	105
INSTRUMENTAL METHODS	106
Fluorescence Measurements	106
Absorbance Measurements	107
Circular Dichroism (CD) Measurements	107
Scanning of Stained Gels	108
GENERAL MATERIALS	111
CHAPTER 4. RESULTS	113
SOME STUDIES ON THE PROTEIN	113
Consideration of Physical Homogeneity	113
Demonstration of Binding Homogeneity	121
Determination of the Molecular Weight of RBP	128
Determination of the Protein Isoelectric Point (pI)	129
Determination of ApoRBP Binding Site Concentration	129
Demonstration of 1 : 1 Binding Stoichiometry	134
Other Studies on the Protein	136
STUDIES ON THE FLAVIN ANALOGS	138
Determination of the Analog Concentrations	138
Consideration of Analog Purity	139
Affinity Chromatography of the Analogs	144

TABLE OF CONTENTS (Cont.)

	Page
EQUILIBRIUM STUDIES ON THE BINDING OF FLAVINS BY APORBP	148
Determination of the Equilibrium Binding Constants	148
Considerations of the Conditions Used in the Equilibrium Binding Studies	153
The Effects of pH and Ionic Composition on the Equilibrium Constant for RF Binding to ApoRBP	157
van't Hoff Analyses for Flavin Analog Binding to ApoRBP	166
STUDIES ON THE OPTICAL AND CD ABSORPTIVITY SPECTRA OF SEVERAL ANALOG-APORBP COMPLEXES	176
Comparison of the Spectra for Native RBP and the Holoprotein Reconstituted with RF	176
Compilation of the Spectra for Several Analog-ApoRBP Complexes	183
KINETIC STUDIES ON THE BINDING OF FLAVINS BY APORBP	194
Verification that the Quenching of Flavin Fluorescence Monitors a Second Order Process	195
Considerations on the Reversible Method of Analysis Used to Analyze the Kinetics of Flavin Binding to ApoRBP	199
Arrhenius Analyses for Flavin Analog Binding to ApoRBP	204
Relaxation Studies on Flavin Analog Binding to ApoRBP	209
CHAPTER 5. DISCUSSION	222
REFERENCES	246

LIST OF TABLES

Table		Page
I	Some Flavin Analogs and Their Structures Relative to that Shown in Figure 1	4
II	The Binding of FMN, FAD, and RF to ApoOYE at pH 9.0, 23°	14
III	Equilibrium Binding to Cytochrome b_5 Reductase at pH 8.1	17
IV	Results of the Scatchard Analyses for the Binding of Flavin Analogs to the Flavodoxin from Azotobacter vinelandii at pH 7.0 and 25 ± 2°	33
V	Relative Affinities for the Binding of Some Flavin Analogs to ApoRBP in 0.078 M NaCl and 0.025 M Na Phosphate, pH 7.0, at 2°	43
VI	Typical Yields of RBP at the Various Stages of Purification	100
VII	Test of Binding Homogeneity for ApoRBP Fractions Eluted from SE Sephadex	123
VIII	Flavin Analog Absorptivities	140
IX	TLC Analysis of Analog Purity	143
X	Equilibrium Energies for the Binding of Some Flavin Analogs by ApoRBP	169
XI	Second Order Rate Constants for the Quenching of RF Fluorescence by ApoRBP at Various Reactant Concentrations	198
XII	Activation Energies for the Second Order Step in the Binding of Some Flavin Analogs by ApoRBP	207
XIII	Activation Energies for the Reverse Reaction Step in the Binding of Some Flavin Analogs by ApoRBP	221

LIST OF FIGURES

Figure		Page
1.	Structure of "Flavin"	3
2.	Fluorimeter Components	48
3.	D. C. Lamp Power Supply	50
4.	A. Fluorimeter Bath in Static Mode	53
	B. Fluorimeter Bath in Stopped-Flow Mode	53
5.	A. Fluorimeter Bath - Top View	54
	B. Fluorimeter Bath - Excitation Side View	55
	C. Fluorimeter Bath - Emission Side View	56
	D. Fluorimeter Bath - View from Side Toward Pushing Assembly	57
6.	Module Positioning Post and Spacer	58
7.	Detail of the Wall on the Emission Side of the Fluorimeter Bath	59
8.	Emission Polarizer Plate and Ring Clamp	61
9.	Static Module	63
10.	A. The Assembled Stopped-Flow Fluorimeter	64
	B. The Ballou Pushing Assembly	65
	C. The Fluorimeter Bath with the Ballou Stopping Assembly Clamped in Place	66
11.	The Mixing Block of the Fluorescence Stopped-Flow Module	68
12.	The Clamp for the Stopped-Flow Mixing Module	69
13.	Face Detail of the Stopped-Flow Mixing Block	70
14.	Connectors Between the Mixing Module and Stopping Syringe	72
15.	The Fluorimeter Bath Cover Plate and Stopping Syringe Assembly Adapter	73
16.	Photomultiplier Housing	75

LIST OF FIGURES (Cont.)

Figure		Page
17.	Photomultiplier Follower and Offset Circuitry	77
18.	Relationship Between Signal Size and Fluorophore Concentration in the Stopped-Flow Mode (A) and in the Static Mode (B)	80
19.	Temperature Correction Curves	81
20.	Mixing Performance of the On-The-Face Mixer of the Stopped-Flow Fluorimeter	87
21.	Dead Time Analysis of the Stopped-Flow Fluorimeter	92
22.	Reproducibility and Signal to Noise Character of the Fluorimeter in the Stopped-Flow Mode	94
23.	Gel Scanning Carriage, Window, and Clamp	110
24.	The Relation Between the Amount of RBP Applied to a Disc Gel and the Area of the Scanned Peak	115
25.	Physical Homogeneity Studies of RBP	117
26.	The Absorbances at 280 nm of the ApoRBP Fractions Eluted from a Column of SE Sephadex by Changes in Ionic Strength and pH Value	122
27.	Scatchard Analyses for Binding of RF by ApoRBP	126
28.	Determination of the Molecular Weight of RBP by SDS Gel Electrophoresis	130
29.	Determination of the pI of RBP by Isoelectric Focusing	131
30.	Determination of ApoRBP Binding Site Concentration	132
31.	Job Analysis for Binding of RF by ApoRBP	137
32.	TLC Analyses of Four Analogs	142
33.	Affinity Chromatography of Crude LF on Sephadex	145

LIST OF FIGURES (Cont.)

Figure		Page
34.	Stoichiometric Binding Analyses of Crude (a) and Purified (b) IsoLF	147
35.	A Typical Fluorescence Quenching Titration	152
36.	The pH Dependence of the Equilibrium Constant for the Binding of RF to ApoRBP at 25°	159
37.	The CD Spectra of Solutions of HoloRBP at Different pH Values	161
38.	van't Hoff Plots for RF Binding to ApoRBP at pH Values Between pH 5 and pH 9	162
39.	The Effect of Ionic Strength (Γ/2) and Anions on the Equilibrium Constant for RF Binding by ApoRBP	165
40.	van't Hoff Plots for the Binding of Five Flavin Analogs by ApoRBP in 0.01 M K Phosphate, pH 7.00	168
41.	CD and Optical Absorptivity Spectra of RBP and RF	178
42.	The Optical and CD Spectra of the Analog Complexes with ApoRBP	185
43.	A Typical Example of the Quenching of Fluorescence Observed on Mixing Equal Concentrations of Flavin Analog and ApoRBP	200
44.	Representative Examples of the Arrhenius Plots for Analog Binding to ApoRBP in 0.01 M K Phosphate, pH 7.00	205
45.	Representative Examples of Relaxation Traces for Dilution Experiments with Analog-ApoRBP Complexes	215
46.	A, B. Relaxation Analyses for the Binding of RF and LF to ApoRBP	217
	C, D. Relaxation Analyses for the Binding of 8 NorLF and 3 OAc^-LF to ApoRBP	218
	E. Relaxation Analysis for the Binding of FMN to ApoRBP	219

LIST OF FIGURES (Cont.)

Figure		Page
47.	A Diagram of the Flavin Binding Site on ApoRBP	230
48.	Entropy-Enthalpy Compensation Plot for the Binding of Flavin Analogs by ApoRBP	232
49.	Compensation Plot of Activation Enthalpy Against Activation Entropy for the Binding of Flavin Analogs by ApoRBP	241
50.	Plot of Log K_a Against Log k_{-1} for Flavin Binding to ApoRBP	244

LIST OF APPENDICES

Appendix		Page
A	Competitive Binding	253
B	Some Considerations on the Equation for Simple Binding	258
C	Considerations on Apoprotein Binding Heterogeneity	261
D	Considerations on Relaxation Kinetics of Flavin Binding to ApoRBP	270
E	Computer Programs	274

LIST OF ABBREVIATIONS

A	ApoRBP
-A	Alloxazine
BSA	Bovine serum albumin
CAT	Computer of average transients
CD	Circular dichroism
CM Sephadex	Carboxymethyl Sephadex
DAAO	D-Amino acid oxidase
DCIP	2,6-Dichlorophenolindophenol
DEAE-cellulose	Diethylaminoethyl cellulose
DMSO	Dimethylsulfoxide
DVM	Digital voltmeter
EPR	Electron paramagnetic resonance
F	Flavin
FAD	Flavin adenine dinucleotide
FET	Field effect transistor
FMN	Flavin mononucleotide
H	Holoprotein
IA	Isoalloxazine
i.d.	Inside diameter
K_a	Association equilibrium constant
K_d	Dissociation equilibrium constant
k_1	Association rate constant
k_{-1}	Dissociation rate constant

LIST OF ABBREVIATIONS (Cont.)

LF	Lumiflavin
NAD	Nicotinamide adenine dinucleotide
NADH	Reduced nicotinamide adenine dinucleotide
OYE	Old yellow enzyme
PCMB	Parachloromercuribenzoate
PE	Polyethylene
pI	Isoelectric point
p.s.i.	Pounds per square inch
PVC	Polyvinylchloride
RF	Riboflavin
r.m.s.	Root mean square
SDS	Sodium dodecyl sulfate
SE Sephadex	Sulphoethyl Sephadex
TCA	Trichloroacetic acid
TLC	Thin layer chromatography
TPN	Triphosphopyridine nucleotide (an older terminology for NAD)
TPNH	Reduced triphosphopyridine nucleotide

CHAPTER 1

INTRODUCTION

A fundamental characteristic of biological systems is the ability of reaction components to recognize each other and to interact in a specific manner. Investigations of these biological interactions, often called binding studies, include the complexing of substrates, effectors, or prosthetic groups to enzymes, antigens to antibodies, hormones or neuromuscular effectors to their receptor sites, a variety of molecules to carrier or storage proteins, and a little bit of everything to serum albumin. Much contemporary effort is being advanced to understand the physical and chemical basis of these interactions.

Flavoproteins serve as excellent examples of biological macromolecules suitable for binding studies, though curiously, they have received relatively little attention with regard to the interaction of the flavin prosthetic group with the specific protein site. Most flavoproteins function as enzymes catalyzing oxidation-reduction reactions. Three general types of flavoenzymes are distinguished on the basis of their reactivity:

1) oxidases, which catalyze the reaction,

$$DH_2 + O_2 \rightleftharpoons D + H_2O_2 \ ,$$

2) dehydrogenases, which catalyze the reaction,

$$DH_2 + A \rightleftharpoons D + AH_2 ,$$

where A is not oxygen, and

3) hydroxylases, which catalyze the reaction,

$$DH_2 + O_2 + XH \rightleftharpoons D + H_2O + XOH .$$

In addition to soluble flavoproteins, there are some membrane-bound enzymes such as those participating in mitochondrial electron transport. Examples of all these types of flavoproteins can be found in the symposia on flavins and flavoproteins (1-3). Flavoproteins thus comprise a large and ubiquitous class of enzymes. In view of their widespread occurrence and importance, investigations of the interaction between flavins and their apoproteins are warranted in order to gain a clearer understanding of the specificity and function of these proteins.

The study of flavin-protein interactions is facilitated by a fortuitous set of flavin spectroscopic properties. Of primary importance to this thesis is the observation that the fluorescence exhibited by oxidized flavins in solution is generally quenched on binding to their apoproteins. Furthermore, the flavin absorption bands with maxima near 450 nm and 370 nm generally change character on binding: maxima often shift to longer wavelengths and absorption bands often change in intensity and show some additional structure. Additionally the weak optical activity of some flavin absorptions is markedly intensified upon the binding of flavins to apoproteins.

SOME ASPECTS OF FLAVIN CHEMISTRY

Nomenclature and Structure of Flavins

Flavin is the common name for the structure shown in Figure 1, an N(10) alkyl derivative of 7,8-dimethyl isoalloxazine:

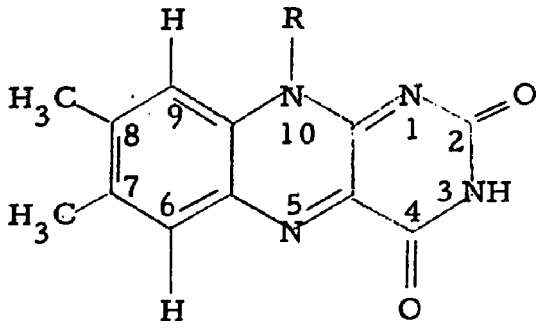

Figure 1. Structure of "Flavin"

For the reader's convenience I have listed in Table I the structures, names and abbreviations of all of the flavin analogs studied or discussed in this thesis. The only naturally occurring flavins known to be prosthetic groups in flavoenzymes are FMN, FAD, and some 8α-substituted derivatives of FAD which are covalently bound to the protein (4).

Some Important Chemical Properties of Flavins

One of the characteristic reactions of flavins is their ability to undergo oxidation and reduction as in the following scheme:

TABLE I

Some Flavin Analogs and Their Structures Relative to that Shown in Figure 1

Abbreviation	Analog	Structure	
		-R Substitution (Figure 1)	Ring Substitution (Figure 1)
IA	isoalloxazine	-H	C_7-CH_3 → C_7-H C_8-CH_3 → C_8-H
LC	lumichrome	-H	
LF	lumiflavin	$-CH_3$	
RF	riboflavin	$-CH_2-(CHOH)_3-CH_2OH$	
FMN	flavin mononucleotide	$-CH_2-(CHOH)_3-CH_2O-PO_3^=$	
FAD	flavin adenine dinucleotide	$-CH_2-(CHOH)_3-CH_2O-PO_2^--O-PO_2^-$- -O-adenosine	
TARF	tetraacetyl riboflavin	$-CH_2-(CHOCOCH_3)_3-CH_2OCOCH_3$	
$RFSO_4^-$	riboflavin sulfate	$-CH_2-(CHOH)_3-CH_2-O-SO_3^-$	
10-ω-CO_2^- BuIA	10-ω-carboxybutyl isoalloxazine	$-(CH_2)_4-CO_2^-$	C_7-CH_3 → C_7-H C_8-CH_3 → C_8-H

deoxy RF	deoxyriboflavin	$-(CH_2)_4-CH_2OH$	
10 EtOHF	10-hydroxyethyl flavin	$-CH_2-CH_2OH$	
3 Me LF	3-methyl lumiflavin	$-CH_3$	$N_3-H \rightarrow N_3-CH_3$
3 Bz LF	3-benzyl lumiflavin	$-CH_3$	$N_3-H \rightarrow N_3-CH_2-C_6H_5$
3 OAc^- LF	lumiflavin 3-acetate	$-CH_3$	$N_3-H \rightarrow N_3-CH_2CO_2^-$
3,4-dihydro F	3,4-dihydroflavin	-R	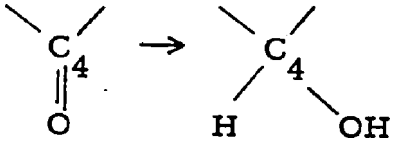
deaza F	deaza flavin	-R	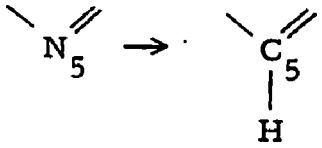
iso F	isoflavin	-R	$C_6-H \rightarrow C_6-CH_3$ $C_8-CH_3 \rightarrow C_8-H$
7 Cl LF	7-chloro lumiflavin	$-CH_3$	$C_7-CH_3 \rightarrow C_7-Cl$
8 Cl LF	8-chloro lumiflavin	$-CH_3$	$C_8-CH_3 \rightarrow C_8-Cl$

TABLE I (Cont.)

Abbreviation	Analog	Structure	
		-R Substitution (Figure 1)	Ring Substitution (Figure 1)
di Cl LF	7,8-dichloro lumiflavin	$-CH_3$	$C_7-CH_3 \rightarrow C_7-Cl$ $C_8-CH_3 \rightarrow C_8-Cl$
8 Nor LF	7,10-dimethyl isoalloxazine	$-CH_3$	$C_8-CH_3 \rightarrow C_8-H$
10 Me IA	10-methyl isoalloxazine	$-CH_3$	$C_7-CH_3 \rightarrow C_7-H$ $C_8-CH_3 \rightarrow C_8-H$
8α hist LF	8α-histidyl lumiflavin	$-CH_3$	$C_8-CH_3 \rightarrow C_8-CH_2$-histidine
3 Me, 8α Morph LF	3-methyl, 8α-morpholino lumiflavin	$-CH_3$	$N_3-H \rightarrow N_3-CH_3$ $C_8-CH_3 \rightarrow C_8-CH_2$-morpholine
Lyx F	L-lyxitylflavin	$-CH_2-(CHOH)_3-CH_2OH$	
Gal F	D-galactosylflavin	$-CH_2-(CHOH)_4-CH_2OH$	
10 For Me F	10-formylmethyl flavin	$-CH_2-CHO$	
7 Cl, 10 Sorb IA	7-chloro, 10-D-sorbityl isoalloxazine	$-CH_2-CO-(CH_2OH)_3-CH_2OH$	$C_7-CH_3 \rightarrow C_7-Cl$ $C_8-CH_3 \rightarrow C_8-H$

Abbreviation	Analog	Structure
A	alloxazine	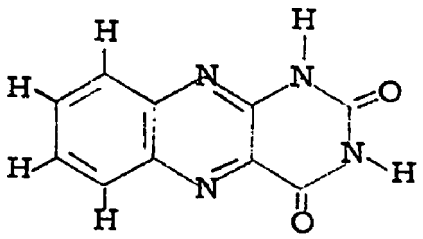
1,3 di Me A	1,3-dimethyl alloxazine	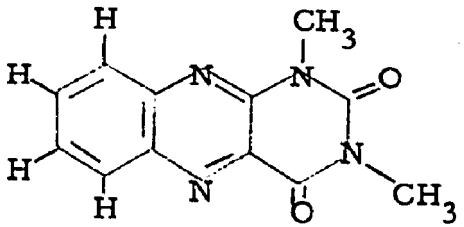
1,3,7,8 tet Me A	1,3,7,8-tetra-methyl alloxazine	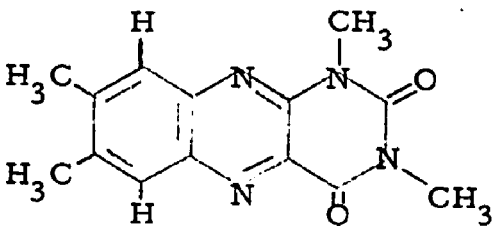
1,3,7,8 tet Me,4 O Me A	1,3,7,8-tetra-methoxy alloxazine	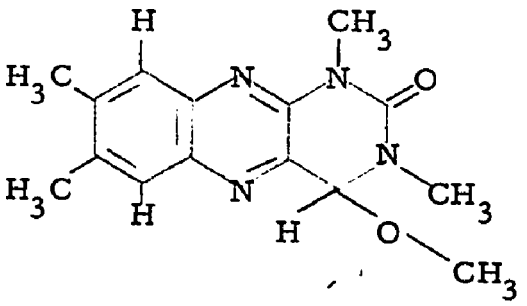

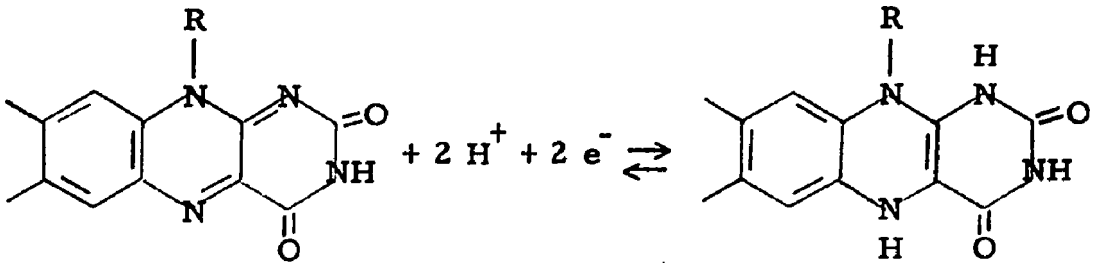

Oxidized Reduced

This reduction can occur by a single two-electron step or by two one-electron steps proceeding through a half reduced state, the flavin semiquinone. The isoalloxazine nucleus can exist as an anion, cation, or neutral molecule in any of its three oxidation states, making a total of nine chemically distinct isoalloxazine species. In the oxidized state the neutral molecule shown in Figure 1 is the flavin species most prevalent over the physiological pH range. Most studies on flavoenzymes have concerned the flavin oxidation-reduction process within the context of the enzyme mechanism and thus involve flavins in more than one oxidation state. Nevertheless the binding studies presented in this thesis are restricted to flavins with the isoalloxazine nucleus in the oxidized (and neutral) state. The reduced or ionic flavin species will be considered only where pertinent.

SOME COMMENTS ABOUT FLAVIN BINDING

The major goal of a flavin binding study is to obtain a complete description of the interaction between the flavin and its apoprotein in the following terms: a) the number of binding sites on the apoprotein

(stoichiometry), b) the strength of the interaction (equilibrium constant, thermodynamic energies), c) the rates of the association and dissociation process for each step in the binding mechanism (rate constants, activation energies), and d) the chemical nature of the interaction. If x-ray data are unavailable, item d) requires the use of different flavin analogs or modified apoprotein in the studies a), b), and c). A comparison of the results then gives some information about the chemical and spatial nature of the interaction. Implicit to the interpretation of quantitative flavin binding studies are the criteria that the removal of the flavin from the holoprotein is reversible, that the reconstituted product is identical with the native species, and that the interacting components are homogeneous with respect to binding.

Flavin binding in its simplest representation involves the reversible one-step reaction:

$$F + A \underset{k_{-1}}{\overset{k_1}{\rightleftharpoons}} H \qquad \text{Equation (1)}$$

where F, A, and H designate flavin, apoprotein, and holoprotein, respectively. K_a, the equilibrium constant for Equation (1), is defined:

$$K_a = \frac{[H]_e}{[F]_e \cdot [A]_e} = \frac{k_1}{k_{-1}} = (K_d)^{-1} \qquad \text{Equation (2)}$$

where $[H]_e$, $[F]_e$, and $[A]_e$ are the equilibrium concentrations of H, F, and A. An extension of reaction (1) is the reversible two-step mechanism, reaction (3)

$$F + A \underset{k_{-1}}{\overset{k_1}{\rightleftharpoons}} FA \underset{k_{-2}}{\overset{k_2}{\rightleftharpoons}} H \qquad \text{Equation (3)}$$

where for this mechanism

$$K_a = \frac{[H]_e}{[F]_e \cdot [A]_e} = \frac{k_1 k_2}{k_{-1} k_{-2}} \qquad \text{Equation (4)}$$

Studies on the complexing of small molecules to proteins, including flavin binding studies, are most frequently considered on the basis of these two relationships.

The Gibbs free energy change, ΔG, for a binding reaction is measured in this thesis by the standard equation

$$\Delta G = -2.30\ RT \log K_a \qquad \text{Equation (5)}$$

The change in enthalpy, ΔH, for the reaction is determined graphically from the slope of log K_a plotted against the reciprocal of the absolute temperature according to the van't Hoff equation

$$\Delta H = -2.30\ R \frac{d(\log K_a)}{d(1/T)}$$

The change in entropy, ΔS, for the reaction is then calculated from the standard equation

$$\Delta G = \Delta H - T\Delta S \qquad \text{Equation (6)}$$

Activation energies for each rate constant k are evaluated using equations from the theory of absolute reaction rates (5, for recent discussion see Moore, 6). $\Delta H^{\ddagger}$, the activation enthalpy, is graphically determined from the slope of log k plotted against 1/T according to the Arrhenius equation

$$E_a = \Delta H^{+} + RT = -2.30\ R \frac{d \log k}{d(1/T)}$$

ΔG^{+}, the activation free energy, is found using the equation

$$\Delta G^{+} = 2.30\ RT \left(\log \frac{kT}{h} - \log k\right) \qquad \text{Equation (7)}$$

where k and h are the Boltzmann and Planck constants. Evaluated at 25°C, Equation (7) gives

$$\Delta G^{+} = (17.4 - 1.36 \log k) \quad \text{kcal/mole} .$$

The activation entropy, S^{+}, is then calculated from H^{+} and G^{+} using an equation similar to Equation (6).

Several flavin binding studies to date have monitored flavoenzyme activity when flavin analogs and apoenzyme are mixed under saturating conditions of substrate. The attempt to understand flavin-protein interactions by interpretation of flavoenzyme activity data is hazardous as can be seen from the following generalized scheme:

$$\begin{array}{ccccc} \text{Apoenzyme} + \text{Flavin} + \text{Substrate} & \rightleftharpoons & \text{Flavoenzyme} + \text{Substrate} \\ \uparrow\downarrow & & \uparrow\downarrow \\ (\text{Apoenzyme - Substrate}) + \text{Flavin} & \rightleftharpoons & (\text{Flavoenzyme - Substrate}) & \rightleftharpoons & \cdots \end{array}$$

$$\cdots \rightleftharpoons \text{Flavoenzyme} + \text{Product}$$

The appearance of product relates to flavin binding in a complicated way because a) the participation of substrate may perturb the interaction between flavin and protein in an unknown manner, b) product

formation includes reaction steps sequential to flavin binding, and c) flavoenzyme activity involves factors other than the interaction between flavin and apoenzyme, e.g., the oxidation-reduction potential of the flavin analog. For these reasons activity studies are difficult to compare to flavin binding studies and will receive only minor attention in the next section.

HISTORICAL BACKGROUND OF FLAVIN BINDING

Old Yellow Enzyme (OYE)

The first detailed investigation on flavin-protein interactions was undertaken by Theorell and Nygaard (7-9) on OYE, TPNH dehydrogenase from yeast. Acid ammonium sulfate precipitation (10) of the protein liberated FMN, the naturally occurring flavin, from the protein. After recovering the apoprotein by centrifugation, the holoprotein could be reconstituted by adding FMN to the redissolved apoprotein at pH values in the range 4 to 10. Theorell and Nygaard (7) were able to study the binding quantitatively because the fluorescence of flavin bound to apoOYE was completely quenched. Although the association process was slow enough to be followed kinetically (quenching $t_{1/2} \sim$ seconds), the degree of dissociation in water or in buffers of weak acids was too small to be measured ($K_d < 10^{-12}$ M) as judged by the absence of fluorescence from free FMN in equilibrium with native OYE under these conditions. However, they noted that the presence of salts of strong acids (the order of the observed effect

was $Br^- > Cl^- > H_2PO_4^-$) greatly increased the dissociation process. At sufficiently high salt concentrations the K_d and apparent k_{-1} were measurable. From dilution experiments of native OYE they concluded a) flavin binding to OYE was reversible, b) quenching of fluorescence monitored a second order process, and c) the assumption that FMN binding to apoOYE was described by Equation (1)*, seemed correct. Values of K_a, k_1, and k_{-1} could be independently calculated which were mutually consistent with this assumption.

Observing that increased salt concentrations led to increased values of k_{-1}, Theorell and Nygaard (8) concluded that an ionic bond existed between FMN and apoOYE, specifically between the negatively charged flavin phosphate group and basic group(s) on the protein. This hypothesis was strengthened by the behavior of k_1 as a function of pH. Measured values of k_1 increased between pH 4 and pH 8 and had a pH profile which resembled that of a dissociable group with pK of 6.0 at 23.5°. This apparent pK shifted to pH 5.8 at 13.5° or in high salt concentrations. These effects were consistent with the hypothesis that the relative magnitude of k_1 depended on the degree of dissociation of the second hydroxyl of the flavin phosphate, i.e., doubly-charged FMN bound faster than singly-charged FMN. The

---

* The molecular weight of OYE determined by ultracentrifugation (11) is twice the minimal molecular weight determined by flavin content (12). OYE thus contains two FMN molecules (per molecule of protein). Judged by the consistency of the binding constants, the interaction between the flavin sites is not highly significant, but may give rise to the small degree of anomaly observed in the binding measurements.

decrease in k_1 observed at pH values above pH 9 was attributed to the dissociation of protons from amino groups involved in the ionic bond. The pH dependence of k_1 was measured at two temperatures, both in the presence and absence of 0.4 M NaCl, and higher rate constants were observed at the higher temperature.

Nygaard and Theorell (9) compared the rate and equilibrium constants for FMN, RF and FAD binding to apoOYE. Their results are given in Table II. Because k_1 for the three derivatives was

TABLE II

The Binding of FMN, FAD, and RF to ApoOYE at pH 9.0, 23° (9)

Flavin	K_a	ΔG	k_1	k_{-1}
	(M^{-1})	kcal/mole	$(M^{-1}sec^{-1})$	(sec^{-1})
FMN	$> 10^{12}$	-17	1.4×10^6	$<10^{-6}$
FAD	5×10^6	-9	0.2×10^6	0.04
RF	5×10^5	-8	0.1×10^6	0.2

relatively constant, they concluded that the strength of the interaction (K_a) depended primarily on the dissociation rate constant (k_{-1}). It can be seen that the free energy change for RF binding could represent as much as half the total free energy change for FMN binding. Thus, the dimethyl isoalloxazine and ribose moieties of FMN contribute significantly to the strength of the interaction.

As part of their investigation, Theorell and Nygaard (9) studied FMN binding to chemically modified OYE. Specific acetylation of protein amino groups and iodination of tyrosyl residues were found to affect both k_1 and k_{-1}. In all cases studied, an overall decreased strength of interaction occurred with an increased extent of reaction. The equilibrium constant for FMN binding decreased by at least 10^4 upon acetylation of 10% of the total number of protein amino groups or di-iodination of 20% of the tyrosyl residues. Although difficult to measure because of the lowered value of K_a, the binding stoichiometry remained 1 mole FMN/mole original apo-OYE sites, even after 50% of the amino groups and 30% of the tyrosyl resides had reacted. These data further substantiated the importance of positively charged amino groups to the binding of FMN by apoOYE and indicated that tyrosyl residue(s) might be involved in the flavin-protein interaction in this flavoenzyme.

In a subsequent communication Theorell, Yagi, Ludwig, and Egami (13) noted that the fluorescence of $RFSO_4$ was not quenched by apoOYE, nor did it interfere with FMN binding. This was quite an unexpected result because FMN and $RFSO_4$ both a) contained the RF moiety known to interact with apoOYE and b) bore a negatively charged group at the terminus of the ribose group on the flavin, also shown to be crucial to the interaction. It must be concluded that the presence of the sulfate group prevented binding.

Cytochrome b_5 Reductase

Undenatured aporeductase could not be prepared from this FAD containing flavoenzyme by the standard acid ammonium sulfate method of Warburg and Christian (10). Instead Strittmatter (14) developed a method involving ammonium sulfate precipitation in the presence of KBr in which the enzyme was subjected to low pH for times shorter than about 10 minutes. Later Strittmatter (15) achieved flavin dissociation by adjusting the enzyme solution to pH 2 using HCl. The flavin was separated from the apoprotein in this latter method by a) passing the pH 2 solution over a Sephadex G25 column or b) adsorbing the flavin onto activated charcoal, then removing the charcoal by centrifugation. He reported that fully active reductase, spectrally indistinguishable from the native species, was obtained when FAD was added to a pH 8.5 solution of the apoenzyme prepared by either of these methods.

Strittmatter (14) investigated the equilibrium binding of FAD, FMN, and RF to cytochrome b_5 aporeductase. Again the fluorescence quenching technique was used to study binding because the flavin in native reductase is non-fluorescent. Table III contains his results for the binding stoichiometries, dissociation constants, and Michaelis constants (K_m) based on reconstitutable enzyme activity (NADH oxidation). The data reveal the importance of the adenosine group and especially the flavin phosphate in binding to aporeductase. However, FMN, and to a lesser extent RF, were able to partially restore

TABLE III

Equilibrium Binding to Cytochrome b_5 Reductase at pH 8.1 (14)

Flavin	Stoichiometry	K_d (2-4°) (M)	K_m (25°) (M)
FAD	1 : 1	$< 10^{-9}$	$< 10^{-9}$
FMN	1 : 1	8×10^{-9}	$2\text{-}4 \times 10^{-8}$
RF		2×10^{-5}	

enzyme activity, thus neither the adenylate nor phosphate ester portion of FAD was an absolute requirement for activity.

Strittmatter (14) concluded this study with an investigation of the effect of group specific reagents on flavin binding to aporeductase. Sulfhydryl groups did not appear to be involved in the interaction with the FMN portion of FAD because FMN binding capacity was not affected when aporeductase had been previously reacted with p-chloromercuribenzoate (PCMB) or N-ethylmaleimide at pH 8.1. A large excess of trinitrobenzene sulfonate caused slow inhibition of FMN binding, suggesting that amino groups were involved in flavin binding, either by participating at the site or by maintaining a functional tertiary protein structure. One specific and very reactive tyrosyl residue appeared to be directly involved in FMN binding because 2.2 moles of iodine per mole of protein completely inhibited binding to the N-ethylmaleimide derivative of aporeductase (5-6 moles of iodine

per mole of protein were required for complete inhibition when the non-sulfhydryl-blocked-aporeductase was used).

As already mentioned, lowering the pH value of the enzyme solution to pH 2 liberated the FAD. Upon raising the pH value back to pH 8.5, the reconstitution process had a half time of the order of minutes and could be followed by changes in a) flavin absorbance, b) flavin fluorescence, c) protein fluorescence, and d) flavin reduction by NADH. Strittmatter (15) observed that the kinetics of renaturation as measured by a) - d) were faster in the presence of FAD (but not FMN) than in its absence. Thus if FAD was not removed during acidification, or was removed and then added back with the Tris* solution used to raise the pH, the rate of subsequent activity return was faster than the rate of activity return if the pH of the apoprotein solution was raised (in this last case the process was monitored by adding FAD at later times). The rate of activity return in the absence of FAD was unaffected by the presence of FMN. FAD appeared to accelerate the renaturation process. Although no kinetic analysis is reported, all traces for experiments in the presence of FAD appear closely second order with a rate constant of about 10^3 $\underline{M}^{-1}$ sec^{-1}. In the absence of flavin or in the presence of FMN, the rate is about a factor of 2-3 slower. In light of the fact that some change in the protein occurs on raising the pH value in the absence of FAD (albeit more slowly) and in light of the results discussed below, the initial

---

* tris-(hydroxymethyl)aminomethane

complexing of FAD to the apoprotein can not be the rate-limiting step and therefore the cause of the apparent second order kinetics. Clarification of this point must await further study.

Strittmatter (15) reacted cytochrome b_5 aporeductase with mercurials and observed that at pH 2, five apoprotein sulfhydryl groups reacted with PCMB or mersalyl. The binding of FAD to this modified aporeductase at pH 8.5 occurred at a much slower rate than to the unmodified aporeductase. More interesting was the observation that FAD binding resulted in the displacement of two of the protein bound mercurials. (In the absence of FAD, the five mercurials remained bound to the aporeductase after raising the pH to 8.5.) The same experiments using FMN instead of FAD showed that no FMN was bound to this mercuriated apoprotein and no mercurials were displaced.

Strittmatter concluded from these studies that FAD was capable of inducing a special sequence of alterations in the protein structure which augmented restoration of flavin binding capacity. Flavin binding to cytochrome b_5 aporeductase appears to be a complicated process involving more steps than the mechanism of Equation (3). This complication makes difficult a thermodynamic study of flavin binding using this system.

D-Amino Acid Oxidase, (DAAO)

Several investigations on the nature of the flavin-protein interaction in DAAO have been made to date. Warburg and Christian

(10) liberated FAD, the naturally occurring flavin in this flavoenzyme, by acid ammonium sulfate precipitation, and from enzyme activity studies measured $K_m = 3 \times 10^{-7}$ M (38°C, pH 8.3).

A more detailed investigation was undertaken by Walaas and Walaas (16). When FAD was bound to apoDAAO prepared by the above method, no appreciable quenching of FAD fluorescence occurred nor were any definite changes observed in absorbance at 375 nm or 450 nm. Walaas and Walaas were thus unable to monitor FAD binding by direct tecyniques and were limited to monitoring flavin binding by the restoration of enzyme activity. Although they made the perhaps unwarranted assumption that relative DAAO enzyme activity measured only the percent of apoenzyme with bound flavin, they concluded from pH and ionic composition studies of flavin binding that interactions may exist between the negatively charged flavin phosphate groups and positively charged groups on the apoprotein, a conclusion similar to that obtained with OYE (8).

Walaas and Walaas (16) also studied the effect of structural analogs of FAD on DAAO activity. FMN and AMP were found to be competitive inhibitors. Ribose-5-phosphate as well as the non-phosphorylated derivatives, RF and adenosine, were slightly inhibitory. Thus to the extent that this inhibition of enzyme activity resulted from inhibition of flavin binding, interactions between FAD and apoDAAO involved the isoalloxazine, ribose(s), phosphate(s), and adenosine

moieties. However, neither FMN or RF alone nor in combination with adenylic acid could reactivate apoDAAO.

Chassey and McCormick (17) extended these studies of the effects of FAD structural analogs on DAAO activity. All analogs differing from FAD either in the flavin side chain or isoalloxazine ring were found to function poorly or not at all as prosthetic groups for apoDAAO. Some analogs which did not function as prosthetic groups inhibited DAAO presumably by displacing FAD from the binding site.

Dixon and Kleppe (18) performed a preliminary kinetic study of flavin binding in native DAAO by following the decrease in enzyme activity after dilution of the enzyme at pH 8.5. They assumed that flavin binding was described by the single step reaction of Equation (1) and that the decrease in activity observed after dilution occurred because of and at the rate of the flavin dissociation. From the initial slope of the decrease in activity, they calculated $k_{-1} = 0.0075\ sec^{-1}$ at 25°. Dilution experiments carried out in the presence of FAD caused a slower rate of activity decrease and indicated that this decrease indeed resulted from FAD dissociation. They asserted that the difference between the rates in the presence and absence of added FAD was due to the association reaction and calculated $k_1 = 3 \times 10^4\ \underline{M}^{-1} sec^{-1}$. The apparent $K_d = 2.8 \times 10^{-7}\ \underline{M}$ calculated from the residual equilibrium activity after dilution agreed well with $k_{-1}/k_1 = 2.5 \times 10^{-7}\ \underline{M}$. In view of the later work of Massey and Curti (19)

discussed below, the mechanism for flavin binding proposed by Dixon and Kleppe (18) is certainly too simple.

Massey and Ganther (20) performed the first direct measurement of the FAD-apoDAAO interaction. From equilibrium dialysis studies covering a six-fold range in DAAO concentration, they determined $K_d = 2.2 \times 10^{-7}$ M at 0-4°C and pH 8.5. This compared well with $K_m = 5.5 \times 10^{-7}$ M measured at 25°. The studies of Massey and Ganther (20) confirmed the implication of Dixon and Kleppe (18) that in relation to many flavoproteins, DAAO has a relatively low affinity for its prosthetic group.

Massey and Curti (19) developed a new method for the preparation of apoDAAO. The observation of Theorell and Nygaard (8) that salts of strong acids tended to dissociate FMN from OYE and the indication of Walaas and Walaas (16) that the same might be true for DAAO prompted Massey and Curti (19) to dialyze DAAO against 1 M KBr in an attempt to prepare apoenzyme. This method produced apoDAAO in higher yields than the method using acid ammonium sulfate precipitation. Reconstituted enzymes from both methods were spectrally and enzymatically indistinguishable.

In contrast to the earlier observations (16), Massey and Curti (19) found that reconstitution of DAAO using FAD plus apoenzyme, could be directly monitored by absorbance changes (maximal at 493 nm) and by both protein and FAD fluorescence quenching. On mixing apoDAAO and FAD, a slow absorbance increase was observed which

followed first order kinetics after an initial lag period. The same value for the rate constant describing this first order absorbance change was observed for a series of experiments in which different concentrations of apoDAAO were mixed with FAD. The observed first order process appeared to represent a binding step subsequent to the initial complexing of flavin and protein. Massey and Curti (19) also performed mixing experiments in which protein fluorescence or flavin fluorescence was monitored. Both types of fluorescence experiments showed an initial rapid quenching of fluorescence which was concentration-dependent, followed by a slow first order quenching which was concentration-independent. These first order changes in fluorescence and absorbance were described by essentially the same rate constant, $k \sim 0.03$ sec^{-1} at 16°, a value faster than that observed by Dixon and Kleppe (18). The initial rapid decrease in fluorescence was consistent with a second order rate constant, about 2×10^{3} $\underline{M}^{-1} sec^{-1}$, a value lower but not incompatible with that of Dixon and Kleppe (18). Restoration of enzyme activity paralleled the slow secondary process. Massey and Curti (19) concluded that reconstitution of DAAO was at least the two step mechanism of Equation (3).

Lipoamide Dehydrogenase

The apoenzyme from lipoamide dehydrogenase, an FAD-containing enzyme, was prepared by Kalse and Veeger (21) using the ammonium sulfate precipitation method. They found that reconstitutability of enzyme activity depended on the procedures used both in the

preparation of apoenzyme and in its reconstitution. Recombination of FAD and apoenzyme showed complicated behavior as judged by the several physical parameters monitored for 30 minutes after mixing. At 5° and 20° fluorescence polarization and enzyme activity with lipoate (an analog of the natural electron acceptor) increased monitonically over the 30 minute period, but increased with different rates. At 5° the vertically polarized component of fluorescence intensity, I_v, increased monitonically with a rate similar to the return of activity with lipoate. However, at 20°, I_v reached a maximum after about six minutes and then slowly decreased during a period when lipoate activity was steadily increasing. At 5° and 20°, enzyme activity with 2,6-dichlorophenolindophenol, an artificial electron acceptor, increased rapidly to a maximum, thereafter decreasing steadily at both temperatures. The different rates and shapes of these progress curves indicate that flavin binding to lipoamide apodehydrogenase is a complicated multi-step process. Kalse and Veeger (21) made thermodynamic and kinetic studies of the reconstitution process using these parameters, but these studies become all the more difficult to relate directly to flavin binding, per se, by their observation that lipoamide apodehydrogenase has a molecular weight about half that of the holoenzyme. Thus, the overall reconstitution reaction must resemble:

2 FAD + 2 apoenzyme monomer $\rightleftharpoons \ldots \rightleftharpoons$ 1 holoenzyme dimer

Visser, McCormick, and Veeger (22) measured some differences in binding to lipoamide apodehydrogenase of FAD and FAD

analogs modified in the 3 position of the isoalloxazine ring. Equilibrium binding studies were performed using polarization of fluorescence to monitor bound flavin; binding stoichiometries for FAD, 3-MeFAD, FAD 3-acetate were approximately 1 mole flavin per 50,000 g apoenzyme; equilibrium constants at 10° for the three derivatives were 3.2×10^{5} $\underline{M}^{-1}$, 1.1×10^{5} $\underline{M}^{-1}$, and 0.3×10^{5} $\underline{M}^{-1}$, respectively. The enzymes reconstituted with the three derivatives were assayed for DCIP and lipoate activity. Their data suggested and they concluded that the activities using analogs modified at the 3 position of the isoalloxazine moiety were less than the activity with FAD. However, a closer examination of their data shows that at the dilute concentrations used in the assay, the relative DCIP activities among the three reconstituted enzymes corresponded directly to the percent of reconstituted enzyme expected on an equilibrium basis. Thus, no difference in DCIP activity among the types of reconstituted enzymes actually existed. Their implicated differences in lipoate activity are also dramatically reduced by this consideration. In contrast to the increase of FAD fluorescence on binding to lipoate apodehydrogenase, Visser and Veeger (23) found that protein fluorescence decreased during binding.

Glucose Oxidase

The binding of FAD, the naturally occurring prosthetic group, to glucose apooxidase was studied by Swoboda (24). Apoenzyme was prepared by the acid ammonium sulfate method. Incubation of the

apoenzyme with various amounts of FAD for an hour, followed by assaying the products for activity, produced a titration curve which showed increasing activity with increasing FAD concentration up to a sharp break point at 1.5 moles FAD per mole glucose apooxidase. From the observation that reconstituted glucose oxidase had a specific activity 75% that of native enzyme and from the apparent 1.5 : 1 stoichiometry, Swoboda concluded that 75% of the apoprotein was undenatured and was able to recombine with 2 moles FAD/mole apoprotein to give fully active glucose oxidase.

Swoboda (24) followed the kinetics of reassociation by several methods: the return of oxidase activity, quenching of FAD fluorescence, and the change in FAD absorbance when FAD and apooxidase were mixed. He observed qualitatively different behavior in the kinetics of these processes depending on which reactant was in excess. Above a five-fold excess of FAD concentration over apoenzyme concentration, the first order progress curves for the return of oxidase activity were superimposible and yielded a rate constant of 0.027 sec^{-1}. In contrast, higher ratios of apoenzyme concentration to FAD concentration caused proportionally higher rates of activity return. From this Swoboda (24) calculated a second order rate constant of 10^5 $\underline{M}^{-1}sec^{-1}$. Experiments in which the quenching of FAD fluorescence was monitored yielded the same rate constants. However, when changes in FAD absorbance were monitored, the rate constant observed for all conditions of excess FAD over apoenzyme was 0.13

sec^{-1}, indicating that another process was occurring much faster than the restoration of activity and quenching of fluorescence. Polarization of fluorescence studies indicated essentially complete binding of flavin had occurred at a time corresponding to about 30% of the total fluorescence quenching. The model proposed to account for these findings involved an interconversion of apoenzyme species, complexation of FAD to each form of apoenzyme, and a succession of unimolecular steps:

$$A_1 \rightleftarrows A_2$$

$$A_1 + F \rightleftarrows (A_1 - F) \rightleftarrows (A_1 - F)^1 \rightleftarrows A_2 - F$$

$$A_2 + F \rightleftarrows A_2 - F$$

Swoboda (25) investigated the effects of FAD analogs on binding. Analogs of adenosine diphosphate (ADP) inhibited the reconstitution of oxidase activity when FAD was mixed with apoenzyme; however, FMN had no inhibitory effect when present in 10^3 excess over FAD. Although the isoalloxazine portion of FAD interacted with protein as evidenced by the fluorescence and absorbance changes accompanying binding, the intensity and polarization of FMN, RF, or LF fluorescence were unaffected by the addition of apoprotein-ADP complex. Moreover, oxidase activity was not reconstituted by mixing apooxidase with a) RF and ADP or b) FMN and adenosine monophosphate. From these results, Swoboda (25) concluded that the adenosyl portion of FAD was crucial for binding and required for oxidase activity. He also concluded that the binding sequence consisted first of an interaction of

the adenosyl moiety with apooxidase followed by some change in the protein which made an isoalloxazine site accessible.

Flavodoxins

Since 1970, the principal investigations on flavin binding have concerned the flavodoxins, FMN-containing electron transfer proteins, from bacteria.

Noting the success of Massey and Curti (19) in removing FAD from D-amino acid oxidase by dialysis against KBr, Mayhew (26,27) removed FMN from the flavodoxins of Clostridium pasteurianum, Clostridium MP, and Peptostreptococcus elsdenii by dialysis against 2 M KBr at pH 3.9. Titration of FMN fluorescence indicated that each apoprotein species was able to rebind one molecule of FMN to form a product identical to the respective native flavodoxin in spectroscopic, catalytic, and oxidation-reduction properties. By measuring the quenching of FMN fluorescence when aliquots of an FMN solution were titrated into a 10^{-7} M solution of P. elsdenii apoflavodoxin, Mayhew (26,27) determined the dissociation constant to be 4.3×10^{-10} M at pH 6.55 and 20°.

Mayhew (27) observed that the kinetics of fluorescence quenching on mixing FMN and P. elsdenii apoflavodoxin corresponded to a second order process. Approximately the same rate constant ($k = 2.6 \times 10^{5}$ $M^{-1}sec^{-1}$ at pH 4.4 and 0.5°) was obtained from experiments run under two conditions: a) the concentrations of FMN and apoprotein were nearly equal, and b) the concentration of apoprotein was in

seven-fold excess over FMN. The rate of association was found to depend both on the pH value and on the ionic composition of the solution. The rate was maximal at pH 4.4 and indicated to Mayhew (27) that the singly-ionized flavin phosphate species was bound more avidly. In phosphate buffer at pH 7, the rate was maximal in 0.017 M Na phosphate, but could be increased by the addition of 0.5 M KCl. At pH 7, the temperature dependence of the association rate constant produced a linear Arrhenius plot between 0.5° and 18° and yielded an activation energy of 8.3 kcal/mole.

Binding constants for other flavin analogs were not measured; however, iso-FMN and 3,4-dihydro-FMN were qualitatively shown to have high affinity for P. elsdenii apoflavodoxin. The fluorescence of these flavins was quenched on addition of apoprotein and the reconstituted products did not lose flavin on extensive dialysis. In contrast, the fluorescence of solutions of FAD, RF, or LF was not quenched on addition of apoprotein and these flavins were readily lost on dialysis. Under the conditions studied, FAD, RF, and LF were not bound at all or had equilibrium constants at least a million-fold lower than FMN. This surprising result indicated to Mayhew (26,27) that binding is very specific for FMN and FMN derivatives and that the phosphate of FMN triggers a protein conformational change in apoflavodoxin which brings the appropriate isoalloxazine site into position, in analogy to the hypothesis that the adenosyl portion at FAD triggers a change in glucose apooxidase (25). Modifications in the isoalloxazine

portion of FMN seemed far less crucial to binding; however, an interaction between the protein and the isoalloxazine clearly occurred as judged by the spectroscopic perturbations which accompanied binding.

Mayhew (26,27) found that FMN binding was completely inhibited by reacting PCMB or N-ethylmaleimide with the apoprotein which indicated that either sulfhydryls interacted directly with the flavin or participated in maintaining a functional site. Preliminary experiments using tetranitromethane implied that nitration of one of the two tyrosines in P. elsdenii apoflavodoxin inhibited flavin binding.

The high affinity of apoflavodoxin for the reduced forms of FMN, coupled with the lack of sufficiently sensitive spectroscopic properties, precluded the direct measurement of the equilibrium constants for the binding to apoflavodoxin of FMNH· or $FMNH_2$, the semiquinone form or fully reduced form of FMN, respectively. One elegant aspect of the work of Mayhew (26,27) concerned his evaluation of these equilibrium constants by an indirect thermodynamic method, using the equilibrium constant for the binding of FMN in conjunction with the oxidation-reduction potentials for the free and bound couples FMN/FMNH· and FMNH· /$FMNH_2$. His results for the binding of FMNH· and $FMNH_2$ to apoflavodoxin are shown in the following thermodynamic cycle.

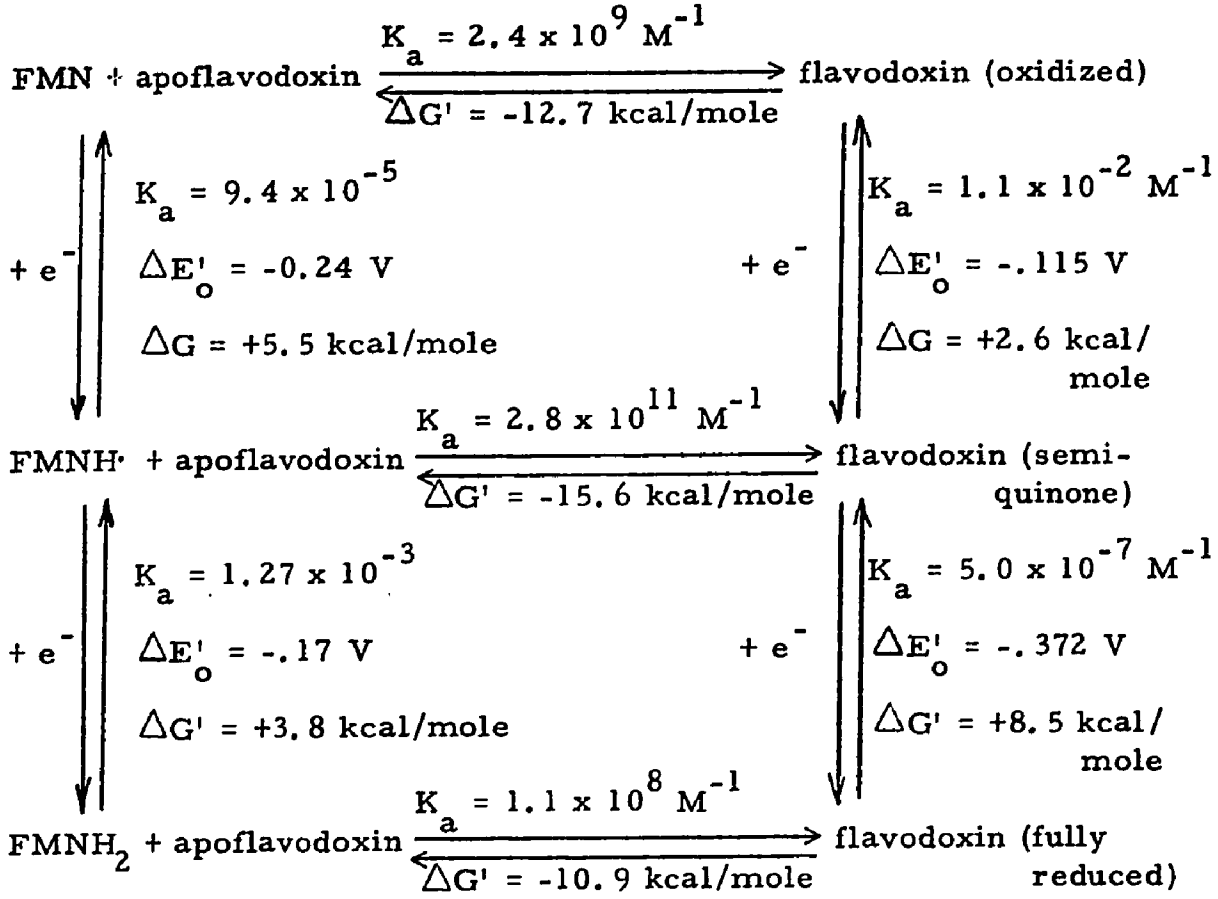

To date the most extensive flavin binding studies employing flavin analogs have been performed on the flavodoxin from Azobacter vinelandii (formerly Shethna flavoprotein). Edmondson and Tollin (28) removed FMN, the naturally occurring chromaphore, from this flavoprotein by precipitation of the apoprotein in 3% trichloroacetic acid. Inclusion of 1 mM dithiothreitol during the precipitation prevented formation of high molecular weight material unable to bind flavin. They studied thermodynamic, kinetic, and spectroscopic aspects of the flavin-apoprotein interaction in the Azotobacter flavodoxin.

Using the fluorescence quenching technique apparent equilibrium constants were determined from modified Scatchard (29) plots in

which $\alpha/[F]_e$ was plotted against $1-$, where $= [H]_e/([A]_e + [H]_e)$, the fraction of total protein complexed with flavin*.

Scatchard plots give characteristic results for simple binding. Thus for flavin binding in which the apoprotein binding sites are homogeneous and independent (and the flavin analogs homogeneous), Scatchard plots are linear with slopes equal to the equilibrium constants. For a single step equilibrium with 1 : 1 stoichiometry (Equation 1), the data points on the modified Scatchard plots of Edmondson and Tollin (28) should have $1-\alpha$ values between 0 and 1 and extrapolate to intercept the origin (30).

Pertinent aspects of the flavin analog binding studies of Edmondson and Tollin (28) are presented in Table IV. The modified Scatchard plots for several flavin analogs were linear (each over a limited range in $1-\alpha$) but intercepted the x-axis at values between 0.2 and 0.6 in $1-\alpha$. From the varying degrees by which these x-intercepts differ from zero, it is evident that some major inhomogeneity existed. Because the flavin analogs were pure when examined by thin layer chromatography, one can only conclude that the A. vinelandii apoflavodoxin was inhomogeneous with respect to the character of flavin binding sites. From the intercept discrepancies and from the limited range in $1-\alpha$ studied, it is not clear whether the inhomogeneity resulted from significant fraction(s) of the apoprotein which bound flavin with weak affinity or which did not bind flavin at all.

---

* The quantities $[A]_e$, $[F]_e$, and $[H]_e$ are defined on page 9.

TABLE IV

Results of the Scatchard Analyses for the Binding of Flavin Analogs to the Flavodoxin from Azotobacter vinelandii at pH 7.0 and 25 ± 2° (28)

Flavin	Apparent K_a	X-Axis Intercept on Modified Scatchard Plot	Range in $1-\alpha$ Covered by Data
	$\underline{M}^{-1}$		
FMN	2.2×10^8	0.24	0.16
deoxyFMN	1.3×10^8	0.18	0.27
3 MeFMN	3.7×10^7	0.44	0.11
isoFMN	4.8×10^7	0.19	0.09
RF	1.8×10^6	0.57	0.20
deoxyRF	2.4×10^6	0.37	0.15
isoRF	1.7×10^6	0.51	0.20
FAD	1.3×10^6	0.58	0.16
LF	$2.2 \times 10^{5*}$	0.5	0.36**
10-ω-CO_2^- Bula	3.1×10^6	0.50	0.15

* This is the value stated by Edmondson and Tollin. The value one obtains from the slope of the line drawn by them through their data points is 1.3×10^5 $\underline{M}^{-1}$.

** The actual range is likely to be smaller than this. See p. 36.

No analogs had x-intercepts less than about 0.2. However, three (including FMN) do cluster around this region, corresponding to an apparent stoichiometry of 0.8 mole flavin bound per mole apoprotein. This stoichiometry would result if the value of the protein concentration used in the Scatchard analyses were about 20% higher than the actual concentration of binding sites.

From the data* of Edmondson and Tollin (28) one can calculate that they used an apoprotein molar absorptivity, $\epsilon_{280} = 2.9 \times 10^4$ $\underline{M}^{-1}cm^{-1}$. However, from the data* of Hinkson (32) one can calculate an $\epsilon_{280nm} = 3.5 \times 10^4$ $\underline{M}^{-1}cm^{-1}$ for the apoprotein on the basis of FMN combining capacity. Thus the apoflavodoxin concentration according to Edmondson and Tollin (28) would indeed be about 20% higher than the actual concentration of FMN binding sites according to Hinkson (32). While this gives a possible explanation why no stoichiometry was found to be greater than 0.8 : 1, it does not answer for the large variation in x-intercepts for the other analogs. Even corrected for the probable error in ϵ^{M}_{280} based on flavin combining capacity, these other analogs show stoichiometries between 0.5 : 1 and 0.8 : 1. The conclusion still remains that their apoprotein preparations contained a considerable degree of binding heterogeneity.

---

* Using the method of Lowry, Rosebrough, Farr, and Randall (31) Edmondson and Tollin (28) found a weight extinction coefficient, $\epsilon^{1\%}_{280\ nm} = 12.7\ cm^{-1}$. They determined the protein molecular weight to be 23,000 g/mole from sedimentation studies and amino acid analyses. By the Lowry et al. (31) method, Hinkson (32) found an $\epsilon^{1\%}_{280} = 13.0\ cm^{-1}$. He also calculated that one mole of FMN would be bound by 27,000 g of A. vinelandii apoflavodoxin.

Edmondson and Tollin (28) falsely assert:

> "The binding of all analogs to the protein was in a 1 : 1 molar ratio, as indicated by the linearity of the binding [Scatchard] plots."

The linearity of these plots does not imply anything about the binding stoichiometry. Rather, the linearity of which they speak implies a constancy of K_a, that is, within the limited range of $1-\alpha$ studied, the apoprotein molecules affecting the equilibrium possess the same intrinsic binding constant. It is disappointing that conditions were chosen which yielded such small ranges in the fraction of apoprotein molecules bound. Only for two* of the ten analogs is the range in $1-\alpha$ seen (Table IV) to be greater than 0.2. In light of the apparent binding heterogeneity of the apoflavodoxin, it is not certain whether the fraction of the apoprotein population affecting each equilibrium determination is the same fraction. It is difficult to know the significance of the binding parameters they measured and comparisons of equilibrium constants and free energies of binding for the several analogs are dangerous. However, it seems likely that phosphorylated flavin analogs are bound more strongly than their non-phosphorylated counterparts judged by higher stoichiometries of flavin binding and higher apparent binding constants.

Quantitative evaluation of these Scatchard analyses is not possible because insufficient information is given by Edmondson and

---

* This could be only for one analog; see discussion of LF binding to apoflavodoxin below.

Tollin (28) to calculate the total apoprotein or total flavin concentration. Even so, some aspects of the Scatchard analysis for LF binding seem questionable. The first concerns the discrepancy between the equilibrium constant for LF binding (2.2×10^5 $\underline{M}^{-1}$) reported by Edmondson and Tollin (28) and the value (1.3×10^5 $\underline{M}^{-1}$) calculated from the slope of the line they drew through their data points. While the difference between 1.3 and 2.2×10^5 $\underline{M}^{-1}$ affects the binding free energy by a mere 0.4 kcal/mole, it causes about a two-fold error in binding enthalpy (about 6 kcal/mole) measured in the subsequent two-temperature thermodynamic analysis of Barman and Tollin (33). The second questionable aspect relates to their method of measuring the relative concentrations of free and bound LF. The molar absorptivity for bound LF, $\epsilon_{LF}^{complex}$, was determined when a five-fold excess of apoprotein was added to a solution of LF. This $\epsilon_{LF}^{complex}$ was then used with the flavin absorbance differences observed when apoprotein additions were made to a solution of LF to determine the equilibrium concentrations of free and bound LF. Because of the low affinity of A. vinelandii apoflavodoxin for LF, it is probable that in the presence of a five-fold excess of apoprotein, a significant portion of the LF is in fact not bound. This would affect the measured concentrations of free and bound LF, the Scatchard plot, and the calculated K_a. Lastly, two of the five points in the Scatchard plot for LF are shown to have $1-\alpha$ values of about 0.90 and 0.99. Because absorbance spectroscopy was used, the total concentration of LF used in this

titration must have been $\gtrsim 10^{-5}$ M, and therefore > K_d. Under these conditions 1-α values of 0.90 and 0.99 would not be expected unless the molar excess of apoprotein over LF were at least eight-fold and about one hundred-fold respectively, although the largest excess anticipated from their stated methodology is five-fold.

Barman and Tollin (33) extended the equilibrium binding studies with A. vinelandii flavodoxin, reporting equilibrium constants but not the Scatchard analyses used to obtain them. Equilibrium constants at 24° for the binding of deaza FMN, deaza RF, and $RFSO_4$ were reported. In addition they reported equilibrium constants for the binding at 10° of FMN, RF, and LF and remeasured the values at 24° for FMN and RF (the latter agree well with the values given by Edmondson and Tollin (28)). Using two point van't Hoff plots, Barman and Tollin (33) attempted to determine the entropies and enthalpies of binding for each derivative*. In view of the well documented examples where such plots are non-linear (34), it is disconcerting that Barman and Tollin (33) studied the binding of each derivative at only two temperatures and assumed the van't Hoff plots would be linear.

Edmondson and Tollin (28) and Barman and Tollin (33) studied the kinetics of binding of flavin analogs to A. vinelandii apoflavodoxin, but it is difficult to know the meaning of much of their stopped-flow and temperature-jump experiments. In view of the aberrant

---

* They did not redetermine the equilibrium constant for LF binding at 24°, instead they used the value given by Edmondson and Tollin (28).

Scatchard plots, it is evident that they could not know the concentration of binding sites in these experiments, yet accurate knowledge of reactant concentrations is of paramount importance in analyzing their kinetics. Thus, on mixing solutions of flavin and apoprotein, ostensibly of equivalent concentration, it is remarkable that linear second order plots were obtained. The rate constants determined from temperature-jump relaxation experiments for the binding of RF and LF in their respective reconstituted holoproteins are likewise subject to considerable error because of this consideration.

The qualitative behavior of these relaxation experiments should be unaffected by uncertainties in the concentration. A truly remarkable difference was found between relaxation experiments using native A. vinelandii flavodoxin (FMN holoprotein) in comparison to the same experiments using holoprotein reconstituted with RF or LF. When subjected to a jump in temperature, the RF and LF reconstituted holoproteins show an increase in fluorescence described by a single exponential, whereas native flavodoxin exhibits biphasic fluorescence behavior: first a rapid decrease (concentration independent) in fluorescence, then a slow increase (concentration dependent) to a level of total fluorescence approximately equal to that which was present before the jump in temperature. Barman and Tollin (33) stated that adequate control experiments had been performed to show that the second relaxation occurring in the native flavodoxin experiments had rates considerably faster than the cooling of the sample cell. They

concluded that the binding of the non-phosphorylated analogs occurred essentially by a one step process (Equation (1)), while binding of FMN involved at least an additional step which they interpreted to be a conformation change occurring subsequent to the second order step of complexation (Equation (3)).

Riboflavin Binding Protein (RBP)

In separating the proteins from the egg whites of the Rhode Island Red chicken using cellulose ion exchangers, Rhodes, Azari, and Feeney (35) isolated a flavoprotein with isoelectric point about pH 4.2. The flavin in this flavoprotein was neither fluorescent nor dialyzable above pH 4, but became both fluorescent and dialyzable at pH values below 4. The flavin dissociated in acid was found to be riboflavin, hence the name riboflavin binding protein. Riboflavin binding proteins have since been found in the yolk of avian eggs and in the serum of birds. These proteins appear to function as transport and storage proteins for riboflavin (36), but no enzymatic function for them is known. Genetic studies have been performed using a mutant Leghorn strain which is unable to produce a protein with flavin binding capacity (37, 38).

Rhodes, Bennett, and Feeney (39) found that under normal dietary conditions half of the total RBP in egg white existed as the flavoprotein and half as the apoprotein. The last steps in their isolation procedure involved the adsorption of the crude flavoprotein-apoprotein onto a carboxymethyl cellulose column at pH 3.5. The flavin

was removed by eluting the column with buffer at pH 3.5. The apoprotein consisted of two separable fractions - one eluting at pH 4.3 and the other at pH 4.5. The two apoprotein fractions were present in egg white in about equal amount and had equal specific flavin binding capacity based on total nitrogen. Recombination of RF with either apoprotein fraction at pH 4.5 gave flavoprotein which was non-fluorescent and non-dialyzable, and which had an absorption spectrum in the flavin region similar to that of the crude flavoprotein-apoprotein. Preliminary experiments suggested the two apoprotein fractions differed in phosphate content; the fractions eluting at pH 4.3 and pH 4.5 respectively, containing 8 and 7 phosphate groups per mole based on a molecular weight of 32,000. Both apoRBP fractions contained carbohydrate and mixtures appeared homogeneous by ultracentrifugal and moving boundary electrophoretic analyses.

Phillips (40) reported molecular weights for Leghorn egg white RBP of 31,800 based on sedimentation equilibrium studies and 31,000 based on RF binding capacity. He also found 7 moles phosphorus and about 30 moles carbohydrate per 31,800 g of this RBP. The flavin binding proteins from both Rhode Island Red and Leghorn chickens appeared similar in composition and physical properties. Disc gel electrophoresis of the Leghorn RBP preparation revealed the presence of small amounts of either high molecular weight or low mobility contaminants. Phillips (40) reported that the relative amount of these

contaminants increased if exposure to light was not minimized during the isolation of RBP.

Farrell, Mallette, Buss, and Clagett (37) determined the amino acid content of RBP and found 16 cysteine residues but no free sulfhydryl groups per 32,000 g RBP. Phillips (40) found that treatment of RBP with mercaptoethanol in 8 M urea followed by alkylation with iodoacetamide derivatized the protein and apparently split it into two subunits. Both subunits were isolated and the larger derivatized polypeptide had a molecular weight of 24,000 determined by sedimentation equilibrium. Treatment of RBP with 8 M urea or 5 M guanidine HCl did not split the protein into subunits. Thus the mercaptoethanol and iodoacetamide treatment appeared to reduce 8 disulfide bonds and dissociate two subunits not connected by a peptide bond. Neither subunit was able to rebind flavin. Recently Cotner and Clagett (41) indicated that under slightly different preparatory conditions the larger alkylated subunit had full flavin binding capacity (1 mole RF bound/mole subunit).

Rhodes et al. (39) studied the affinity of apoRBP for some flavin analogs and found that all these analogs had their fluorescence quenched by binding to apoRBP, but more than 1 mole of apoRBP per mole flavin was required to achieve complete fluorescence quenching. Equilibrium constants were not directly measured; instead, the affinity of apoRBP for the analogs was compared relative to the affinity for RF. Many of the flavin analogs were inactive in the

microbiological assay. Thus when a) the analog and RF were added to apoRBP, b) the mixture was dialyzed, and c) a portion of the dialysate which passed through the dialysis bag was used to grow bacteria, the amount of RF displaced by the analog could be assayed and related to the relative binding of analog and RF (Table V). Although the equation used by Rhodes et al. (39) may have been in error (See Appendix A, Part II), their conclusion that RF was bound with greater affinity than any of the other analogs is unaffected. Although FMN and FAD could not be tested by the above method because of their microbiological activity, apoRBP was found to have greater affinity for RF than for FMN or FAD. This was shown by dialyzing the holoproteins reconstituted with FMN or FAD against a solution of RF where the ratio of the total molar amount of RF to the total molar amount of protein was $\geq 1 : 1$. The holoRBP obtained after dialysis was found to contain only RF.

Nishikimi and Yagi (42) measured the changes in visible RF absorbance which accompanied binding to apoRBP. Maximum visible absorbance for bound RF occurred at 455 nm and had an absorptivity of 1.1×10^4 $\underline{M}^{-1} cm^{-1}$ based on a free RF absorptivity of 1.25×10^4 $\underline{M}^{-1} cm^{-1}$ at 455 nm. The visible circular dichroism spectrum of RBP had a maximum absorptivity difference near 455 and $\epsilon_L - \epsilon_R$ could be calculated to be 7.2 $\underline{M}^{-1} cm^{-1}$ at this wavelength. Phillips (40) extended these circular dichroism studies into the ultraviolet region and found considerable differences between RBP and apoRBP in the

TABLE V

Relative Affinities for the Binding of Some Flavin Analogs to ApoRBP in 0.078 M NaCl and 0.025 M Na Phosphate, pH 7.0, at 2° (39)

Analog	Relative Affinity* of the Analog and RF for ApoRBP
RF	1.00
3 Me RF	0.156
Lyx F	0.060
Gal F	0.049
LF	0.014
3 Me LF	0.015
10 For Me F	0.015
7 Cl, 10 Sorb I A	0.002

* These values were calculated from experiments described above in the text using the equation

$$\text{Relative Binding Affinity} = \frac{\text{ug RF displaced}}{\text{ug RF bound}} \times \frac{\text{total umoles RF}}{\text{total umoles analog}}$$

Rhodes et al. (39) did not give the source or the derivation of this equation; however, the discussion in Appendix A, Part II indicates it may be in error.

190-240 nm region. Between 220 and 240 nm, apoRBP had $\epsilon_L - \epsilon_R$ values much more negative than holoRBP. Negative maxima occurred for holoRBP at 204 nm and for apoRBP at 212 nm, both with values of $\epsilon_L - \epsilon_R$ about -500 $\underline{M}^{-1}cm^{-1}$.

Some protein modifications of RBP affect flavin binding. Rhodes et al. (39) observed flavin binding capacity was lost on incubation of apoRBP with trypsin and chymotrypsin and RF was dissociated from RBP in 8 M urea. However, flavin binding capacity was unaffected by heating apoRBP to 100° for 15 minutes (0.05 M Tris, pH 7.0). Farrell et al. (37) found that neither iodination of RBP with a two-fold excess of reagent necessary to diiodinate all the tyrosyl residues, nor alkylation with 1-tosylamido, 2-phenylethylchloroketone in 10-fold excess necessary to react all the histidine residues affected the binding capacity of RBP. However, they observed that reaction with H_2O_2 decreased binding capacity. Farrell et al. (37) stated "At a ratio of 2 moles of H_2O_2 per 8 moles of tryptophan in the protein, 90% of the flavin binding capacity was lost," although this stoichiometry was not apparent from their data. Their Figure 2 indicated 90% loss in flavin binding capacity occurred after addition of 6 μmoles of H_2O_2 to 0.083 μmoles of protein; that is, 72 moles H_2O_2 per mole RBP or 9 moles H_2O_2 per mole tryptophan in the protein. Tryptophan was oxidized as monitored by the decrease in absorbance at 280 nm and increase in absorbance at 340 nm (oxidized indole). Nevertheless, H_2O_2 is a relatively non-specific oxidant and the high molar excess of

H_2O_2 to protein needed for inactivation does not preclude the possibility that the loss of binding capacity corresponded to the oxidation of another group(s), e.g. disulfides (43). Guanidine·HCl, 5 M, dissociated the flavin from RBP and the effect was found to be reversible.

Physical and chemical studies on an RBP from egg yolk have been performed and indicate that this protein (of 36,000 molecular weight) is similar to the egg white RBP but differs slightly in phosphate composition and relative amino acid distribution (44-46). Preliminary results of flavin binding studies using egg yolk RBP were reported at the Konstanz Conference on Flavins and Flavoproteins, 1972 (47). The stoichiometry of binding was 1 mole RF per mole apoprotein. At 25° and pH 7 the values of K_a, k_1, and activation energy for RF binding were 3.3×10^8 M^{-1}, 4.6×10^7 $M^{-1}sec^{-1}$, and 3.5 kcal/mole, respectively.

RESEARCH OBJECTIVE

The aim of the present investigation is to undertake a detailed thermodynamic, kinetic, and spectroscopic analysis of the binding of flavin analogs to egg white apoRBP. This protein was chosen for study because its apoprotein bound a variety of flavin analogs (with quenching of fluorescence) tested in a preliminary study (48). Because of its high affinity for uncharged flavin derivatives, RBP provides an excellent system on which to study the interaction between the isoalloxazine moiety of flavin and the protein site. That RBP is

cheaply and easily purified in gram quantity and is exceptionally stable with respect to binding are additional favorable qualities. Insofar as RBP has a flavoprotein semiquinone absorbance spectrum (42, 49) and free radical electron paramagnetic resonance (EPR) signal (42, 49) characteristic of flavoproteins with blue semiquinone spectra (50), it is hoped that the studies of flavin-protein interactions in RBP may serve as a model for flavin binding in dehydrogenase flavoenzymes.

During the early stages of this research, it became evident that fluorimetric equipment was mandatory in order to perform the necessary equilibrium and kinetic flavin binding studies. To assure the continued availability of an instrument with sufficient sensitivity and to gain shop experience, I designed and constructed, with the aid of Dr. David Ballou, an inexpensive, dual-purpose fluorimeter capable of both static and stopped-flow operation. The details of construction and evaluation of this instrument are found in Chapter 2.

CHAPTER 2

A FLUORIMETER CAPABLE OF BOTH STATIC AND STOPPED-FLOW OPERATION

FLUORIMETER CONSTRUCTION AND ASSEMBLY

The components of the fluorimeter are outlined in Figure 2. To make their description easier, components have been classed into three groups. Group I concerns the production, stabilization, and selection of the light used to excite the fluorescence. Group II comprises those components affecting the sample and its fluorescence emission: modules positioning the sample, equipment controlling sample temperature, and filters selecting the emission passband to be observed. Group III contains the electronic units detecting, amplifying, measuring, and recording the fluorescence signal. Following the details of construction and assembly of the fluorimeter is an evaluation of its performance.

Group I Components: Excitation

A Sorenson A. C. voltage regulator, model ACR 1000, regulates the line voltage, nominally 115 VAC but subject to excursions as great as +3%. The output from this device, adjustable between 110

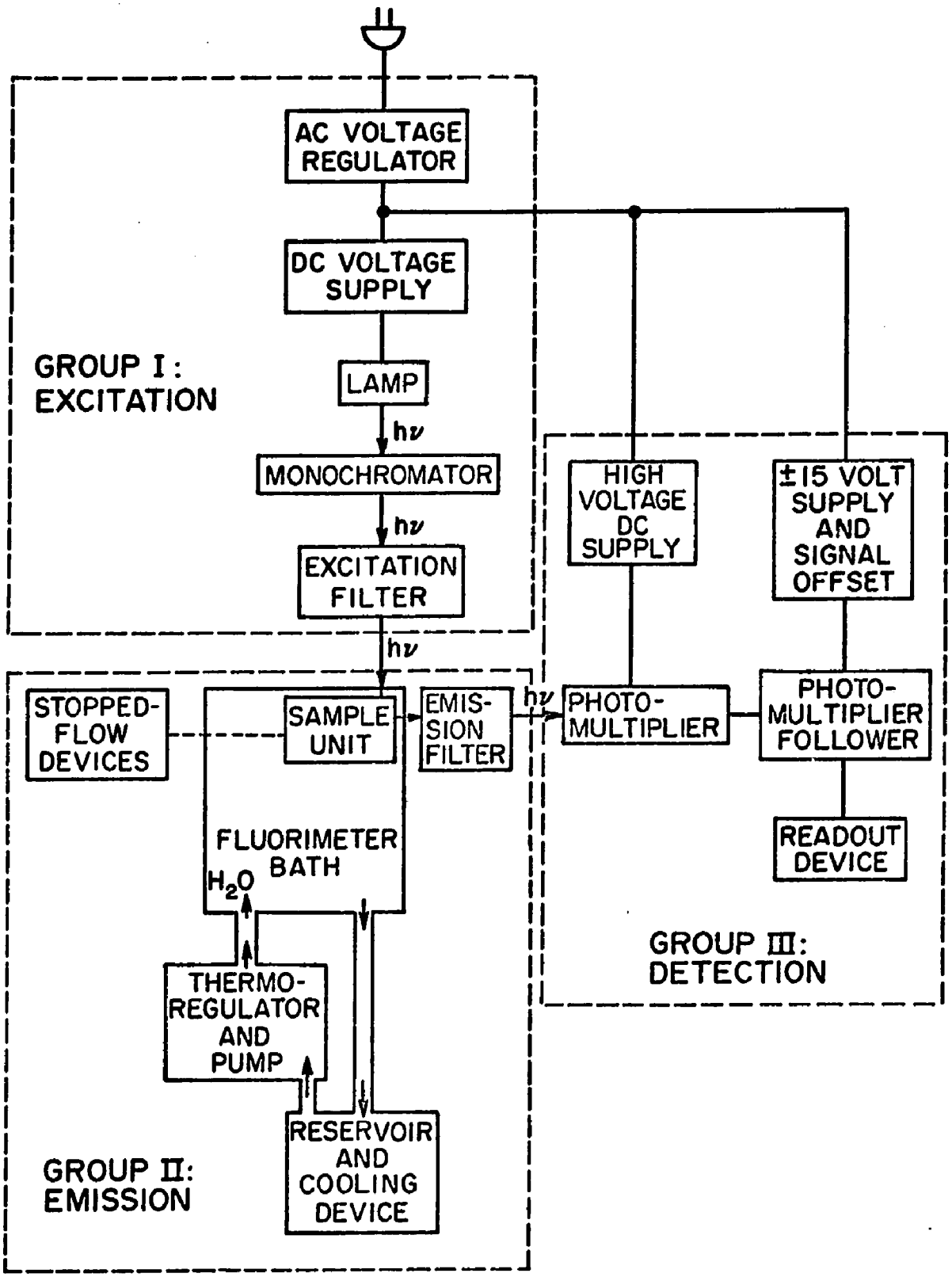

Figure 2. Fluorimeter Components

and 120 VAC, is specified as constant to 0.1% under load and line changes to 10%.

Figure 3 shows a wiring diagram for the homemade D.C. voltage supply powering the lamp. A solid state bridge rectifier converts the regulated A.C. voltage to D.C. and a twin LC smoothing circuit reduces output ripple to less than 0.1%. The rectifier, inductors, and capacitors are mounted on an aluminum chassis base and enclosed in an expanded metal cage. All circuitry and components can carry 10 amps, thus the supply is capable of providing a kilowatt of power. Note that this device supplies approximately +55 V.D.C. and -55 V.D.C. with respect to earth ground. No attempt should be made to establish either output lead as common to earth ground without installing an isolation transformer before the D.C. supply.

The lamp used as the source of radiation for the fluorimeter is a 500 watt narrow-filament, tungsten-halogen lamp, Sylvania 500 Q/CL, screwed into a Sylvania S-4 Mini-Can base and mounted in a modified 35 mm slide projector, TDC Vivid model Mainliner 300. The lamp base is fastened to a slotted plate providing front-to-back lamp adjustment and this lamp assembly replaces the corresponding items originally in the projector. The remainder of the lamp positioning device, heat filter (which rejects radiation of wavelength longer than 800 nm, while transmitting > 80% of the radiation between 350 nm and 620 nm), spherical mirror, and collimating lenses of the projector are retained, while the slide changer, focusing assembly, small fan,

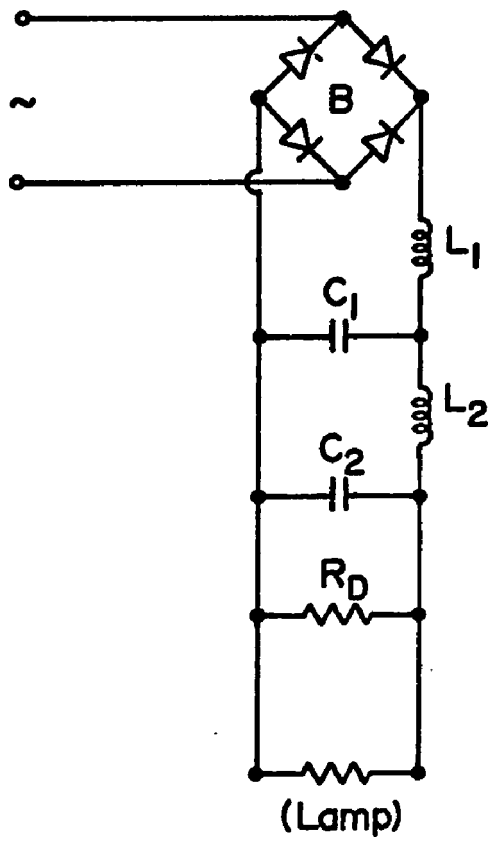

Figure 3. D.C. Lamp Power Supply

B = Motorola bridge rectifier, MDA 962-5; $C_1 = C_2 = 6000$ μfarad, Computamite capacitors, FAH 602-150; $L_1 = L_2 = 0.010$ henry, Stancor inductors, C 2688; $R_D = 22\ k\Omega$, safety discharge resistor. All components are available from Allied Electronics.

and original lamp wiring are removed. An aluminum tube and plate are attached to the front of the projector to prevent light from leaking sideways into the eyes of the experimenter. The projector stands on an aluminum chassis box 5" x 6" x 9" which contains a fan for forced air cooling. The fan, a 19 watt Pamotor model 4500A, fastened inside the rear-facing end of the box, draws air in through a hole cut from the box end and covered with a 1/4" mesh screen. A hole cut from the box top permits a constant stream of forced air to circulate gently around the lamp and heat filter, eventually exhausting out of the top of the projector through louvres.

A Jarrell Ash monochromator model 82-410 selects the wavelength region used to excite the sample fluorescence (or to characterize fluorescence emission). This monochromator is equipped with two gratings of dispersion 1.65 nm/mm and 3.3 nm/mm blazed at wavelengths 300 nm and 600 nm. In conjunction with easily changed slits of widths 0.15, 0.5, 1, 2, and 5 mm, sufficient variability in bandwidth selection is available to obtain fluorescence emission and excitation spectra, as well as to perform the thermodynamic and kinetic studies described in this thesis.

Under conditions demanding that stray light be reduced below the 0.2% value specified for the monochromator (e.g., for extremely dilute flavin solutions where the small amount of scattered stray light in the emission passband would exceed the flavin fluorescence), an interference filter (Baird Atomic #11-92-7) is used in series with the

monochromator. This one inch filter of 15 nm half bandwidth centered at 450 nm (transmitting 58% of peak wavelength illumination, while rejecting greater than 99.9% of the radiation outside 3 half bandwidths) is clamped in a mount which can be inserted into the excitation filter compartment on the fluorimeter bath described below.

Group II Components: Fluorescence Emission

The sample is contained in either a standard 10 mm x 10 mm path fluorescence cuvette positioned by a static module or in the reaction chamber of a stopped-flow module, both detailed below. A novel feature of this fluorimeter is the interchangeability of these modules. Figure 4A is a photograph of the fluorimeter bath with the static module clamped in place, while Figure 4B shows the stopped-flow module in place. Attached to the bath can be seen the filter assemblies (A), photomultiplier flange (B), inlet (C) and outlet (D) pipes for bath fluid, and connecting port (E) to the stopped-flow pushing assembly. Figures 5A, B, C, and D are diagrams of the bath assembly. The sample positioning post (detailed in Figure 6) forces the appropriate sample module against the walls of the bath. "O" ring seals in the walls of the bath prevent bath fluid from leaking through the excitation and emission ports drilled through the bath walls. The wall on the emission side of the bath is shown in detail in Figure 7.

Two filter assemblies, one for excitation and one for emission, are attached to the exterior of the bath. Both filter assemblies shown in Figure 5 consist of a compartment which can accomodate 2" x 2"

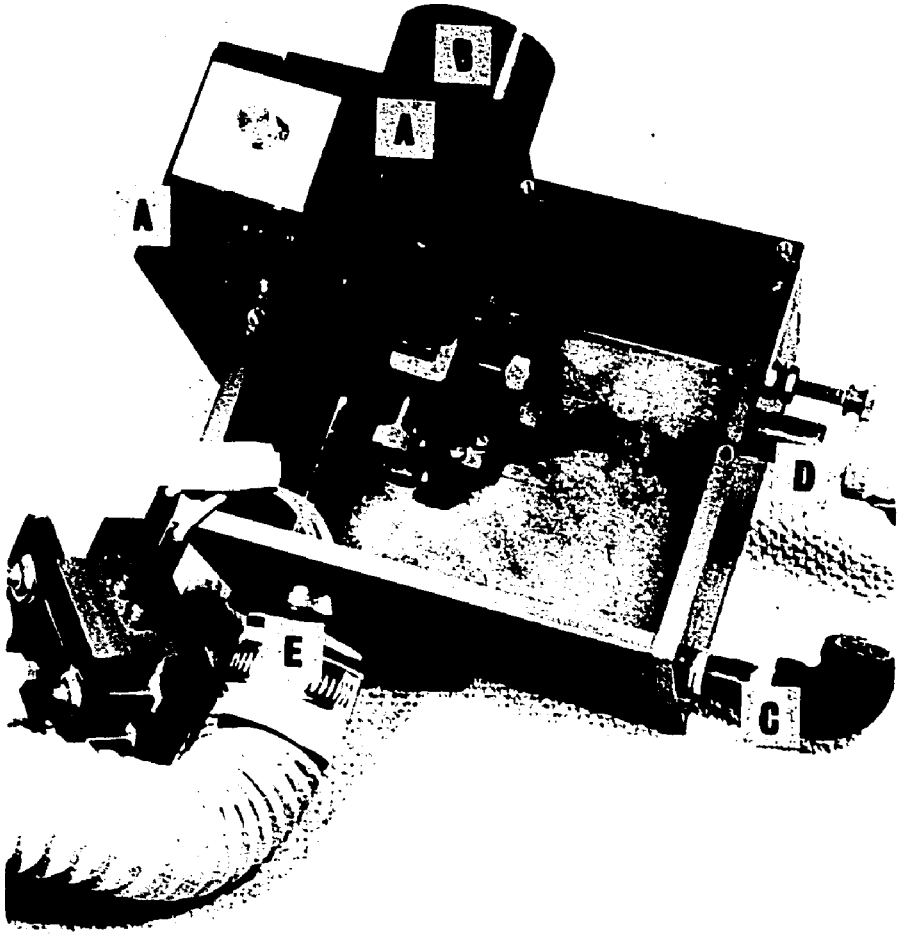

Figure 4A. Fluorimeter Bath in Static Mode
See text for details.

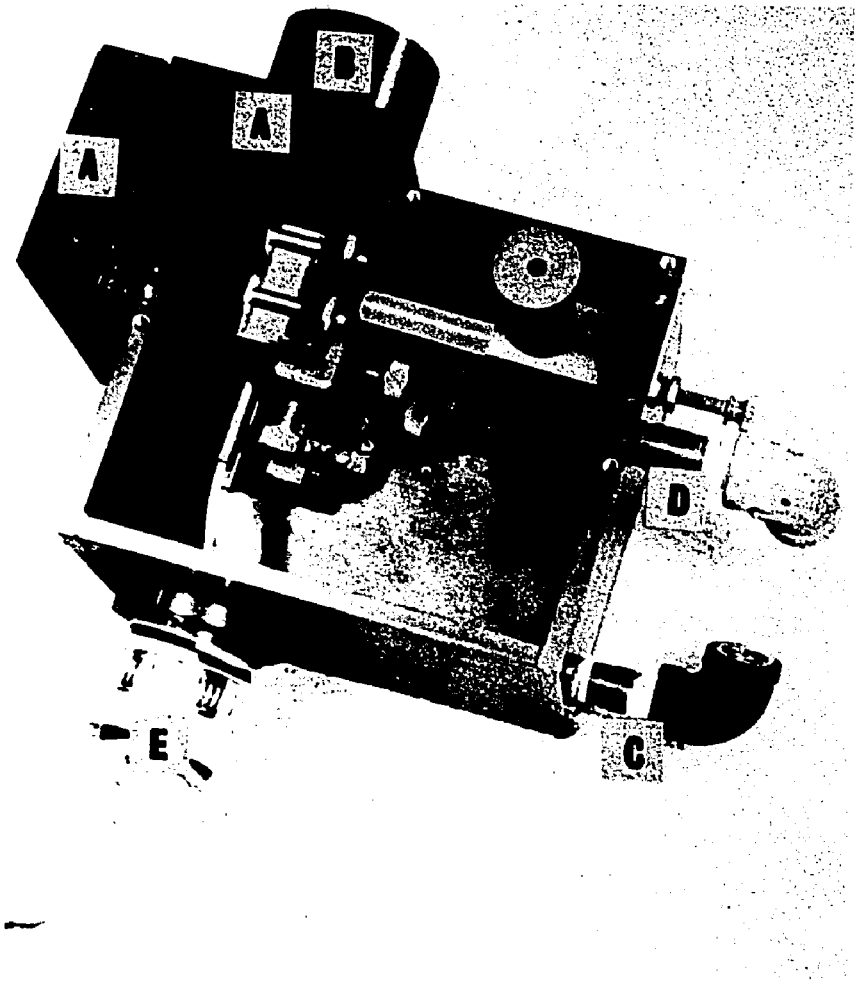

Figure 4B. Fluorimeter Bath in Stopped-Flow Mode. See text for details.

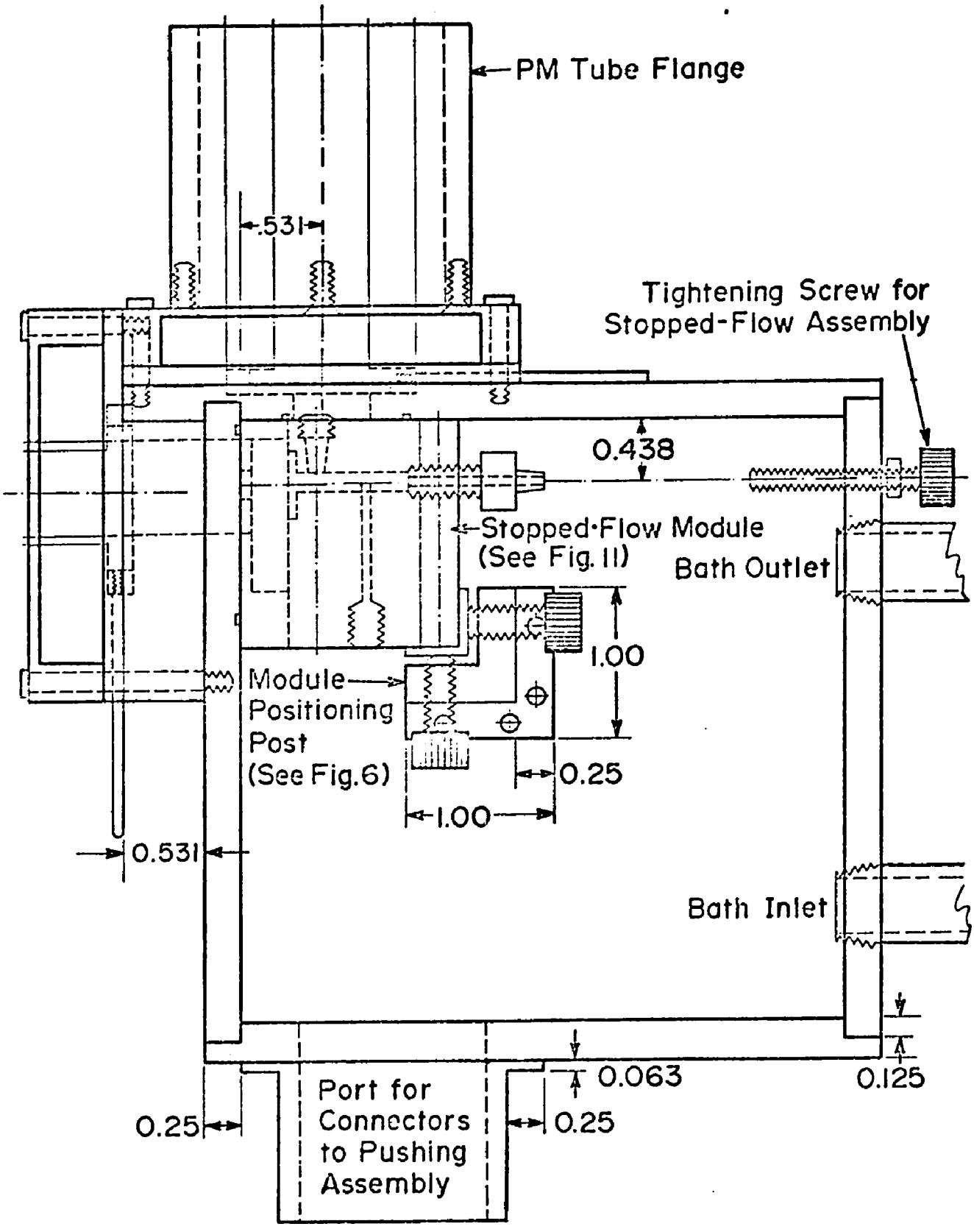

Figure 5A. Fluorimeter Bath - Top View.

All parts areanodized 10-24 aluminum except where noted. The dimensions in all diagrams are in inches except where noted.

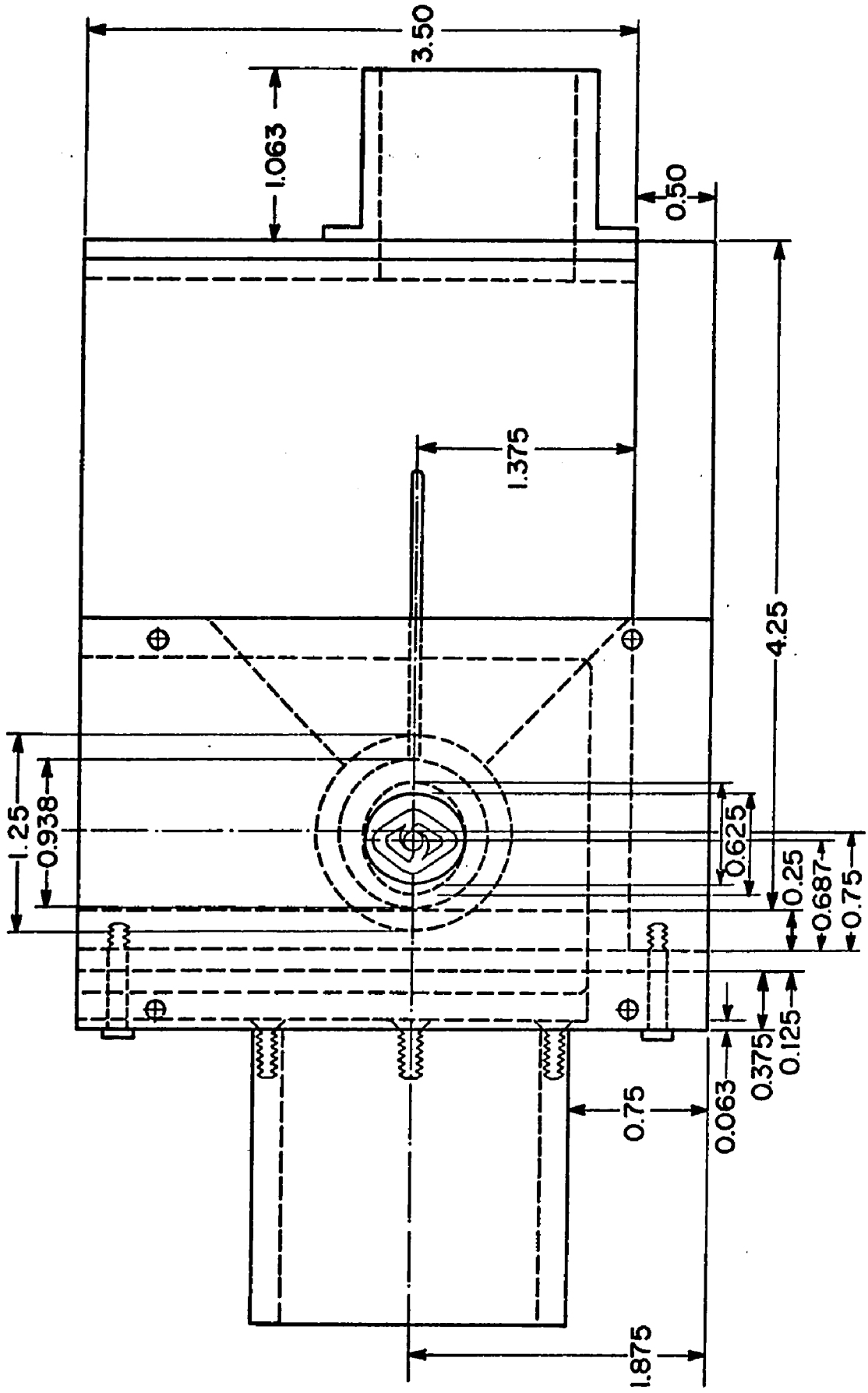

Figure 5B. Fluorimeter Bath - Excitation Side View

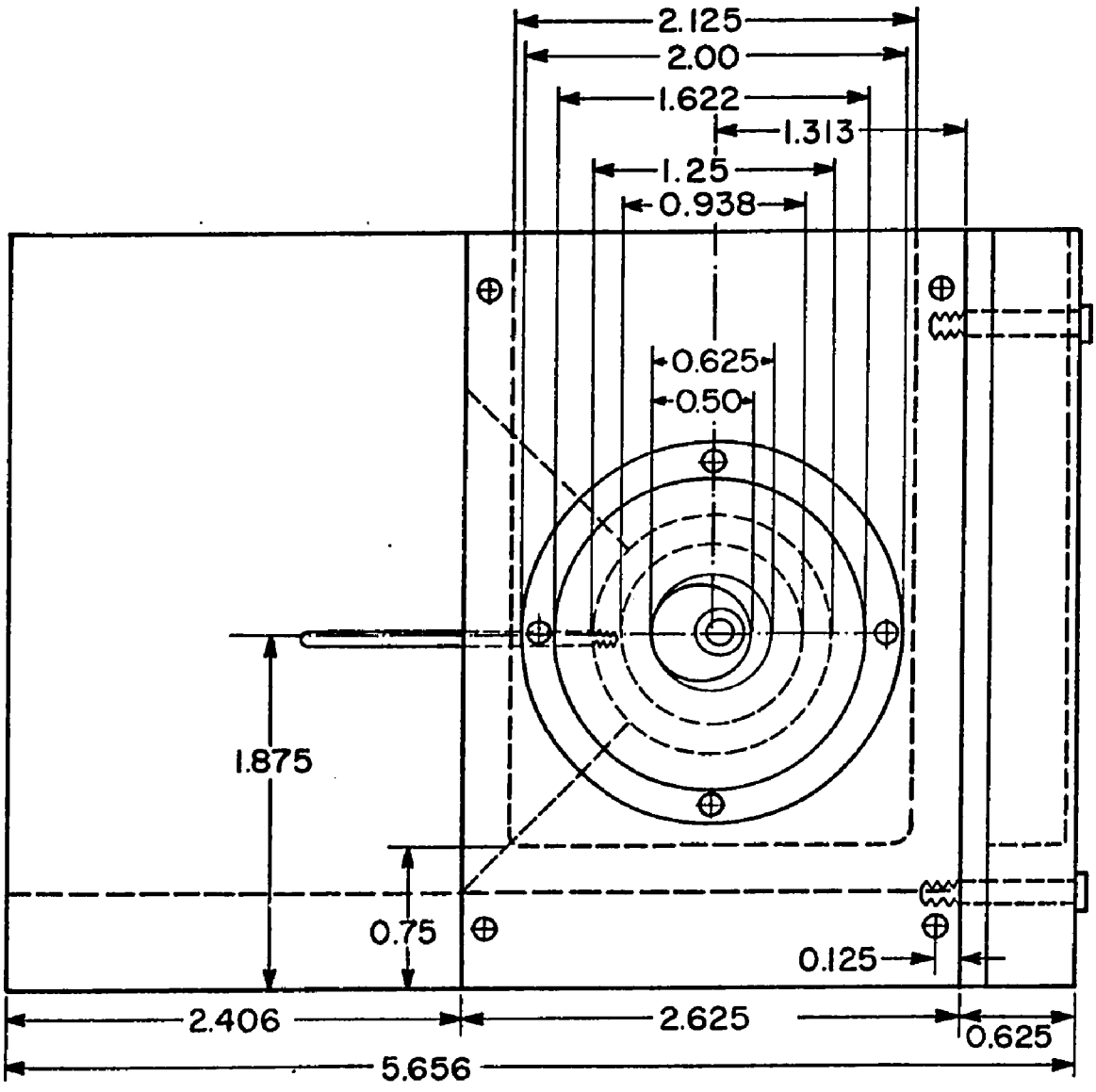

Figure 5C. Fluorimeter Bath - Emission Side View

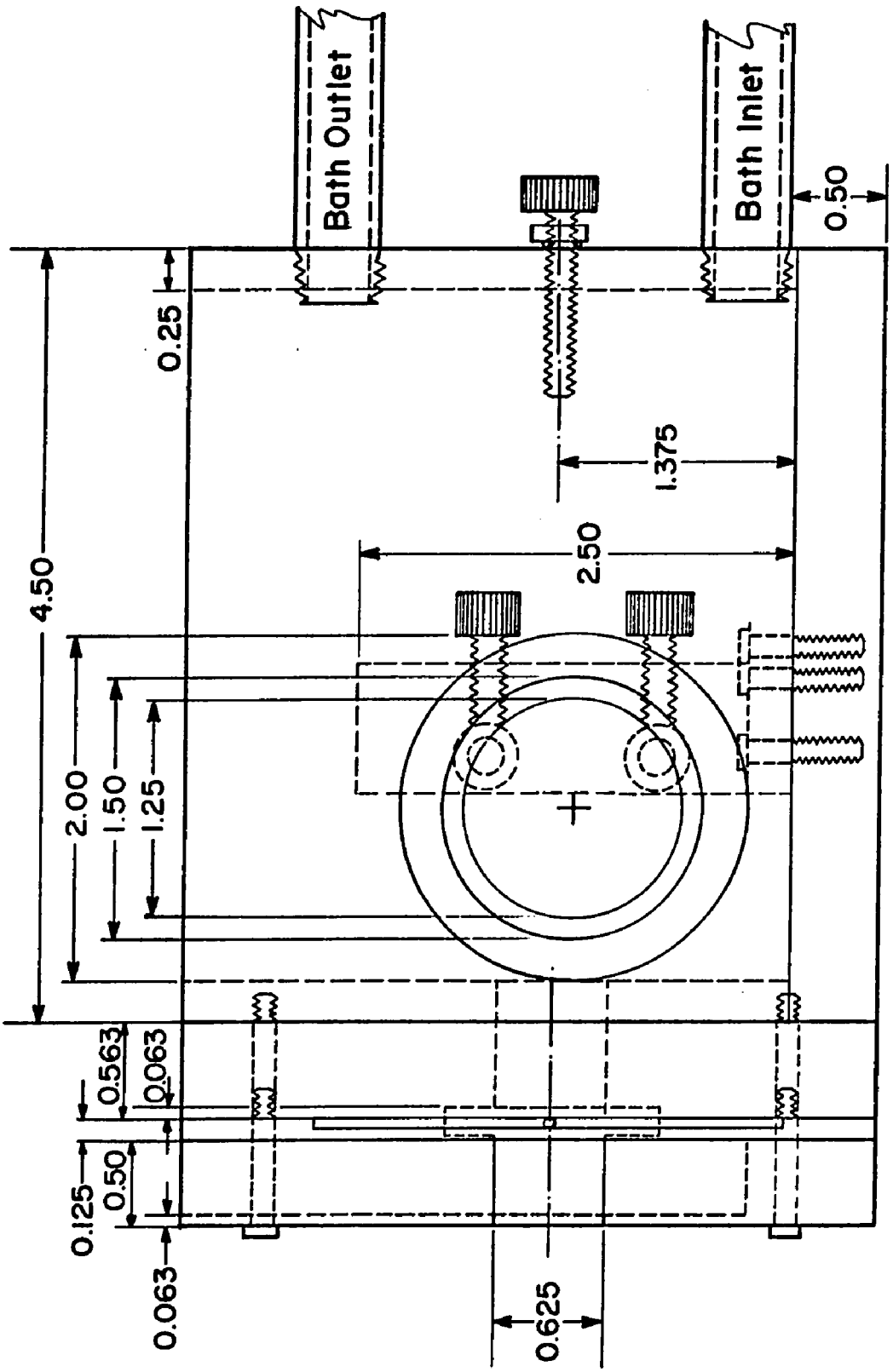

Figure 5D. Fluorimeter Bath - View from Side Toward Pushing Assembly

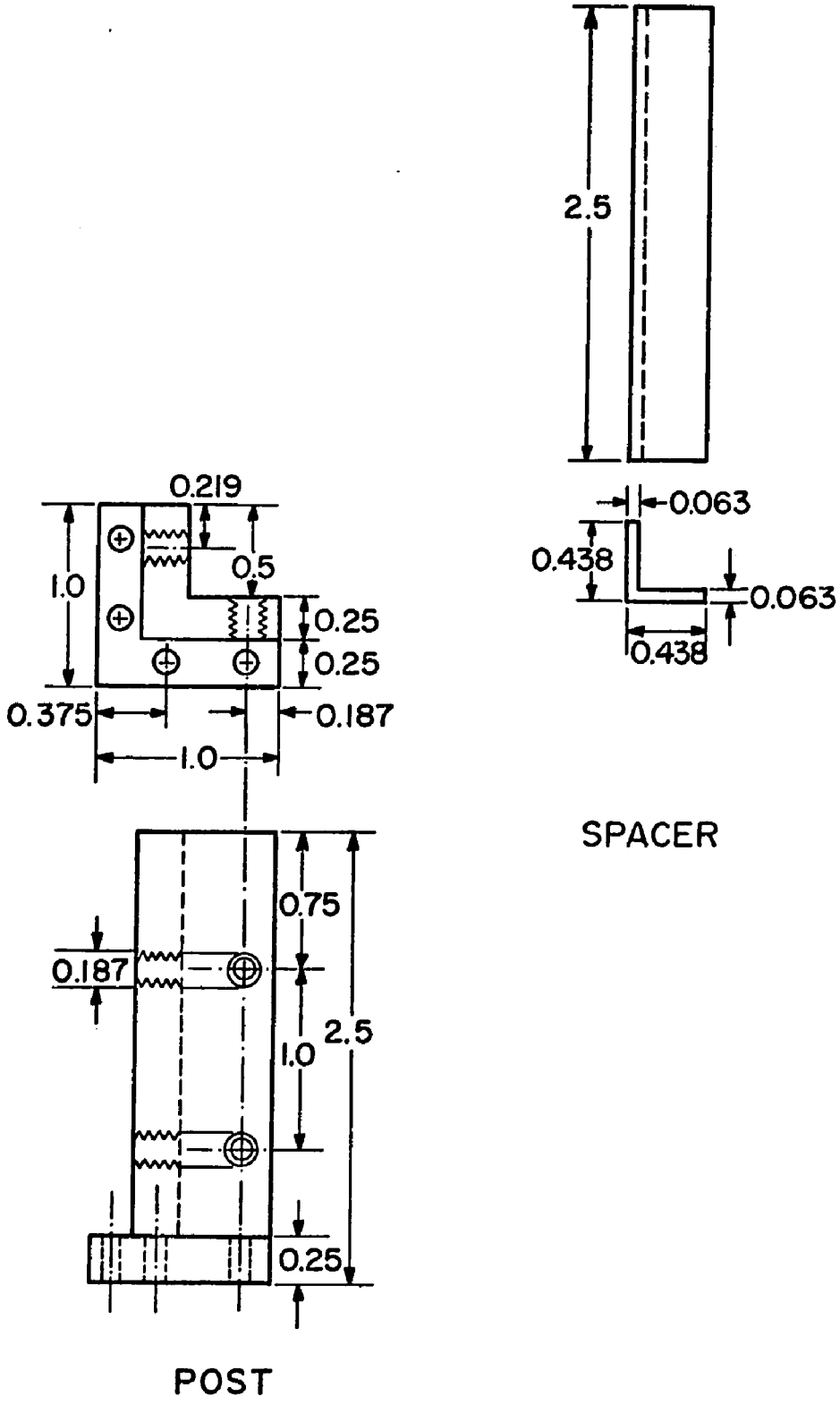

Figure 6. Module Positioning Post and Spacer

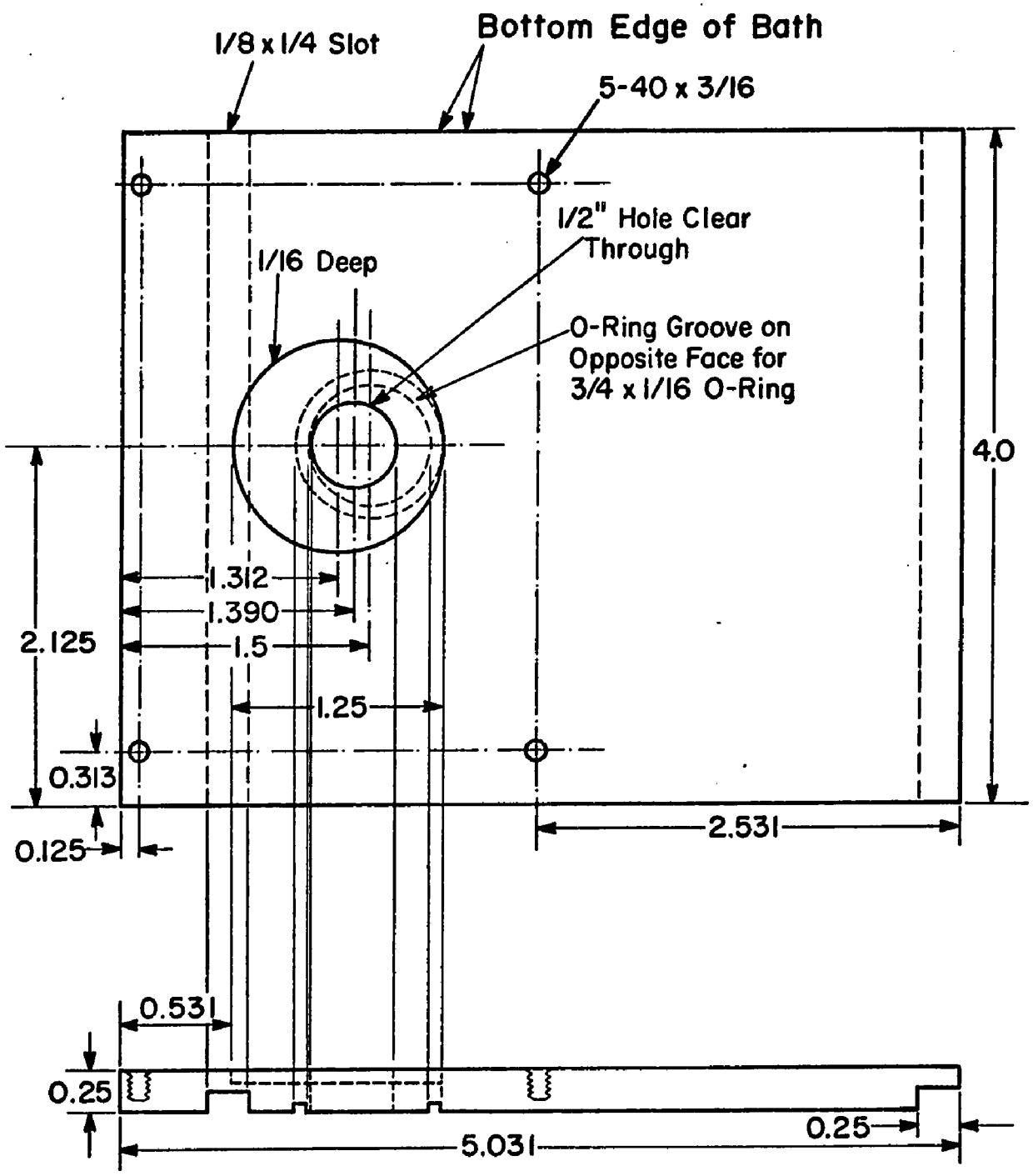

Figure 7. Detail of the Wall on the Emission Side of the Fluorimeter Bath

filters (allowable thickness is 7/16" for excitation and 5/16" for emission) and a plate detailed in Figure 8 containing a circular filter holder rotatable through 90° for polarization of fluorescence studies. (This latter capability has never been tested.) The lids of the filter compartments are not diagrammed. A tubular flange (Figures 4A, B) attached to the emission filter holder positions the photomultiplier housing. Black flocking paper gummed on one side (Edmund Scientific Co.) is glued onto the inside of this flange and is used here and elsewhere to insure light tightness.

From a 5-gallon reservoir (Coleman cooler) located on the floor, a Haake temperature controller and pump Model ED circulates water through rubber tubing into the bath via pipe C in Figure 4. Water drains by gravity from pipe D back to the reservoir. A Jumo 0-50° thermoregulator available from Cole-Parmer Co. is used with the Haake controller to achieve better than 0.05°C temperature constancy, adjustable over the range of 0°-50°C. Because the Haake controls temperature only by intermittant heating, cooling capacity must be provided to obtain temperatures below ambient. This is provided by a) cold tap water circulated through a heat exchanger consisting of 8 feet of 3/16" i.d. copper tubing wound in a coil and submersed in the reservoir, or b) a homemade refrigeration unit consisting of a Bendix-Westinghouse #H25-1-A compressor and heat exchanger, a Singer Controls Company of America #204C expansion valve, a Sporlan Valve Co. Model C-082 Catch-All refrigeration

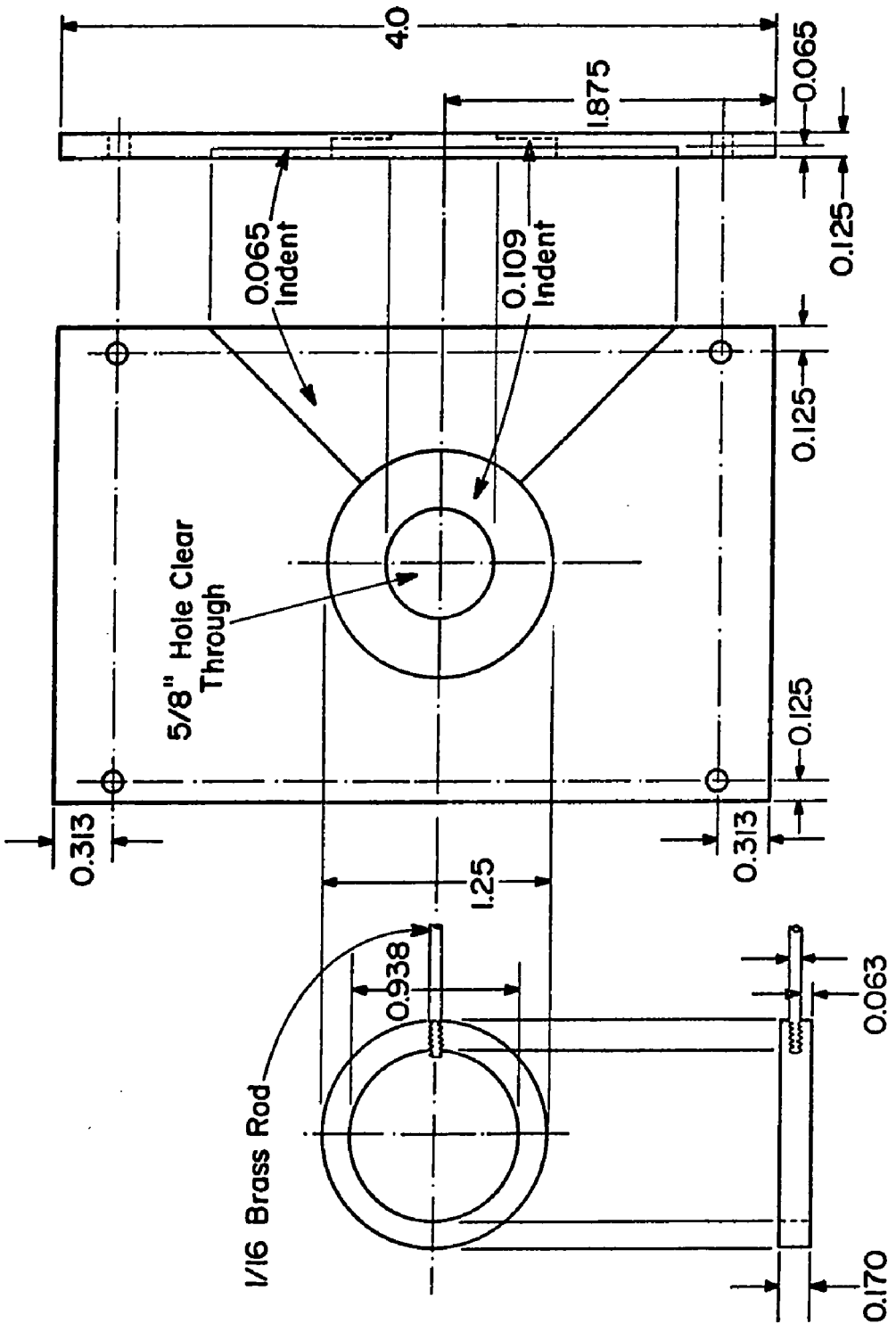

Figure 8. Emission Polarizer Plate and Ring Clamp. The excitation polarizer plate is its mirror image except positioning screw holes are 0.500 from top and bottom.

filter, 20 feet of 1/4" i.d. and 6 feet of 1/2" i.d. copper tubing wound in a coil submersed in the reservoir, and sufficient Freon 12 to fill the system.

In the winter in Ann Arbor, cold tap water is below 8°C and the heat exchanger method can lower the system temperature to 10°C. The refrigeration method is capable of maintaining temperatures below 0° if the reservoir is filled with appropriate antifreeze solution. Bath temperature is monitored using a calibrated Sargent Welch Model S-80210A thermometer.

The two halves of the static module (Figure 9) are cemented with Dow-Corning RTV silastic and clamped together with two stainless steel bolts and nuts. Before cementing the two halves together, small pieces of black flocking paper are placed in milled-out depressions opposite the excitation and emission ports, forming light traps to reduce scattered light.

Figures 10A, B, and C are photographs of the assembled stopped-flow fluorimeter together with detailed photographs of the components. Reactant solutions are forced through polyethylene (PE) tubing using the pushing assembly of Ballou (51). This device uses gas at about 40 p.s.i. in a pneumatic piston (Bimba model 092-D actuated by a Skinner VG-6 solenoid valve) to drive syringe plungers and thus solution through Hamilton Gastight 1001 syringes connected to the two PE tubes. When exhausted, the syringes are easily refilled from reactant reservoirs connected to the syringes by Hamilton

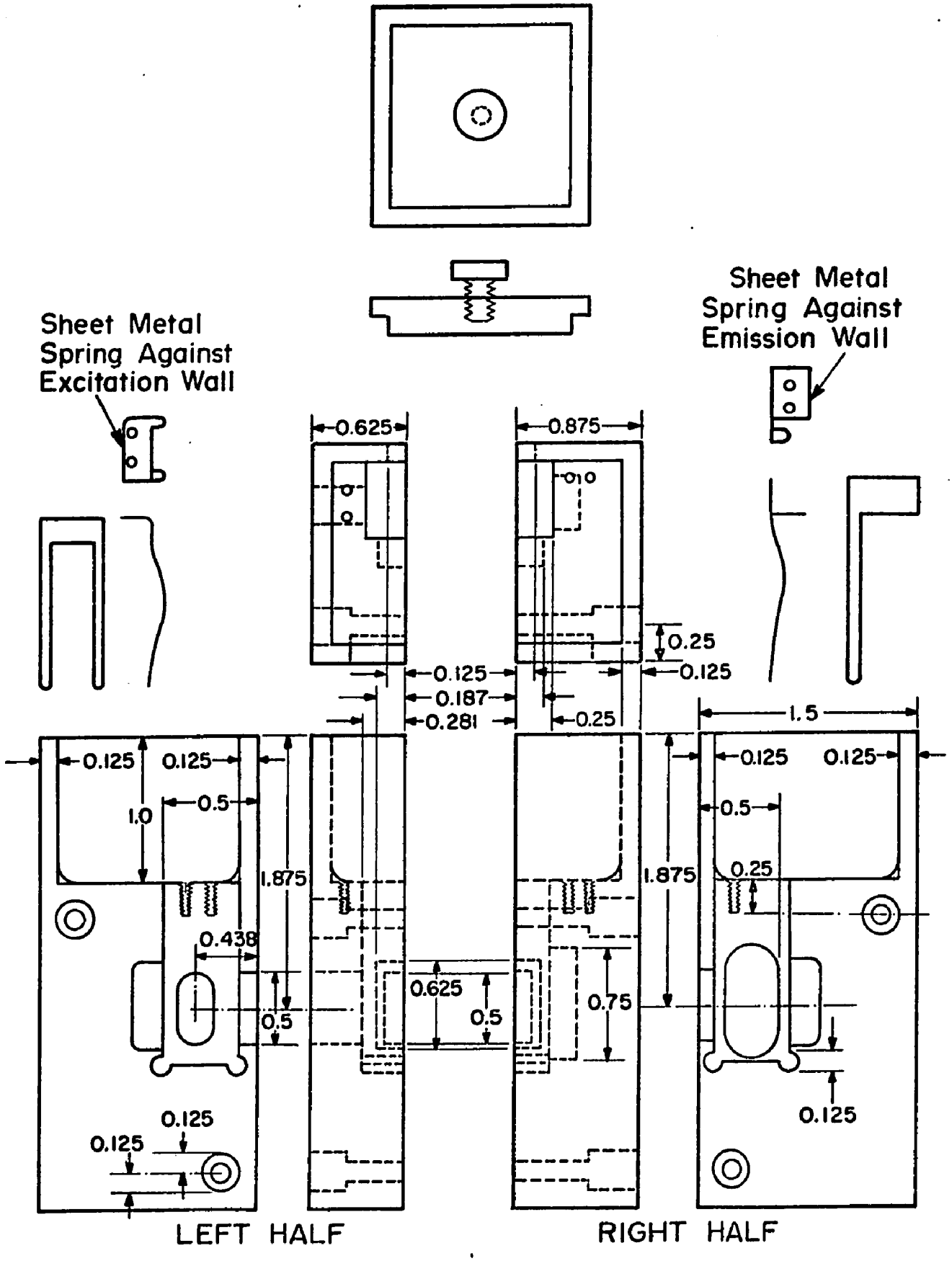

Figure 9. Static Module

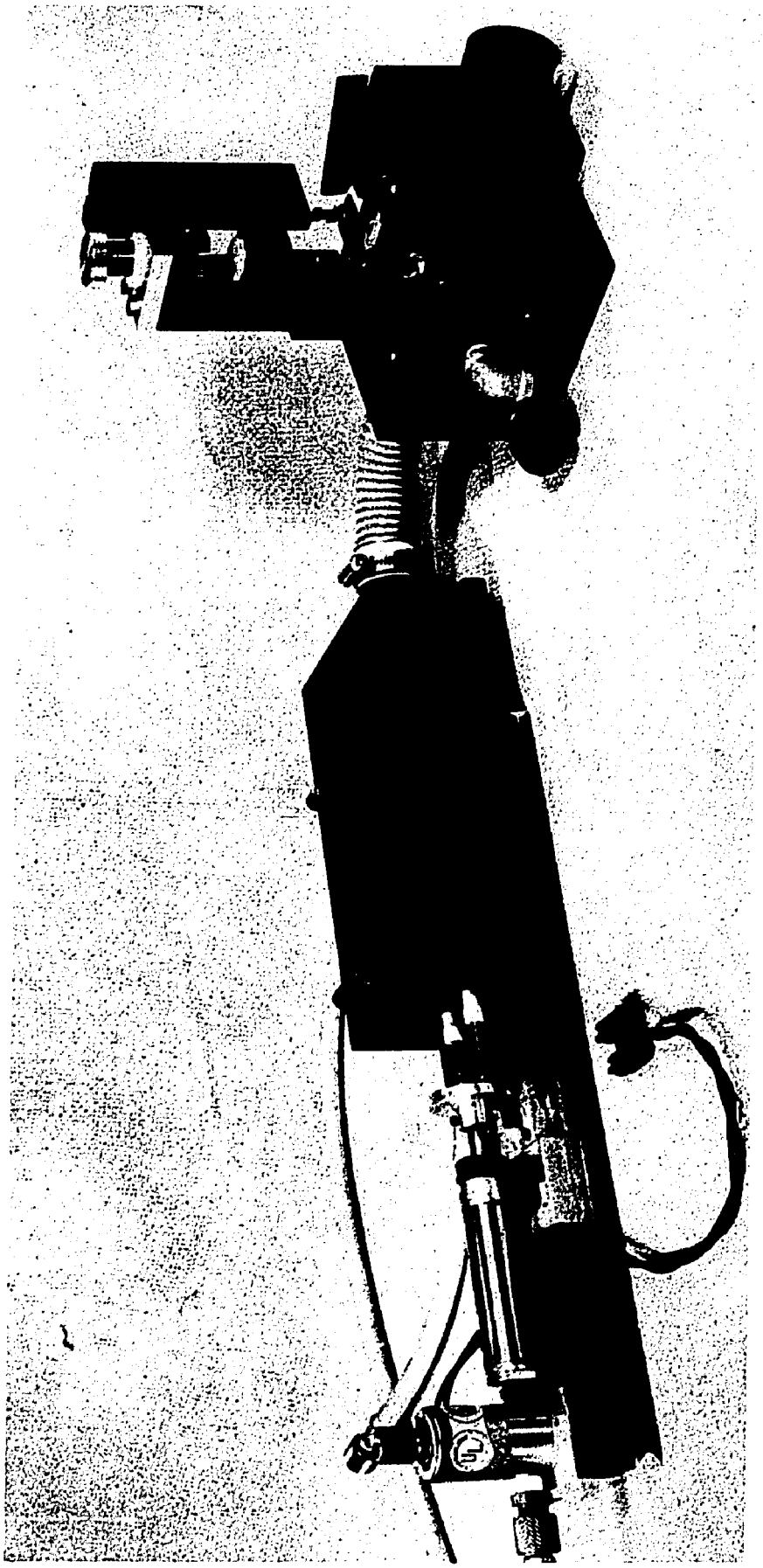

Figure 10A. The Assembled Stopped-Flow Fluorimeter

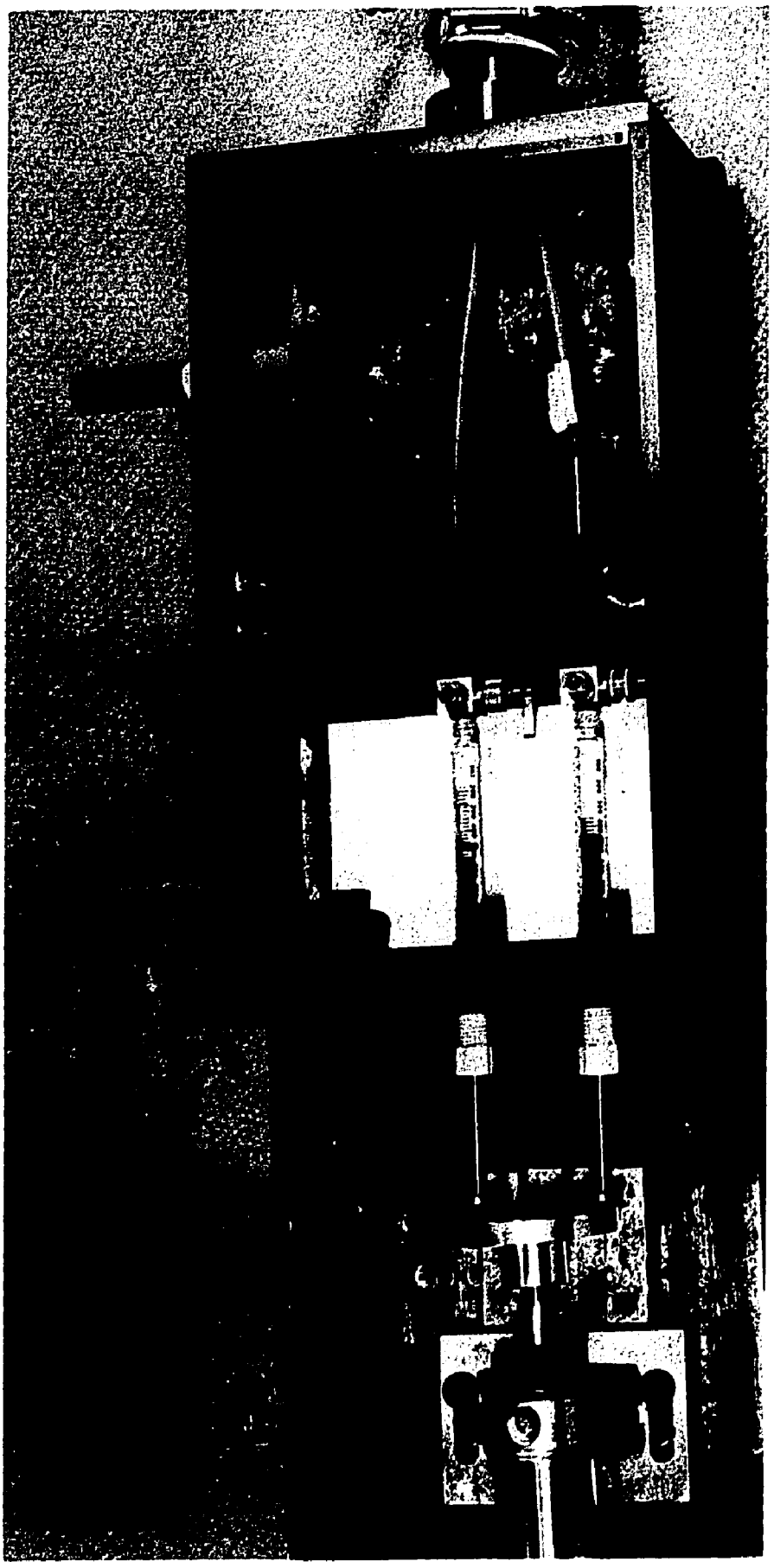

Figure 10B. The Ballou Pushing Assembly

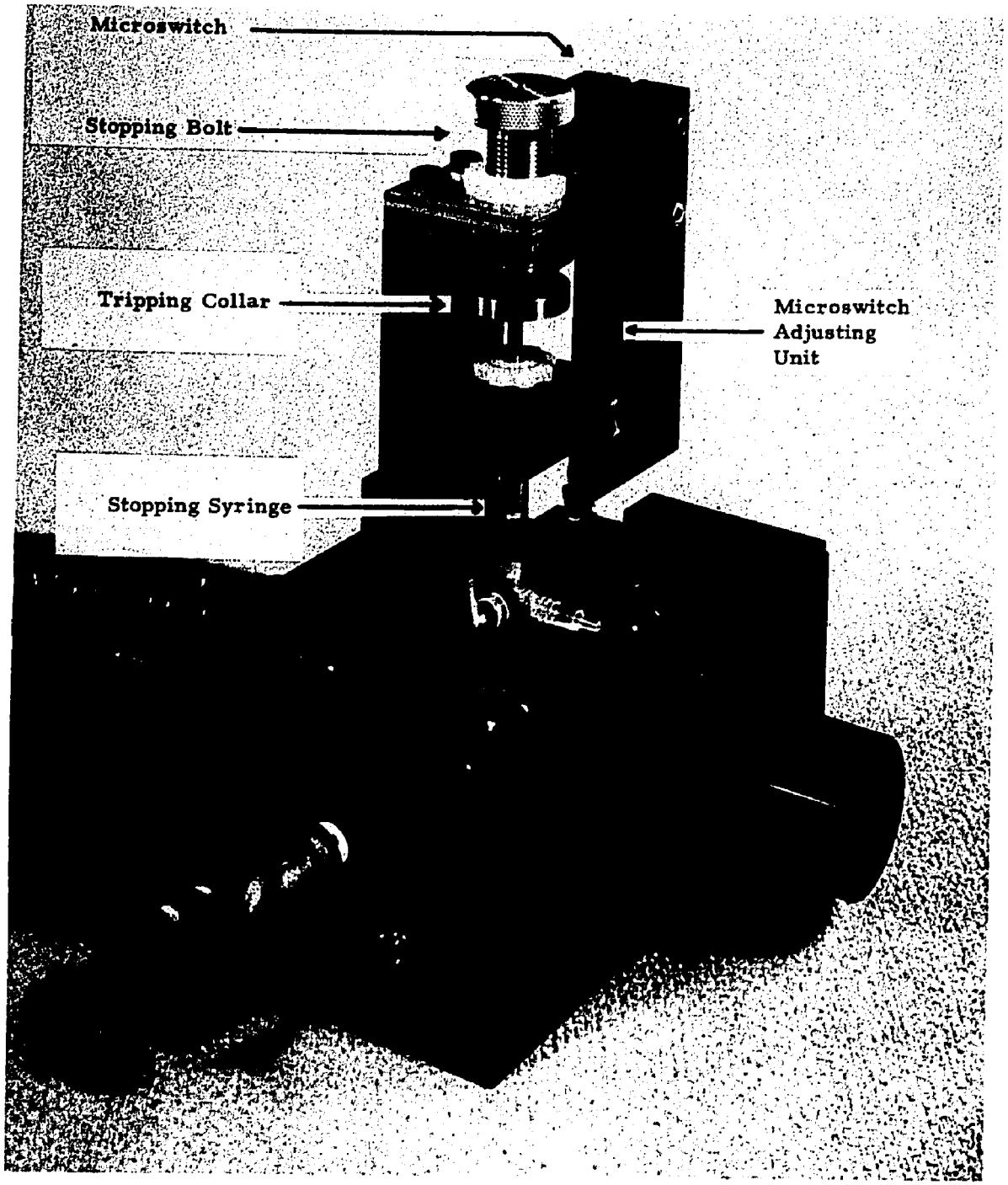

Figure 10C. The Fluorimeter Bath with the Ballou Stopping Assembly Clamped in Place

3MFF3 three-way valves. The syringes, valves, and tubing connections are mounted in a water bath filled by the Haake circulator. The PE tubes are fed through a 1.375" conduit connecting the pushing assembly bath with the fluorimeter bath, and are completely immersed. Proper adjustment of the height of the baths maintains a constant flow of water through the conduit. The ends of the PE connecting tubes are crimped according to the method of Ballou (51) such that the reactants never contact metal. The tubes are held in place between the pushing block and the mixing module by 1/4-28 threaded brass connectors. Similar connectors are made by Chromatronix, Inc.

Components of the stopped-flow mixing module are shown in Figures 11 and 12. A 1/4" thick x 1" diameter quartz plate is pressure fitted against the face of the polyvinylchloride (PVC) mixing block (Figure 11) by a clamping device made of two aluminum plates (Figure 12) and four stainless steel bolts and nuts. A novel feature of this mixing block is the design of the mixer. Extending the original design of Ballou (51), the new mixing block provides for all non-orthogonal channels to be on the face of the block, thus greatly facilitating its manufacture. Reactants enter the mixing block through two holes, make a 90° turn inside the block, and flow towards the quartz plate. Channels milled in the face (detailed in Figure 13) of the mixing block and sealed against the quartz plate divide each reactant stream into two streams and direct them toward the two points of first mixing.

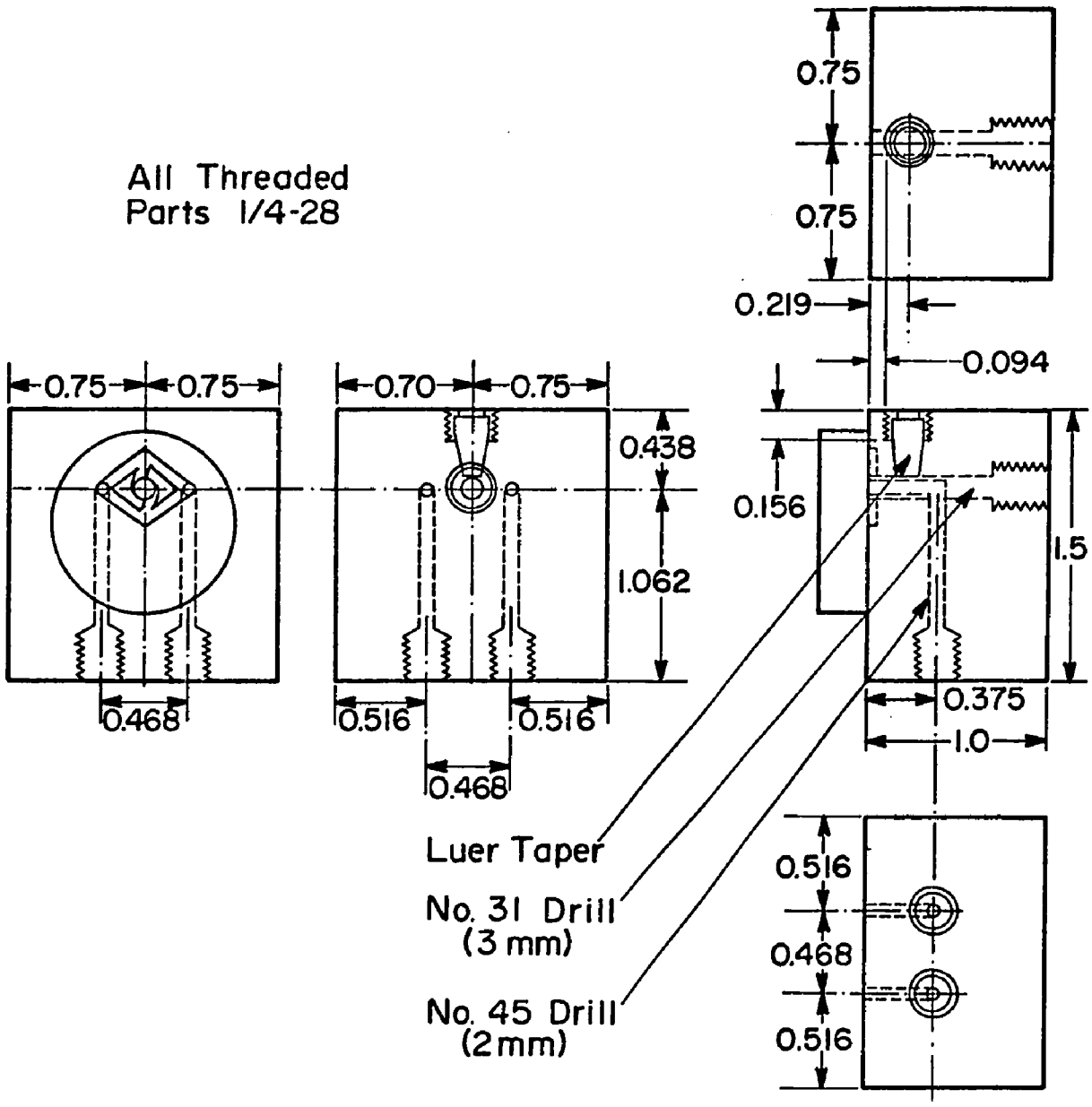

Figure 11. The Mixing Block of the Fluorescence Stopped-Flow Module

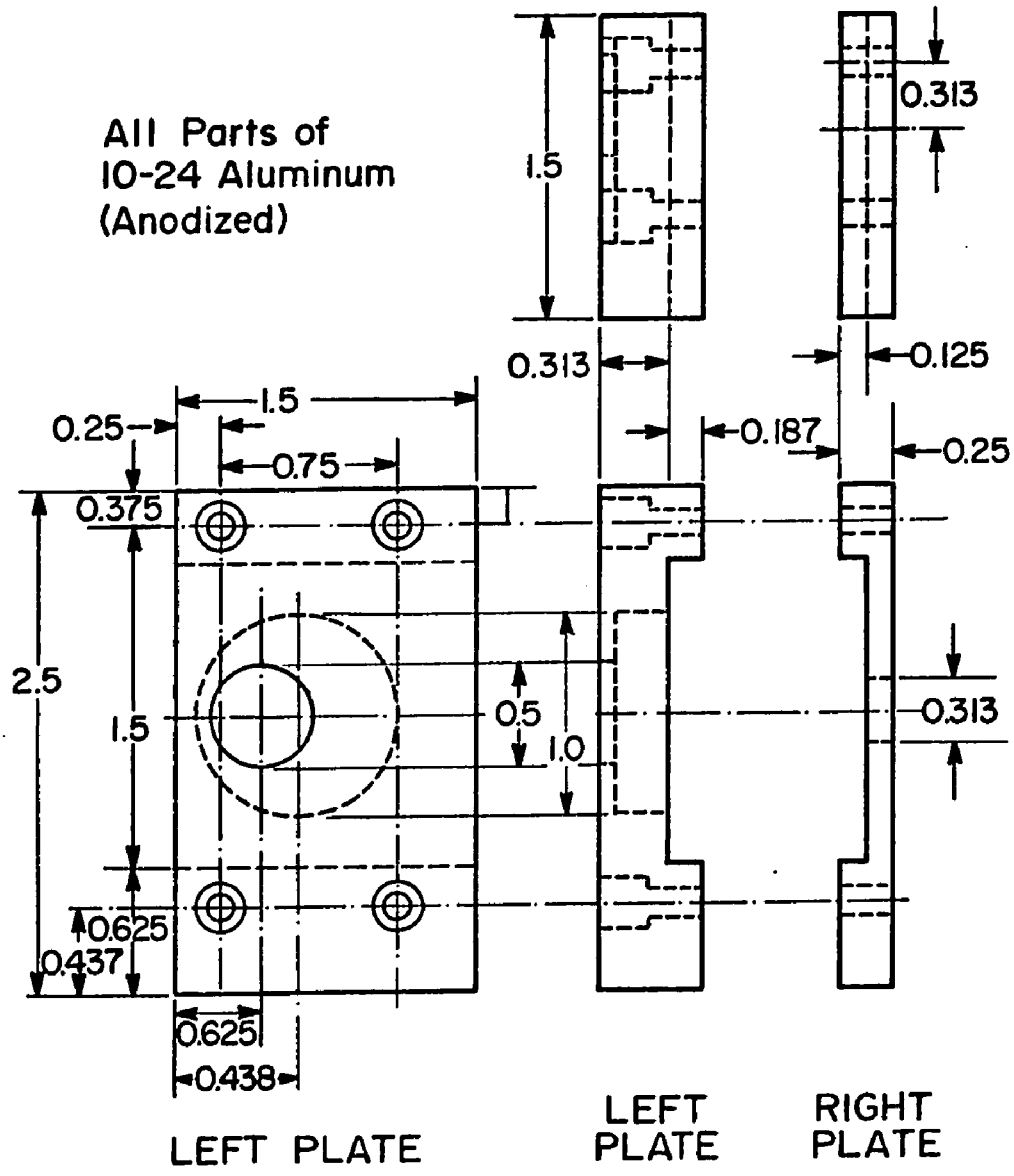

Figure 12. The Clamp for the Stopped-Flow Mixing Module

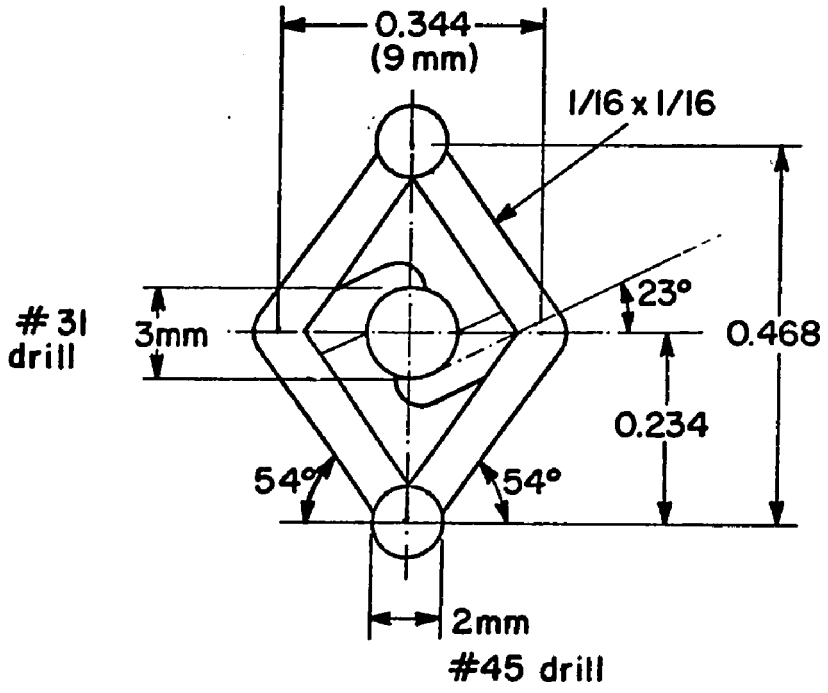

Figure 13. Face Detail of the Stopped-Flow Mixing Block

Still in channels on the face of the mixing block, the two freshly-mixed streams collide almost head on at the final mixing point directly in the excitation beam. The reaction mixture then flows away from the mixing face, down the 3 mm diameter reaction tube, past the observation port, and out of the mixing block. Close attention is paid in the design to keep the total cross sectional area of flow nearly constant in successive channels. This minimizes cavitation.

The observation window in the stopped-flow module is a solid lucite Luer taper held in the mixing block by a 1/4-28 threaded brass ring. The very small dead space formed from fitting the flat end of the Luer taper tangent to the cylindrical reaction channel is a necessary consequence of keeping the window out of the excitation beam. The choice of a Luer taper and position of the window are a good compromise among the considerations of ease in construction, tightness of seal, minimization of transport and resolution times, and maximization of sensitivity.

Solution exhausting from the mixer flows through connectors A, B, and C (Figure 14) designed in order to adapt the stopping assembly of Ballou (51) to fluorimeter operation. The Ballou stopping assembly is fastened by means of an adapter section to the fluorimeter bath plate (Figure 15). A tightening bolt (Figure 5) on the bath secures the Luer joint between connectors A and B. Solution passes through the bath plate via connector C. During a shot, solution fills the stopping syringe and forces the syringe plunger upward until it hits

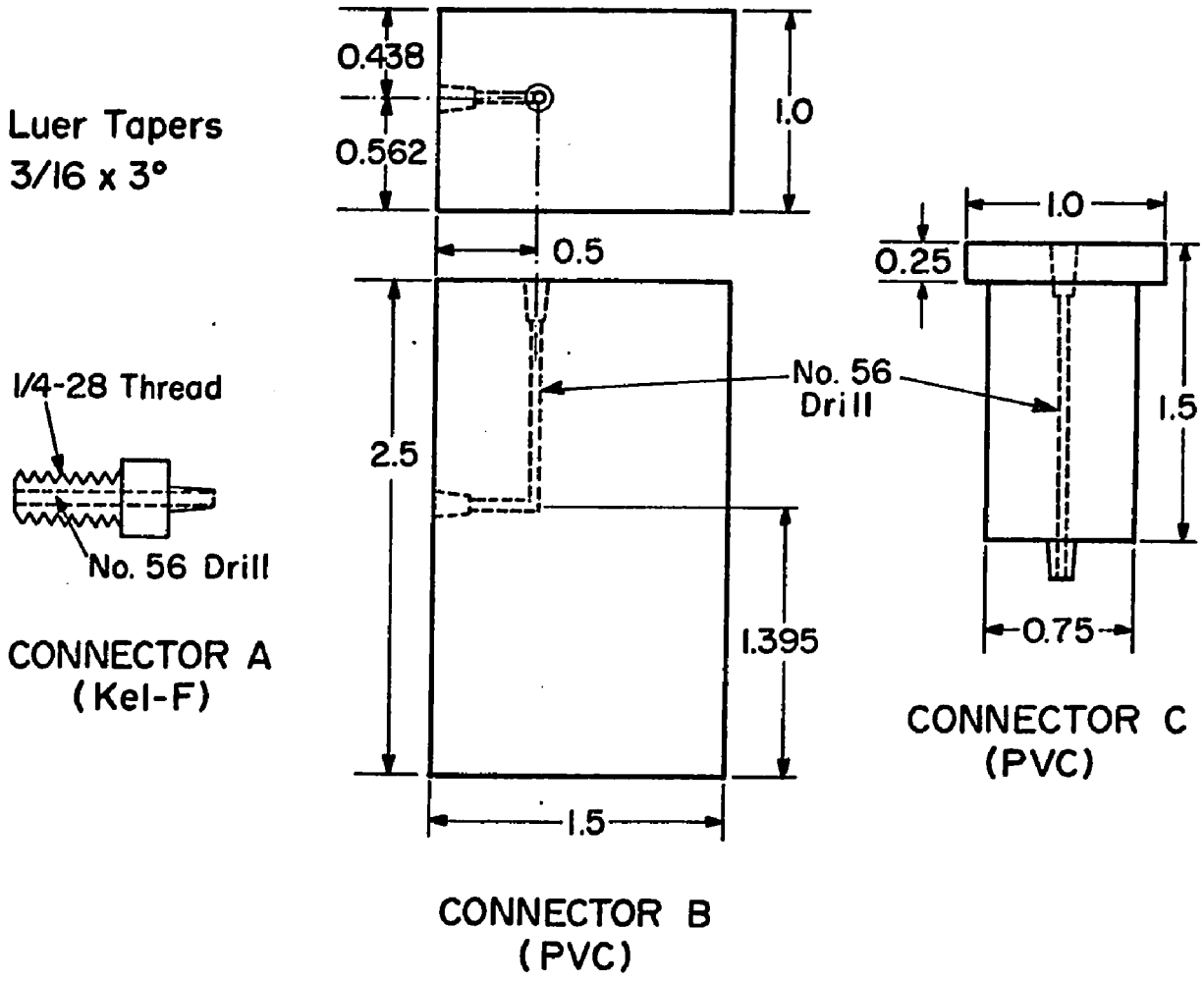

Figure 14. Connectors Between the Mixing Module and Stopping Syringe

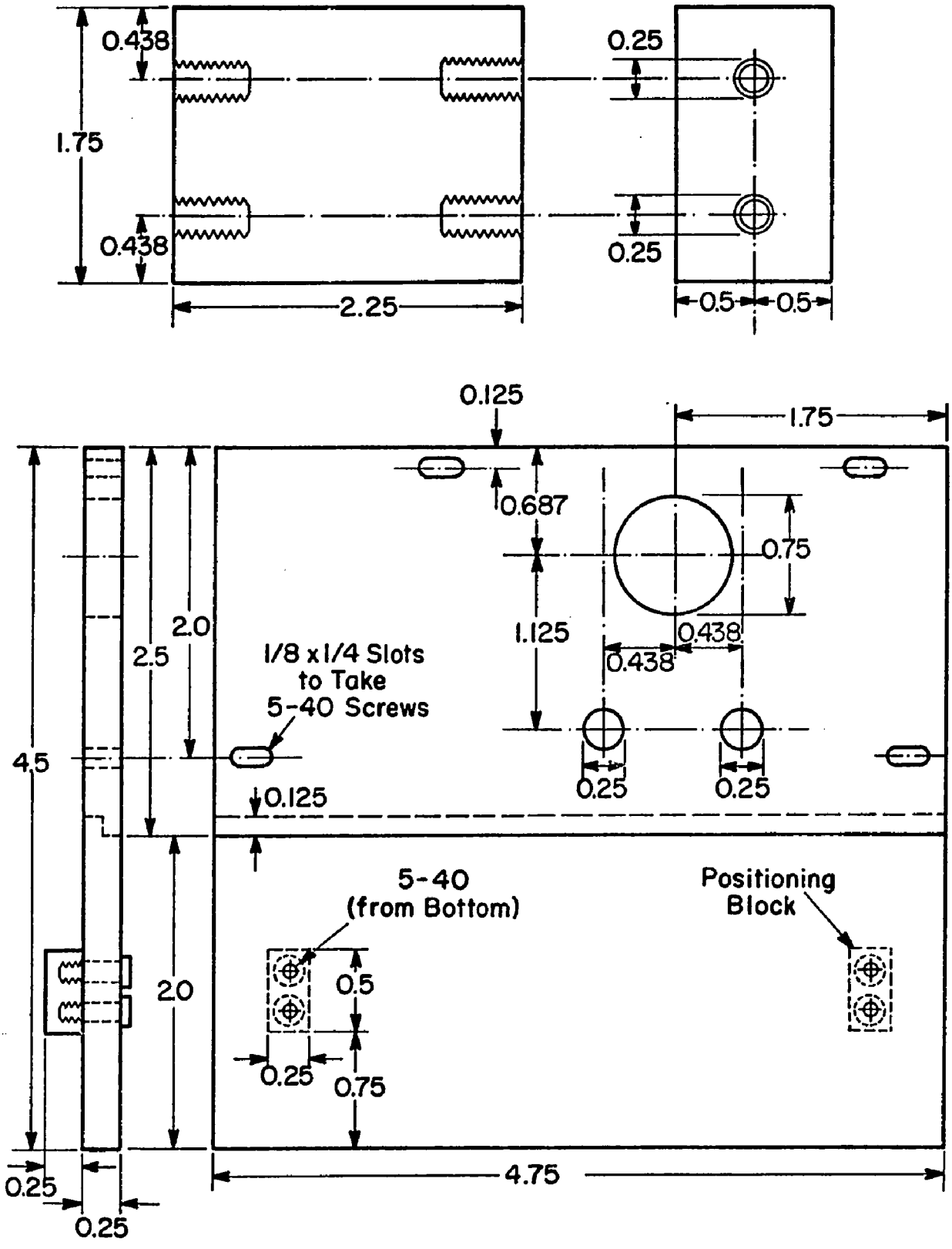

Figure 15. The Fluorimeter Bath Cover Plate and Stopping Syringe Assembly Adapter

a stopping bolt. The volume pushed during a shot can be adjusted by this stopping bolt. After a shot, solution is emptied from the stopping syringe via a Hamilton three-way valve. Attached to the top end of the syringe plunger is a collar which passes by and trips a microswitch during the traverse of a shot. The microswitch, a Robertshaw BZ 2RS, can be variably positioned and triggers the kinetic recording device.

Group III Components: Detection

The detector used in this fluorimeter is an 11 stage EMI 9592B photomultiplier tube with S-10 response. The photomultiplier housing is shown in Figure 16. The magnetic shield (Co-netic Magnetic Shield Division 1.25" x 4.5" mu metal shield) is at cathode potential and is insulated from the remainder of the housing by a delrin spacer. The rear of the shield fits snugly into and is positioned by a delrin cylinder which holds the tube socket, thereby the tube, and dynode chain. The wiring diagram for the dynode chain is that suggested by EMI (52). Signal voltage (carried by coaxial cable), common voltage, and photomultiplier high voltage pass through a brass bulkhead separating the photomultiplier section from the follower section of the housing. Photomultiplier high voltage (carried by a shielded coaxial cable in the rear section of the housing) comes from a Hewlett Packard Model 6516A supply modified to include an on/off switch in the output function. The desired voltage is dialed digitally in increments of 10, 100,

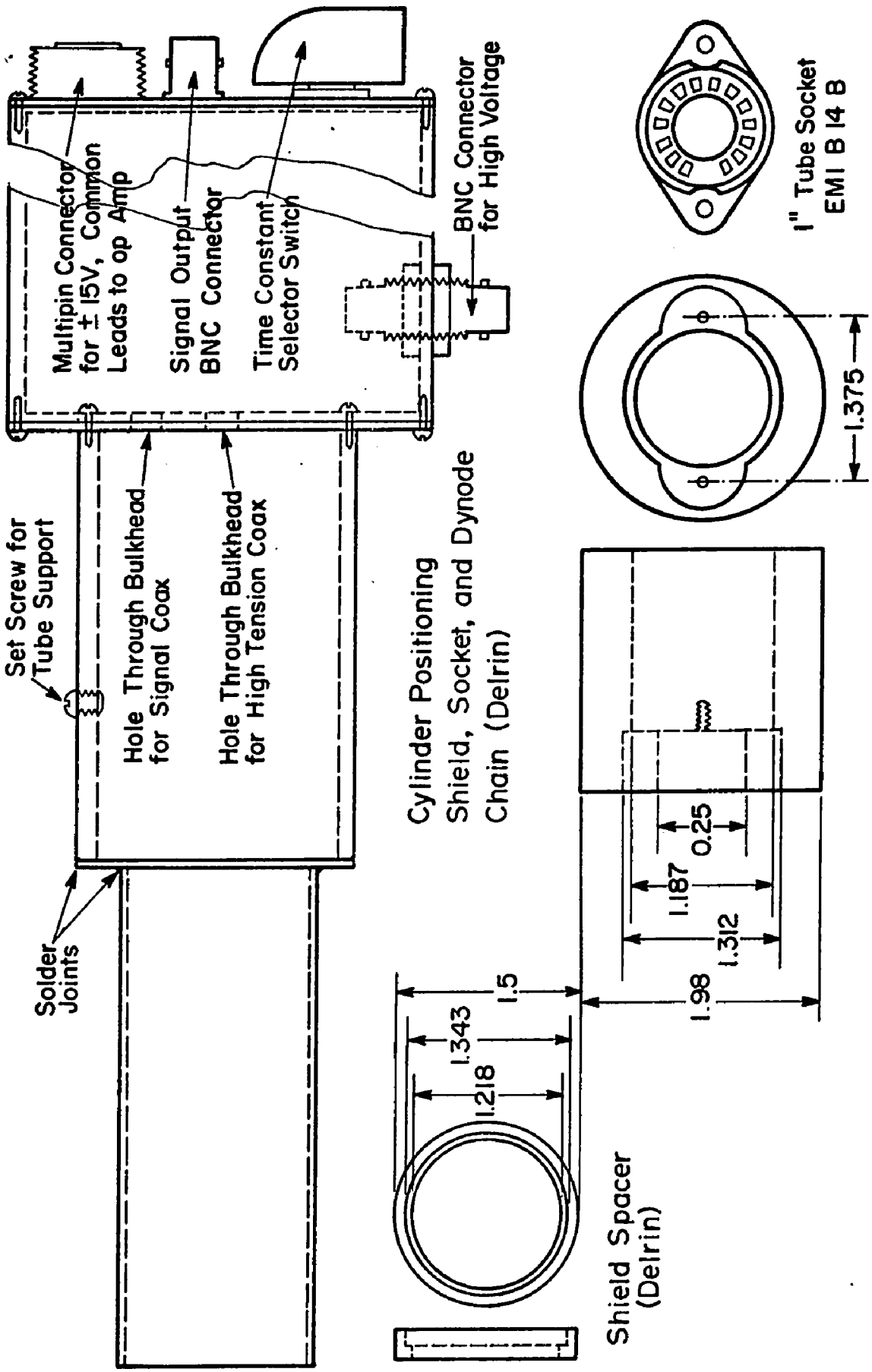

Figure 16. Photomultiplier Housing

or 1000 volts up to 3000 volts, on top of which may be added a continuously variable voltage between 0 and 10 volts.

The wiring diagram for the follower is shown in Figure 17. Attaching the time constant capacitors across the load resistor is not usual practice, but inexpensively allows a wide range of output time constants to be designed into a small space. The only requirement which must be satisfied in this arrangement is that the capacitor leakage resistance be the same for all capacitors or much greater than load resistance. Otherwise the load resistance and therefore the signal magnitude will appear different for each capacitor (time constant). This requirement is satisfied in this instrument to better than 1% except for the use of the 0.1 uf capacitor (one second time constant) which yields a signal 85% as large as the signal with the other capacitors. Selection of the desired time constant capacitor is made by a twelve position switch mounted on the rear of the housing. An FET operational amplifier is used in a follower configuration to provide a high input impedance to the signal. A Philbrick PR 30C supply provides $\pm$ 15 V for the operational amplifier. Figure 17 also diagrams an offset circuit located in the supply chassis box which allows a constant voltage to be subtracted from the signal. This device is used when one wishes to display only the small change atop a large signal.

A digital voltmeter, Keithley Model 160, is used to read-out static fluorescence signals, while kinetic fluorescence traces are

FOLLOWER CIRCUIT IN PHOTOMULTIPLIER HOUSING

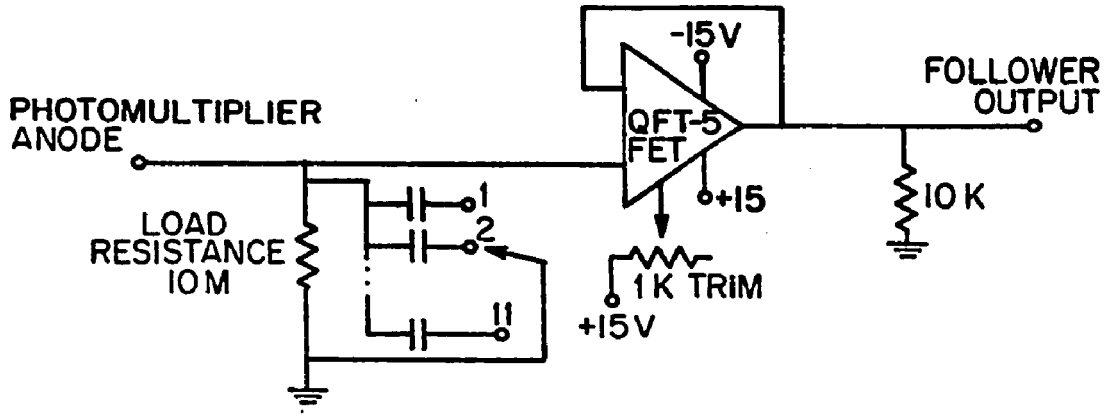

Position	Capacitance	Time Constant (msec)
1	parasitic	0.2
2	22 pf	0.4
3	100 "	1
4	200 "	2
5	500 "	5
6	0.001 uf	10
7	0.002 "	20
8	0.005 "	50
9	0.01 "	100
10	0.02 "	200
11	0.1 "	1000

OFFSET CIRCUIT IN ±15V SUPPLY CHASSIS BOX

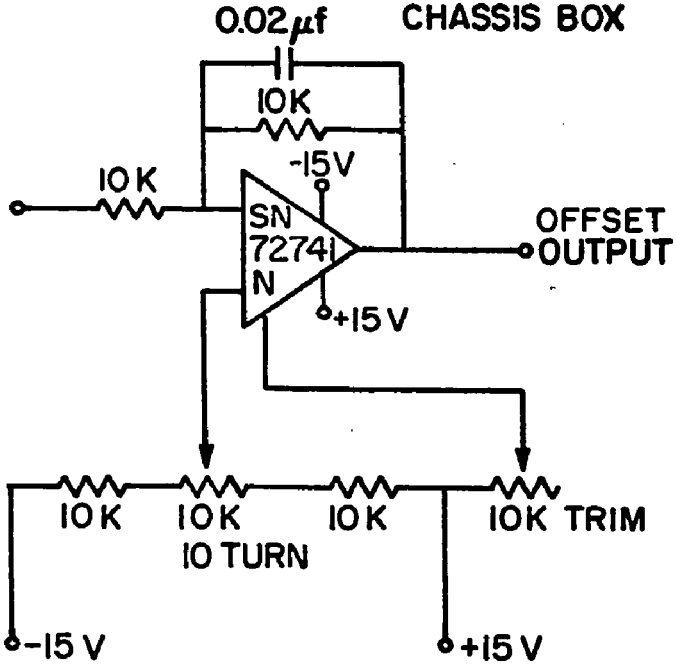

Figure 17. Photomultiplier Follower and Offset Circuitry

recorded with a Textronix Model 564 recording oscilloscope or a Varian Model C-1024 Time Averaging Computer (CAT) in conjunction with a Moseley Model 680M strip chart recorder.

FLUORIMETER PERFORMANCE

Since the fluorimeter was built specifically to obtain the data presented in this thesis, performance was evaluated with flavin studies in mind. The first four criteria concern operation in either the static or stopped-flow mode: 1) overall system stability, 2) linearity between fluorescent species concentration and signal magnitude, 3) sample temperature measurement, and 4) sensitivity at low concentrations of the fluorescent species. The evaluation section concludes with specific considerations of performance in the stopped-flow mode, namely: 5) dead time, 6) response time, 7) reproducibility, and 8) mechanical performance.

1) Overall System Stability

This is one of the most important requirements in a "single beam" device (one in which the signal is not continually or intermittently compared with a reference and thereby corrected for fluctuations or drift in lamp output and electronics performance). After some early pitfalls* had been circumvented, the system was

* The most notable of these was the inclusion of a Variac (several were tried) in the lamp supply between the AC voltage regulator and the bridge rectifier. Even after cleaning the Variac windings and lubricating with electrical contact dope, the slidewire contact with

consistently stable to within $\pm$ 0.1% for periods longer than an hour, the major instability being slow drift.

2) Linearity of Signal Magnitude with Sample Concentration

Strict linearity is imperative since the instrument is used primarily to determine free flavin concentrations (under various conditions) from fluorescence measurements, as opposed, for instance, to determining fluorescence spectra. Over all ranges of flavin concentrations used in the fluorimeter and in both modes of operation, signal size was linearly proportional to flavin concentration. Figure 18 displays the results of some of these tests.

3) Sample Temperature Measurement

Sample temperature was determined in either mode of fluorimeter operation using a Sargent-Welch S80210A thermometer (range -1° to 51° with scale divisions every 0.1^{o}) partially immersed in the fluorimeter water bath. To obtain the sample temperature the thermometer reading was adjusted using the curve in Figure 19 which corrects both for thermometer inaccuracy and for the difference between bath and sample temperatures. To correct for inaccuracy, the thermometer was calibrated against a Brooklyn thermometer tested and certified by the National Bureau of Standards. A slight difference between water bath and sample temperatures was observed and resulted from the non-insulating quality of the aluminum walls

---

the windings wandered, resulting in erratic lamp voltage, lamp output, and signal size.

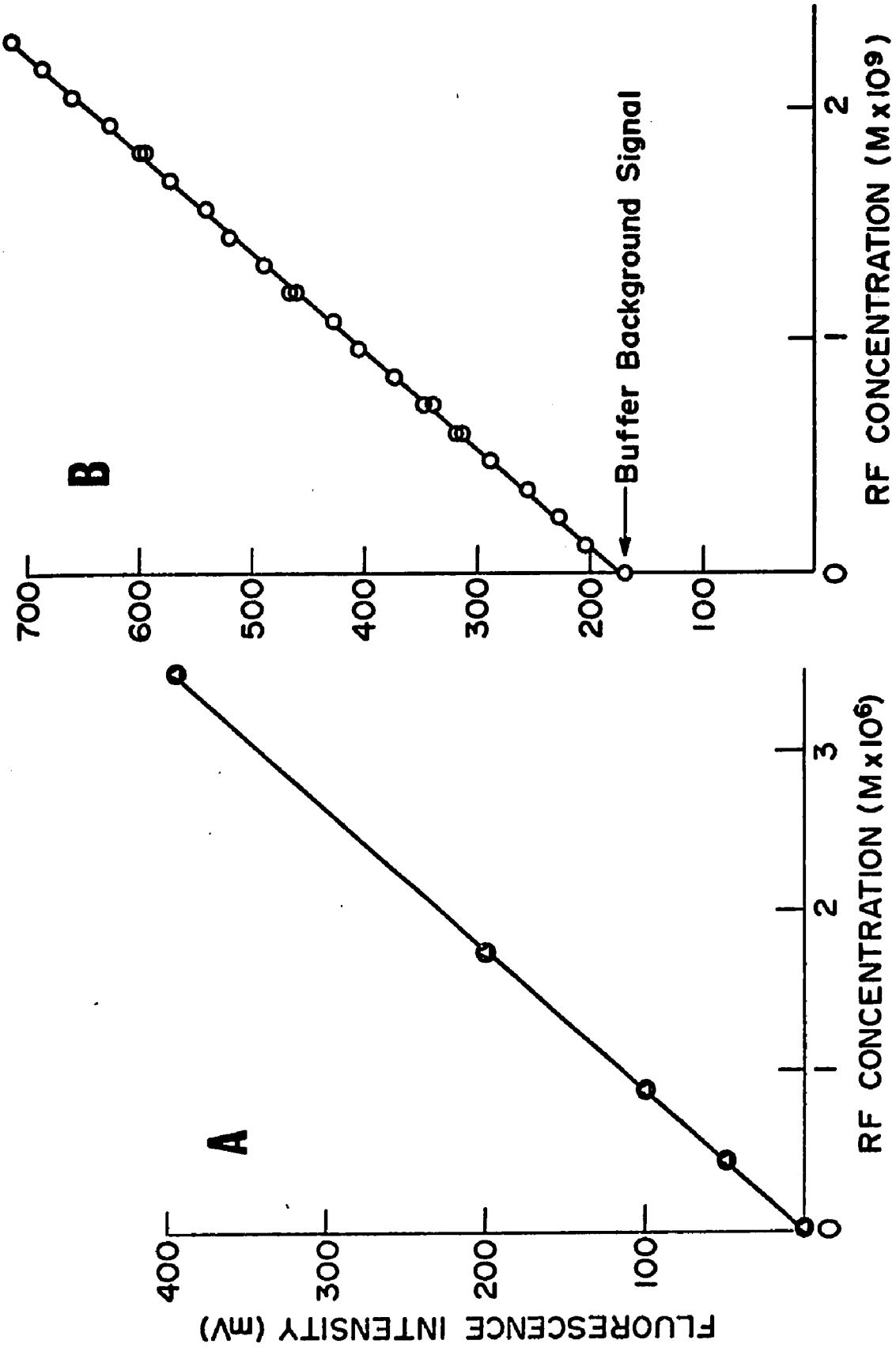

Figure 18. Relationship Between Signal Size and Fluorophore Concentration in the Stopped-Flow Mode (A) and in the Static Mode (B)

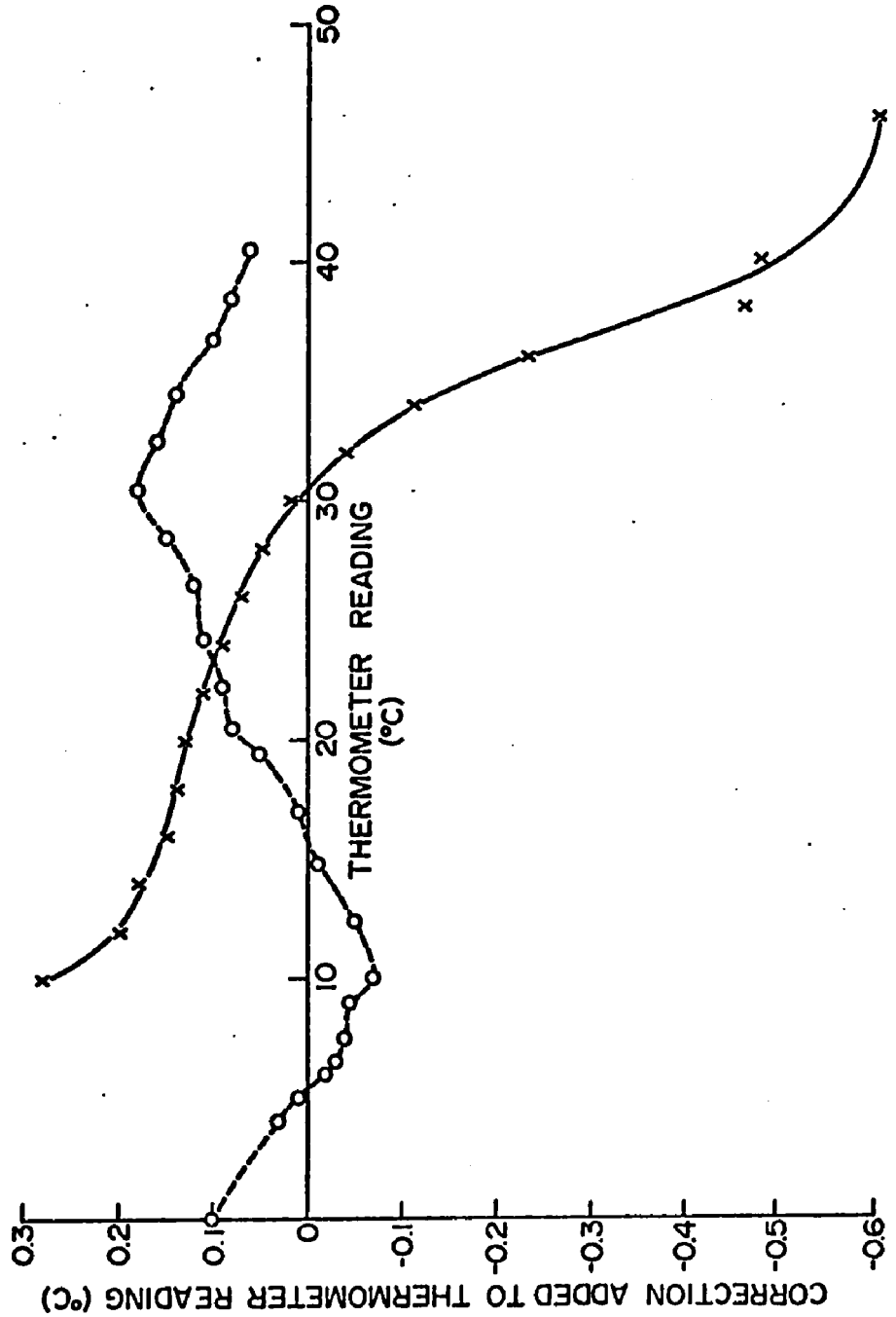

Figure 19. Temperature Correction Curves. The ordinate values indicated by x——x must be added to the Sargent Welch S80210A, 703-1005 thermometer reading to obtain the sample temperature. x——x corrects both for thermometer inaccuracy and for the difference between the bath and sample temperatures. o---o corrects only for thermometer inaccuracy.

surrounding the water bath. This difference was the larger, the farther the bath temperature was from ambient. Any studies requiring bath temperatures different from ambient by more than 20° should use a bath wall design modified to include thermal insulation.

Upon changing the bath temperature, the time required for complete reequilibration of module temperature was about 10 minutes for the static module and about 20 minutes for the stopped-flow module. A sample cuvette at ambient temperature inserted into the static module came to thermal equilibrium with the module in less than 5 minutes.

4) Sensitivity

In the static mode sensitivity is equated with the minimum detectable concentration, m.d.c., of the fluorescing species, where the m.d.c. is defined as that concentration giving a signal which differs from the pure solvent signal, here referred to as background, by an amount equal to the root-mean-square (rms) noise level of the signal*. This can be approximated using Equation 8.

$$\text{m.d.c.} = \frac{(\text{concentration of test solution})}{(\text{total test signal minus background})} \times \frac{(\text{peak-to-peak noise signal})}{5} \qquad \text{Equation 8}$$

Under the test conditions used to obtain the data in Figure 18, a riboflavin concentration of 10^{-9} M gave a signal of 410 mV. For a

* For the ATSM method used to determine m.d.c. see Udenfriend (53).

background signal of 170 mV and for the observed peak-to-peak noise level of 20 mV (time constant of 0.2 sec), the m.d.c. calculated from Equation 8 is 1.7×10^{-11} M. This small m.d.c. value is a good indication of the instrument sensitivity in the static mode.

This m.d.c. value, however, is slightly too small because background is not the constant value assumed above. Instead, for these small fluorescence signals, one observes that background increases with each successive addition of reagent*. This phenomenon is attributed to the deposition and accumulation of dust and lint in the cuvette coming from the surfaces of the micropipette and plastic stirrer, to which they may be electrostatically attracted. Routine dusting of all fluorimeter surfaces close to the static module and drying the tip of the micropipette with lint-free lens paper reduced this increase in background, but did not eliminate it. Other mixing methods which were attempted proved to be unsatisfactory.

Although lint accumulation increases the m.d.c. only slightly (to m.d.c. $\sim 2 \times 10^{-11}$ M), the effect is quite detrimental in titration experiments where errors accumulate. The background increase resulting from lint accumulation greatly influences the measured values of the binding K_a for those flavin derivatives which must be

---

* The reader is to understand that the term "addition" here includes the mixing of the cuvette solution by the method employed throughout these studies - rapidly cycling a Calbiochem plastic plumper up and down in the cuvette 5 to 10 times, taking care to avoid scraping the sides of the cuvette.

studied under conditions where the background signal becomes of comparable magnitude to the flavin fluorescence signal. As a "rule of thumb", background increases resulting from lint accumulation can be expected and will adversely influence measured K_a values when the photomultiplier voltages in the static mode of this fluorimeter exceed 700 V.

Sensitivity in the stopped-flow mode includes the additional consideration of the speed of the reaction. A test of this sensitivity is to evaluate not only how small a fluorescence change can be measured, but also how fast can the change occur and still be followed. Thus a good criterion is to determine how large a second order rate constant can be measured by the instrument. Referring to the analysis presented in Figure 21, the second order rate constant calculated from trace d is 6×10^7 $M^{-1} sec^{-1}$. Although this rate constant is not large for a fluorescence instrument, the experiment can be used to ascertain how much larger a rate constant could have been measured. The half time observed for the concentration change from 8.4×10^{-8} M to 4.2×10^{-8} M in Figure 21 is nearly 200 msec, obtained with an instrument time constant of 2 msec. Obeying the "rule of thumb" that the instrument time constant should not exceed one-tenth of the half time of the process being recorded, a second order process with half time of 20 msec could have been followed. The inset to Figure 21 shows that the instrument had sufficient signal/noise quality to allow such an analysis. Thus the instrument is capable of measuring rate

constants for the quenching of flavin fluorescence at least as large as 6×10^8 $\underline{M}^{-1}sec^{-1}$. In fact, the instrument was used to quantitate (to within several percent) second order rate constants approaching 3×10^8 $\underline{M}^{-1}sec^{-1}$ for quenching of flavin fluorescence (Figure 44). For fluorophores with higher quantum yield than flavins, larger rate constants could be measured by this instrument.

Additionally it may be noted from slopes a and b in Figure 21 that processes with half times less than 4 msec can be accurately followed. Thus fluorescence changes with first order rate constants larger than 170 sec^{-1} can be measured with this instrument.

5) Dead Time

This instrument, like many stopped-flow instruments, initiates reactions by mixing reactants at a point separated in position and thus in time from the observation point. There is therefore a time interval, called the dead time, during which the reaction proceeds without being observed. This unobserved interval depends in a complex way on 5a) the dead volume, 5b) flow characteristics, and 5c) mixing efficiency of the instrument.

5a) The dead volume is that volume between the points of first mixing and the midpoint of observation, which for this instrument is 0.036 ml. The time necessary to flush the mixed solution through this volume defines an interval called the transport time. Using flow traces obtained with a velocity transducer, flow velocities are calculated to be 28 ml/sec at 40 p.s.i. and 32 ml/sec at 50 p.s.i.,

yielding transport times of 1.3 msec and 1.1 msec, respectively. Dead time would equal transport time if reactants were transported via plug flow (see 5b), mixing were instantaneously complete (see 5c), and observations were made of a point volume rather than over a volume containing reactants of different age (see 5d).

5b) Plug flow is an idealized concept where the flow velocity is constant throughout the cross section of the channel. Although plug flow is physically impossible, it is closely approximated by turbulent flow. Turbulent flow within the mixing block is assured since flow through every channel has a Reynolds number* > 5000 when syringe driving pressure is $\geq$ 40 p.s.i.

5c) Mixing can be considered complete when the two reactants are interspersed to the extent that diffusional processes become the limitation to the reaction. By studying a reaction which is diffusion controlled, therefore having a rate several orders of magnitude greater than the fastest possible mixing rate, the observation of an apparent rate of reaction indicates mixing incompleteness and is actually a measure of the rate of mixing for the instrument (55). The mixing performance of this instrument is demonstrated in Figure 20 from the study of a diffusion controlled reaction. Fluorescein is fully

---

* Reynolds number = $V\rho d/\eta$, where V is linear flow velocity in cm/sec, ρ is density in gm/cm^3, d is channel or equivalent diameter in cm, and η equals viscosity in poise. In this calculation the values used are ρ = 1 gm/cm^3, and η = 0.01 poise, i.e., the values for water. For straight pipes, flow yielding a Reynolds number greater than 2000 is turbulent (54).

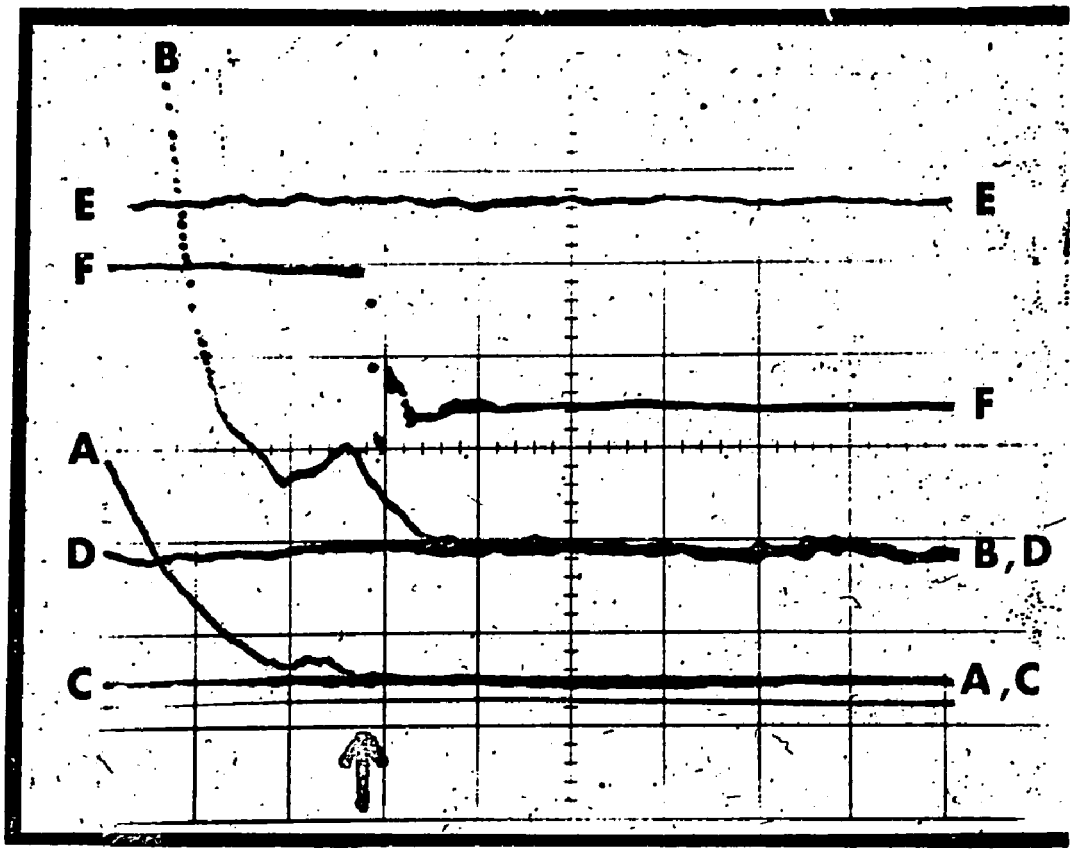

Figure 20. Mixing Performance of the On-The-Face Mixer of the Stopped-Flow Fluorimeter. Approximately 10^{-6} M fluorescein in 0.010 M NaOH was mixed against 0.011 M HCl at room temperature. The measured pH value of the mixture was pH 2.9. The traces are recorded at 2 msec per division. The vertical sensitivity is 0.1 V per division for traces A, C, and E and is 0.02 V per division for traces B and D. Flow stops at the time indicated by the arrow. See text for further details.

fluorescent at high pH values, is non-fluorescent at low pH values, with a pK about 6. A dilute solution of fluorescein ($\lesssim 10^{-6}$ M) in 0.010 M NaOH is reacted in the stopped-flow against 0.011 M HCl and results in trace A. Trace B is a duplicate shot recorded using a five-fold more sensitive vertical scale. The equilibrium signals recorded about half a second after each of these two shots are shown in traces C and D. Trace E results from reacting fluorescein in base against water instead of acid and is used to quantitate the fluorescein concentrations in A and B. Trace F is the velocity transducer output recorded simultaneously with trace B. The following protocol is used to obtain traces A and B in Figure 20. In both shots, one syringe contains the fluorescein solution at basic pH. After flushing with water, the second syringe is loaded with acid solution and some solution is pushed into the connecting tube to move the acid/water interface toward, but not into the mixing block. A shot is then recorded. At early times during the shot recorded in trace B, water mixes with fluorescein giving a huge fluorescence signal (off scale). After about one-third of the push ($\sim$ 2 msec) the acid/water interface passes by the mixer and then by the observation port. Therefore after $\sim$ 2 msec fluorescein is mixing with acid and its fluorescence would be completely quenched except for the incompleteness of mixing. Trace B of Figure 20 shows that after 3 msec but before the stopping of flow an approximately steady state fluorescence signal is established which corresponds to $3 \pm 1\%$ unreacted material. Thus mixing is 97%

complete during the transport time. One millisecond after the stopping of flow greater than 99.5% complete mixing is achieved. For experiments not following the complicated procedure given above, i.e., when acid is directly mixed against fluorescein in base, the observed results mimic those shown in Figure 20 near and after cessation of flow*.

5d) The stopped-flow observation port views a finite volume instead of a point volume and thus observes reactant mixtures of slightly different ages after mixing; this results in the so-called slit error (55). To minimize kinetic imperfections associated with this averaging process, the interval of ages viewed at any time should be small compared to the half time of the fastest process recorded. The Luer taper window views a volume of approximately 0.025 ml, therefore the age of the reactant mixture observed is uncertain corresponding to a volume of 0.0125 ml, or 0.4 msec at a flow velocity of 30 ml/sec. This age uncertainty represents about one-tenth of the half time of a process with a rate constant of 170 sec^{-1}.

The apparent dead time of a stopped-flow instrument is the interval between the true zero time of the reaction and the time when the reaction mixture is observed. True zero time can be evaluated

---

* The velocity trace F shows flow to be constant during nearly the last 6 msec before stop, but that a ringing phenomenon exists for approximately 1 msec thereafter. This ringing may be electrical (from the transducer) rather than represent oscillation within the stopping syringe, although this latter possibility has not been eliminated.

for a kinetic process using a graphical method which linearizes the time course of the observable of the reaction (e.g., plotting log (observable) against time if the reaction is known to be first order, or in the example studied here, plotting (observable)$^{-1}$ against time when reactant concentrations are equivalent and reaction is known to be second order). True zero time occurs when the linearized time course of the observable is extrapolated to the 100% unreacted value. Mixing inefficiencies and flow abnormalities will manifest themselves in apparent dead times shorter than the transport time. Satisfactory mixing and flow performance is demonstrated if dead time equals transport time.

To directly evaluate the dead time of the stopped-flow fluorimeter, the quenching of fluorescence when RF is mixed against apoRBP was studied at several values of equivalent reactant concentrations. The results of these experiments are presented in Figure 21. In order to compare the results of experiments at different concentrations, the kinetic traces have been normalized by dividing the signal at any time by the signal expected if no reaction occurs. Dead time is seen to be about 1.0 to 1.2 msec, that is, equal to the transport time within the 0.4 msec time resolution of the instrument. The initial curvature in the fastest trace is attributed to the slight inefficiency of mixing mentioned earlier. Deviation from linear second order behavior is seen after two half lives at 10^{-6} M (trace c), and shortly after the first half life at 10^{-7} M (trace d). This phenomenon results

Legend to Figure 21

Equimolar solutions of apoRBP and RF in 0.01 M potassium phosphate, pH 7.0, were mixed at 25° to give the final concentrations indicated. In order to plot the results at the different concentrations in the same figure, the fluorescence values as a function of time were normalized by dividing by the fluorescence value found when RF was mixed against buffer. [Normalized Fluorescence]$^{-1}$ values of 2 and 4 correspond to the points in the reaction at which 50% and 75% of the RF fluorescence was quenched and the time interval, $\tau_{2\rightarrow4}$, between these two points in the reaction corresponds to the second half-life of the reaction. (The second half-life of the reaction was chosen for comparison at the different concentrations because the first half-life of the reaction at the highest concentration was over in the dead time of the instrument.) The left and right halves of Figure 21 contain the same data and differ only in time scale. For convenience, however, some of the data plotted in the left half have been omitted in the right half. The three shots seen in the inset were obtained at after-mixing reactant concentrations of 1.25×10^{-7} M and are those analyzed in the trace labelled d. The fluorescence signal sensitivity for these shots was 0.1 V per division and the three traces were recorded at 20, 50, and 100 msec per division. Under the same buffer and temperature conditions, 1.25×10^{-6} M apoRBP mixed against 1.25×10^{-7} M RF (concentrations after mixing) had a pseudo-first order rate constant of 55 sec^{-1}. This corresponds to a second order rate constant of 4.4×10^{7} M^{-1}sec^{-1}.

After-Mixing Reactant Concentrations	Number of Shots Plotted	Trace Label	$\tau_{2\rightarrow4}$	Second Order Rate Constant Calculated from $\tau_{2\rightarrow4}$	Total Reactant Concentration Not Complexed at Equilibrium	Second Order Rate Constant Calculated from Reversible Analysis
(M)			(msec)	(M^{-1}sec^{-1})	(%)	(M^{-1}sec^{-1})
1.25×10^{-5}	8	a	3.2	5.0×10^{7}	1	4.6×10^{7}
		b	3.4	4.6×10^{7}		4.5×10^{7}
1.25×10^{-6}	7	c	28.8	5.6×10^{7}	3	4.8×10^{7}
1.25×10^{-7}	3	d	254.	6.3×10^{7}	9	4.4×10^{7}

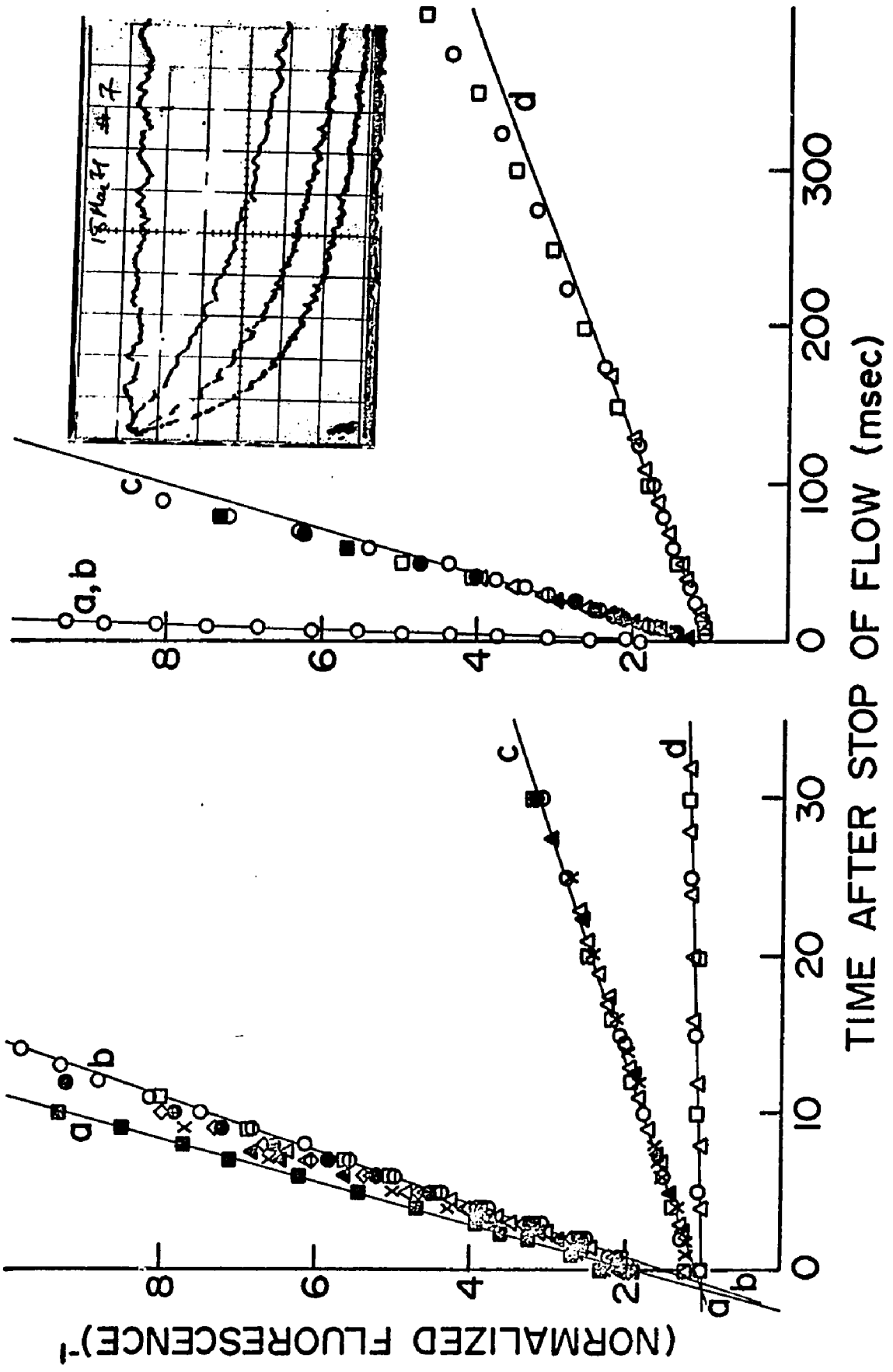

Figure 21. Dead Time Analysis of the Stopped-Flow Fluorimeter

from the reversible nature of the binding reaction and causes the apparent second order rate constants calculated from the slope of the plots to be the larger, the more dilute the reactant solutions. However, the rate constants agree with each other and with the rate constants calculated under pseudo first order conditions when calculated according to a reversible reaction analysis as shown in the legend to Figure 21. The overlap of the many shots plotted is a demonstration of the reproducibility of the instrument.

6) Response Time

Trace B in Figure 20 permits evaluation of the lower limit on instrument response time; the fastest response may be even faster than is shown. The approximate half time for the approach to steady state (before stopping) is seen to be 0.4 msec. Following the "rule of thumb" that no distortion will occur from the recording of a kinetic phenomenon if the recording device has an intrinsic time constant 8 to 10 times smaller than the phenomenon, this instrument can follow processes with half lives at least as small as 3 to 4 msec with no distortion in the observed kinetics. This corresponds to first order rate constants of about 200 sec^{-1}.

7) Reproducibility

Already evident from the superposition of the analyses presented in Figure 21, the excellent reproducibility of this stopped-flow fluorimeter is directly observable in Figure 22. This figure exhibits duplicate shots recorded at three different, fast sweep rates of RF

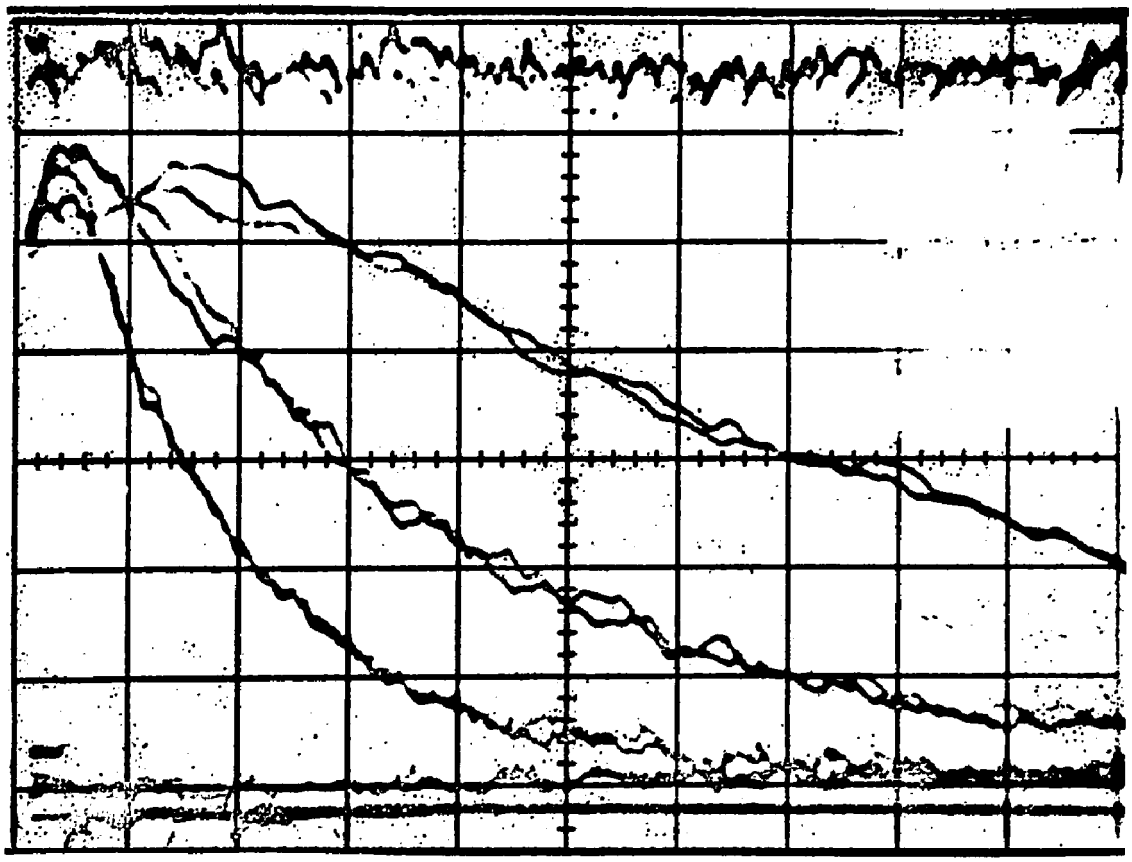

Figure 22. Reproducibility and Signal to Noise Character of the Fluorimeter in the Stopped-Flow Mode.

1.25×10^{-7} M RF was reacted at 25° against 1.25×10^{-6} M apoRBP (concentrations are after mixing) and the quenching of fluorescence monitored. Duplicate shots were recorded at 2, 5, and 10 msec per division with 0.2 msec time constant. The sensitivity was 0.1 volt per division. Traces for RF mixed against buffer and for buffer alone are also shown. The pseudo first order rate constant calculated from these shots is 55 sec^{-1} which corresponds to a second order constant of 4.4×10^{7} $M^{-1} sec^{-1}$.

fluorescence quenching on mixing with apoRBP under pseudo first order conditions. The total fluorescence decrease represents a change in concentration of 1.2×10^{-7} M.

8) Mechanical Performance

Mechanical differences in the two halves of the delivery system (e.g., unequal friction of the barrels inside the pushing syringes, unequal expandability of the PE connecting tubes) can give rise to delivery of unequal volumes of reactants during the cessation of flow. Aberrant results, especially in relaxation studies, caused by unequal volume delivery are to be anticipated when the syringe barrels, connecting tubes, etc. are replaced. Whenever such component replacement was necessary, appropriate measures were taken to eliminate unequal delivery as tested by the following experiment. a) A stock fluorophore solution in syringe 1 was mixed against buffer in syringe 2, then b) buffer in syringe 1 was mixed against the stock fluorophore solution in syringe 2. Proper delivery had been achieved when the fluorescence signal was the same in a) and b) and was the same during and after flow.

The pushing time varies with the volume collected in the stopping syringe and with the pressure of gas driving the pushing assembly piston. A typical value for the pushing time is about 7 msec when a total volume of 0.20 is pushed at 40 p.s.i. An abnormally long pushing time usually indicates a partial blockage of flow in some component and the lowered flow velocity causes inefficient mixing and

must be corrected. Blockage sometimes occurred from the constriction of a connecting tube when the brass tube holding the connecting tube in place was excessively or repeatedly tightened. For this reason the stopped-flow module was normally not disconnected from the connecting tubes. When not in use, the module was lifted out of the bath as seen in Figure 4A.

CHAPTER 3

EXPERIMENTAL METHODS

CHEMICAL METHODS

Preparation of RBP

All steps in the following preparations were carried out at 4°C. The separated whites from ten dozen Leghorn eggs (total volume about four liters) were diluted 1 : 1 with 0.1 M sodium acetate (NaOAc) buffer, pH 5.3 (Buffer I), and 50 mg of solid RF was added in order to convert all the RBP to holoprotein. After stirring the preparation for 30 minutes, the coagulated material was removed by filtration through several layers of cheesecloth, then through a double layer of Miracloth. 700 ml of a thick DEAE slurry (slurry is used here to mean the suspension which results from mixing equal volumes of buffer and equilibrated, packed DEAE) in buffer I was added to the filtered solution and this suspension was stirred for 20 minutes. The DEAE was then allowed to settle, the supernatant discarded, and the residue packed into a 4.5 cm diameter column. After washing with several liters of buffer I, the yellow RBP was eluted with 0.2 M NaCl in buffer I. The yellow eluate was diluted four-fold with distilled water and siphoned onto a 2.2 x 50 cm DE52 column equilibrated with buffer I. The column was washed with 500 ml of 0.05 M NaCl in

buffer I, then developed with a linear salt gradient formed from 400 ml volumes of 0.05 M NaCl in buffer I and 0.35 M NaCl in buffer I. RBP eluted at approximately 0.12 M NaCl in buffer I. Ten ml fractions were collected and their absorbances measured at 275 mm and 455 mm. Those fractions with $A_{275}/A_{455} = R < 6.3$ were pooled.

The pooled fractions were concentrated by a) diluting the pooled fractions with four volumes of distilled water, b) adding a sufficient amount of DE52 slurry in buffer I to bind all the yellow material, c) stirring the resulting suspension ten minutes, d) settling and then packing the settled DE52 into a small column, and 3) eluting the RBP with 0.3 M NaCl in buffer I. The very concentrated RBP eluate was then placed onto a Biogel P-60 column (4.5 x 60 cm) which was developed at the rate of about 50 ml per hour with 0.15 M tris chloride, pH 7.4. Fractions with the lowest R values, typically $\lesssim 6.1$, were pooled for preparation of apoprotein. Fractions with a higher ratio were saved and added to the DE52 column step of the next preparation.

Preparation of ApoRBP

The pH of the P-60 eluate was adjusted to 3.8 with 0.1 M acetic acid. After dilution with an equal volume of distilled water, the protein solution was applied to a 2.2 x 30 cm column of SE Sephadex A-50 equilibrated with 0.05 M NaOAc, pH 3.8. The column was washed with this buffer until the protein band at the top of the column appeared as an opaque white zone in the translucent column material

and until the column eluant became non-fluorescent under irradiation with a u.v. lamp.

Elution with buffer I or with a linear salt gradient constructed from one liter volumes of 0.1 M NaOAc, pH 4.1, and 0.5 M NaCl in 0.1 M NaOAc, pH 4.1, caused the opaque zone to migrate down and off the column, whereupon the fractions which contained the apoRBP were found to be completely transparent and colorless. The central 80% of the protein peak was pooled and the pH adjusted to 6.8 with 0.5 M dibasic potassium phosphate. The protein was either dialyzed against 0.1 M potassium phosphate, pH 6.8 (buffer II), or, if the preparation were less than 10^{-5} M, concentrated by a) batch adsorption onto a minimal quantity of DE52 equilibrated with buffer II, b) preparation of the DE52 into a column, and c) elution with 0.2 M KCl in buffer II. Dialyzed or concentrated apoRBP was routinely stored in plastic bottles and either frozen at -10°C or kept for short periods at $+4^{\circ}$C. Typical amounts of RBP present at several stages of the preparation are summarized in Table VI.

Disc Gel Electrophoresis

A homemade apparatus permits samples to be electrophoresed independently and consists of ten removable upper reservoir assemblies, a rack to hold them, a common lower reservoir, and upper and lower electrodes. Each upper reservoir is composed of a 1" x 4" plexiglas tube mounted vertically and plugged at the base with a short segment of a one-hole rubber stopper. The glass tube which holds the

TABLE VI

Typical Yields of RBP at the Various Stages of Purification*

Step	Volume	A_{455}	A_{281}	RBP
	(ml)	($\underline{M}^{-1}cm^{-1}$)	($\underline{M}^{-1}cm^{-1}$)	(gm)
1. 10 dozen egg whites	4000	---	---	---
2. pH 5.3 filtrate	7100	0.05**	---	2.0
3. DEAE column eluant	190	2.1	---	1.2
4. DE52 column eluant	172	1.91	---	0.90
5. P60 column eluant	71	3.60	22.0***	0.72
6. SE Sephadex column eluant	570	0.00	1.71	0.61

* This is a composite table derived from several preparations.

** This absorbance was recorded before excess RF was added and represents RBP which was 45% holoprotein.

*** This value is the absorbance at 275 nm and yields $R_{\frac{275}{455}} = 6.11$.

gel is pushed into the hole in this rubber stopper and makes each reservoir chamber watertight. The upper reservoir assemblies are held by the rack so that the glass tubes are partially submerged into the lower buffer reservoir. Thermal disruption of electrophoretic patterns as a result of excessive Joule heating in the gels is avoided if the gels in the glass tubes are held completely below the surface of the buffer in the lower reservoir. The upper electrodes, wired in parallel, consist of 2", 30 gauge platinum wires attached to the jack portions of single-pin and socket connectors. The jacks are forced through rubber stoppers and these rubber stoppers and connectors permit safe and easy disconnection of individual electrodes while the high voltage is on. A platinum wire along the bottom of the lower reservoir comprises the lower electrode. A Heathkit IP-17 supply provides up to 100 mA of high voltage variable between 0 and 400 VDC.

Disc gel electrophoresis was performed at pH 9 using a slightly modified form of the method of Davis (56) and at pH 6 using system #1599 of Chrambach and Rodbard (57). In the latter method gels were constructed so that the stacking phase had a pH value about 5 in order that all protein species in the RBP preparation would bear a net negative charge and therefore migrate into the separating phase which had a running pH value of 6. For both disc electrophoretic methods (pH 9 and pH 6) separations were carried out in 8% to 12% polyacrylamide gels and 5 to 50 µl of protein sample was mixed with approximately 20 µl of 10% sucrose before layering atop the concentrating gel. A

current of 0.5 amp/gel was applied until the protein had migrated into the gel; thereafter 1.5 amp/gel. After the run, gels were removed from the tube by rimming with a fine needle while continually ejecting water from a syringe. A short section of 30 gauge copper wire was pushed into the gel at the position of the bromphenol blue marker front, using a 22 gauge needle to align the wire before insertion. Gels were stained several hours in 0.3% aniline blue black in methanol-water-acetic acid (volume ratio 5 : 5 : 1) and passively or electrophoretically destained in 7% acetic acid. A simple homemade destainer was used for this purpose and consists of a slotted plexiglas plate (0.25" x 3.5" x 5.0") which divides the destaining bath into two compartments. Parallel slots 4 mm wide milled through the plate firmly holds gels to be destained; unused slots can be filled with rubber tubing. Electrophoretic destaining was accomplished in less than 30 minutes at 5 ma/gel after passive destaining of the gels for an hour. A watertight seal between compartments was not necessary, but shortened destain time. Some gels shrink during destaining, so care was exercised to prevent loose gels from floating out of their slots by wrapping a layer of cheesecloth around the gels in the plate. Destained gels were stored in 7% acetic acid until analyzed.

Sodium Dodecyl Sulfate (SDS) Gel Electrophoresis

Two methods were used for the preparation of samples for electrophoresis. The first was a modified form of the method of

Shapiro (58), in which samples were dialyzed for 24 hours in 0.01 M sodium phosphate, pH 7.0, containing 0.1% SDS and 0.3% 2-mercaptoethanol. The second method followed the procedure of Weber, Pringle, and Osborn (59). Samples were dialyzed against 0.01 M sodium phosphate, pH 7 to remove precipitating cations (potassium) and to decrease the ionic strength of the protein solutions. Samples were then made 0.9% in SDS and 0.9% in 2-mercaptoethanol and a) incubated for an hour at room temperature, b) heated to 100° for 2 minutes, or c) heated to 100° for 5 minutes. Electrophoresis was carried out on gels from 8 to 15% in acrylamide and .1% SDS. Gels were stained with aniline blue black or with 0.05% Coomassie blue in 12% TCA and passively or electrophoretically destained. Molecular weight determinations were made using the method of Weber and Osborn (60).

Gel Electrofocusing

This was performed by the method of Dale and Latner (61) as modified by Percival, Dunckley, and Purves (62). Eight percent polyacrylamide gels containing 1 or 2% Ampholine, pH range 3 to 10, and 20 to 50 ug of sample, were cast in glass tubes 5 mm by 65 mm using RF as photocatalyst. The disc electrophoresis apparatus was used with the upper reservoirs containing the cathodal solution, 2.5×10^{-4} M NaOH, and the lower reservoir containing the anodal solution, 3.6×10^{-4} M H_2SO_4. 100 V was applied for 15 min, then increased to 300 V. After an additional 2 to 3 hours, electrofocusing

was complete and the run was stopped. Continuation for longer times caused the pH gradient to become shallower and the entire gradient to migrate off the cathodal end of the gel. The electrofocused gels were fixed in 20% trichloroacetic acid (TCA). This fixation precipitated proteins in opaque zones which were photographed with dark background and side illumination.

Riboflavin Purification

RF was purified in the dark by a method suggested by Müller (63). About three grams of Sigma riboflavin dissolved in 100 ml of 0.10 M NaOH was treated with two grams of Darco activated charcoal, stirred ten minutes, then filtered through a Buchner funnel with Whatman #1 paper overlayed with Celite Analytical Filter Aid (Johns Manville). The first 10 ml of the deep orange filtrate was discarded but the remainder was added to 40 ml of boiling 2 M acetic acid. Immediately after precipitation began, the solution was filtered through Whatman #1 paper in a heated funnel. Approximately one quarter of the flavin precipitated on the paper and was discarded. The filtrate was cooled to room temperature overnight. The fluffy bright orange precipitate which resulted was washed twice with acetone, dried in a vacuum, and stored in the dark until used.

FMN Purification

The method of Massey and Swoboda (64) was employed with DE52 instead of DEAE. The FMN fraction was then passed over G-50 Sephadex as discussed below.

Flavin Purification by Chromatography

This was performed on a Sephadex G-50 (fine) column (4.5 x 70 cm, equilibrated with 0.01 M potassium phosphate, pH 7.0, buffer III, wrapped in aluminum foil). The flavin sample to be chromatographed was dissolved in buffer III and filtered before application to the column. The column was developed with buffer III at a flow rate about 50 ml per hour and it was found that flavins usually preceeded impurities off the column. Peak flavin fractions were pooled, stored in the dark without freezing (7 Cl LF bleaches when frozen in buffer), and used as soon as possible. Samples for TLC analysis were concentrated in darkness using a rotary evaporator*.

Thin Layer Chromatography (TLC)

TLC of flavins was performed using ascending development in the dark on 4 x 20 cm sheets cut from commercial plates (with and without fluorescent indicator). Samples dissolved in dimethyl sulfoxide (DMSO) or glacial acetic acid were spotted 2 cm from the bottom of the plates using a nichrome wire loop. Impurities were estimated visually from serially diluted samples run simultaneously. The solvent systems employed and the ratios by volume of their components were I) chloroform:methanol (96 : 4), II) n-butanol:water:0.1 M dibasic potassium phosphate (60 : 15 : 25), III) n-butanol:n-propanol:

---

* The presence of 0.01 M potassium phosphate resulted in a considerable amount of salt when these samples were dried. Equilibration of the G-50 column with < 1 mM potassium phosphate buffer might prove more satisfactory in this regard.

ethanol:25% ammonium hydroxide:water (40 : 40 : 10 : 45 : 15),

IV) toluene:chloroform:dimethyl formamide (4 : 4 : 1).

INSTRUMENTAL METHODS

Fluorescence Measurements

These were made with the lab-assembled fluorimeter described in Chapter 2. Fluorescence of flavins absorbing in the 450 nm region was routinely excited with the monochromator (5 mm slits) in tandem with the Baird Atomic interference filter. For flavins not absorbing in this region, the monochromator (slits 1 or 2 mm) alone was used and the excitation wavelength was selected which gave the highest ratio of free flavin fluorescence signal to background.* Wratten filters #2E, 8, and 12 were used as emission filters and the one which gave the highest signal to background ratio was used. Standard 1 cm path fluorescence cuvettes (Hellma #111 QS) were used in the static analyses. The photomultiplier voltage was chosen so that the largest signal to be read during a titration was < 200 mV because this took fullest advantage of readout capability of the Keithley digital voltmeter. The time constant in static mode operation was typically 0.2 to 1 second. In the stopped-flow mode the photomultiplier voltage was chosen such that the largest signal during a shot was about half a volt. A practice shot was normally used to optimize the sweep rate and to select a time constant < 1/10 the reaction half time. When signal to noise quality was poor,

* For the binding studies, all flavins were excited in the region of their long wavelength maxima (Table VIII).

several shots were accumulated in the CAT and the average of the shots was analyzed.

Absorbance Measurements

Spectra were recorded using either a Zeiss DMR 21 or Cary 15 recording spectrophotometer. Measurements were routinely made at ambient temperature using 1 cm path cuvettes, except for protein absorption spectra in the 220 nm region where cylindrical cuvettes of path lengths 0.1, 0.5, and 1 mm were used.

Circular Dichroism (CD) Measurements

CD spectra were recorded at ambient temperature with a Durrum-Jasco UV 5 scanning spectropolarimeter equipped to measure circular dichroism and altered to include the Sproul Scientific SS-20 modification. Concentrations of the different flavin derivative holoproteins ranged from 8×10^{-6} M to 4×10^{-5} M. The choice of path lengths and instrument sensitivities used to record CD spectra depended on the absorbance of the holoproteins in the wavelength regions. A 4 cm pathlength cuvette and an instrument sensitivity of 6.06×10^{-5} ΔA/cm were used from 600 nm to 320 nm, while these were 1 cm and 6.06×10^{-5} ΔA/cm from 320 nm to 250 nm, 0.05 cm and 6.06×10^{-5} ΔA/cm from 250 to 220 nm, and 0.01 cm and 3.03×10^{-5} ΔA/cm from 220 nm to 190 nm.

The spectra presented here have been corrected for baseline non-ideality and were averaged from at least two scans made with appropriate time constants and scan speeds. The circular dichroic

absorption coefficient, $\Delta\epsilon$, is obtained from the measured difference in absorption between left and right circularly polarized light, $A_L - A_R = \Delta A$, according to Equation (9).

$$\Delta\epsilon = \epsilon_L - \epsilon_R = \frac{A_L - A_R}{C \cdot l} \qquad \text{Equation (9)}$$

where C is the molar concentration and l the pathlength in cm. The instrument was routinely calibrated with solutions of d-10-camphorsulfonic acid (65).

Scanning of Stained Gels

Designed to obtain a quantitative record of the relative intensity of stained bands in disc gels, a scanning device was constructed which can accomodate transparent slabs up to 5 cm long and 1 cm thick.

The scanner utilizes a homemade drive unit and gel holding assembly (below) in conjunction with a Gilford model 220 O. D. Converter. The simple drive unit consists of a Hurst model SM synchronous motor (30 rpm) mounted on a frame and coupled to a 3/16 inch diameter brass drive shaft by an "O" ring and pulley mechanism. The Gilford carriage positioning rod formerly in the thermostatted cell unit is removed and replaced by the 10 inch drive shaft, which is 10-32 threaded for 4 inches at the end opposite the pulley. By means of the 10-32 tapped nut in the carriage base which had previously permitted alignment of the cuvette in the light beam, the brass shaft couples to the cell carriage and drives it through the light beam. An auxiliary slit, 0.11 mm by 3 mm, made from two razor blades held on a 3.25

inch x 4.5 inch thin copper plate masks the collimated light beam to obtain higher band resolution. The copper plate rests between the carriage and the compartment wall next to the monochromator. The slit is horizontally centered on the plate and is 1.50 inches from the floor of the compartment.

The components of the gel holding assembly (Figure 23) are the carriage block, which has the dimensions of a standard four place cuvette holder, two double-channelled window clamps, and two windows. The parallel channels in the window frames are spaced to partially compress the cylindrical gel between the windows and thus a constant thickness and volume of the gel material is in the light beam throughtout the scan. The Gilford is operated on an absorbance scale suitable for a given gel, but the wavelength is chosen so that the maximum absorbance does not exceed 1.0. The Gilford is balanced on a clear portion of the gel.

Appropriate performance tests for an inexpensive, homemade device of this kind were deemed to be a) linearity of drive, b) reproducibility of scans, and c) constancy of stained band R_f values. a) How uniformly a sample is driven through the light beam was tested by taping a transparent ruler with index marks onto the carriage block and scanning. Linearity of drive was established to be better than 97% throughout a drive length of 4.5 cm. b) For the sake of convenience in comparing a series of gels, one wishes that scans be reproducible. A test of this criterion is to see how superimposable are the

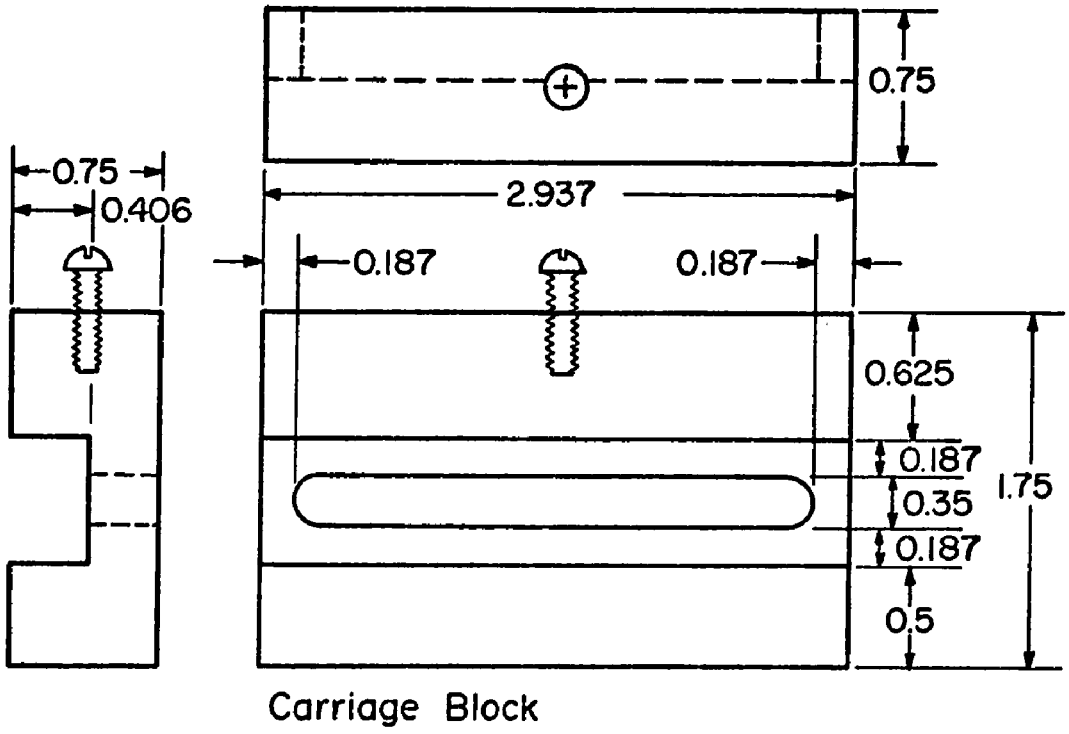

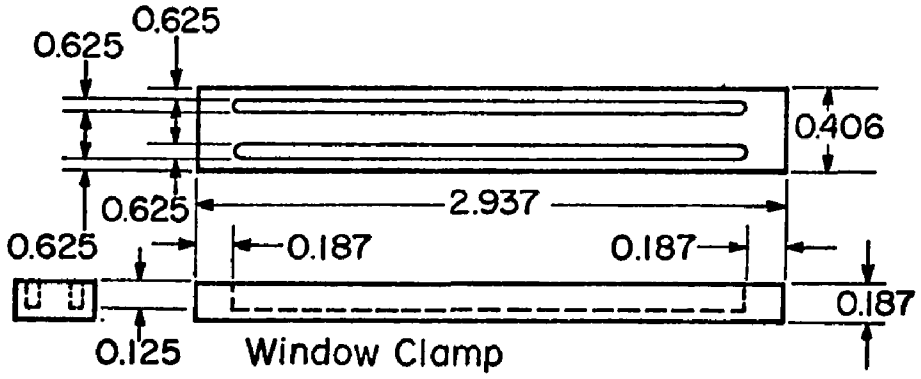



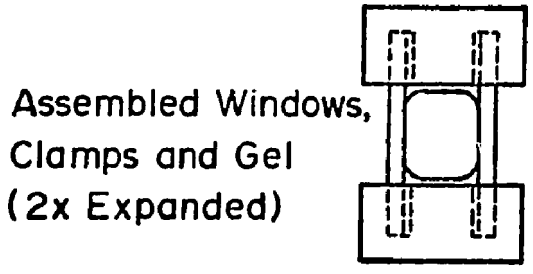

Figure 23. Gel Scanning Carriage, Window, and Clamp.

successive scans of the same sample. Scans of the ruler were recorded with a two hour lapse and with disassembly and reassembly of the apparatus between two series of scans. Reproducibility was better than 99%. c) this criterion is an attempt to test the scanning method under conditions more closely approximating actual working conditions. Greater than 99% reproducibility for the R_f value of RBP was obtained in the following two experiments. a) A series of scans was made in which one gel was scanned, removed, and rescanned. b) Scans were made of gels electrophoresed for different lengths of time (and therefore having RBP bands which had migrated different distances into the gels).

GENERAL MATERIALS

Riboflavin and FMN were obtained from Sigma Chemical Co., and FAD from Calbiochem. TARF was prepared by Dr. Graham Palmer. Deaza RF was the gift of Dr. Dale Edmundson. 8-Nor LF, 3 Bz LF, 8α hist LF, 3 Me, 8α Morph LF were the gift of Dr. Sandro Ghisla. The remainder of the flavin derivatives used in these studies were the gift of Dr. Vincent Massey and Dr. Franz Müller.

The DEAE cellulose was Schleicher & Schuell and DE52 (microgranular DEAE cellulose) was purchased from Whatman. CM Sephadex A-50, SE Sephadex A-50, and Sephadex G-50 were purchased from Pharmacia. Biogel P-60 was obtained from Bio-Rad Laboratories. 20 cm x 20 cm TLC plates MN Polygram Sil G/UV_{254} (with

fluorescent indicator) and MN Polygram Sil G (without fluorescent indicator) were obtained from Brinkman. Dialysis tubing was purchased from Union Carbide Corp. and boiled in a dilute EDTA solution then washed with glass distilled water before use. Millipore filters of 5, 0.8, 0.45, and 0.22 micron pore sizes and Swinnex filter holders were obtained from the Millipore Corporation.

Acrylamide, N, N-methylenebisacrylamide and N, N, N', N'-tetramethylenediamine were obtained from Canalco. Ampholine 3-10 was purchased from LKB. Trizma (base) was purchased from Sigma Chemical Co. and bovine serum albumin from Armour. Other chemicals were reagent grade and all buffers were prepared using glass distilled water.

CHAPTER 4

RESULTS

SOME STUDIES ON THE PROTEIN

Two aspects of RBP homogeneity were examined: a) the homogeneity of the preparation in terms of the size, shape, and net charge, and b) the homogeneity of the preparation with respect to the flavin binding constant.

Consideration of Physical Homogeneity

One anticipates that protein contaminants in the RBP preparation will resemble RBP to a considerable extent in size and charge character because the isolation of RBP involves differential adsorption to ion exchange resins and separation by molecular sieving. Thus, the apoRBP preparation will consist of protein molecules with isoelectric points near pH 4.5 and molecular weights near 3×10^4 Daltons. Sensitive analytical techniques are available however, which distinguish among closely related protein species even if they differ by as little as a few percent in molecular weight (disc gel or SDS gel electrophoresis) or by as little as one in net charge (disc gel electrophoresis, gel electrofocusing).

In these techniques, the separated protein components are fixed and/or stained in the gels for visualization. In a given test the degree of homogeneity is determined by the fraction of total applied protein which appears in the major peak. These tests are semi-quantitative to the degree that the stained band intensity is proportional to the amount of protein in the band and to the degree that all protein species stain similarly. These criteria are considered in Figure 24 for the studies on RBP, where the relation between the amount of RBP applied to a gel and the scanned area of the peak is seen to be linear for amounts of protein below 25 ug. Different proteins are likely to stain with unequal intensity. However, comparison of the stained areas for 5 ug of BSA and 5 ug of RBP in Figure 24 shows the intensity of staining for the two proteins agrees to better than a factor of 2. Noting that as little as 0.5 ug of RBP was detectable and assuming non-homogeneous components stained no less than half so intensely as RBP, contaminants which represented as little as 1% of the total preparation should have been estimable when 100 ug of RBP were run per gel. However, I often found that applying this amount of protein overloaded the gel and caused broadened peaks. Thus, whenever overloading was a problem, tests for non-homogeneous components consisted of a series of gels to which a range of sample was applied, e.g., 100, 25, 2 ug/gel, where the smallest amount applied provided an internal standard for estimation of minor components.

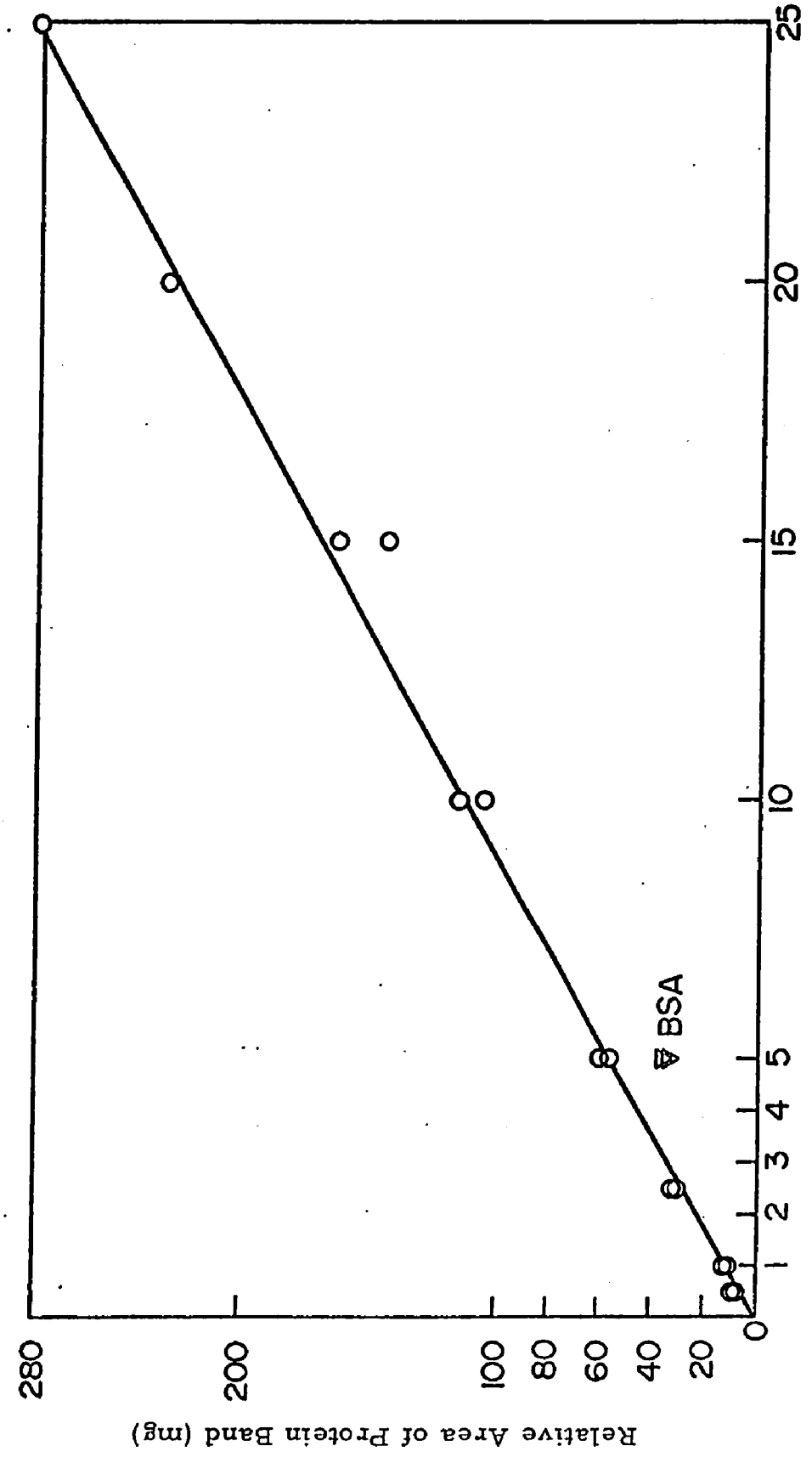

Figure 24. The Relation Between the Amount of RBP Applied to a Disc Gel and the Area of the Scanned Peak.

The absorbance of the stained bands at 600 nm was recorded as a function of distance migrated. The areas corresponding to the peaks were cut out and the weights in mg of the peaks were plotted on the ordinate axis.

The results of the analytical gel techniques used to ascertain the physical homogeneity of the RBP preparations are summarized in Figure 25. Photograph A demonstrates that the protein migrated in 10% acrylamide gel, pH 9, as a homogeneous peak and that non-homogeneous material comprised less than 2% of the total stained intensity. On electrophoresis of his RBP preparation at pH 9, Phillips (40) observed slower migrating minor bands and suspected that their relative proportion increased by exposing the protein to light during the isolation procedures. This observation had not come to my attention at the time I was isolating the protein so that the RBP electrophoresed in Figure 25A was prepared under normal room lighting - with no precaution being made to exclude light at the various preparative stages. The homogeneous behavior seen at pH 9 does not support Phillips' (40) hypothesis that his slower migrating proteins were products of the photodecomposition of the RBP.

Slightly heterogeneous behavior is seen on disc electrophoresis of RBP in 10% acrylamide gel at pH 6 (Figure 25, Photograph B). At this pH value, RBP is resolved into two components which differ slightly in mobility. Using a curve resolver on the recorded gel scans, the minor RBP component was estimated to be about 25% of the total stained intensity, while the two bands together represented about 98% of the total stained intensity. Electrophoresis of RBP at pH 6 was performed only once and observation of yellow color associated with the region of the 25% component was not ascertained. However, in

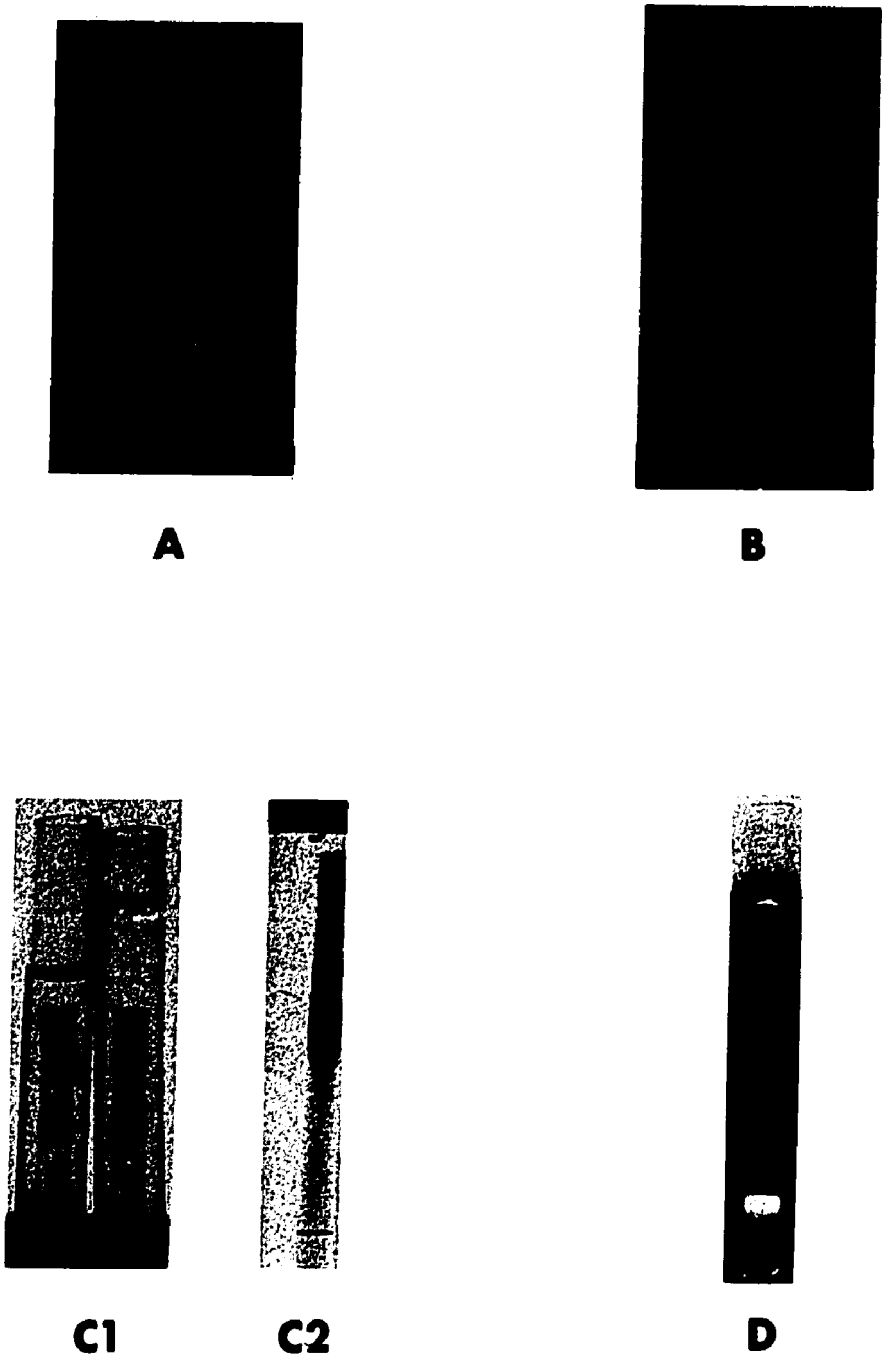

Figure 25A, B, C1, C2, D. Physical Homogeneity Studies of RBP. Disc gel electrophoresis at pH 9 (A), samples of 2, 10, and 100 ug/gel were stained with aniline blue-black. Disc gel ectrophoresis at pH 6 (B), samples of 6, 25, and 100 ug/gel were stained with aniline blue-black. SDS gel electrophoresis (C1 and C2), samples of 12 and 50 ug/gel were stained with aniline blue-black in C1 and 100 ug/gel was stained with Coomassie blue in C2. Gel electrofocusing of 50 ug of RBP (D).

light of the isoelectric focusing results below, both bands in Photograph B of Figure 25 are presumed to contain RBP. Verification of this point must await further investigation.

SDS gel electrophoresis of RBP in 8% acrylamide gels produced the results seen in Photographs C1 and C2 of Figure 25. The tiny dots seen near the tops of the gels in Photograph C1 were staining artifacts* and do not represent protein. The band trailing the major peak in Photograph C2 represents about 5% of the total stained intensity. Because this technique tests for protein homogeneity on the basis of size only, these results indicate that the sample electrophoresed was more than 95% homogeneous with respect to molecular weight. This method did not differentiate the two components which separated slightly on electrophoresis at pH 6.

The absence of stained intensity near the position of the copper wire inserted at the position of the bromphenol blue front in the gel in Photograph C2 indicates the absence of small molecular weight protein material in the sample electrophoresed, yet material of about 8,000 Daltons is expected on the basis of the studies of Phillips (40), Phillips, Mallette, and Clagett (66), and Cotner and Clagett (41). They found that RBP splits into two unequal fragments under reduction with 2-mercaptoethanol and alkylation with iodoacetamide; the larger subunit consisting of a glycopeptide of 24,000 Daltons and the smaller

---

* They were specks of amido black on the gel surfaces and were independent of the sample or amount electrophoresed.

subunit of a glycopeptide of about 8,000 Daltons. The fragments could not be dissociated in 8 M urea or in 5 M guanidine·HCl. Clagett (67) proposed that the two subunits are covalently connected by two of the eight (37) disulfide bonds in RBP. The RBP samples which produced the results seen in Photographs C1 and C2 of Figure 25 were made 0.1% in SDS and 0.3% in 2-mercaptoethanol in 0.01 M Na phosphate, pH 7.0, and dialyzed 24 hours against the same buffer. It is likely that this treatment would have separated two subunits linked only by disulfide bonds and that the two subunits would then have separated during electrophoresis. If the two fragments stained with equal intensity on a weight basis, a band containing 25% of the total stained intensity in Photograph C2 of Figure 25 should have been apparent near the position of the copper wire.

In order to eliminate the possibilities that the 8,000 Dalton subunit passed through the dialysis bag during the 24 hour incubation period or ran ahead of the bromphenol blue front and escaped off the end of the 8% acrylamide gels, the experiments were repeated under slightly different conditions. Samples of holoRBP, insulin, and spinach ferredoxin were prepared by one of the methods of Weber, Pringle, and Osborn (59): solutions of the proteins in 0.9% SDS, 0.9% 2-mercaptoethanol, 0.2 M Na phosphate, pH 7.0, were heated to 100° for 5 minutes. Additional samples of RBP were prepared in which the heat treatment was limited to 2 minutes or eliminated and replaced by incubation at room temperature for 12 hours. The flavin

in the RBP samples showed intense yellow-green fluorescence on excitation with an ultraviolet lamp - indicating that protein denaturation in the region of the binding site had occurred. The protein samples were applied onto 15% gels containing 0.1% SDS, 0.1 M Na phosphate, pH 7.2, and electrophoresed until the bromphenol blue fronts had migrated about half the length of the 7 cm gels. The gels were stained for 6 hours in Coomassie blue and electrophoretically destained. The gel containing 20 ug of insulin (two peptide chains of total molecular weight 5,700 Daltons) showed a broad band near the copper wire inserted at the position of the front. The gel containing 10 ug of spinach ferredoxin (one peptide chain of 10,600 Daltons) showed a sharp band with R_f about 0.6. The gels containing from 20 to 50 ug of RBP showed a single intense band with R_f less than 0.3 and no stained intensity in the region of an 8,000 Dalton peptide chain. These results indicate that the RBP molecule is unlikely to contain 2 peptide subunits covalently connected by disulfide bonds.

Photograph D of Figure 25 shows the results of gel isoelectric focusing experiments with RBP. This gel was electrofocused for 3 hours before fixing and photographing. The slight heterogeneity seen in Photograph D confirms the slight charge heterogeneity found on gel electrophoresis at pH 6. In each of the several isoelectric focusing experiments performed on holoRBP, a yellow zone began to form after about 30 minutes at the position which later corresponded to the position of the fixed protein. Before the yellow color faded as the RF

diffused from RBP, the intensity distribution across the zone indicated that the major and minor bands in Photograph D of Figure 25 were both colored and therefore contained RBP.

I conclude from these results that the RBP used in the studies presented in this thesis consisted of a single polypeptide chain which is homogeneous in size but slightly heterogeneous in total charge.

Demonstration of Binding Homogeneity

It is possible that the apparent slight charge heterogeneity in RBP seen in the last section might cause or accompany differences in flavin binding among the differently charged protein species. Thus an attempt to fractionate the preparation on the basis of charge (by ion-exchange chromatography) might separate the species to a sufficient degree that fractions could be found to have altered equilibrium constants. This possibility was examined for apoRBP fractions eluted from a column of SE Sephadex by a salt gradient (Figure 26). The fractions were combined as indicated into fractions I, II, III, and IV and these fractions were used (along with a sample of a previous apoRBP preparation) to measure equilibrium constants for LF binding at 17° and 33° (Table VII). At a given temperature and within the limits of error, the binding constants for the apoprotein samples were the same. To the extent that the apoRBP molecules which differ in net charge are separable by ion-exchange chromatography on SE Sephadex, the results of the tests in Table VII indicate that the

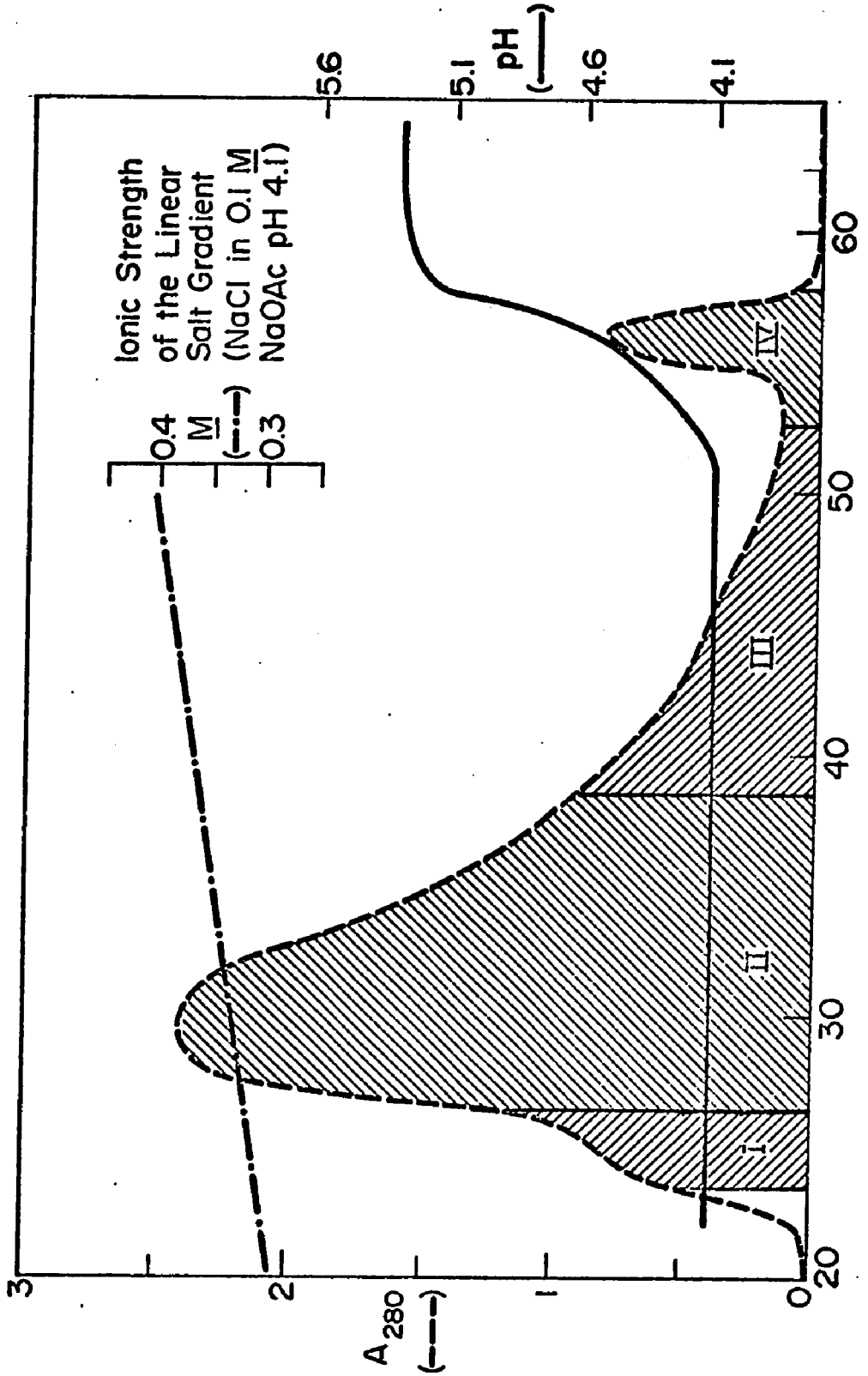

Figure 26. The Absorbances at 280 nm of the ApoRBP Fractions Eluted from a Column of SE Sephadex by Changes in Ionic Strength and pH Value.

The fractions were pooled as indicated and the pools were tested for binding capacity and homogeneity as described in the text.

TABLE VII

Test of Binding Homogeneity for ApoRBP Fractions Eluted from SE Sephadex

Fraction (Figure 26)	% of Total Eluted Protein Represented by Fraction	ϵ_{281}^{apoRBP} *	K_a^{LF} (17°)**	K_a^{LF}(33°)**
	%	$\underline{M}^{-1}cm^{-1} \times 10^{-4}$	$\underline{M}^{-1} \times 10^{-7}$	$\underline{M}^{-1} \times 10^{-7}$
I	3	5.5	4.7	1.2
II	62	4.9	4.7	1.0
III	23	5.0	4.9	1.1
IV	12	5.1	4.7	1.1
Previous*** preparation	--	4.9	5.0	1.1

* The absorptivity of apoRBP at 281 nm, ϵ_{281}^{apoRBP}, was determined by the method given on page 138.

** The equilibrium constant for the binding of apoRBP of LF, K_a^{LF}, was determined by the method given on page 148.

*** This is the apoRBP stock used to obtain the equilibrium binding energies in Table X.

differently charged apoprotein molecules are identical with respect to their binding properties.

The results in Table VII also show the stability of the protein with regard to binding. The sample labelled "previous preparation" had been stored for more than seven months at $4^{\circ}C$, yet within experimental error this sample gave the same K_a values for the binding of LF as were found seven months earlier (Table X) and the same K_a values for LF binding as were found using the freshly prepared apoprotein.

The values of $\epsilon_{281}^{\text{apoRBP}}$ are seen in Table VII to be slightly higher for fractions I and IV than the values of $\epsilon_{281}^{\text{apoRBP}}$ for the central fractions - presumably indicating the presence of protein in these side fractions which did not bind RF. For this reason the tails of the apoprotein peak eluted from SE sephadex were routinely omitted from the apoRBP stock used in the binding experiments and were added at a previous purification step in a subsequent preparation.

The second method of testing for binding homogeneity of the apoRBP preparation employed a Scatchard (29) analysis (Figure 27A, B). To obtain the data for this analysis, one of the reactants (RF) participating in the complex (holoRBP) was kept at a constant total concentration (except for dilution) and was titrated by incremental additions of the other reactant (apoRBP). Because the initial concentration of RF in these titrations was near the value of K_d for the complex, wide ranges in both $\bar{\nu}_F$ and $\bar{\nu}_A$ were covered, where

Legend to Figure 27A, B

Scatchard Analyses for Binding of RF by ApoRBP

Titrations at 25° consisted of additions of 9.6×10^{-8} M apoRBP* in 0.01 M potassium phosphate, pH 7.0 (buffer III), containing 1.7×10^{-6} M BSA**, to 3.00 ml of RF solutions of the stated concentrations in buffer III. Data have been corrected for dilution. The lines have been drawn to best fit the data and yet pass through the ordinate value of 8.6×10^{8} M^{-1}, the reciprocal of the mean K_d value, one K_d value being calculated for each of the data points in Figure 27A or 27B.

Data points	RF concentration before additions, M x 10^{10}	Average K_d value for the titration M x 10^{10}	Range in apoRBP concentration* represented by data points, M x 10^{10}
□	5.8	11.0	3.9 ⟶ 21.7
×	39.2	12.4	4.7 ⟶ 135.
△	29.5	11.4	4.7 ⟶ 135.
○	29.5	12.8	6.3 ⟶ 129.

* This is the concentration of binding sites as determined by the method on page 129.

** The presence of BSA was independently shown to have no effect on the titrations.

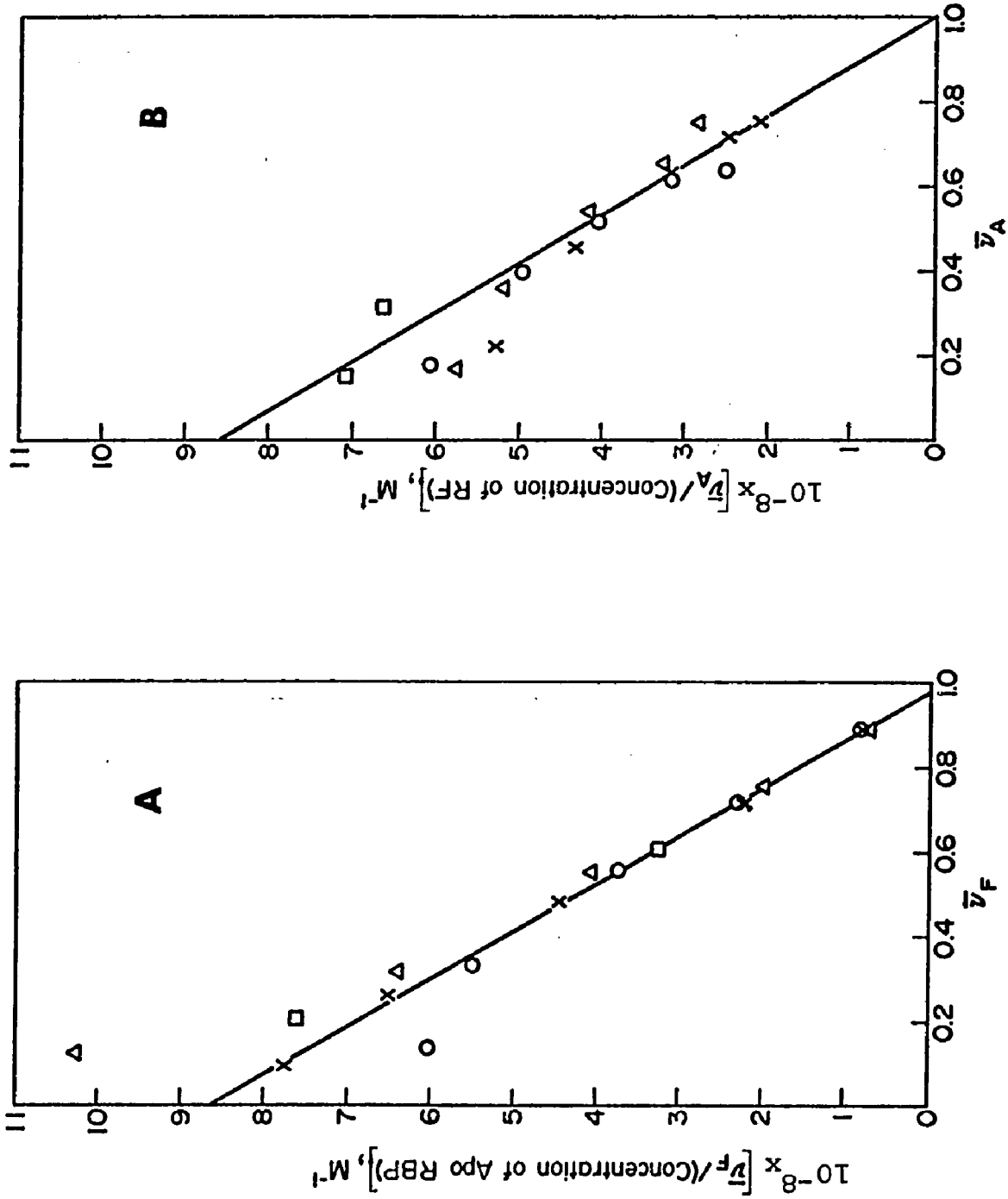
A
B
10^{-8} x [$\bar{\nu}_F$/(Concentration of Apo RBP)], M^{-1}
10^{-8} x [$\bar{\nu}_A$/(Concentration of RF)], M^{-1}
$\bar{\nu}_F$
$\bar{\nu}_A$
0
1
2
3
4
5
6
7
8
9
10
11
0.2
0.4
0.6
0.8
1.0

Figure 27A, B.

$\bar{\nu}_A = \frac{[H]_e}{[A]_e+[H]_e}$ and $\quad F = \frac{[H]_e}{[F]_e+[H]_e}$ in the nomenclature of the introduction*. This allowed Scatchard analyses to be made with respect to both $\bar{\nu}_F$ and $\bar{\nu}_A$. The higher data point scatter in Figure 27B than in Figure 27A results from the greater statistical error associated with measuring $\bar{\nu}_A$ than with measuring $\bar{\nu}_F$. ($\bar{\nu}_F$ is directly calculable from the fluorescence titration data, whereas $\bar{\nu}_A$ is obtained by several arithmetic operations on the titration data, and the operations tend to accumulate and compound the small errors.) The higher data point scatter for $\bar{\nu}_F$ values less than 0.3 and $\bar{\nu}_A$ values at the extremes is common (68) and results from the technical difficulties in measuring the small concentrations involved. Edsall and Wyman (30) have discussed the type of Scatchard analysis expected for binding to molecules A which have multiple binding sites with different intrinsic equilibrium constants. The curvature in the Scatchard plot which results in the multiple binding site case is strikingly evident. By analogy, a distribution of intrinsic equilibrium constants (i.e. non-homogeneity of binding) within the apoRBP population would also be expected to produce curvature in Scatchard plots (see Appendix C). The plot in Figure 27A is linear for $\bar{\nu}_F$ values between 0.2 and 0.9 and extrapolates to an x-intercept of 0.98. The data points in Figure 27B cover a range in the fraction of apoprotein sites complexed from 0.15 to 0.75. Although some scatter is evident, the data points in

---

* This formalism assumes binding stoichiometry is 1 : 1.

Figure 27B are well fit by a straight line with x-intercept equal to 1.0 and y-intercept equal to the reciprocal of the mean of the dissociation constants for all the data points. That these plots are linear over wide ranges in the fraction of reactant complexed and have x-intercept values of 1 indicates that the binding sites "counted" during the determination of the binding site concentration obey the same equilibrium constant for RF. ApoRBP is therefore homogeneous with respect to binding.

The plots in Figure 27A, B do not, by themselves, indicate 1 : 1 binding stoichiometry. Scatchard analyses often are used to determine stoichiometry, but in order to be so used, the plots must be based on the concentrations of molecular species participating in the binding reaction. The apoprotein concentration used in Figure 27 was the concentration of binding sites, not the concentration of apoprotein molecules. ApoRBP molecules with more than one site or even a population of apoRBP molecules with mixed numbers of sites would have produced intercepts of 1.0 - if each site was equivalent and independent. ApoRBP binding stoichiometry is considered on page 134.

Determination of the Molecular Weight of RBP

The molecular weight of RBP has been determined to be 32,000 Daltons by sedimentation studies and amino acid, sugar, and phosphate residue content (40). I estimated the molecular weight of my RBP preparation using SDS gel electrophoresis as described by Weber and

Osborn (60) under conditions which would have reduced all the disulfide bonds in RBP. The value of 30,000 Daltons I obtained (Figure 28) is in close agreement with the weight of apoprotein which binds one mole of RF (see page 134), but is not consistent with the hypothesis that RBP consists of subunits of 24,000 and 8,000 Daltons which are linked by disulfide bonds (40, 41, 66).

Determination of the Protein Isoelectric Point (pI)

I redetermined the pI value for RBP using the gel electrofocusing technique. A series of gels containing RBP were electrofocused simultaneously with the one fixed and photographed in Figure 25D. The gels were removed at intervals, sliced laterally into 3 mm segments, and each segment was equilibrated with 1 ml of 0.1 M KCl. Measurement of the pH value of the equilibrated segments resulted in the pH profiles of Figure 29. The position of RBP in the fixed gels indicated the protein has a pI = 4.5, a value slightly higher than that originally determined by Rhodes et al. (39).

Determination of ApoRBP Binding Site Concentration

Binding site concentration was routinely determined by titrating freshly prepared RF solutions with apoRBP and monitoring the quenching of flavin fluorescence (Figure 30). (Because RF dissolves slowly in aqueous buffers, fresh solutions were passed through 5 um Millipore filters and equilibrated in the dark before use.) In each of these titrations $[RF]_{total}$ was chosen to be much larger than the value of K_d. $[RF]_{total}$ was sufficiently large that 1) several

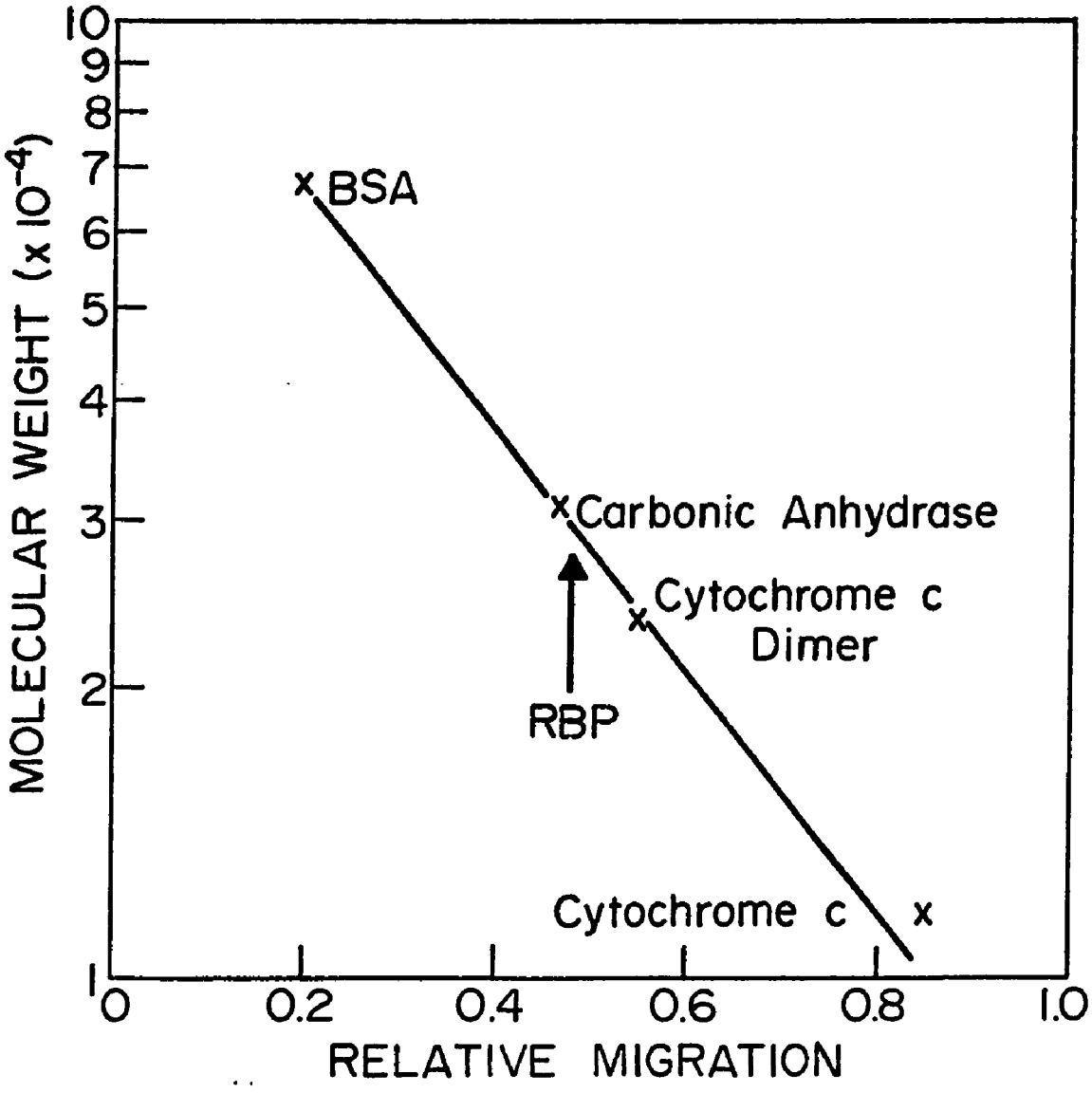

Figure 28. Determination of the Molecular Weight of RBP by SDS Gel Electrophoresis.

Samples were dialyzed against 0.1% SDS and 0.3% 2-mercapto-ethanol prior to electrophoresis on 8% acrylamide gels.

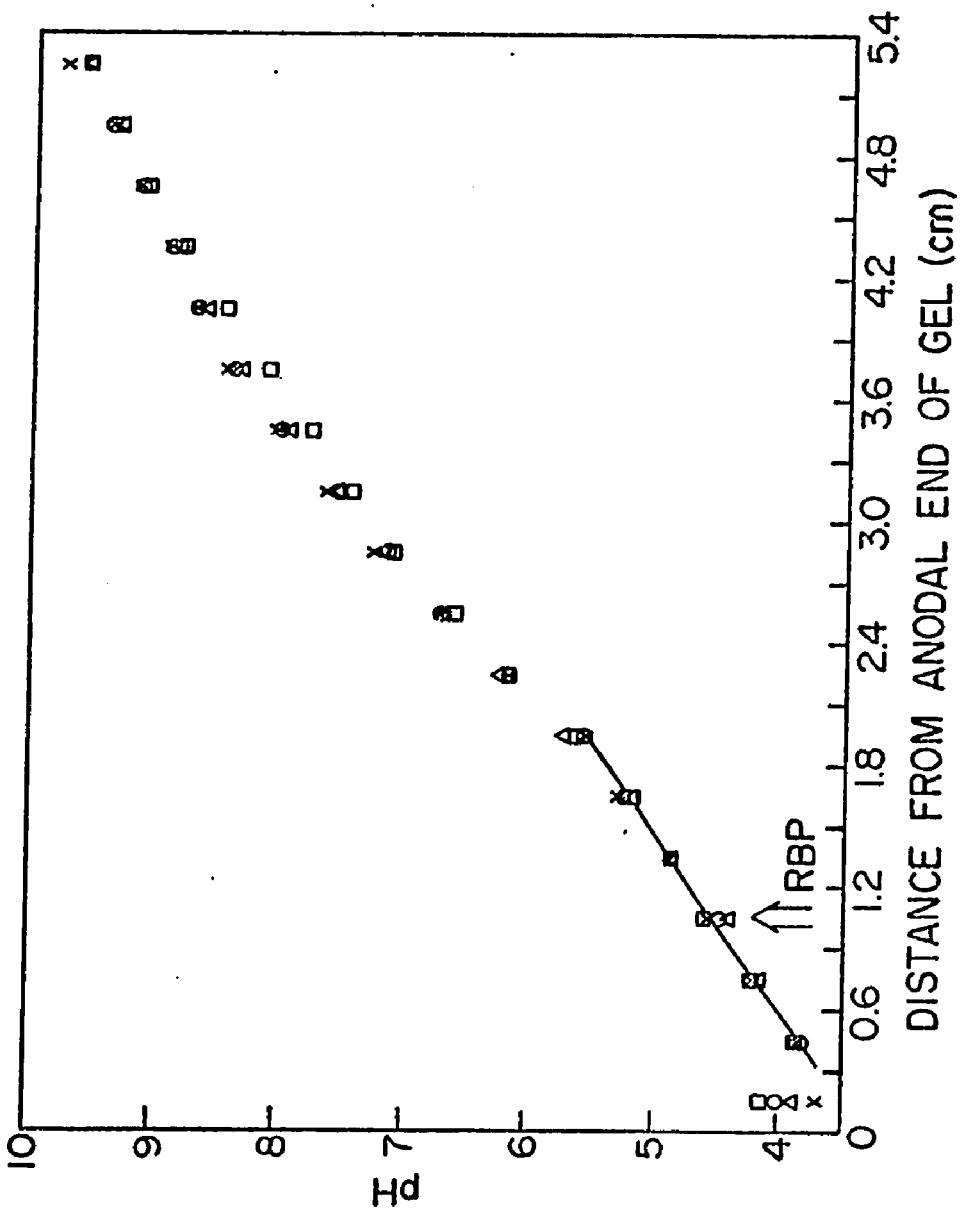

Figure 29. Determination of the pI of RBP by Isoelectric Focusing.
pH values of the gel segments after two hours (x), after 2.5 hours (o), after three hours (Δ), after 3.25 hours (□).

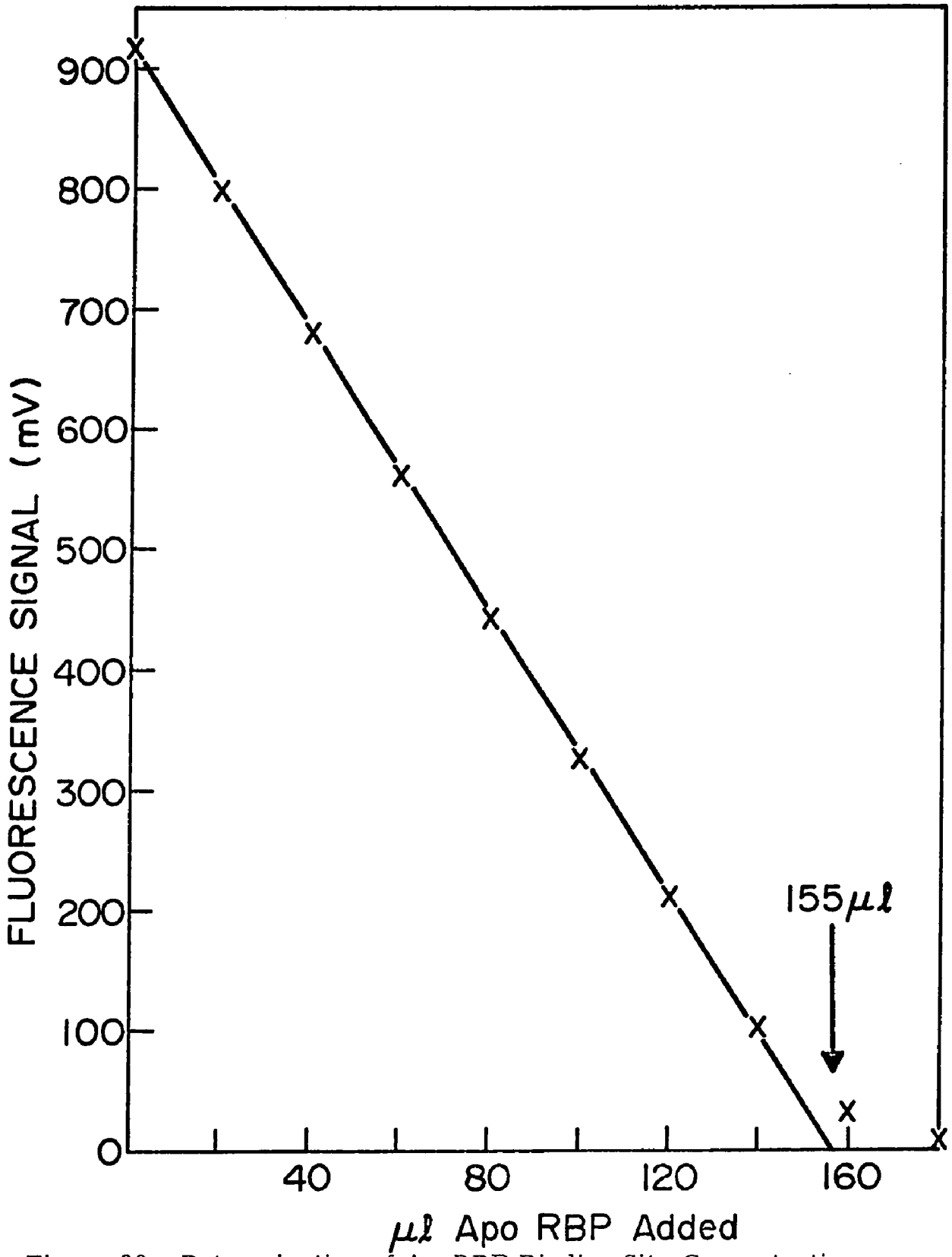

Figure 30. Determination of ApoRBP Binding Site Concentration. 3 ml of 1.25×10^{-6} M RF was titrated with stock apoRBP and the fluorescence signal corrected for dilution. The equivalence point corresponds to a binding site concentration of 2.42×10^{-5} M.

successive additions of apoRBP resulted in stoichiometric* binding of the added apoprotein, and 2) these additions of apoRBP quenched a large fraction of the initial RF fluorescence. At RF concentrations $> 10^{-6}$ M** and at 15°, the quenching of flavin fluorescence was linearly proportional to the volume of stock apoRBP added until the fluorescence had been reduced to less than 20% of the initial value. However, the last few additions of apoprotein in the experiment shown in Figure 30 produced fluorescence readings which fall above the line drawn through the initial titration points. The fluorescence values for the non-linear points correspond to the concentrations of RF free in solution expected on an equilibrium basis (Appendix B). By extrapolation of the linear portion of the titration to the abscissa, I determined the volume of apoRBP which contained the number of sites equal to the total amount of RF present in the titrated solution. Assuming a value for the absorptivity of RF at 444 nm, $\epsilon_{444}^{RF} = 1.25 \times 10^4\ M^{-1} cm^{-1}$ (69), one value for ϵ_{281}^{apoRBP} was determined per titration and the mean of ten titrations was found for each apoRBP preparation. ϵ_{281}^{apoRBP} was consistently equal to $4.9 \pm 0.1 \times 10^4\ M^{-1} cm^{-1}$.

---

* The working definition of "stoichiometric binding" was that at any instant > 99% of all possible complexes were in fact formed.

** Fluorescence studies performed on solutions of < 95% transmittance would usually require a correction for the reduction in transmittance. This correction was neglected in my studies because the free flavin and bound flavin solutions of the same concentration have approximately the same % transmittance in the excitation region. (Experimentally, titration of RF solutions of 99, 90, and 75% transmittance were found to yield the same concentration for stock apoRBP.)

Demonstration of 1 : 1 Binding Stoichiometry

As mentioned on page 128, the Scatchard analysis of Figure 27 did not demonstrate a 1 : 1 binding stoichiometry for RBP because binding site concentration was used in these plots. However, two kinds of evidence demonstrate that one mole of apoRBP binds one mole of RF. The first utilizes the RF fluorescence quenching results of Figure 30 to show that the gram molecular weight of protein necessary to quench the fluorescence of one mole of flavin is equivalent to the molecular weight of apoRBP determined by physical methods. The dry weight analysis of Palmer and Hunter (70) established the absorbance of a 1% solution of the apoprotein to be 17.0 cm^{-1} at 280 nm. The binding site molecular weight calculated from this is 2.9×10^4 Daltons*. The protein molecular weight as determined from sedimentation equilibrium studies (40) is 3.2×10^4 Daltons, while that determined from the SDS gel electrophoresis studies above is 3.0×10^4 Daltons. The agreement between these values indicates that one mole of apoprotein contains one mole of binding sites.

The evidence just presented demonstrates that each apoRBP molecule has one binding site with high affinity for RF. However, there is a possibility that a set of secondary binding sites with low affinity for RF also exists but is undetectable under the conditions used in

---

* The dry weight analysis was performed using a relatively less pure apoRBP sample than is obtained by the purification procedure in this thesis. This means that the binding site absorptivity at 280 nm for the apoRBP used by Palmer and Hunter (70) would be about 5.2×10^4 $\underline{M}^{-1} cm^{-1}$, which yields a binding site molecular weight of 3.1×10^4 Daltons.

Figures 27 and 30. Hypothetical sites which bind RF with quenching of fluorescence and have values of $K_a < 10^5 \underline{M}^{-1}$ would produce negligible (< 2%) (see Appendix C) deviation from linearity when $[RF]_{total} \lesssim 10^{-6} \underline{M}$ (e.g. Figure 30). Similarly, secondary sites with K_a values greater than $10^5 \underline{M}^{-1}$, but which bind without quenching of fluorescence, could also be consistent (see Appendix C) with the data observed in Figures 27 and 30. The existence of the latter set of sites seems to be contradicted by the observation that a sufficient excess of apoRBP added to a solution of RF essentially causes complete quenching of fluorescence. However, the difference in K_d values between $10^{-9} \underline{M}$ and, for example, $10^{-5} \underline{M}$ is probably sufficient for the high affinity sites to effectively partition all the RF molecules from the secondary sites under the conditions of these experiments: $[A]_{total} < [F]_{total} \lesssim 10^{-6} \underline{M}$.

A method more suitable than fluorescence titrations for detecting secondary sites of weak affinity is the method of continuous variation, attributed to Job (71). To use this analysis an observable must be found which is proportional to the concentration of the complex, rather than to one of the reactants, and this observable is plotted as a function of the relative mole fraction of one of the reactants. Making the critical assumption that any flavin bound to apoRBP will have a visible CD intensity of about the same order of magnitude as the CD intensity for the interaction with high affinity, the CD absorbance at 458 nm was chosen as the variable of study in the Job

analysis. Maximum CD intensity developed when the mole fractions of apoRBP and RF were 0,5 (Figure 31). This value convincingly demonstrates (72) the existence of one and only one RF binding site on apoRBP with a K_a value greater than about 10^3 $\underline{M}^{-1}$.

Other Studies on the Protein

I determined the sugar content in RBP by the method of Dubois, Gilles, Hamilton, Rebers, and Smith (73) using glucose as reference and found 9 ± 1 moles of equivalent glucose residues per 32,000 grams of RBP. (This method does not measure amino sugars.) The result is in good agreement with the value of 10 sugar residues per mole of protein obtained by Phillips (40).

Dr. Stephen Dinka kindly determined the sialic acid content of RBP for me by a modification of the method of Warren (74). Using pneumoccal neuraminidase in one instance and dilute sulfuric acid in another to release the sialic acid residues from the protein, he found that RBP contained 4.4 ± 0.6 moles of sialic acid per mole of protein. This value for the sialic acid content contrasts considerably with the value of 0.5 mole/mole (0.5% by weight) previously found by Feeney, Rhodes, and Anderson (75).

No lipid was detected in RBP using the Sudan Black B staining method of Sargent (76).

Many flavoprotein oxidases form adducts with sulfite producing altered visible absorbance spectra (77). When a 4×10^{-5} $\underline{M}$ solution of native holoRBP in 0.2 $\underline{M}$ tris Cl, pH 8.0, was made 0.1 $\underline{M}$ in

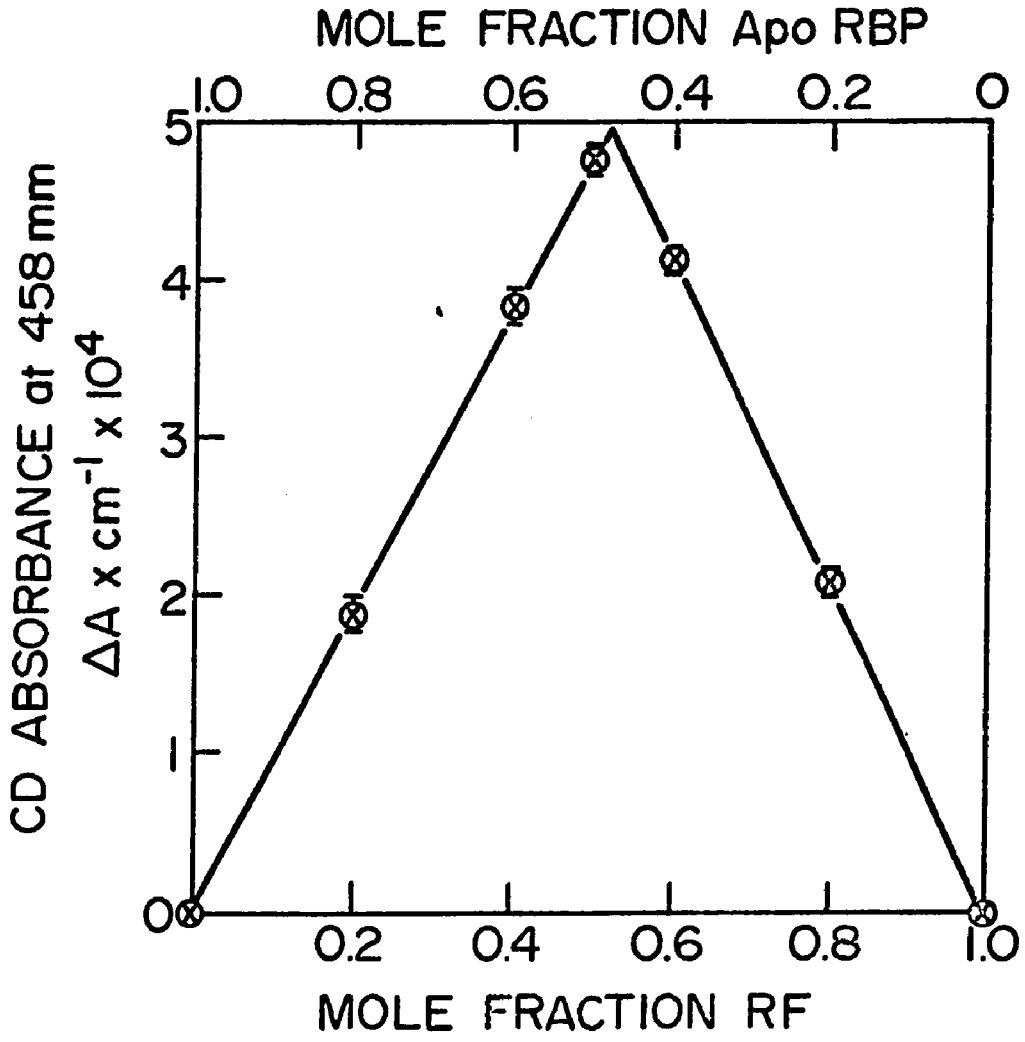

Figure 31. Job Analysis for Binding of RF by ApoRBP.

Mixtures were prepared from stock RF and stock apoRBP solutions of 1.20×10^{-4} M and the peak visible CD absorbances were recorded. The concentration of apoRBP was determined by fluorescence quenching titrations. (A similar Job plot would have been obtained had the concentration of apoRBP been determined on the basis of the protein molecular weight (40) and the weight absorptivity (70)). The concentration of RF was based on an $\epsilon_{444} = 1.25 \times 10^{4}\ \underline{M}^{-1}\,cm^{-1}$ (69). The CD signals have been corrected for the small CD intensity of RF at 458 nm.

sodium sulfite no change in the spectrum at wavelengths greater than 300 nm was observed over a 48 hour period. This result is consistent with the observation that the semiquinone form of RBP has the spectral properties of a dehydrogenase type flavoprotein.

ApoRBP in the presence of excess RF, FMN, or FAD lacked the ability to mediate reduction of cytochrome c in the presence of spinach ferredoxin when tested in the ferredoxin-TPN reductase activity assay of Foust, Mayhew, and Massey (78).

STUDIES ON THE FLAVIN ANALOGS

Determination of the Analog Concentrations

Having chosen the excitation and emission conditions which maximized the fluorescence signal/noise for the particular flavin analog being studied, its concentration was determined by a fluorescence quenching method similar to the one used to obtain the apoRBP concentration (Figure 30). Under the condition $[F]_{total} \sim 10^{-6}$ M (i.e. Figure 30) the fluorescence quenching titrations for many of the analogs curved after the first few apoprotein additions and the linear region corresponded to a relatively small proportion of the total fluorescence. However, as discussed in Appendix B, this behavior is just what is expected for a binding system described by Equation (1) when $[F]_{total}$ is not sufficiently large with respect to K_d. Moreover, to produce stoichiometric binding of half of the total flavin (resulting in the linear quenching of 50% of the fluorescence), $[F]_{total}$ must be

$> 100\ K_d$. For a majority of analogs this conditions was satisfied in the titrations used to calculate the analog concentrations. The linear region was maximized by performing the titrations at 10-15° and by employing the highest concentrations commensurate with solubility and solution absorbance. The volume of apoRBP in each addition was chosen so that the linear portion of the fluorescence quenching plot consisted of at least five points. A preliminary determination was made of the K_d for the analog at that temperature to assure that the conditions for stoichiometric binding had in fact been met. The analog concentrations determined by this method were used to calculate the absorptivities of the analogs at their long wavelength maxima (Table VIII).

Consideration of Analog Purity

TLC was the routine method of testing the flavin analogs for purity. Since all the flavin analogs studied were fluorescent, they were conveniently visualized after TLC by irradiation with the 366 nm or 254 nm lines from a mercury vapor lamp, whereupon the analogs appeared as bright spots on a dark background. The sensitivity of this fluorescent method was sufficient to detect fluorescent impurities in the flavin analog if the impurity represented more than 1% of the total sample, assuming the impurity and analog had the same quantum efficiency for fluorescence emission.

Non-fluorescent impurities which absorb at 254 nm were detected using TLC plates with fluorescent indicator, whereupon the

TABLE VIII

Flavin Analog Absorptivities

Analog	Absorptivity ($M^{-1}cm^{-1} \times 10^{-4}$) at wavelength	Number of titrations Averaged
RF	1.25 at 444 nm	(from Beinert (69))
LF	1.28 at 441	8
LC	1.15 at 356	5
10 EtOHF	1.25 at 443	4
TARF	1.19 at 445	3
FMN	1.24 at 445	(from Beinert (69))
FAD	1.13 at 450	(from Beinert (69))
3 MeLF	1.26 at 443	6
3 BzLF	1.30 at 444	3
3 OAc^-LF	1.25 at 445	2
3,4 dihydroRF	1.28 at 403	3
deaza RF	1.28 at 397	2
isoLF	0.83 at 447	3
7 ClLF	1.27 at 441	3
8 ClLF	1.34 at 439	2
diClLF	1.27 at 440	2
8 NorLF	0.99 at 444	5
10 MeIA	0.98 at 430	5
3 Me, 8 αMorphLF	1.4 at 448	2
1,3 diMeA	0.71 at 384	3
1,3,7,8 tet MeA	1.18 at 355	2
1,3,7,8 tet Me,4 OMeA	1.20 at 361	3

impurities appeared as dark spots on a bright field when the plates were illuminated with the 254 nm mercury vapor line. Detection of non-fluorescent impurities was not so sensitive as detection of fluorescent impurities because absorbance methods are inherently less sensitive than fluorescence methods. Moreover, quantitation of non-fluorescent impurities proved difficult because convenient estimation of the relative amounts of flavin analog and non-fluorescent impurity was not possible (e. g. by comparison of the relative absorbances of the spots at 254 nm) because the flavin analogs were fluorescent under these conditions and were usually brighter than the background fluorescence of the plate. As a consequence, amounts of non-fluorescent impurity smaller than about 5-10% of the total sample were not detectable without severely overloading the plates.

Figure 32 presents a typical TLC analysis of four derivatives chromatographed with solvent system II on plates with indicator and photographed under 254 nm and 366 nm illumination. The samples (purified RF, purified TARF, Sigma FMN, and crude LC) cover a range in purity. In comparison to the serially diluted samples run on plate 2, the samples on plate 1 are seen to be 98, 95, $\sim$ 90, $<$ 50% pure assuming the three left-hand derivatives contained no non-fluorescent impurities just below the level of detection. Overloading, a common occurrence, is seen in the FMN sample and to a lesser extent in the LC sample on plate 1. Table IX summarized the TLC analyses of all the flavin analogs used in the binding studies. The

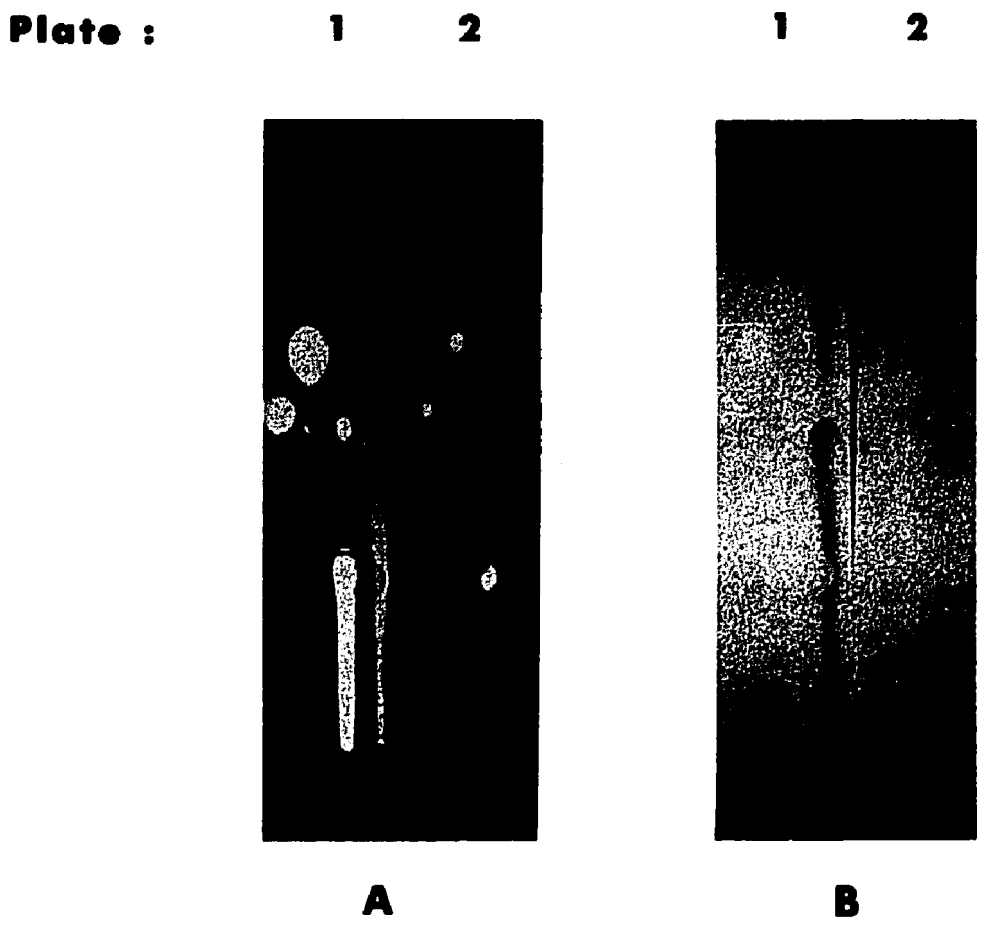

Figure 32A, B. TLC Analyses of Four Analogs

The same two TLC plates (1,2) are photographed with illumination at 366 nm (A) and at 254 nm (B). From left to right the samples applied to each plate were purified RF, purified TARF, Sigma FMN, and crude LC. The spot of each sample applied to plate 2 contained one-twentieth of the amount applied to the corresponding spot of plate 1. The two plates were developed with solvent system II.

TABLE IX

TLC Analysis of Analog Purity

Analog	Rf in Solvent System*				% Purity+	Presence of Nonfluorescent Impurity
	I	II	III	IV		
RF	0	0.57	0.61	0.03	>98	-
LF	0.31	0.53	0.74	0.39	>95	-
LC	0.27	0.92	0.91	0.85	>95	+
10 EtOHF	0.10	0.61	0.73	0.19	>95	-
TARF	0.30	0.73	0.87	0.65	93	-
FMN	0	0.30	0.32	0	95	-
FAD	0	0.04	~0.4	0	~ 90	-
3 MeLF	0.96	0.60	0.87	0.82	95	-
3 BzLF	0.85	0.85	0.95	0.90	>95	-
3 OAc LF	0.64	0.30	0.61	0	>85	+
3,4 dihydro RF	0	0.75	0.60	0.03	70	+
deaza RF	0	0.55	0.65	0.04	90	+
iso LF	0.39	0.56	0.70	0.63	94	-
7 ClLF	0.30	0.69	0.73	0.61	95	+
8 ClLF	0.04	0.72	0.74	0.82	>90	-
di ClLF	0.05	0.77	0.80	0.70	95	-
8 Nor LF	0.02	--	0.60	0.52	>90	-
10 MeIA	0.24	0.48	0.61	0.52	95	-
3 Me, 8 Morph LF	0.83	0.58	0.89	0.80	75	+
1,3 di MeA	0.90	0.89	0.87	0.83	>90	-
1,3,7,8 tet MeA	0.92	0.89	0.78	0.95	--	+

* Solvent systems: I) chloroform:methane (96 : 4), II) n-butanol: water:0.1 M dibasic potassium phosphate (60 : 15 : 25), III) N-butanol: n-propanol:ethanol:25% ammonium hydroxide:water (40 : 40 : 10 : 45 : 15), IV) toluene:chloroform:dimethyl formamide (4 : 4 : 1).

+ With respect to fluorescence homogeneity.

estimate of purity is based only on the fluorescent components; a separate column indicates the presence or absence of detectable non-fluorescent impurities.

Affinity Chromatography of the Analogs

Early in my thesis research, some analogs which had been judged of good purity by TLC were found a) to have absorbance peaks not common to the normal flavin spectrum, or b) to exhibit anomalous fluorescence quenching behavior when titrated with apoRBP.

a) the absorbance spectrum of the LF sample as originally obtained had a peak at 327 nm with $A_{327} > A_{444}$; however, no evidence for the substance absorbing at 327 nm was seen on TLC analysis. The ratio A_{327}/A_{444} was improved slightly by crystallization of the sample dissolved in formic acid after neutralization with sodium hydroxide*. Purines appear to have differential affinity for Sephadex, as indicated by the separation of allopurinol from alloxanthine during chromatography on G-25 Sephadex (79). To see if Sephadex would also show differential affinity for flavins and their impurities, the crude LF sample was passed over G-50 Sephadex. Figure 33 shows that indeed the flavin and the impurity were readily separated by this method. Both fractions eluted from the column behind the zone corresponding to the buffer in which the crude sample was dissolved - indicating that both the flavin and the impurity had affinity for the Sephadex.

* A method suggested to me by Dr. Franz Muller (63).

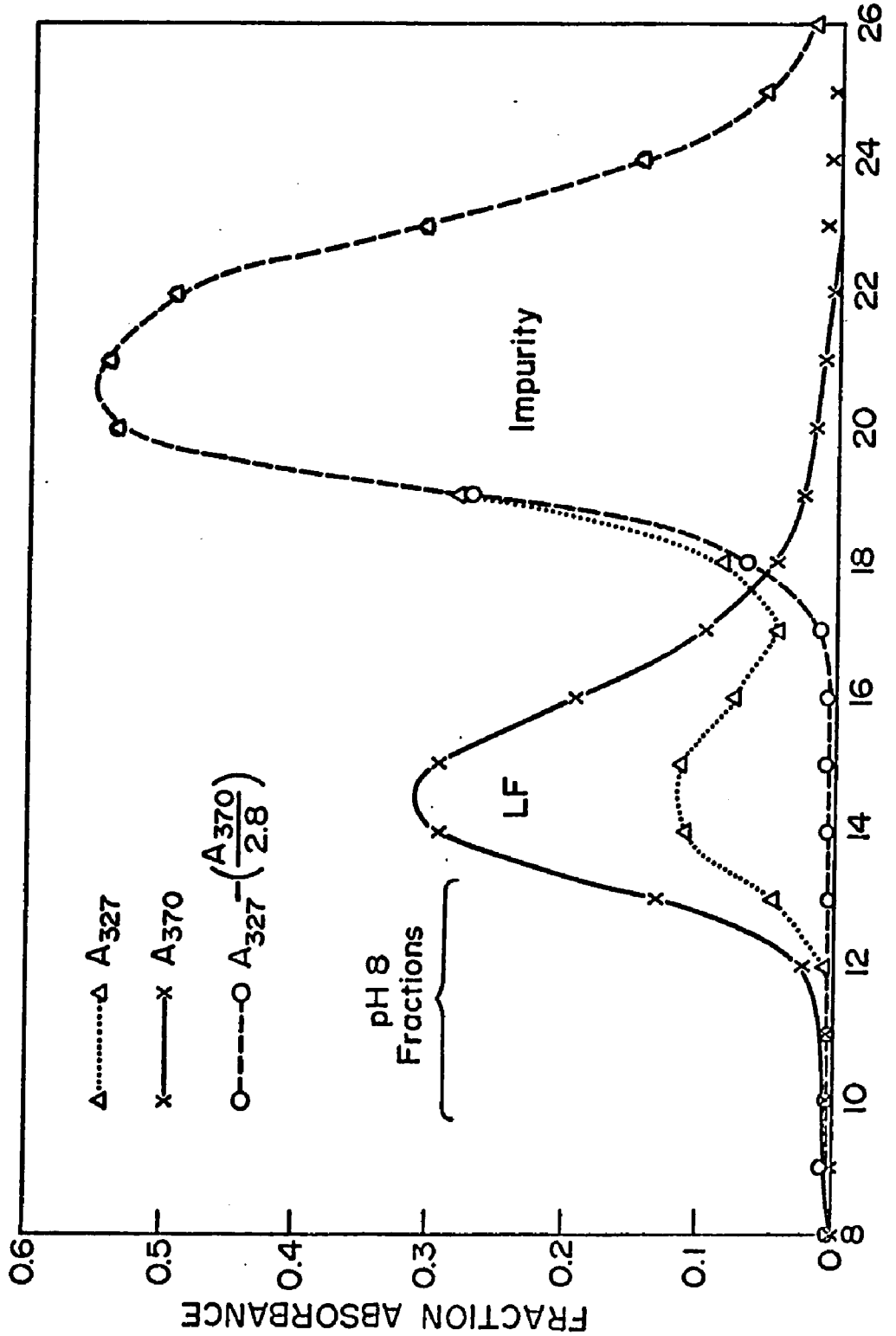

Figure 33. Affinity Chromatography of Crude LF on Sephadex.
10 ml of a crude LF sample dissolved in pH 8 buffer was applied to a G-50 Sephadex (fine) column and developed with 0.01 M potassium phosphate, pH 7.0. (o--o) represents an attempt to subtract the LF absorbance expected at 327 nm from that observed. The numbering of the fractions was arbitrarily started just before the flavin eluted.

Anticipating that the LF impurity would interfere* with the binding studies, no analyses were made with the unpurified LF sample. However, experiments inadvertently performed with impure isoLF samples directly demonstrated the effect an impurity can have on binding studies.

b) The starting isoLF sample (judged 95% pure by TLC analysis) gave curve a of Figure 34 when titrated with apoRBP in the stoichiometric binding analysis. After passing the isoLF sample over the G-50 Sephadex column, curve b was obtained. Two anomalies are apparent in titration a by comparison with titration b. The linear portion of titration a markedly differs in slope from titration b and titration a possesses a curvature or lag for the first few apoRBP additions. The difference in slope between titrations a and b could result from a non-fluorescent impurity which has no absorbance at 446 nm but which has affinity for apoRBP of about the same order of magnitude as isoLF**.

---

* The impurity is likely to be a starting reactant in the lumiflavin preparation, a side reaction product, or the product of an impurity in one of the starting reactants. To the extent that it resembled flavin, it could "consume" some apoRBP and therefore interfere with the binding studies.

** An unbound or weakly bound non-fluorescent species absorbing at 446 nm would cause titration a to have a steeper slope than titration b (rather than the shallower one observed) because of the normalization procedure used for the abscissa. Regardless of its absorbance at 446 nm, a non-fluorescent species which was much more tightly bound than isoLF would completely consume some of the initial additions of apoRBP and give rise to a titration with no initial quenching followed by a breakpoint and slope equal to titration b.

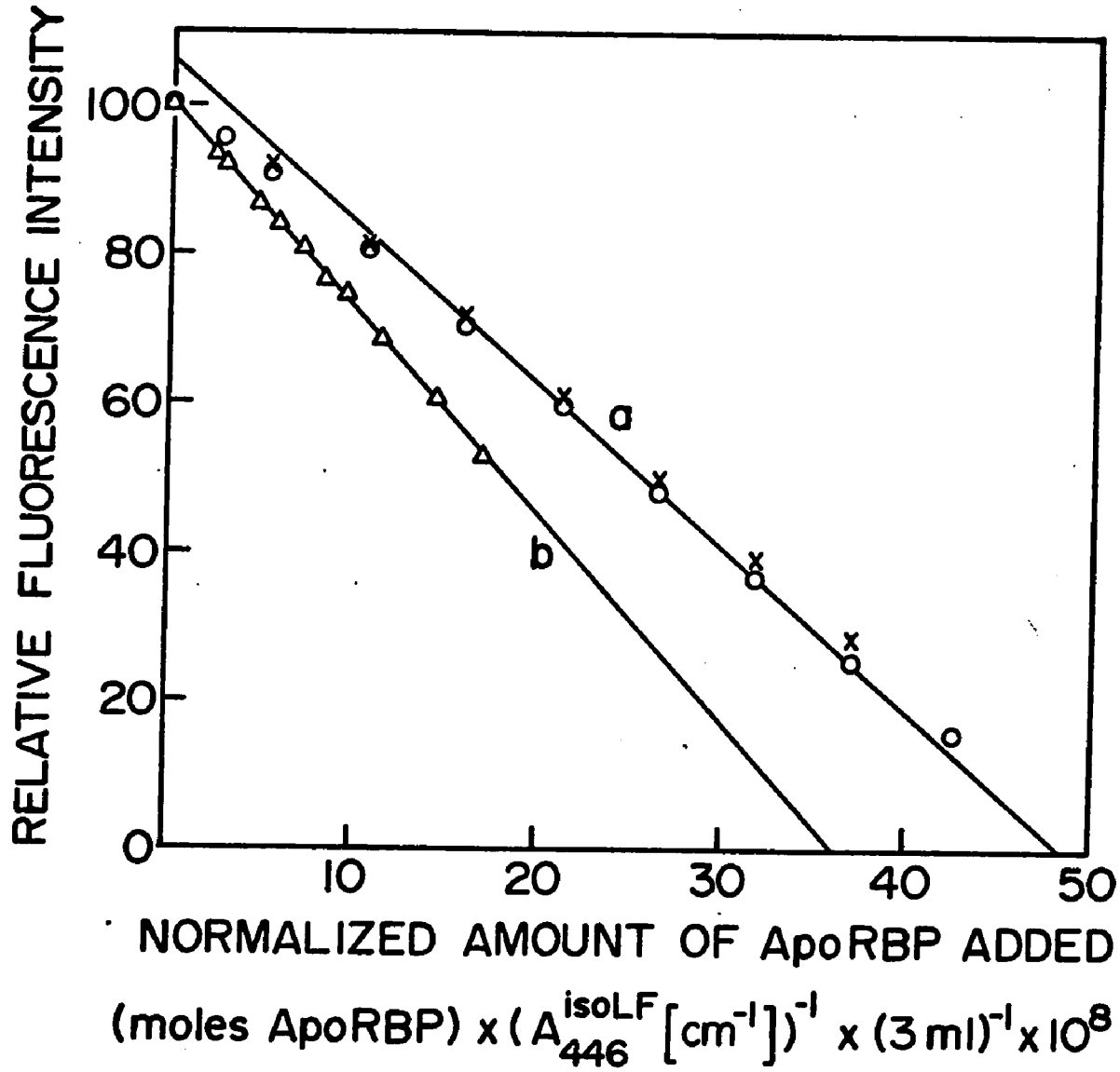

Figure 34. Stoichiometric Binding Analyses of Crude (a) and Purified (b) IsoLF.

Duplicate titrations for each sample were performed as described in the text. In order to compare the titrations for purified and unpurified sample (made under different conditions of concentration and photomultiplier gain), the axes have been normalized. The ordinate gives the percent of fluorescence (corrected for dilution) remaining after successive additions of apoRBP. The abscissa gives the cumulative moles of apoprotein divided by the absorbance at 446 nm of the isoLF solution (before titration) divided by the volume of the isoLF solution being titrated. The x-intercept is the reciprocal of the sample absorptivity at 446 nm. Note that the absorptivities of purified and crude isoLF samples differ by about 30%.

The appearance of a lag in titration a indicates that successively more flavin fluorescence is quenched with each apoprotein addition in this region, as if a non-fluorescent impurity (other than the one causing the anomalous slope) in the flavin has a greater affinity for apoRBP and is therefore preferentially consuming the flavin binding sites in the initial additions of apoRBP. The unpurified isoLF sample yielded absorptivity and concentration values about 30% smaller than those of the purified material. Further binding studies were not performed using the unpurified isoLF sample.

In order to avoid these complications, the flavin analogs used in the binding studies were routinely chromatographed on G-50 Sephadex - or other wise purified - prior to use. This affinity method was not useful in distinguishing among flavin species however, since a mixture of RF, LF, 3 Me LF, 7 Cl LF, and TARF only resolved into two poorly separated peaks.

EQUILIBRIUM STUDIES ON THE BINDING OF FLAVINS BY APORBP

Determination of the Equilibrium Binding Constants

As mentioned in the introduction, the studies of flavin binding to apoRBP were made possible primarily by the observation that while flavins free in solution are fluorescent, complexes with apoRBP are not*. Assuming that binding is the one-step equilibrium of Equation (1),

* The working criterion used to demonstrate that the analog-apoRBP complexes were non-fluorescent was to show that > 95% of the analog fluorescence was quenched by adding a sufficient excess of apoRBP.

an expression (Equation 11) for K_d results from substitution of the conservation Equations (10) into Equation (2):

$$[A]_{total} = [A] + [H]$$
$$[F]_{total} = [F] + [H] \qquad \text{Equations (10)}$$

$$K_d = \frac{\{[A]_{total} - ([F]_{total} - [F])\} \cdot \{[F]\}}{[F]_{total} - [F]} \qquad \text{Equation (11)}$$

Having previously determined $[A]_{total}$ and $[F]_{total}$ from stoichiometric binding titrations at high reactant concentrations, Equation (11) was used to calculate the K_d values for analog binding at sufficiently low total reactant concentrations that appreciable concentrations of both free and bound reactants were present in equilibrium. The one unknown quantity, [F], in Equation (11) was readily evaluated by comparing the fluorescence intensity produced by a known concentration of the analog with the fluorescence intensity remaining after successive additions of apoprotein. Each experiment consisted of a series of apoprotein additions designed to reduce the initial fluorescence intensity

---

The > 95% quenching criterion was met for all the flavin analogs studied, with three exceptions. The maximum percentage of fluorescence quenched for FAD; 3 Me, 8 α Morph LF; and 8 α Hist LF were 74%, 72%, and 19%, respectively. The difficulty encountered with the binding studies of these derivatives was the large value of K_d calculated in each case, i.e. extremely concentrated mixtures of analog and apoRBP would be needed to theoretically achieve > 95% quenching. From the behavior observed in the quenching titrations in which the above quenching percentages were obtained, I believe higher values would have been reached had more concentrated stock solutions of apoRBP been available. The K_d values for these derivatives were calculated assuming the complexes were non-fluorescent.

by 10, 30, 50, 70, and 85-90%. A simple computer program (see Appendix E) which corrected for dilution and background fluorescence was used to calculate the K_d value for each titration point. In addition to the K_d values, the computer printout included the concentrations of A, F, and H and the percent of the initial flavin fluorescence quenched for each titration point. The mean of the K_d values for a titration was used in the determination of each K_a value plotted in the van't Hoff analyses.

Figure 35 gives a) the results of an actual (typical) fluorescence quenching titration, b) the results expected for the ideal binding system (Equation (1)) under the conditions of $[A]_{total}$ and $[F]_{total}$ which actually obtained and which obeyed the mean of the K_d values calculated from the observed titration points, and c) graphical representations of the quantities $[F]_{total}$, $[A]_{total}$, [F], [A], and [H]. This figure reveals why the points for the small values of $\bar{\nu}_F$ in the Scatchard plot of Figure 27A have poorer signal/noise values than the other points. The absolute magnitude of the error in [F] is relatively constant for all data points. However, because [A] and [H] are determined by difference measurements involving $[F]_{total}$, $[A]_{total}$, and [F], the relative error in [A] and [H] is considerably larger for the data point corresponding to the first apoprotein addition than for all the others. This large relative error results in substantial "noise" in the determinations involving this data point.

Legend to Figure 35

The data points (o) give the relative fluorescence signals (corrected for background and dilution) observed in a titration of RF by apoRBP and correspond to the data points (o) in Figure 27A, B. Thirty µl of 2.99×10^{-7} M RF was added to 3.00 ml of 0.01 M potassium phosphate, pH 7.00, and titrated at 25° with aliquots of 9.6×10^{-8} M apoRBP in 0.01 M potassium phosphate, 1.7×10^{-6} M BSA, pH 7.0. The K_d values calculated for each apoprotein addition were:

Cumulative apoRBP added	Relative Fluorescence Intensity Remaining	K_d value (M) $\times 10^9$
(ul)		
20	0.862	1.42
50	0.670	1.22
100	0.443	1.18
170	0.280	1.21
470	0.114	1.38
	Average	1.28

The solid line is the theoretical quenching curve expected for $K_d = 1.28 \times 10^{-9}$ M, the average K_d value for the titration. The dashed line is the graphical representation of $([F]_{total} - [A]_{total})$. For fluorescence values > 0, this line corresponds to the fluorescence quenching curve expected if each apoRBP addition resulted in complete complexation of a corresponding amount of flavin - i.e. the stoichiometric binding curve. The length of the vertical arrows is equivalent to the concentration of the corresponding reactant species at the position of the arrow with respect to the x-axis.

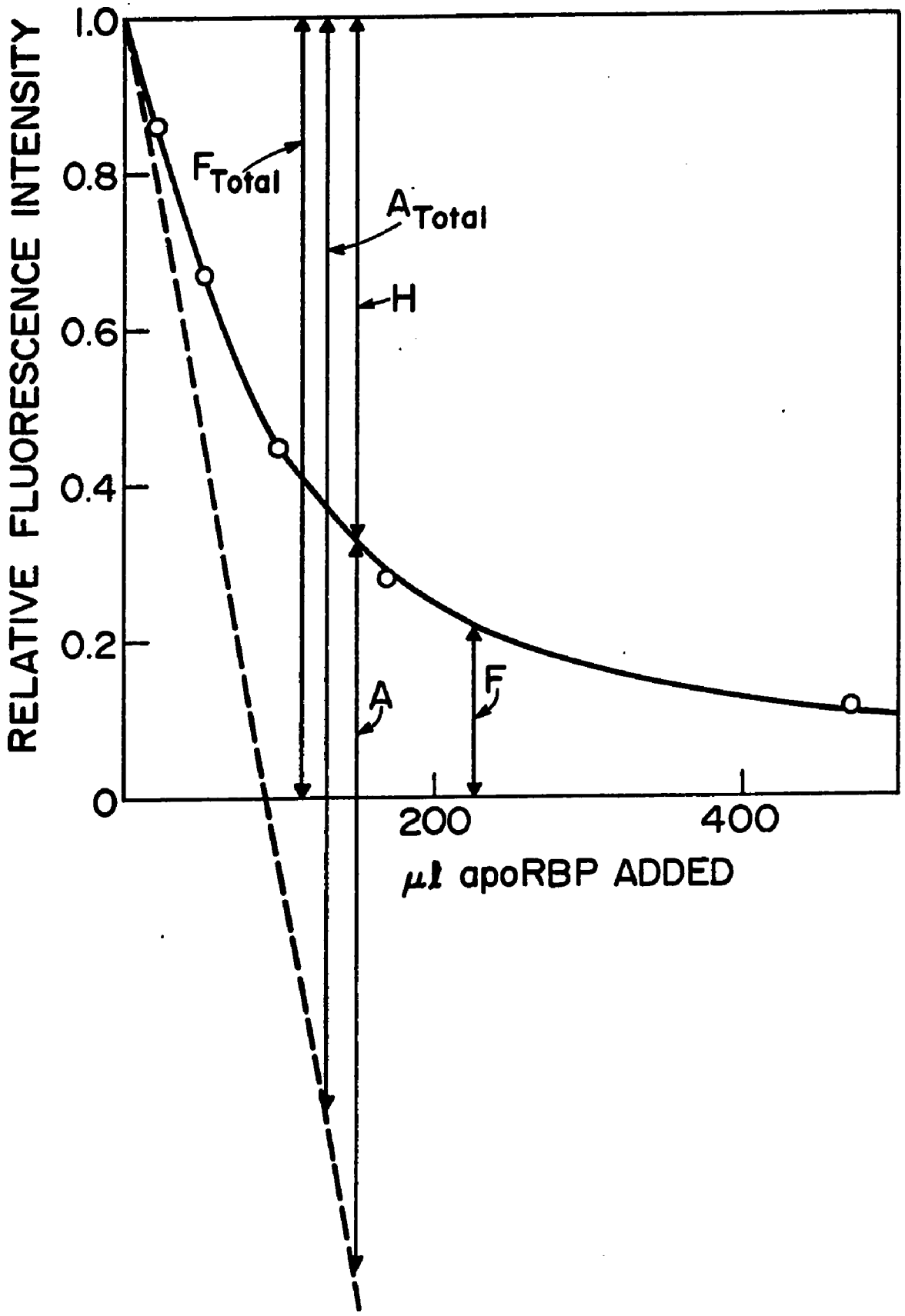

Figure 35. A Typical Fluorescence Quenching Titration.

Considerations of the Conditions Used in the Equilibrium Binding Studies

Averaging the K_d values for flavin binding over a wide range (10-90%) in the amount of the initial fluorescence quenched served two purposes. First the averaging process provided a statistically more reliable value for each K_d. Secondly, the method gave some qualitative information concerning the homogeneity of the flavin analog under consideration. This assumes that the results for the many analogs where relatively little variation* in K_d occurred over the quenching range from 10 to 90% of the initial fluorescence continued to indicate that the protein was homogeneous with respect to binding. A significantly greater variation in K_d over the 10%-90% quenching range observed for a given flavin analog was interpreted as indicating a degree of non-homogeneity in the analog (e. g. the 3, 4 dihydro RF sample, which appeared to be contaminated with RF).

Up to this point no mention has been made of the working concentrations of reactants employed in the quenching titrations. For the reasons discussed below, all the titrations used to obtain the K_a values plotted in the van't Hoff analyses were performed on flavin analog solutions satisfying the condition

$$K_d < [F]_{total} < 3\,K_d .$$

---

* Minor variations were often observed. These variations amounted to the K_d values observed at 90% of the initial fluorescence quenched being 5 to 30% higher than the K_d value at 10 or 30% of the initial fluorescence quenched.

This required knowledge of the approximate magnitude of K_d over the temperature range 10-40°. Therefore preliminary titrations (with $[F]_{total} \sim 10^{-6}$ M) were made at about 15 and 35°. The log $[(K_d)^{-1}]$ for the two titrations was plotted against 1/T and the straight line connecting the points was used to determine the approximate $(K_d)^{-1}$ values at selected temperatures between 10 and 40°. One stock solution of each analog was then prepared so that an addition of 5 to 100 ul of the stock to 3 ml of buffer would give a solution with $[F]_{total} \sim 2\ K_d$ over the entire temperature range. Because $[F]_{total} \sim 2\ K_d$, the volumes of stock apoRBP which needed to be added to give approximately 10, 30, 50, 70, and 90% quenching of the initial flavin fluorescence were easily determined using the protocol in Appendix B.

To have satisfied the condition $[F]_{total} \sim 2\ K_d$ may appear to have been a tedious approach because it required preliminary titrations to evaluate K_d. However, several arguments are put forward to justify this approach. The first argument is statistical. When $[F]_{total} = [A]_{total} = 2\ K_d$, the concentrations of all reactant species are equal: $[F] = [A] = [H] = K_d$. As a result of the equilibrium equation, the equivalence of all reactant concentrations means that the uncertainty in each concentration is the same, and this produces a minimum in the relative uncertainty in K_d. In the terminology of Weber (80), the condition of equivalent reactant concentrations corresponds to the point of "maximum information" content for a single determination of K_d. The condition $[F]_{total} \sim 2\ K_d$ also represents

the best compromise between poor signal to noise quality in the K_d value determined for the first few apoprotein additions if $[F]_{total} >> K_d$ on the one hand, and on the other, the large range in $[A]_{total}$ which would be required to achieve the range in fluorescence quenching from 10% to 90% of the initial value if $[F]_{total} < K_d$.

A second argument for satisfying a condition such as $[F]_{total} \sim 2\ K_d$ is that this kind of approach gives a consistent basis for comparison among the binding energies for all the analogs studied. Had all the van't Hoff analyses been performed at flavin concentrations which gave excellent signal to noise quality (e.g. at 10^{-6} M), some studies would have satisfied $[F]_{total} \sim K_d$ (e.g. FMN) while others would have satisfied $[F]_{total} \sim 10^3\ K_d$ (e.g. RF). As discussed in Appendix C, the equilibrium constants obtained with $[F]_{total} >>> K_d$ are sensitive to small percentages of impurities with low binding affinity in either the apoprotein population or the flavin analog population and the energies obtained could be greatly influenced by these weaker interactions. However, under the condition $[F]_{total} \sim 2\ K_d$, the equilibrium constants and energies would reflect the majority of interactions. A comparison of the energies for the different analogs obtained under different ratios of $[F]_{total}$ to K_d could be a comparison of different interactions from those intended. This same argument is true within a given van't Hoff analysis. Over the temperature interval from 10° to 40°, the value of K_d for an analog can vary by considerably more than a factor of ten. Were all titrations to be performed using

the same $[F]_{total}$ (e.g. ~ 2 K_d at 40°), the K_d value determined at successively lower temperatures could be progressively more influenced by a small percentage of either reactant with weaker affinity.

Certain trends in the equilibrium binding studies evaluated in this thesis indicated the possibility that one of the reactant populations contained a small percentage(s) of molecules with lesser affinity than the majority - even though this is counter to the evidence for apoRBP apparent in the linear Scatchard analyses of Figure 27A, B. These trends included a) the observation that the K_d value obtained for quenching 90% of the initial fluorescence for many analogs (but not all) tended to be 1.1 to 1.3 times as large as the values obtained at smaller percentages of the initial fluorescence quenched, and b) the preliminary van't Hoff plots for RF binding were non-linear (see Figure 38). The degree of this non-linearity amounted to the K_a values at 5° falling from 10 to 40% below the line drawn through the K_a values at 25° and 45°. Real curvature in these van't Hoff plots would indicate significant values of heat capacity for the reaction. However, as seen in Figure 40, the non-linearity was not real. As discussed on page 163, this artifact (non-linearity) may have partly resulted from using $[RF]_{total} \sim 5 \times 10^{-9}$ M in the determination of the K_a values plotted in Figure 38. Thus the ratio of $[F]_{total}$ to K_d was different at each temperature. The possibility that discrepancies a) and b) were caused by additional, as yet unidentified, systematic

errors has not been eliminated. Nevertheless, the justification for satisfying the condition $[F]_{total} \sim 2\ K_d$ is that if either reactant population has a slight degree of heterogeneity, this condition minimizes the effect the heterogeneity has on the binding results.

The Effects of pH and Ionic Composition on the Equilibrium Constant for RF Binding to ApoRBP

Before flavin binding to apoRBP was studied as a function of temperature, some preliminary investigations were undertaken to determine how buffer conditions affected the interaction. First, the equilibrium constant at 25° for the binding of RF to apoRBP was studied as a function of pH. The results of fluorescence quenching titrations in 0.1 M acetate, phosphate, and tris buffers in the range from pH 5 to pH 9 are shown in Figure 36. The K_a values for this interaction are nearly constant between pH 6 and pH 9 and are independent of the buffering agents tested. Also plotted in Figure 36 are the K_a values determined at other pH values from CD measurements. These K_a values were determined under the assumption that the CD intensity of the complex and of the free reactants is constant as a function of pH. Changes in ΔA_{458} were therefore assumed to represent changes in the relative concentrations of the reactant species in equilibrium. K_a could not be determined from CD studies at pH values below pH 3 because the CD spectra of the holoprotein solutions at these pH values were within the instrument noise level of the CD spectra which result from RF alone. Only upper limits to K_a could be

Legend to Figure 36

The pH Dependence of the Equilibrium Constant for the Binding of RF to ApoRBP at 25°.

Data points (x) indicate K_a values determined from fluorescence quenching titrations. These studies were made with $[RF]_{total}$ from 3 to 10 x 10^{-9} M in the following 0.1 M buffers: Na acetate from pH 4.8 to 6.0, K phosphate from pH 6.0 to 8.0, tris Cl from pH 7.0 to 9.0, and glycine Cl at pH 10.4. Data points (o) indicate K_a values determined from CD measurements. 0.1 M KCl solutions which contained equivalent RF and apoRBP concentrations from 3 to 8 x 10^{-5} M were adjusted to the desired pH value with 1 M HCl or 1 M NaOH. K_a values were determined from the CD absorbance at 458 nm assuming the holoprotein absorptivity was constant as a function of pH. See text for further details.

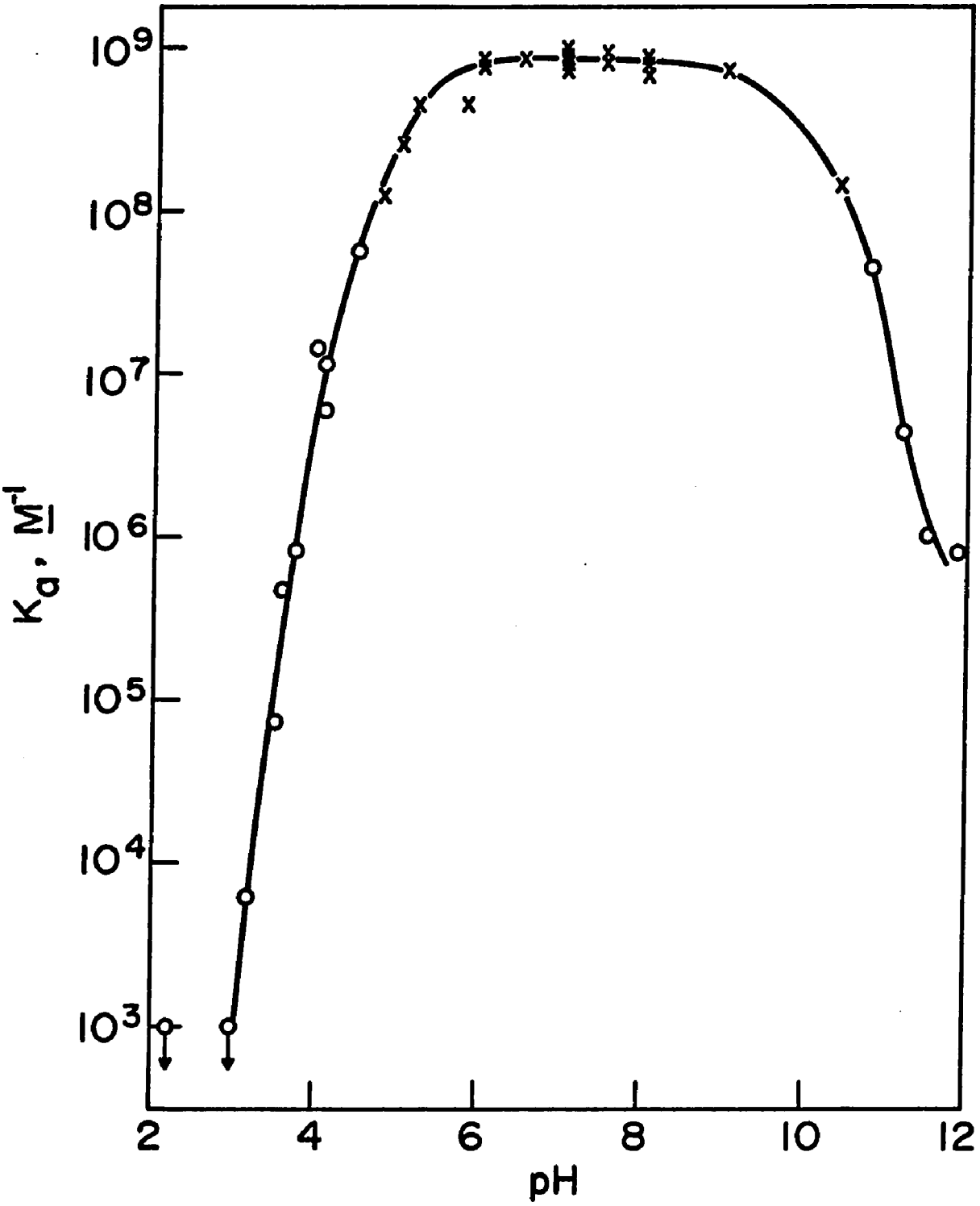

Figure 36.

ascribed at these pH values and are indicated in Figure 36 by (⚲). In similar manner, the CD absorbances of holoRBP solutions brought to pH values between 5 and 10 were identical* within the noise level of the instrument. Thus in this pH range only a lower limit (10^8 $\underline{M}^{-1}$) on K_a could be established. For clarity these points have been omitted in Figure 36. The dissociation of RF from apoRBP as a result of adjusting the solution pH to 2.2 or 11.9 was reversible. The original CD absorbance spectrum was recovered when the solution pH value was readjusted to neutrality.

The congruence of the fluorescence quenching data and the CD data in Figure 36 supports the assumption that the CD spectrum of holoRBP does not change as a function of pH. Additional evidence in support of this assumption is given in Figure 37 where the CD spectra of holoRBP solutions at different pH values are shown. In each case the total concentrations of RF and apoprotein were equal to 2.9×10^{-5} $\underline{M}$. The relative intensities of the CD maxima are the same in the three spectra, as are the shapes and positions of the peaks, indicating the absence of species with different spectral character from that of holoRBP at neutral pH values.

The next consideration of the effect of the buffer on binding was to determine how pH affected the temperature dependence of the equilibrium constant. Figure 38 shows the results of van't Hoff analyses

---

* Identical optical absorptivity and CD absorptivity spectra were obtained for holoRBP solutions in 0.1 $\underline{M}$ acetate, carbonate, phosphate, tris, borate, or glycine buffers in the pH range from 5 to 10.

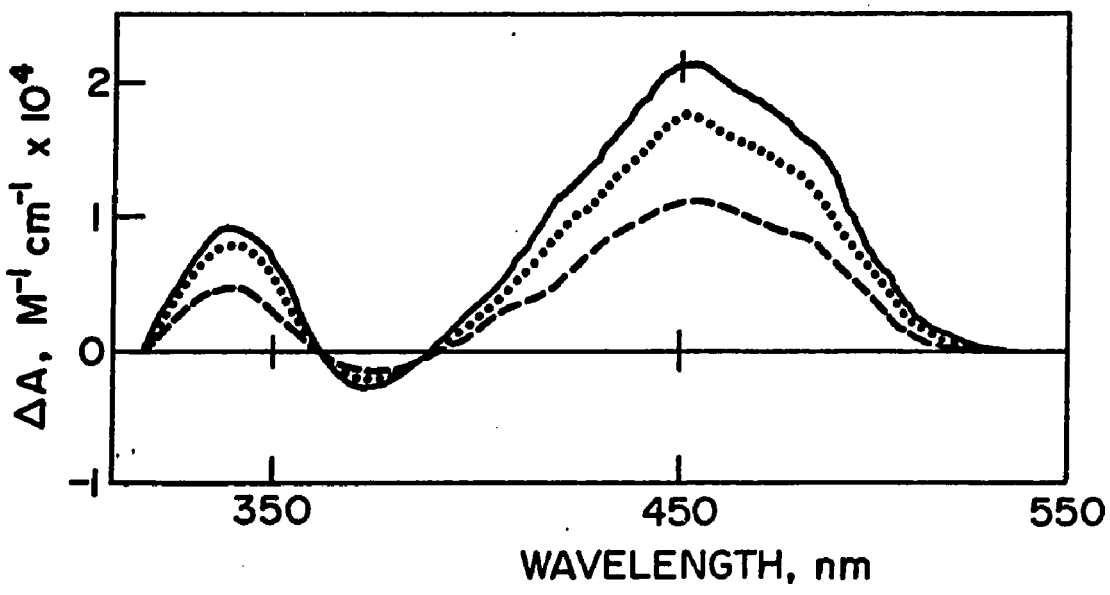

Figure 37. The CD Spectra of Solutions of HoloRBP at Different pH Values.

Unbuffered solutions of 2.9×10^{-5} M native holoRBP in 0.1 M KCl were adjusted to the following pH values and the CD spectrum recorded at room temperature: pH 3.5 (----), pH 11.9 (····), any pH value between pH 5 and pH 10 (——).

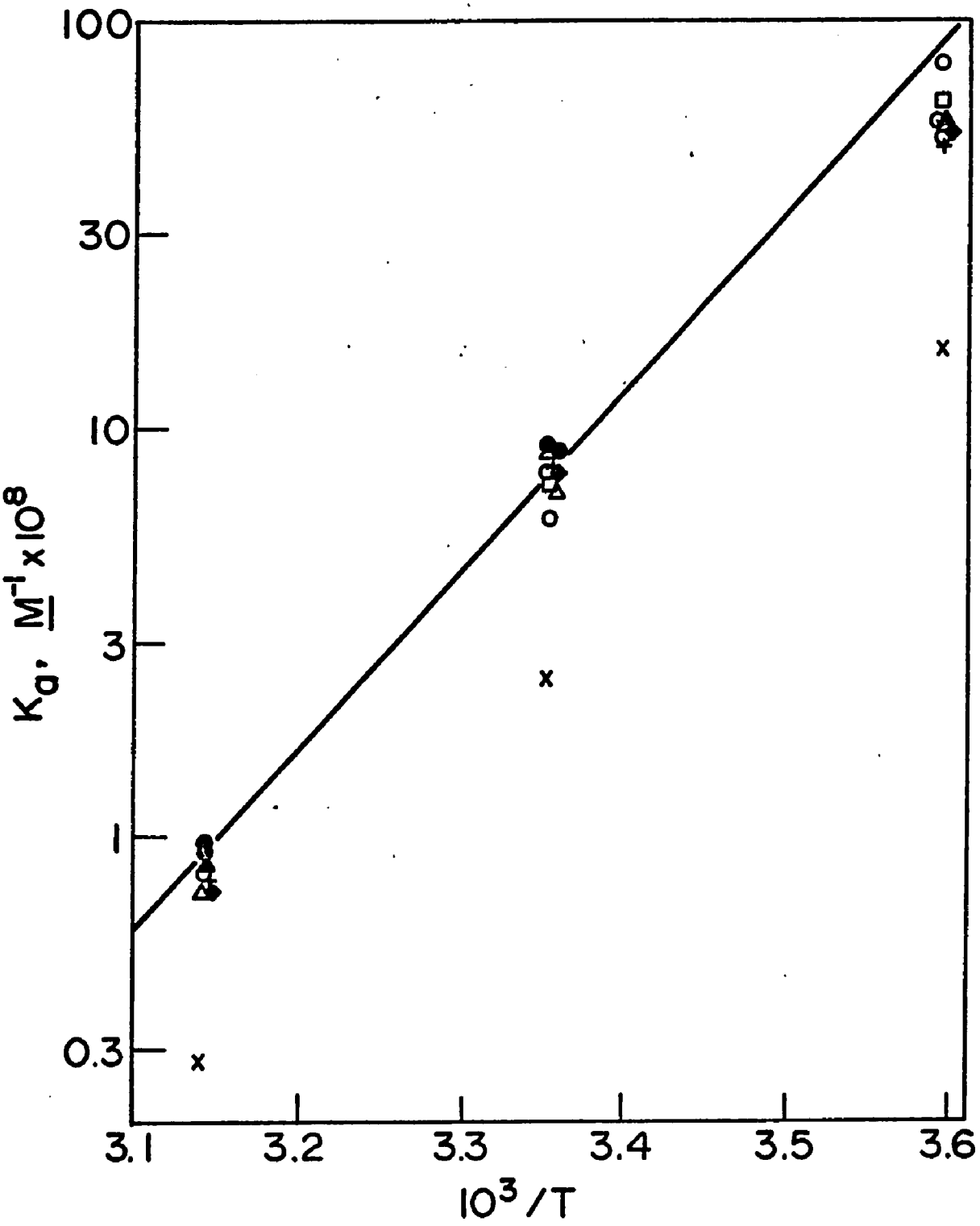

Figure 38. Van't Hoff Plots for RF Binding to ApoRBP at pH Values Between pH 5 and pH 9.

Data points indicate conditions of buffer and pH: x, + are for 0.1 M Na acetate, pH 5, 6; ♦, ●, ▲ are for 0.1 M K phosphate, pH 6, 7, 8; o, △, □ are for 0.1 M tris Cl, pH 7, 8, 9. The line shows the van't Hoff plot for RF binding to apoRBP in Figure 40.

(at three temperatures) for RF binding to apoRBP under different conditions of pH and buffering ions. The non-linearity of the plots was disconcerting when first observed and will be explained below. At the three temperatures the K_a determinations obtained at pH 5 differ markedly from the K_a determinations obtained at other pH values, and the latter are seen to fall in clusters. The important aspect to notice, however, is that the temperature dependence of the equilibrium constant at all pH values between 5 and 9 is quite similar.

The non-linearity in Figure 38 resulted from two factors. The first is that the determinations are made with $10\ K_d < [F]_{total} < 15\ K_d$ at 5°, $[F]_{total} \sim 3\ K_d$ at 25°, and $[F]_{total} \sim K_d$ at 45°, conditions which could cause a slight non-linearity if either or both of the reactants were slightly heterogeneous with respect to binding. This slight non-linearity gave the original stimulus to perform all the binding experiments with $[F]_{total} \sim 2\ K_d$. A second and more significant reason why the K_a values at 5° were too small to fall on a line drawn through the points at the other temperatures is that at the time of these experiments, I was unaware of the problem of the increase in fluorescence background as a result of lint accumulation in the cuvettes (page 83). The experiments at 5° in Figure 38 were performed with the photomultiplier at high gain and a significant error must have resulted. Because the van't Hoff plot was subsequently shown to be linear (Figure 40), and because the temperature dependence at the different pH values is clearly evident in Figure 38, the

experiments were not deemed important enough to be repeated with the background increases taken into account.

Some experiments were performed which examined the effect of ions on the binding of RF to apoRBP. The results of these experiments are summarized in Figure 39. Insignificant variation in the K_a at 25° for RF binding to apoRBP was found among fluorescence quenching in determinations 0.01 M or 0.1 M K phosphate, pH 7.0, in the presence and absence of 0.1 M KCl. The addition of solid KBr or $(NH_4)_2SO_4$ in sufficient quantities to bring the final concentrations to 1 M and 2 M caused no change in the observed CD spectrum of native holoRBP in 0.1 M tris Cl, pH 7.5. This established a lower limit of 1.4×10^8 M^{-1} for the K_a under these conditions.

The observation (19, 26) that flavins can be dissociated from flavoproteins by dialysis against KBr solutions at low pH value prompted a study of the K_a of RF binding to apoRBP as a function of the concentration of KBr. As already mentioned, KBr apparently had little effect on the binding at pH 7.5. However, Figure 39 shows that increasing concentrations of KBr dramatically decreases the K_a for the binding of RF to apoRBP at low pH values. NaCl has a similar but less dramatic effect at pH 3.8. These observations are consistent with the effect found by Mayhew (26) for flavodoxins. The relatively greater effect of Br^- than Cl^- is consistent with the order and approximate magnitude of the effect observed for O.Y.E. by Theorell and Nygaard (8). The interpretation is that Br^- tends to further destroy

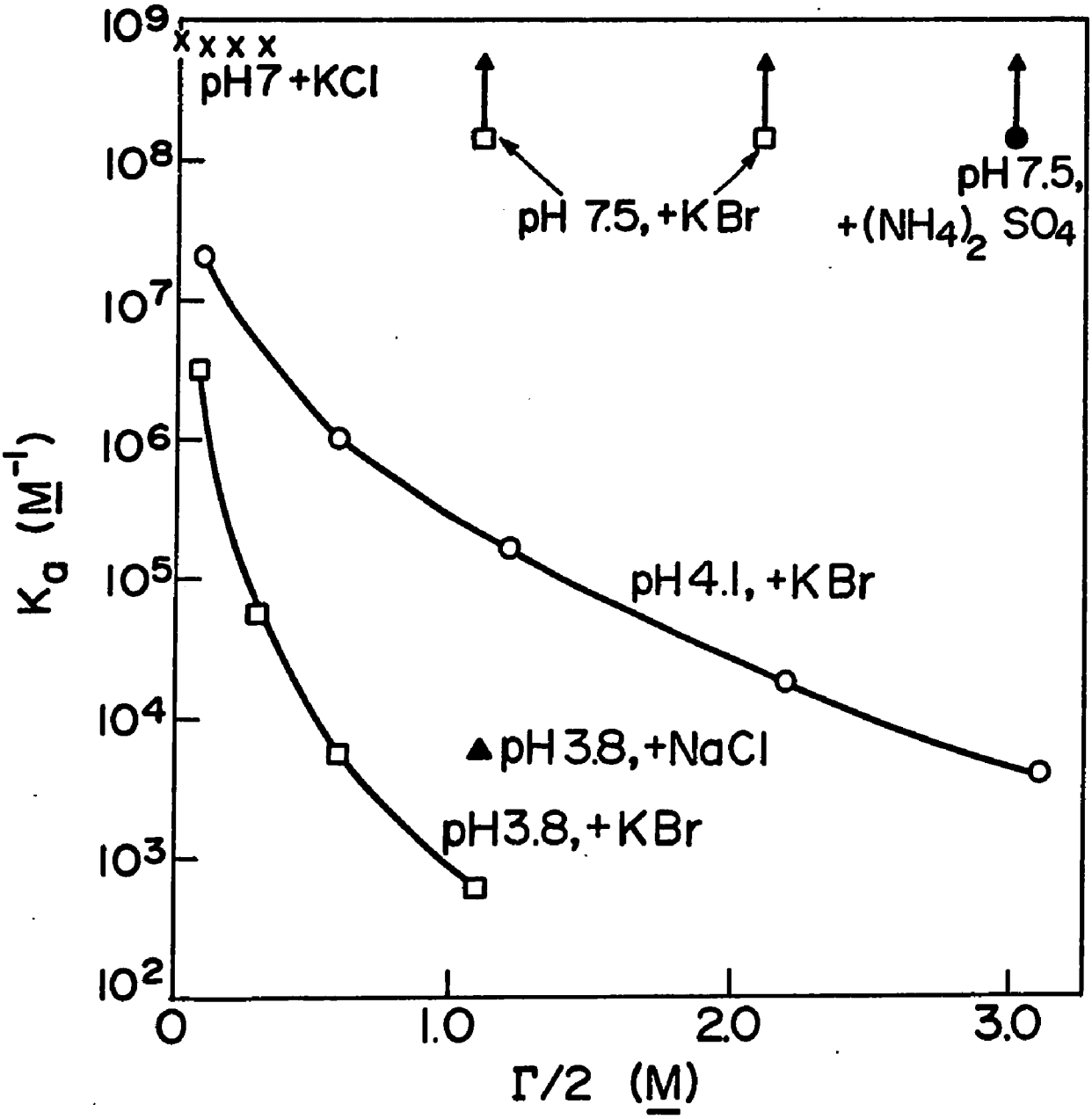

Figure 39. The Effect of Ionic Strength ($\Gamma/2$) and Anions on the Equilibrium Constant for RF Binding by ApoRBP.

(x) Fluorescence quenching studies done in 0.01 M K phosphate or 0.1 M phosphate, pH 7.0 with KCl added. (↑) CD studies at pH 7.5 using 0.1 M tris Cl. Neither KBr (↕) nor $(NH_4)_2SO_4$ (↕) changed the spectrum, thus only a lower limit on K_a was established. (O) CD studies in 0.1 M NaOAc, pH 4.1, with KBr added to give the final $\Gamma/2$ values. (□) CD studies in 0.1 M NaOAc, pH 3.8, with KBr added to give the final $\Gamma/2$ values. (▲) One CD study in 0.1 M NaOAc, pH 3.8, with NaCl added.

the integrity of the site in RBP after a sufficient number of critical electrostatic linkages have been broken by lowering the pH value to near or below the isoelectric point of the protein. Because RF is uncharged, the effects of salts at a low pH value, and of a low pH value itself, on the K_a for flavin binding to RBP can not be interpreted as the disruption of direct salt linkages between flavin and apoprotein suggested by Swoboda (25) as a general case for most flavoproteins.

Although the preliminary investigations (48) of flavin analog binding to apoRBP had been performed in 0.02 M tris Cl, pH 8.1, phosphate was selected as the buffering agent in the present studies for the following reasons. 1) The pK of tris is known to have a considerable temperature dependence (81), a property which could interfere with the determination of K_a as a function of temperature for those analogs (e.g. FMN) with a pK near the pH of the medium. 2) Of the common buffers acetate, phosphate, and tris, both acetate and tris would have interfered with CD studies because of their absorbance at wavelengths below about 220 nm. The concentration and pH of K phosphate used in the following studies was arbitrarily chosen to be 0.01 M and pH 7.00.

van't Hoff Analyses for Flavin Analog Binding to ApoRBP

Fluorescence quenching titrations for more than twenty flavin analogs were carried out over the temperature range 10 to 40°C and the logarithm of the average value of $(K_d)^{-1}$ was plotted against 1/T. The plots generally consisted of more than one titration at each of

at least five temperatures spaced over the temperature range. Representative examples of these van't Hoff plots are shown in Figure 40. No indication of curvature was observed for any of the analogs. Δ H for each analog was calculated from the slope of the line which "best fit" log $(K_d)^{-1}$ against 1/T. "Best fit" was determined by a standard least squares analysis which minimized the squares of the residuals, $([\log K_a]^{observed}-[\log K_a]^{line})^2$, using the computer program LINEAR in Appendix E. Error limits on each ΔH value were established from the 95% confidence interval on the slope of the "best fit" line. $\Delta G(25^o)$ was calculated from the value of K_a at 25° on the "best fit" line. Each error limit in $\Delta G(25^o)$ represents the relative standard deviation of the differences between the observed K_a values at all temperatures and the "best fit" line. $\Delta S(25^o)$ was evaluated using ΔH and $\Delta G(25^o)$ in Equation (6) and the error limit in ΔS was was set equal to the larger of the error limits in ΔH and $\Delta G(25^o)$. Both $\Delta G(25^o)$ and $\Delta S(25^o)$ were converted to the corresponding unitary quantities by correction for the cratic contribution (82): $\Delta S_u(25^o)$ is 8 e.u./mole more positive than $\Delta S(25^o)$ and $\Delta G_u(25^o)$ is 2.4 kcal/mole more negative than $\Delta G(25^o)$. Table X summarizes the results of the equilibrium studies on the binding of flavin analogs by apoRBP.

To a first approximation, the equilibrium energies for the binding of these flavin analogs by apoRBP are the same. All the energies within a given column have the same sign. The binding

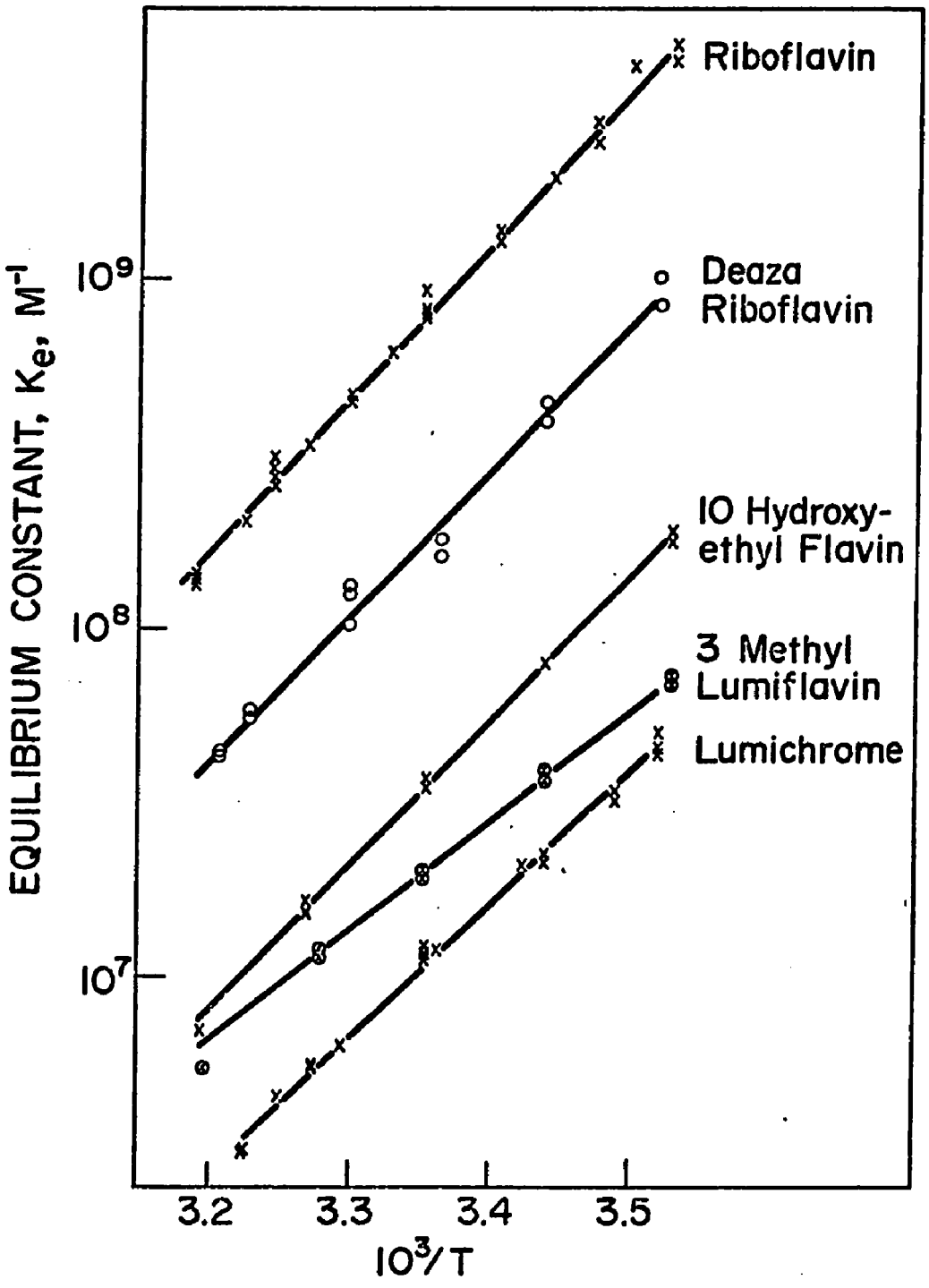

Figure 40. van't Hoff Plots for the Binding of Five Flavin Analogs by ApoRBP in 0.01 M K Phosphate, pH 7.00.

TABLE X

Equilibrium Energies for the Binding of Some Flavin Analogs by ApoRBP

Fluorescence quenching titrations were conducted in 0.01 M K phosphate, pH 7.0.

Flavin	$K_a(25^\circ)$	$\Delta G_u(25^\circ)$	ΔH	$\Delta S_u(25^\circ)$	$[F]_{total}^{(25^\circ)}$	Number of Titrations (points) in the van't Hoff Analysis
	M^{-1}	kcal/mole	kcal/mole	e.u./mole	M	
RF	7.9×10^8	-14.7 ± 0.2	-20.3 ± 0.2	-19 ± 1	2.9×10^{-9}	25
LF	2.13×10^7	-12.4 ± 0.2	-17.3 ± 0.1	-17 ± 1	9.3×10^{-8}	12
LC	1.08×10^7	-12.0 ± 0.2	-17.3 ± 0.2	-18 ± 1	2.6×10^{-7}	18
10 EtOHF	3.5×10^7	-12.7 ± 0.1	-18.7 ± 0.3	-20 ± 1	5.9×10^{-8}	10
TARF	5.3×10^5	-10.2 ± 0.3	-20.3 ± 0.3	-34 ± 2	1.9×10^{-6}	12
FMN	7.3×10^5	-10.4 ± 0.3	-20.1 ± 0.5	-33 ± 3	2.1×10^{-6}	11
FAD	$< 7 \times 10^4$	> -8	---	---	4×10^{-6}	--
3 Me LF	1.98×10^7	-12.4 ± 0.2	-14.6 ± 0.2	-7 ± 1	1.20×10^{-7}	10
3 Bz LF	1.05×10^8	-13.3 ± 0.2	-17.2 ± 1.0	-13 ± 3	3.1×10^{-8}	9
3 OAc^- LF	2.2×10^6	-11.1 ± 0.1	-14.8 ± 0.4	-13 ± 2	9.4×10^{-7}	7

3,4 dihydro RF*	3.6×10^{7}	-12.7 ± 0.3	-16.2 ± 0.3	-12 ± 1	5.7×10^{-8}	9
deaza RF	1.7×10^{8}	-13.7 ± 0.3	-18.9 ± 0.4	-18 ± 2	1.70×10^{-8}	14
iso LF	1.21×10^{7}	-12.1 ± 0.1	-15.4 ± 0.2	-11 ± 1	1.75×10^{-7}	10
8 Nor LF	2.10×10^{6}	-11.0 ± 0.1	-14.4 ± 0.2	-11 ± 1	8.4×10^{-7}	11
10 Me IA	2.7×10^{6}	-11.2 ± 0.1	-15.0 ± 0.1	-13 ± 1	5.0×10^{-7}	11
7 Cl LF	4.9×10^{7}	-12.9 ± 0.1	-18.1 ± 0.2	-18 ± 1	3.6×10^{-8}	11
8 Cl LF	1.23×10^{7}	-12.1 ± 0.1	-16.2 ± 0.1	-14 ± 1	1.51×10^{-7}	10
7,8 di Cl LF	2.4×10^{7}	-12.5 ± 0.2	-15.9 ± 0.4	-12 ± 2	9.4×10^{-8}	11
3 Me, 8α Morph LF	2.0×10^{5}	-9.7 ± 0.3	-17.5 ± 1.0	-26 ± 3	2.2×10^{-6}	5
8α hist LF	$< 5 \times 10^{3}$	> -7	---	---	8×10^{-6}	--
1,3 di Me A	2.5×10^{7}	-12.5 ± 0.3	-13.4 ± 1.1	-3 ± 4	2.23×10^{-7}	8
1,3,7,8 tet Me A	2.4×10^{7}	-12.5 ± 0.2	-17.1 ± 0.5	-16 ± 3	2.4×10^{-7}	9
1,3,7,8 tet Me, 4 O Me A	4.1×10^{6}	-11.4 ± 0.2	-15.1 ± 0.8	-12 ± 3	1.4×10^{-6}	8

* The values for 3,4 dihydro RF are subject to some uncertainty as a result of the apparent contamination of this analog with RF.

reactions all show favorable enthalpy changes and unfavorable entropy changes with resultant net favorable free energy changes in the direction of complex formation. The binding of any of these analogs to apoRBP results in $\Delta G_u(25^o) = -11 \pm 4$ kcal/mole, $\Delta H = -17 \pm 4$ kcal/mole, $\Delta S_u(25^o) = -18 \pm 16$ e.u./mole. Only from a detailed examination of the data are trends, correlations, and paradoxes apparent.

Consider first the analogs with modifications at the N 10 position. Comparing the data for LC, LF, 10 EtOHF, and RF, there is a trend toward more negative ΔH values with the increase in side chain length. This is accompanied by relatively constant ΔS_u values and results in more negative ΔG_u values as the residue on N 10 gets progressively longer and contains more hydroxyl groups. Hydrogen bonds or, at least, favorable interactions are implicated as the moiety on position 10 is lengthened in successive analogs. Comparing the results for TARF and FMN with those for RF, the ΔH values remain unchanged at about -20 kcal/mole, while a significant effect is observed in the ΔS_u values. As the bulkiness of the side chain increases (TARF) or as the chain acquires a bulky, negatively charged group (FMN), the ΔS_u value becomes considerably more negative. Because many effects are being added to give the net overall differences in ΔH, ΔG_u, and ΔS_u values seen for the different analogs, I do not pretend to be able to explain the various contributions in terms of bonds broken or formed nor changes in the degrees of freedom of

water, flavin, or protein molecules. However, from the trends in the above results, I would predict that the observed ΔG_u value (more positive than -8 kcal/mole) for FAD is the result of a ΔH value near -20 kcal/mole and a ΔS_u value near -40 e.u. Obviously, only future experiments can prove or disprove this prediction.

Comparing the results for the analogs of LF modified in the three position to the results for LF, a less clear picture emerges. For 3 MeLF, the ΔH and ΔS_u values are both significantly less negative than the same values for LF, but the resulting ΔG_u value for 3 MeLF is identical with that for LF. This is an example of enthalpy-entropy compensation, a subject considered on page . 3 BzLF is bound about a factor of five more strongly at 25° than is 3 MeLF, which may indicate an interaction of the phenyl residue with the protein; however, other possibilities exist. The data indicate only that 3 BzLF has a more favorable ΔH value and slightly less favorable ΔS_u value than 3 MeLF, both effects resulting in the more negative ΔG_u value for 3 BzLF. The result does indicate that a residue of some bulk (benzene) can be attached to the flavin molecule at this position and not decrease the binding affinity to apoRBP. A comparison of the results for 3 OAc^-LF with those for 3 MeLF shows that the negatively charged carboxyl residue decreases the ΔG_u value as a result of a ΔS_u value less favorable for binding (more negative).

Comparing 1) the energies for 3, 4 dihydroRF with those for RF, and 2) the energies for 1, 3, 7, 8 tetMe, 4 OMeA with those for

1, 3, 7, 8 tetMeA indicates that reduction of the C(4) = O group causes ΔG_u to be more positive by 1 to 2 kcal/mole as a result of more positive ΔH values which are not completely offset by more positive ΔS_u values. This may indicate that the C(4) = O group is involved in a hydrogen bond with the apoprotein. Comparisons of the energies in cases 1) and 2) is, however, not strictly valid since the reduced derivative is in one case an alcohol and in the other an ether. An additional complication in the interpretation of the results for the analogs with reduced 4 position carbonyl residues concerns stereospecificity. Each of the two reduced samples was composed of unknown relative proportions of 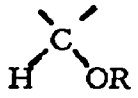 and 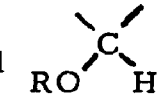. The affinity of apoRBP for these isomers is unlikely to be the same, and in fact, some evidence for a difference in affinity was found. Of all the analogs used in the equilibrium studies, 3, 4 dihydroRF and 1, 3, 7, 8 tetMe, 4 OMeA (along with dezazRF) showed the greatest variation in the K_a values determined in a given fluorescence quenching titration. The K_a values determined at the 90% quenching point were sometimes a factor of two larger than the values determined at the 10-30% quenching points*. This is just the result expected if impurities are present

---

* The justification for using the results with these analogs was that the van't Hoff plots were linear and had the same slopes when the results for the average K_d or the results for the K_d at any specific percentage of the fluorescence quenched were used in the van't Hoff plots. Thus the ΔH values were the same. A factor of 2 difference in K_a corresponds to a difference in the ΔG_u value of 0.3 kcal/mole or about equal to the standard deviation of the ΔG_u values for these analogs. The K_a values used in the van't Hoff plots for these analogs were determined

because the first additions of apoRBP will preferentially bind the analog molecules with highest affinity. A closer examination of this point seems warranted in future studies.

Comparing the energies for deazaRF with those for RF, an insignificant change is found in the ΔS_u value, coupled with a ΔH value more positive by about 1 kcal/mole for deazaRF. Thus replacement of the nitrogen at position 5 with a CH moiety produced a resultant ΔG_u value less favorable for binding by about 1 kcal/mole.

Significant differences are found between the energies for 8 NorLF and LF. Both ΔH and ΔS_u are more positive for 8 NorLF, with the net result that replacement of the methyl group at position 8 with a hydrogen produces a ΔG_u value less favorable for complexation by about 1 kcal/mole. Moreover, the energies for 10 MeIA in comparison to the energies for 8 NorLF show that replacement of the second methyl on the benzene ring of IA with a hydrogen produces small compensating changes in the ΔH and ΔS_u values with little resultant change in the ΔG_u value. Comparing now the values for isoLF with those for 8 NorLF shows that replacement of the hydrogen at position 6 in 8 NorLF with a methyl group to give isoLF produces little change in the ΔS_u value but a more negative ΔH value with resultant ΔG_u value for isoLF more favorable toward complexation by about 1 kcal/mole. Thus exchanging the methyl group at position 8 in LF with

---

in the same manner as those for the rest of the analogs - namely, the reciprocals of the average K_d values for the quenching titration.

the hydrogen at position 6 (yielding isoLF) causes minor change in the ΔG_u value, again as a result of nearly compensating changes in the ΔH and ΔS_u values.

Replacement of either or both methyl residues at positions 7 and 8 in LF with chlorine residues produces minor changes in the ΔH, ΔG_u, and ΔS_u values. 7 ClLF has a ΔG_u value slightly more favorable toward complexation than the ΔG_u value for LF. DiClLF has a ΔG_u value intermediate between the values for the monochloro analogs and essentially equal to the ΔG_u value for LF as a result of compensating ΔH and ΔS_u values.

Attaching a large substituent at the 8α position causes considerable change in the equilibrium binding energies. Comparing the energies for 3 Me, 8α MorphLF with those for 3 MeLF shows that introduction of the morpholino residue is not favorable to binding. The 3 kcal/mole more favorable enthalpy change is overwhelmed by a 6 kcal/mole less favorable entropy change. Curiously, the enthalpies for 3 Me, 8α MorphLF and for LF are similar. The introduction of the histidyl residue at position 8α produces an even less favorable interaction. My prediction in this case is that the binding of 8α histLF has a ΔH value near -17 kcal/mole and a ΔS_u value more negative than -35 e.u./mole.

Comparing the results for 1, 4, 7, 8 tetMeA with those for 3 MeLF should show the effect of shifting the methyl residue from position 10 to position 1 of the isoalloxazine ring. This shift produces

a more favorable ΔH value and a less favorable ΔS_u value. These energy changes compensate to produce little net change in the ΔG_u value.

One might expect the comparison of the energies for 1, 3 diMeA and 1, 3, 7, 8 tetMeA (Pair A) to be similar to the comparison of the energies for 10 MeIA and LF (Pair B). The substituents at the 7 and 8 positions of the IA ring differ in the same way for both pairs. In both pairs the replacement of the 7 and 8 methyl residues with hydrogens produces less favorable ΔH values and more favorable ΔS_u values. In the case of Pair A , the changes in ΔH and ΔS_u values compensate to yield the same ΔG_u value for both analogs. In contrast, the differences between the ΔH and ΔS_u values for Pair B do not compensate, but yield a ΔG_u value for 10 MeIA about 1 kcal/mole less favorable for complexation than the ΔG_u value for LF, as has already been discussed. The reasons for the differences between the results for Pair A and Pair B may indicate that the free energy differences associated with a series of structural changes are not additive.

STUDIES ON THE OPTICAL AND CD ABSORPTIVITY SPECTRA OF SEVERAL ANALOG-APORBP COMPLEXES

Comparison of the Spectra for Native RBP and the Holoprotein Reconstituted with RF

One of the most extensively investigated characteristics of flavoproteins has been their optical absorbance spectra and to a much

lesser degree their CD absorbance spectra. Insofar as the electronic transitions giving rise to the flavin absorption bands are sensitive to the environment of the flavin, the optical and CD spectral changes observed when flavins bind to apoproteins give useful information about the interaction with the apoprotein site. Because RBP lacks any known enzymatic activity, its spectral properties provide a means of ascertaining the degree of reconstitutability of the protein. Figure 41 compares the optical and CD absorbance spectra of native holoRBP, apoRBP, RF, and the reconstituted RF-apoRBP complex. The concentration of reconstituted holoRBP was based on fluorescence quenching results and an absorptivity for RF at 445 nm of 1.25×10^4 $\underline{M}^{-1}cm^{-1}$ (67). For purposes of comparison, the native holoRBP concentration was calculated on the assumption that native and reconstituted holoRBP had the same absorptivity at 455 nm (1.10×10^4 $\underline{M}^{-1}cm^{-1}$). To the extent that these spectra are sensitive to the uniqueness of the interaction, the close spectral indistinguishability of the native and reconstituted holoproteins gives as much evidence as is available at this time that no irreversible change in RBP occurs during the preparation of the apoprotein nor in its subsequent recombination with RF.

The apoprotein has an optical absorbance spectrum in the near ultraviolet similar to that of many proteins containing aromatic amino acids. The absence of intensity in the visible regions of the optical and CD spectra of the apoprotein indicates the complete removal of flavin.

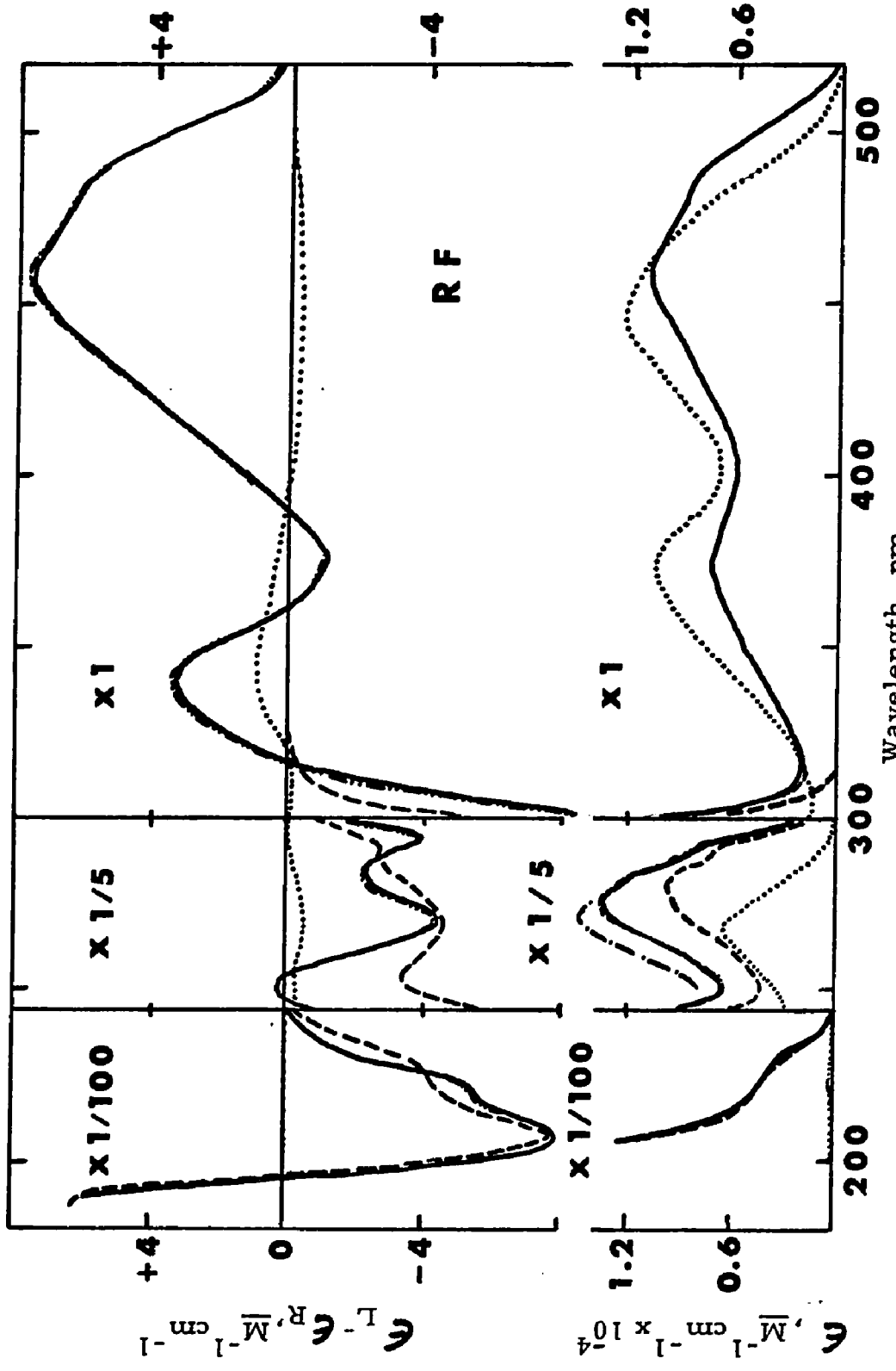

Figure 41. CD and Optical Absorptivity Spectra of RBP and RF.
The curves are native holoRBP (——), apoRBP (- - -), RF (· · ·), holoRBP reconstituted from apoRBP + RF (-·-·-·), and the arithmetic sum of the optical absorbances of apoRBP and RF in the region 250-280 nm (-·-·-).

The optical absorptivity spectrum of RF bound to apoRBP in comparison to that of RF free in solution shows several features which are characteristic of many flavoproteins (83), namely: 1) hypochromism in the 270, 370, and 450 nm peaks, with the decrease in absorptivity at 370 nm being greater than at 270 and 450 nm; 2) a red shift of approximately 10 nm in the 450 nm peak with little shift in the 370 nm peak, and 3) the appearance of additional structure in the 450 nm peak (a pronounced shoulder at 480 nm and a perceptible shoulder at 430 nm).

Because the isoalloxazine ring lacks an asymmetric center and is therefore optically inactive, LF lacks CD intensity. The small amount of optical activity observed for RF in Figure 41 results from the centers of chirality on the ribose side chain. When RF is complexed to apoRBP, however, the shape of the CD spectrum in the visible region changes completely and a large intensity increase occurs concomitant with the smaller change in optical absorptivity. This increase in optical activity results from protein induced asymmetry (extrinsic Cotton effect).

The shape of the 450 nm peak in the visible CD spectrum of holoRBP is very similar to the same peak in the optical absorbance spectrum, both having maxima at about 455 nm and pronounced shoulders near 480 nm. Nishikimi and Yagi (42) pointed out that Moffit and Moscowitz (84) had shown theoretically that such a similarity is expected for electronic transitions in which both the electric

and magnetic dipole moments of the transition are insensitive to nuclear displacement. A negative peak in the visible CD spectrum of holoRBP corresponds to the 370 nm optical absorbance peak and a positive peak with greater dichroic intensity than the 370 nm peak which occurs at 340 nm. The latter peak has no apparent counterpart in the optical absorbance spectrum.

The shape of the visible CD spectrum for holoRBP shown in Figure 41 is similar to that previously reported, and indeed the value of the 450 nm maximum (7.7 $\underline{M}^{-1}cm^{-1}$) agrees well with the spectra shown by Nishikimi and Yagi (42) and by Phillips (40) from which values for $\epsilon_L - \epsilon_R$ at 450 nm of 7.2 and 7.7 $\underline{M}^{-1}cm^{-1}$ can be calculated. About the same variation is seen among the $\epsilon_L - \epsilon_R$ values at 340 nm; namely, 3.7, 3.0, and 3.5 $\underline{M}^{-1}cm^{-1}$, respectively. However, somewhat greater differences in the value at 370 nm exist, -2.1, -2.0, and -0.2 $\underline{M}^{-1}cm^{-1}$, respectively.

In the near ultraviolet region, the CD spectra for apoRBP and holoRBP show similarities. Both have negative extrema at 270 nm of nearly equal intensity. The shoulder or small peak in the apoRBP curve at 292 nm appears to intensify on complexation with RF. Although qualified by the uncertain dichroic contributions of bound RF in this region, the intensified 294 nm peak seen for holoRBP may indicate that binding of RF perturbs tryptophan residue(s) as suggested by Phillips (40) on the basis of his CD data. The trough observed at 254 nm in the CD curve for apoRBP corresponds to a

small positive peak at 251 nm in the holoRBP spectrum. The apoprotein extremum in this region may or may not result from a smaller contribution of the same positive band(s) producing the positive dichroism seen for holoRBP. The near ultraviolet spectrum for apoRBP shown by Phillips (40) agrees well with that seen in Figure 41. However, his spectrum for holoRBP has negative peaks at 270 and 292 nm with $\epsilon_L - \epsilon_R$ values of 14 $\underline{M}^{-1}cm^{-1}$ or about two-thirds as intense as the same peaks shown in Figure 41.

The far ultraviolet CD peaks of apoRBP and holoRBP both have a mean residue ellipticity of about 11,000 deg $cm^2 dmole^{-1}$ at 208 nm. This value is calculated from the observed $\epsilon_L - \epsilon_R$ and the amino acid residue analysis of RBP reported by Farrell et al. (37). (The protein content of RBP is 27,800 g/mole and the mean residue molecular weight is 118 g.) Model polypeptides in alpha helical form have negative CD extrema at 208 nm and 222 nm with similar mean residue ellipticity of about 35,000 deg $cm^2 dmole^{-1}$ (85, 86). Comparison of the model polypeptide ellipticities at 208 nm with those of apoRBP and holoRBP suggest that both of the latter may be composed of as much as 30% alpha helix.

Chen et al. (86) compiled the far ultraviolet CD spectra for ten protein examples for which estimates of the content of helix, β structure, and unordered form were available from x-ray data. Of these, the spectrum for egg white lysozyme (and to a lesser extent insulin) bears a striking resemblance to holoRBP, even though the

published amino acid compositions for lysozyme (87) and RBP (37) are quite different (on a mean residue basis, however, both contain the same number of disulfides). Both have maximal negative dichroism at 208 nm with a pronounced shoulder at 220 nm. The mean residue ellipticity for lysozyme is somewhat larger (about 13,500 deg $cm^2 dmole^{-1}$). The ratio of the ellipticity at 220 to the ellipticity at 208 nm is 0.76 for lysozyme while it is 0.70 for holoRBP. By comparison, the same ratio for insulin is 0.81; in contrast, the following proteins have ratios > 0.9: the six other proteins reviewed by Chen et al. (86) having peaks near 208 and 220 nm, and, in addition, glucose oxidase (88), flavodoxins from four bacteria (88), and lipoamide dehydrogenase (89). Both lysozyme and holoRBP also lack a positive maximum in their CD spectra at wavelengths greater than 190 nm and have similar dichroism intensities at 190 nm relative to their intensity at 280 nm. (The signal to noise quality of the RBP spectra rapidly deteriorated at wavelengths below 195 nm, so the latter comparison is approximate.) Chen et al. (86) calculate that the fractions of lysozyme residues in helical, β, and unordered form are 29, 16, and 55%, respectively, as determined from the x-ray structure of Blake et al. (90). On the basis of the similarity between the far ultraviolet CD spectra for lysozyme and holoRBP, the fractions of holoRBP residues in helical, β, and unordered form may approximate the respective values in lysozyme - again indicating that holoRBP may contain 25-30% alpha helix.

Compilation of the Spectra for Several Analog-ApoRBP Complexes

The CD and optical absorptivity spectra of twenty flavin analogs and their complexes with apoRBP are given in Figure 42A, B, C, D, and E. After drawing attention to the general features common to either the set of optical absorptivity spectra or the set of CD spectra for the complexes, I will mention the specific correlations and differences observed within that set.

Qualitatively the optical absorptivity spectrum of each analog-apoRBP complex relates to the spectrum of the free analog in the same way that the optical absorptivity spectrum of RF holoRBP relates to the spectrum of RF. All the complexes except that for LC have the same number of optical absorptivity maxima as the free analog. Comparing the optical spectrum of each analog with that of its apoRBP complex, the maxima for the complex show hypochromism at wavelengths greater than 300 nm (with two possible exceptions: the 400 nm maximum for the deazaRF complex and the 370 nm maximum for the 7, 8 diClLF complex). Comparing the long wavelength optical maximum for analog and complex, the peak for the complex shows 1) a bathochromic shift (an exception may be LC, for which a shift is indeterminable), 2) greater resolution as judged by shoulders near 480 nm (the complexes with 10 MeIA, isoLF, 8 NorLF are important exceptions. More will be said about this on page 190), and 3) resultant tailing toward the red (no exceptions). In contrast to the complex with RF (where little wavelength shift occurs in the 370 nm peak), most of

Legend to Figure 42A, B, C, D, E

Each page of this figure contains the CD and optical absorptivity spectra of four flavin analogs and their complexes with apoRBP. The buffer was 0.01 M K phosphate, pH 7.0. The other conditions are given in Materials and Methods. The concentrations of the complexes used to obtain absorptivities were not the total equimolar apoprotein and analog concentrations present, but were the concentrations calculated from the equilibrium data in Table X. The CD spectrum for free deazaRF was not recorded. All other analogs for which no CD spectrum is shown were optically inactive.

.... Spectra for the free analogs.

—— Spectra for the analog-apoRBP complexes.

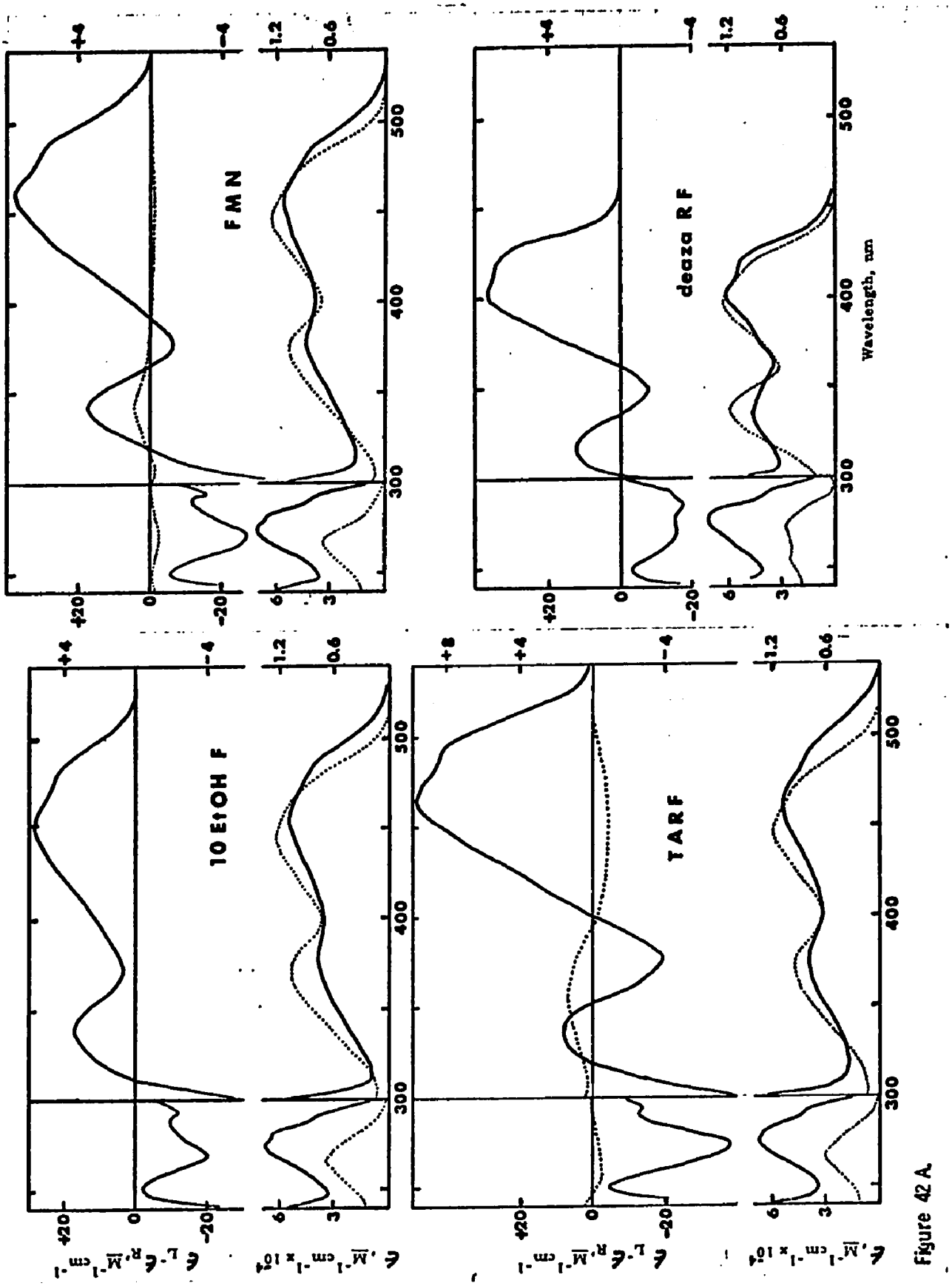

Figure 42 A.

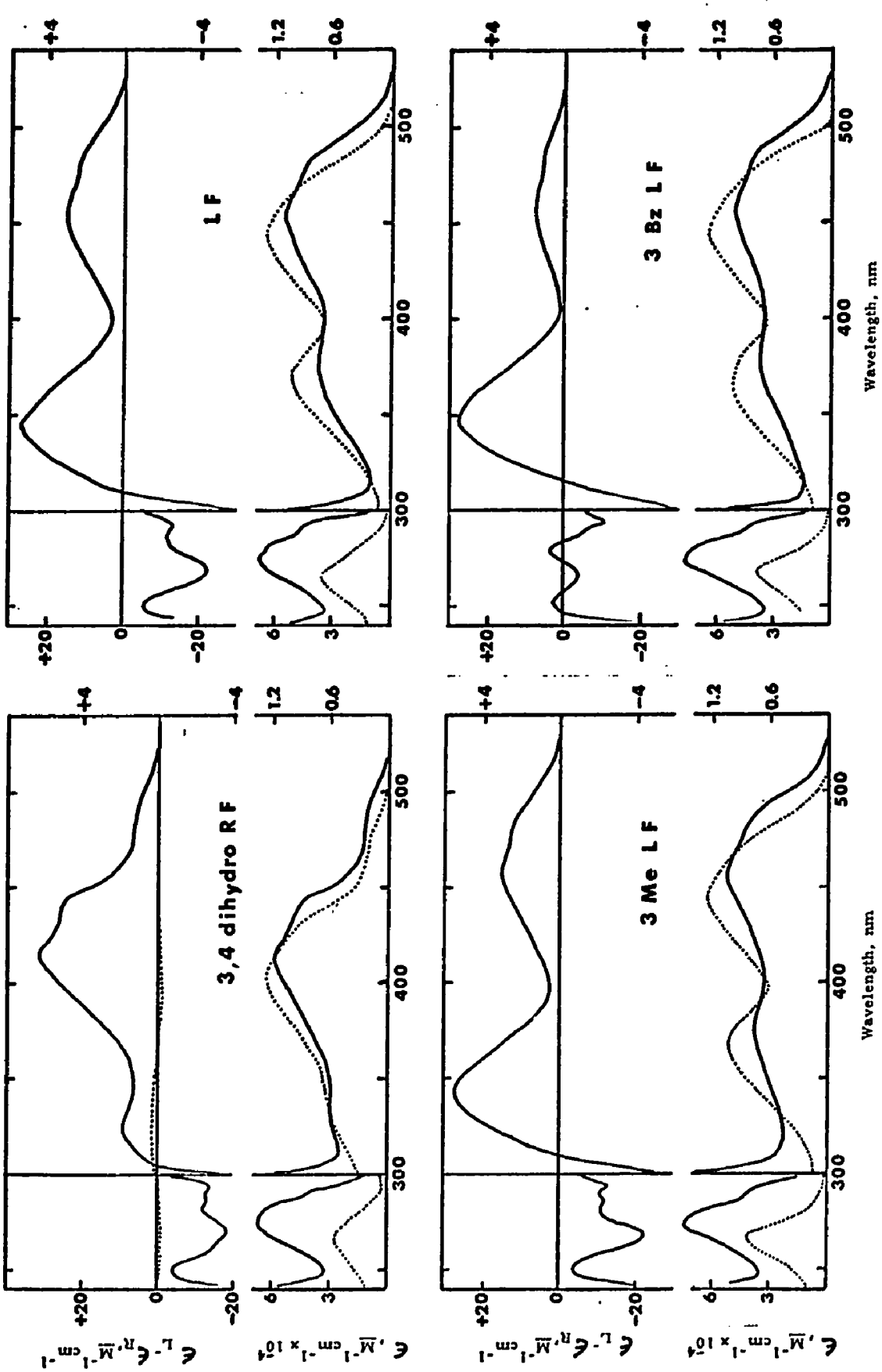

Figure 42 B.

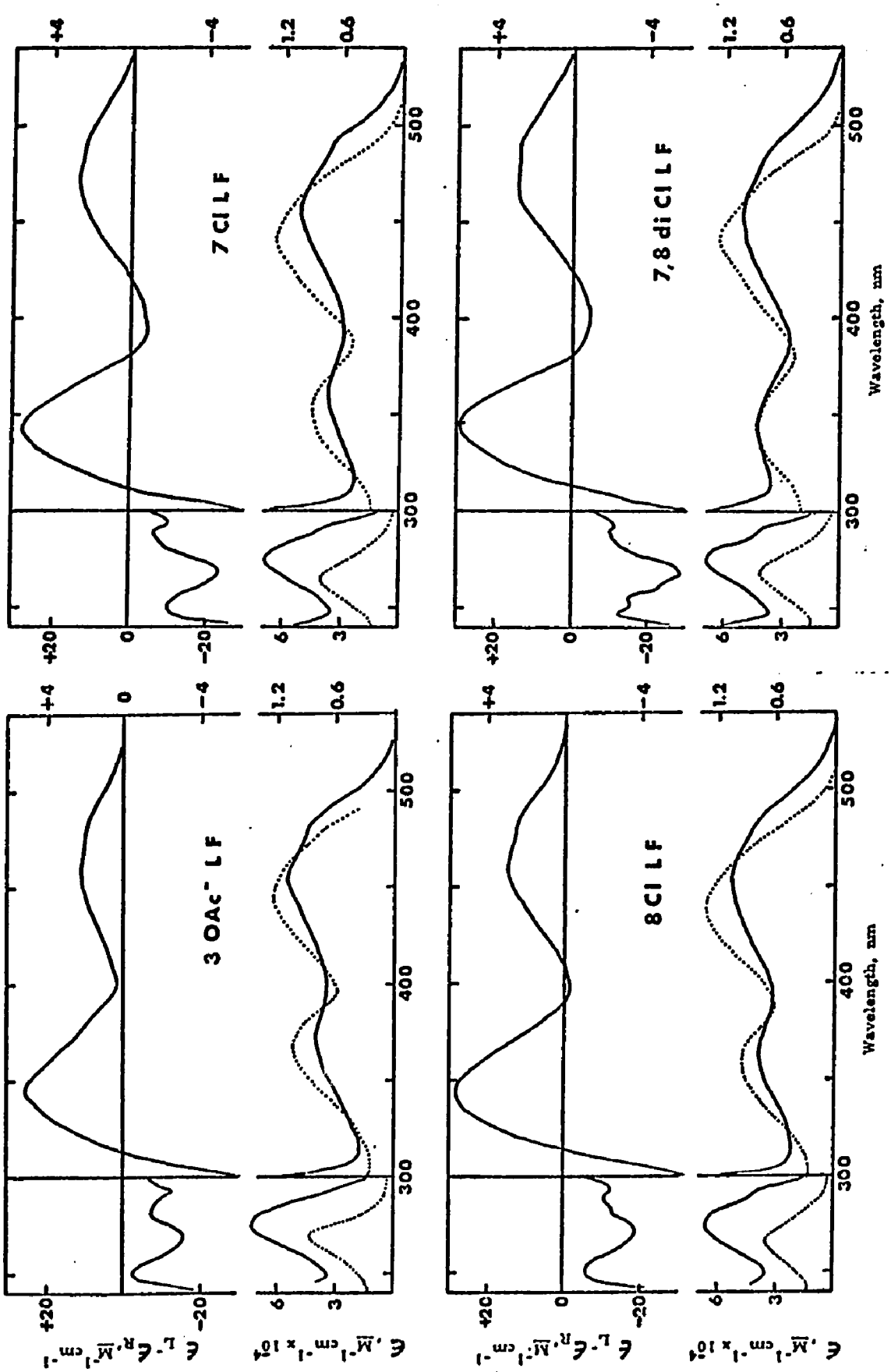

Figure 42 C.

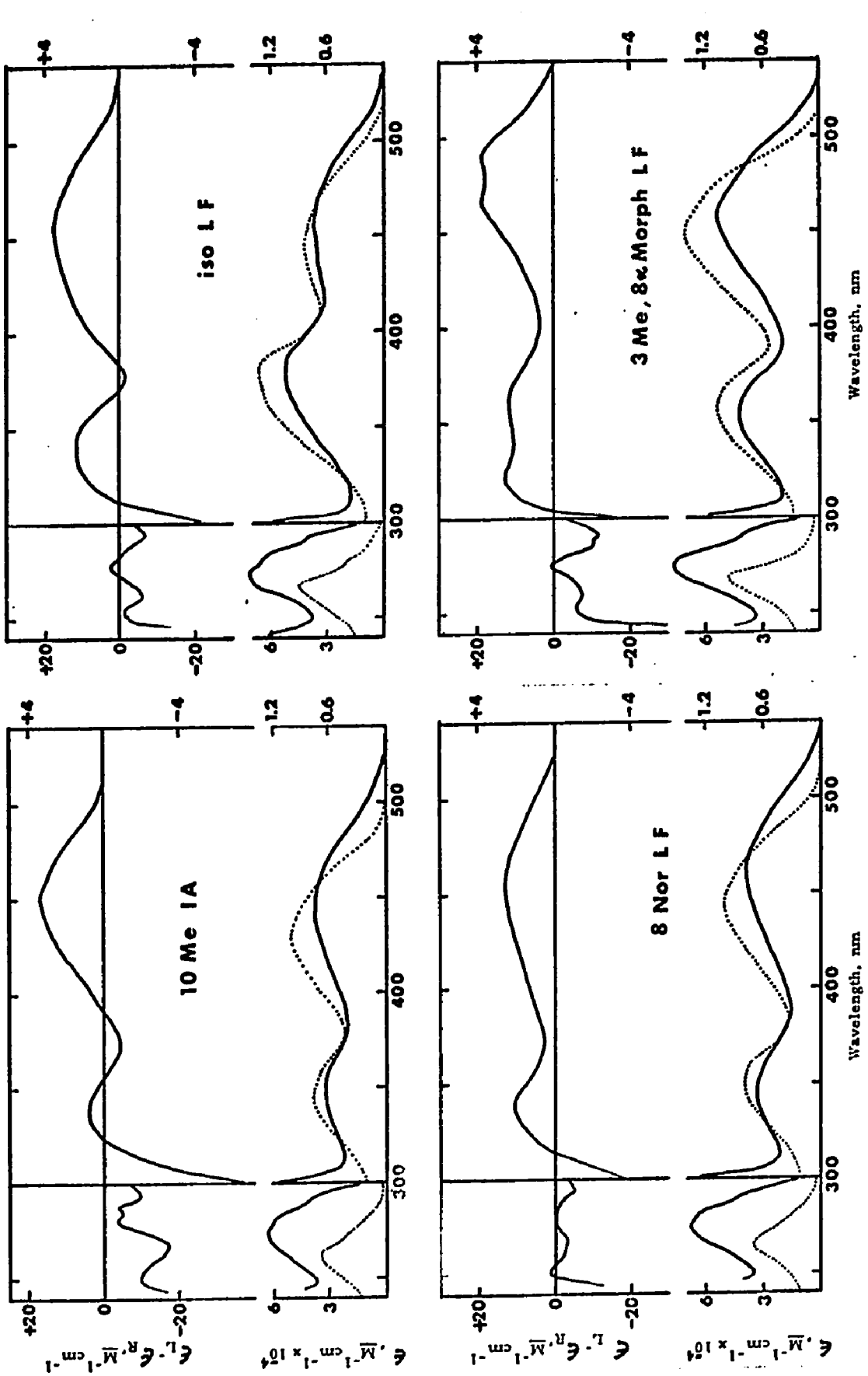
iso L F
3 Me, 8α Morph L F
10 Me I A
8 Nor L F
Wavelength, nm
Wavelength, nm

Figure 42 D.

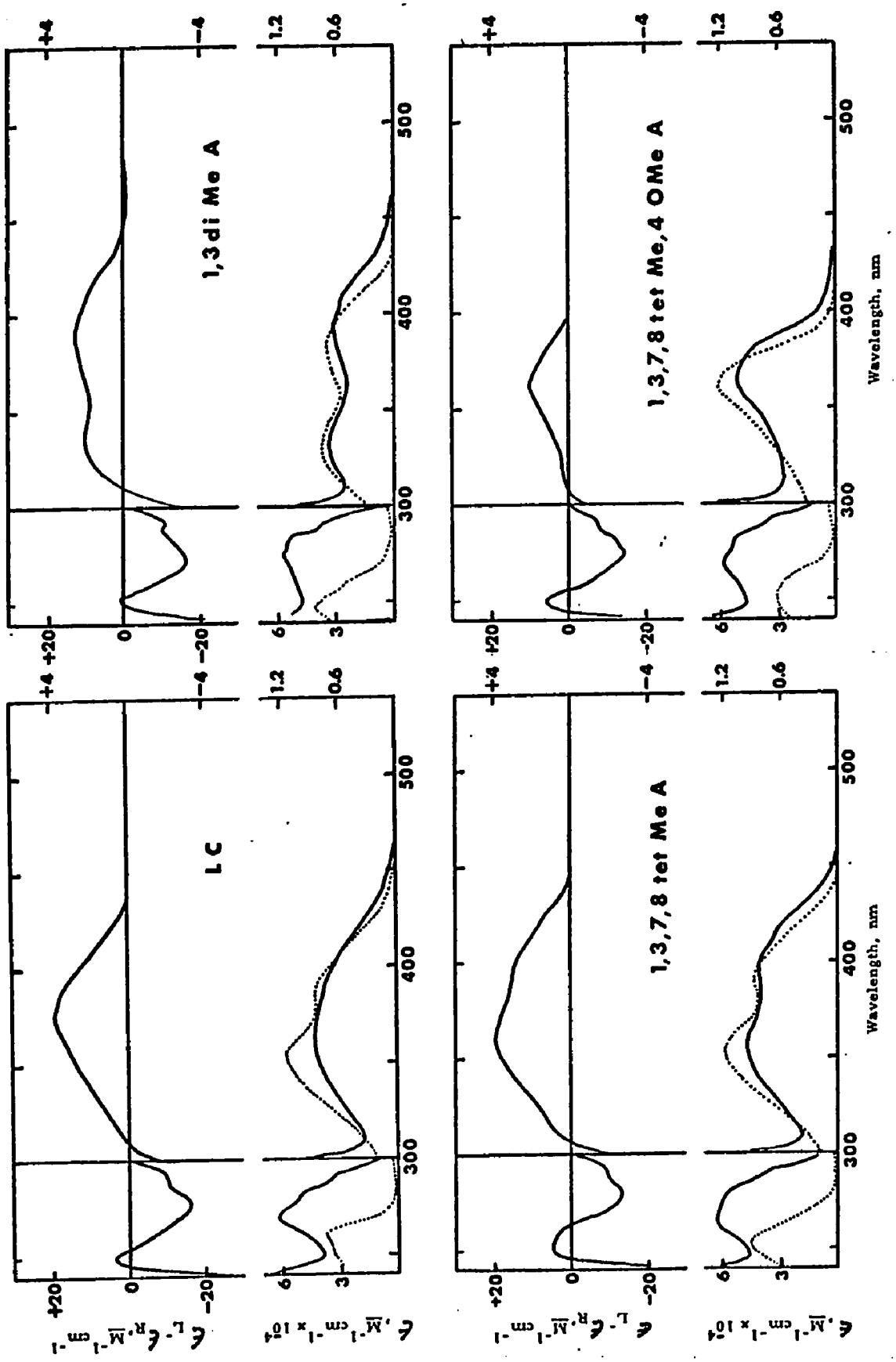
1,3 di Me A
1,3,7,8 tet Me A
1,3,7,8 tet Me,4 OMe A
L C
Wavelength, nm
Wavelength, nm

Figure 42 E.

the analog-apoRBP complexes shown in Figure 42A, B, C, and D have bathochromic shifts in the 270 nm peak. However, the complexes with deazaRF, 8 NorLF, and 3 Me, 8 α MorphLF show hypsochromic shifts, while the complexes with 8 ClLF, diClLF and possibly isoLF show apparently little wavelength shift for this peak. The 275 nm maxima of the complexes are dominated by the protein contribution at this wavelength, but all apparently show some degree of hypochromism in the analog contribution.

As mentioned above, the optical absorptivity spectra for the complexes of apoRBP with 8 NorLF, 10 MeIA, and isoLF differ from the spectra of the other complexes in that their 450 nm peaks lack or have far less pronounced shoulders in the 480-490 nm region. In addition, the optical spectra for the complexes with 8 ClLF and 7, 8 diClLF have markedly reduced shoulders in this region. The common structural feature which distinguishes this set of analogs is the replacement of the methyl residue at position 8 of the "normal" flavin with another moiety (a hydrogen or a chlorine residue)*.

---

* This correlation had not been realized when the spectra were normalized and redrawn from the original. In spite of my painstaking effort to accurately transfer the spectra, it is possible that some unintentional emphasis might have been added or deleted - especially in a feature so sensitive to error as a spectral shoulder. A check of the originally recorded spectra shows that the stated effects mentioned here and elsewhere are as dramatic as seen in Figure 42. While the method of redrawing spectra is subject to small error, it provides a convenient means for many spectra to be visualized. I doubt that I would have discerned the correlation from a tabulation of absorptivities or from tracings of the absorbance spectra at different concentrations of complexes.

The appearance of a shoulder at 410 nm in the optical spectrum of the complex with 1, 3 diMeA is apparently an exception to this correlation. However, the CD spectrum of this complex has little shoulder near 410 nm, a result which is in agreement with the class of analogs with hydrogens at position 8, as discussed below.

In general, the CD spectra of the analog-apoRBP complexes relate to the optical spectra of the complexes in similar fashion as the CD spectrum of native holoRBP relates to its optical spectrum.

1) The number of positive dichroic maxima at wavelengths > 300 nm is the same as the number of maxima in the optical spectra (exceptions: 3 Me, 8 α MorphLF which has 4 CD maxima but 2 optical maxima, and 1, 3, 7, 8 tetMeA which has two optical maxima but only one CD maximum (plus another definite shoulder)).

2) The peak wavelengths of the long wavelength band are nearly identical for both the CD and optical spectra of the complexes (exceptions: 3 Me, 8 α MorphLF and 1, 3, 7, 8 tetMeA).

3) The shape of the long wavelength CD peaks for the complexes strongly resembles the shape of the optical absorptivity peaks in this region (exceptions: the complex with 3 Me, 8 α MorphLF which shows greater resolution in the long wavelength CD maximum; the complexes with 1, 3 diMeA and 3 OAc^-LF which show less resolution in their CD maxima, and the complex with 1, 3, 7, 8 tetMeA, for which this is difficult to discern).

4) Each complex which has two optical absorptivity maxima at wavelengths > 300 nm has a positive CD maximum in the region 320-350 nm and the position of this peak is at a shorter wavelength than the optical maximum (exception: the complex with 1, 3, 7, 8 tetMeA, which has two optical peaks, does not have a CD maximum between 300 and 350 nm).

5) The CD spectra of the complexes in the near ultraviolet region all show evidence for negative CD extrema at about 295 nm, have negative maxima between 260 and 270 nm and have negative extrema (or small positive maxima) near 250 nm.

Some strong correlations among the CD spectra are apparent.

1) The complexes with all of the analogs containing a methyl residue, a hydrogen, or no residue at position 10 have long wavelength maxima less intense than 4 $\underline{M}^{-1}cm^{-1}$, while all of the analogs containing ribose moieties at position 10 have long wavelength maxima of intensity greater than 6 $\underline{M}^{-1}cm^{-1}$. The complex with 10 EtOHF has a somewhat intermediate value of 5.6 $\underline{M}^{-1}cm^{-1}$, while the CD intensity at 458 nm for the complex with TARF is considerably increased (9.8 $\underline{M}^{-1}cm^{-1}$).

2) With three definite exceptions (see 4) below) the complexes with analogs containing methyl residues at position 10 have CD peaks at 340 nm considerably more intense than their CD peaks at 450 nm. The complexes with LF, 3 MeLF, 3 BzLF, 3 OAc^{-}LF, 7 ClLF, 8 ClLF, and diCl LF all show this effect and have relatively the same CD

intensity at 340 nm, namely about 5.5 $\underline{M}^{-1}cm^{-1}$. In addition, they all have CD intensity near 460 nm about 3 $\underline{M}^{-1}cm^{-1}$ (except for 3 BzLF which shows $\Delta\epsilon_{460} \sim 1.5\ \underline{M}^{-1}cm^{-1}$). Whether significance or coincidence should be attached to the following observation is uncertain: the complexes with LF, 3 MeLF, 3 OAc^-LF, and 3 BzLF do not have negative CD intensity near 400 nm, while the complexes with 7 ClLF, 8 ClLF, and diClLF do.

3) With three definite exceptions (see 4) below), all the complexes with analogs containing residues other than hydrogen at position 10 have long wavelength bands showing resolution (shoulders or peaks near 480 nm).

4) The three exceptions to 2) and 3) are the complexes with 8 NorLF, 10 MeIA, and isoLF, the same analogs whose complexes had optical spectra which lacked definite shoulders near 480 nm. The complexes with these analogs have smaller CD intensity in the 340 nm peak than in the 450 nm peak and show essentially featureless 450 nm peaks. Two of the three complexes (i.e. for 8 NorLF and isoLF) have considerably reduced intensity in the 250-280 nm region (but in this regard, so does the complex with 3 BzLF). The CD spectrum for the complex with 3 Me, 8α MorphLF is somewhat of a paradox in relation to those of the other analogs modified in the 8 position. The presence of the morpholino residue at the 8α position causes the CD spectrum of the complex to have such a pronounced shoulder at 480 nm that it has become a peak. This effect is consistent with the correlation

between the presence of a moiety (other than hydrogen) at position 8 and the appearance of spectral structure near 480 nm. However, the peak for the 3 Me, 8α MorphLF complex near 330 nm is considerably smaller than is expected on the basis of 2) above. In addition the CD spectrum of this complex shows a positive peak near 370 nm - a peak which is not observed in any of the other analogs with a residue (except H) in the 10 position.

Clearly the replacement of the 8 methyl residue by a hydrogen in 8 NorLF, 10 MeIA, and isoLF produces profound effects on the spectral character of the complexes of these analogs with apoRBP.

KINETIC STUDIES ON THE BINDING OF FLAVINS BY APORBP

In order to complete the description of the energetics of flavin binding to apoRBP, the temperature dependence of the individual rate constants for the reaction must be studied. This requires determining the number of steps in the reaction sequence and finding techniques by which the individual rate constants can be evaluated. Because the stoichiometry in this case is one mole of flavin bound per mole of protein, the step when apoRBP and flavin initially interact is likely to be a second order step. If a kinetic process can be found which is strictly second order with respect to the concentrations of apoprotein and flavin, it is highly probable that this process monitors the initial complexation step. As demonstrated in the first section below, the quenching of flavin fluorescence by apoRBP is such a process. The

next topic considered is the evaluation of second order rate constants for reversible binding of flavins by apoRBP. The third section in this chapter considers the temperature dependence of the quenching process, for even if the binding reaction consists of a complicated sequence of steps, the temperature dependence of the second order step can give useful information about this binding reaction. The results of some relaxation studies on flavin binding are given in the last section of this chapter. These studies attempt to answer the question whether flavin binding to apoRBP is a single step reaction.

Verification that the Quenching of Flavin Fluorescence Monitors a Second Order Process

The observation that the fluorescence of flavins was quenched by apoRBP prompted the use of fluorescence in the initial studies of the kinetics of binding. Results of preliminary studies were disconcerting, however, because the observed rate constant for quenching was apparently neither first nor second order - as measured by standard plotting methods. In these experiments, nominally equal concentrations of RF and apoRBP were mixed in the stopped-flow fluorimeter and the ensuing decrease in fluorescence monitored. Plotting either the log [fluorescence intensity] or [fluorescence intensity]$^{-1}$ as a function of time produced non-linear plots. I learned afterward that the concentration of apoprotein was about 13%

higher than had been calculated* in preparing the solutions. This is a relatively small error considering the effect it had on the results and points out the necessity of using reactant solutions of strictly equal concentration in this type of analysis.

Subsequent to determining the apoRBP concentration by stoichiometric binding titrations, plots of [fluorescence intensity]$^{-1}$ against time such as those in Figure 21 were obtained. When $[RF]_{total} = [apoRBP]_{total} \sim 10^{-5}$ M, the plots were linear and therefore encouraging; however, when $[RF]_{total} = [apoRBP]_{total} \lesssim 10^{-6}$ M curvature was observed and the rate constants obtained under the latter conditions were always higher than those obtained at the higher concentrations**.

After preliminary kinetic experiments with LF (see the example for 8 ClLF binding in Figure 43), it became apparent that these flavin binding reactions were proceeding to an equilibrium fluorescence level. Thus these binding reactions were not irreversible as had been assumed in deriving the equation on which the above plotting

---

* These experiments were performed before the stoichiometric quenching titrations were employed to determine the apoprotein concentration. The concentration was determined using a value of 17 cm^{-1} for the absorbance of a 1% apoprotein solution (70) and the only value of the protein molecular weight available at that time: 36,000 Daltons (39). As shown on page 134, the molecular weight based on binding is 32,000 Daltons, a difference of about 13%.

** At that time, the small residual fluorescence observed long after mixing equimolar solutions $< 10^{-6}$ M was assumed to be some "background" fluorescence. These concentrations of flavin required relatively high gain - a condition which, after all, would result in a larger background signal. Only later was my error apparent.

method was based (for example, see Moore (6)). The legend to Figure 21 indicates that an equation (page 201) derived on the assumption that flavin binding to apoRBP is a reversible reaction gives nearly identical values for the rate constant at all concentrations used in the reactions plotted in Figure 21.

Reactions in which a ligand is bound can be driven in the direction of complete complexation of the ligand by addition of an excess of the binding species (i.e. under pseudo first order conditions). Accordingly, some mixing experiments were conducted using solutions of apoRBP and RF at equal concentrations and others using concentrations of apoprotein in excess. Table XI summarizes the results of these experiments. The reaction velocity varied by 10,000-fold for the group of experiments conducted under equimolar apoRBP and RF concentrations and by 10-fold for the group of experiments under conditions of excess apoprotein, yet the values of the rate constant describing the quenching process are seen to be quite similar within each group and between the two groups. Even though the actual quenching process may occur at a step(s) after the second order step, any such step(s) is seen to occur sufficiently fast that the second order step is rate limiting*. Quenching of fluorescence, therefore, monitors the complexation step and can be used to determine k_1

* To what extent the slight decrease in the value observed for the experiment when $[\text{apoRBP}]_{\text{total}} = [\text{RF}]_{\text{total}} = 5.9 \times 10^{-6}$ M represents a real trend is uncertain. If real, such a decrease might indicate the presence of another step in the binding reaction.

TABLE XI

Second Order Rate Constants for the Quenching of RF Fluorescence by ApoRBP at Various Reactant Concentrations

Solutions of apoRBP and RF in 0.01 M K phosphate, pH 7.00, were mixed in the stopped-flow fluorimeter at 20.3°C.

Shot	Concentrations 1.7 x [ApoRBP]	After Mixing 1.7 x [RF]	$10^{-7} \times k_1$ Pseudo First Order Analysis	$10^{-7} k_1$ Reversible Analysis
	M	M	$M^{-1} sec^{-1}$	$M^{-1} sec^{-1}$
1	10^{-7}	10^{-7}		4.0 ± 0.2
2				4.1 ± 0.2
3	10^{-6}	10^{-6}		4.1 ± 0.2
4				3.9 ± 0.2
5	10^{-5}	10^{-5}		3.9 ± 0.3
6				3.6 ± 0.3
7	10^{-5}	10^{-7}	4.1 ± 0.2	
8			4.2 ± 0.2	
9	10^{-5}	10^{-6}	4.1 ± 0.2	
10			4.1 ± 0.3	
11	10^{-6}	10^{-7}	3.8 ± 0.2	
12			3.8 ± 0.2	
13	10^{-6}	10^{-7}	4.0 ± 0.2	
14			4.2 ± 0.2	
		Averages:	4.0 ± 0.2	3.9 ± 0.2

of Equation (1). Furthermore, the reversible analysis gives values for the rate constant which are consistent with 1) the values obtained under pseudo first order conditions and 2) values obtained from an irreversible analysis of experiments done at high equimolar reactant concentrations. The reversible analysis therefore yields an accurate measure of the value for the second order rate constant.

Considerations on the Reversible Method of Analysis Used to Analyze the Kinetics of Flavin Binding to ApoRBP

When a solution of apoRBP was mixed with an equal concentration of any flavin analog other than RF, the recorded fluorescence quenching traces proceeded to a value at equilibrium which represented an appreciable fraction of the initial fluorescence. As an example, the binding of 8 ClLF to apoRBP is shown in Figure 43. Attempts to obtain linear plots from such traces using analyses which assumed irreversible binding proved fruitless - as with hindsight they should. Most of these reactions were so fast as to require reactant concentrations $< 10^{-6}$ M in order that quenching occur after the instrument dead time. At these concentrations, an appreciable equilibrium fluorescence intensity was observed, and the value of this intensity corresponded to the amount of free flavin expected from the previously determined equilibrium constants. Clearly, binding is reversible in this system.

As a first approach, the kinetic traces were analyzed by Equation (12), the standard integrated rate equation (91) derived

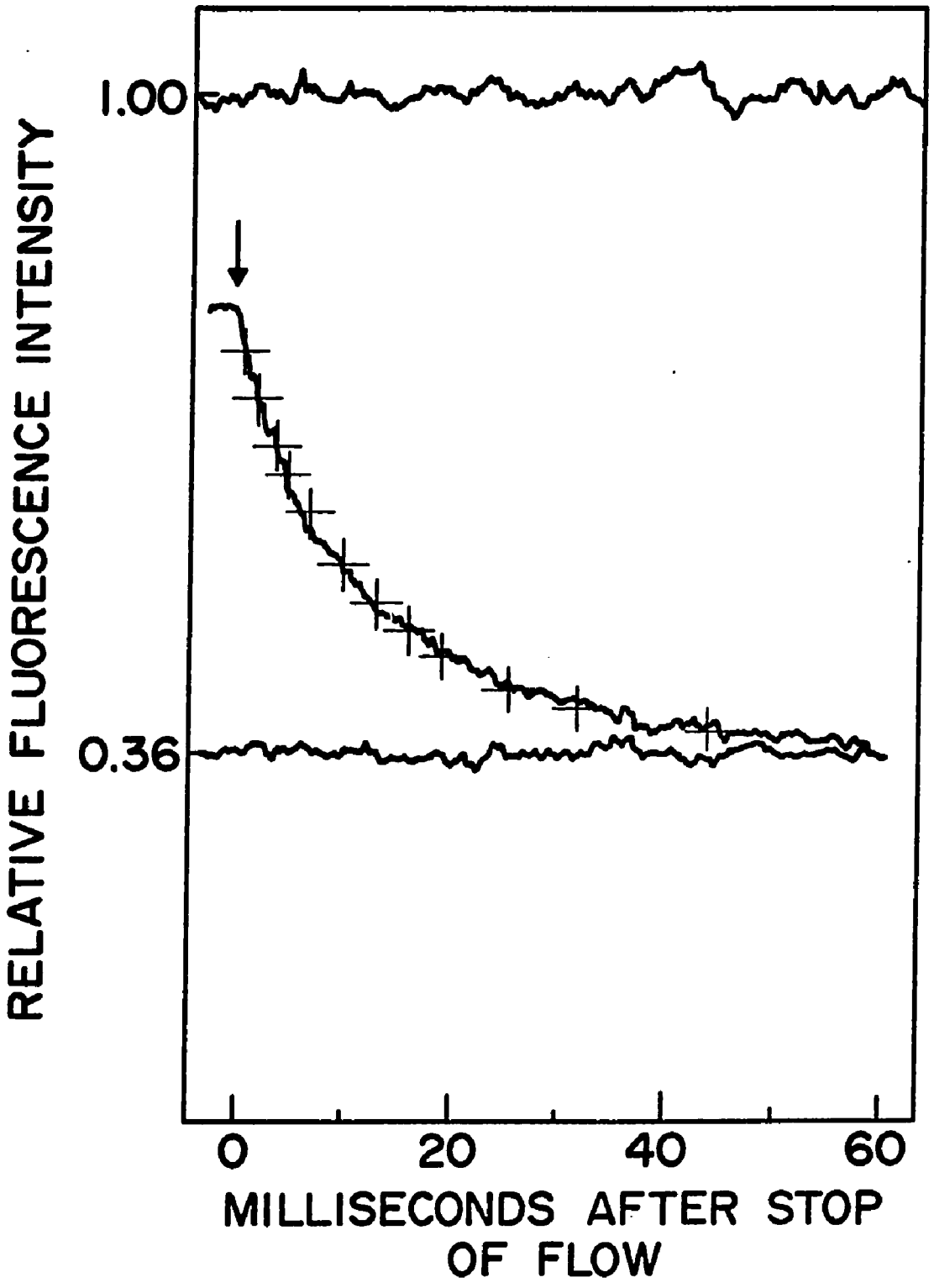

Figure 43. A Typical Example of the Quenching of Fluorescence Observed on Mixing Equal Concentrations of Flavin Analog and ApoRBP.

In this instance 8 ClLF and apoRBP were reacted at final concentrations of 5.0×10^{-7} M in 0.01 M K phosphate, pH 7.00, at 25.4°C. See text for further details.

under the assumption of a one-step reversible reaction (Equation (1)) for mixing of equal concentrations of binding sites and ligand molecules.

$$k_1 t = \frac{2.303[H]_e}{([F]_{total})^2 - ([H]_e)^2} \log \frac{[H]_e \times \{([F]_{total})^2 - [H][H_e]\}}{([F]_{total})^2 \times ([H]_e - [H])}$$

Equation 12

where [H] is the concentration of complex at any time t.

Equation (12) determines a value for the rate constant at any point on the quenching trace. Accordingly, a computer program (REVERSIBLE of Appendix E) was written by Mr. David Sun which requires as inputs the values $[F]_{total}$ and $[H]_e$ together with as many data pairs (t, [H]) as desired. By iteration, a single value of k_1 is found which best fits all the data pairs. "Best fit" minimizes the residuals $([H]_{observed} - [H]_{calculated})^2$, where $[H]_{calculated}$ is the value of [H] expected from the iterated k_1 value at the given value of t. The computer printout includes the 95% confidence interval on k_1 based on the Students' t-distribution.

Kinetic data were routinely recorded with a CAT and printed out on a strip chart recorder. Since each of its 1024 channels is able to store only one accumulated number, the CAT is unable to superimpose all the traces in Figure 43. Furthermore the 1024 channels can be divided into only two independently addressable halves. The CAT is therefore not conveniently able to record all the information necessary to compute k_1. This difficulty was circumvented with the

use of a digital voltmeter (DVM) in conjunction with the CAT. After a trial shot, a suitable time base was selected such that both the kinetic trace and the equilibrium value could be recorded in one 512 channel section. Two to six kinetic shots were accumulated and therefore averaged in channels 1-512 and the equilibrium fluorescence signal of individual shots were recorded with the DVM. The same number of shots of buffer against flavin were accumulated in channels 513-1024 and also individually recorded with the DVM. Buffer background (which in some cases was a significant percentage of the total fluorescence signal) was then recorded with only the DVM. Suitable normalizations of the fluorescence signals and strip chart distances allowed the rate constants to be calculated in units of $\underline{M}^{-1}\text{sec}^{-1}$. In practice, ten data points spread over three "half-lives" of the recorded fluorescence change were used in the computer analysis. The data points were not equally spaced along the time axis, rather they were more closely spaced at earlier times where the change in fluorescence is greater. This method makes k_1 more representative of the whole kinetic trace rather than unduly weighting the points nearer equilibrium*.

---

* Studying the binding kinetics for several analogs presented me with one of two dilemmas: 1) Higher reactant concentrations would improve signal-to-noise quality but, because of the large value of k_1 in some cases, would also cause a large percentage of the reaction to occur within the instrument dead time. The lack of adequate signal-to-noise quality at sufficiently low concentrations of the alloxazine analogs prevented the analysis of their binding kinetics. 2) Analogs with large k_1 values but small K_a values required a compromise between working at "lower" or at "higher" reactant concentrations. At "lower"

The plus marks in Figure 43 indicate the "best fit" fluorescence values calculated from the values on the kinetic trace at these times. Good agreement is seen between the recorded trace and the trace expected for a reversible one-step reaction. The 95% confidence limits on the calculated k_1 value in the analysis of the trace in Figure 43 were less than 2% of the k_1 value. Of the nearly 160 shots used in the Arrhenius analyses, about 120 of them had 95% confidence limits which were < 2% of the calculated k_1 values. In no case was this limit greater than 6% of the k_1 value. In a given Arrhenius analysis the largest 95% confidence limit tended to be associated with the rate constants measured at the highest temperature - i.e. where the reaction rates were the fastest and where the change in fluorescence recorded was the smallest percentage of the fluorescence corresponding to $[F]_{total}$. For each analog the equilibrium fluorescence value reached in a given kinetic trace corresponded to the concentration of flavin expected on the basis of the equilibrium value for the binding of the analog at that temperature.

---

concentrations the rate of reaction was slow enough to occur after the dead time but the equilibrium fluorescence intensity was a very large fraction (sometimes 1/2) of the total fluorescence intensity when the analog was mixed with buffer; thus the change in fluorescence intensity covered by the kinetic trace was restricted. At "higher" concentrations the kinetic trace could cover a greater change in fluorescence intensity but was subject to doing so within the instrument dead time. For these analogs, equimolar reactant concentrations were used which maximized the total change in fluorescence observed in the kinetic traces.

Arrhenius Analyses for Flavin Analog Binding to ApoRBP

The binding kinetics for the reaction of apoRBP with 16 flavin analogs were studied over the temperature range 10-40°C and the logarithm of the rate constant (calculated assuming a reversible reaction) was plotted against 1/T. The Arrhenius plot for a given analog generally consisted of more than one point at each of several temperatures over the interval. Figure 44 shows four representative examples of the quality of the results found. Curvature was not evident in the plots for which data at more than two temperatures was taken, with the exception that the rates of some analogs at 40°C were slightly below the line drawn through the other points (e.g., RF, LF in Figure 44). The line which "best fit" log (k_1) against 1/T was used to calculate $\Delta H^{\ddagger}$ from the Arrhenius energy, $E_a = \Delta H^{\ddagger} + RT$. The computer program LINEAR in Appendix E was used to determine the "best fit" line which minimized the squares of the residuals, $([\log (k_1)]^{observed} - [\log (k_1)]^{line})^2$. Error limits on each $\Delta H^{\ddagger}$ value were established from the 95% confidence interval on the slope of the "best fit" line. $\Delta G^{\ddagger}(25^{\circ})$ and $\Delta S^{\ddagger}(25^{\circ})$ were calculated using the equations given on page 11 and were converted to the corresponding unitary activation parameters, $\Delta G_u^{\ddagger}(25^{\circ})$ and $\Delta S_u^{\ddagger}(25^{\circ})$, by correction for the cratic contribution (82) in a similar way as was done for the equilibrium energies on page 167. The standard deviation of the differences between the observed k_1 values for a given analog and the k_1 values on the "best fit" line was used to determine the error limits

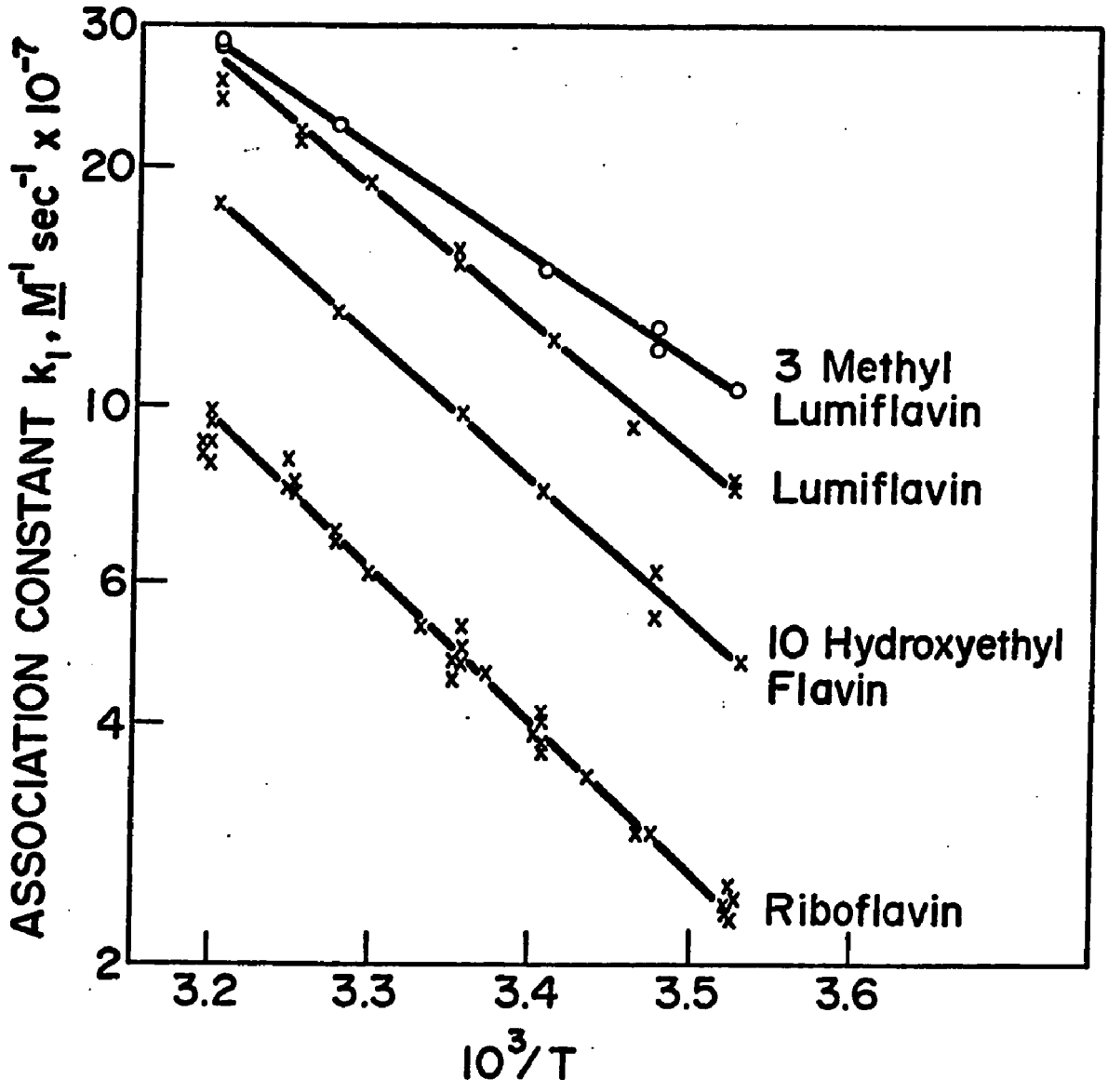

Figure 44. Representative Examples of the Arrhenius Plots for Analog Binding to ApoRBP in 0.01 M K Phosphate, pH 7.00.

on ΔG_u^+. The larger of the error limits on ΔH^+ or ΔG_u^+ was used to set the error limit on ΔS_u^+. Table XII summarizes the results for the Arrhenius analyses of the second order step in analog binding to apoRBP.

As is observed for the equilibrium binding energies (Table X), the activation energies for the binding of the different flavin analogs to apoRBP (Table XII) look remarkably similar from analog to analog. The values for the binding of any of these analogs to apoRBP are $\Delta G_u^+ = 4.5 \pm 0.9$ kcal/mole, $\Delta H^+ = 6.2 \pm 1.8$ kcal/mole, and $\Delta S_u^+ = 7 \pm 9$ e.u./mole.

The second order rate constants increase for the binding of analogs in this series: RF, 10 EtOHF, LF, LC. This seems to indicate the shorter the residue in the 10 position of the isoalloxazine ring, the faster the rate of reaction. The rates for RF and TARF are similar; indicating that the rate is apparently unaffected by this further increase in size of the 10 position residue. However, the largest difference between the ΔH^+ values in Table XII is between the values for RF and for TARF.

The rate constant for the binding of FMN is about a factor of 6 smaller than that for RF. This may result from the negative charge on the phosphate moiety of FMN. Such an interpretation is consistent with the comparison of the rate constants for 3 MeLF and 3 OAc^-LF. The value for the negatively charged analog is decreased by about a factor of 4-5 from the value for the uncharged analog. However, the

TABLE XII

Activation Energies for the Second Order Step in the Binding of Some Flavin Analogs by ApoRBP

Stopped-flow experiments were conducted in 0.01 M K phosphate, pH 7.00.

Flavin Analog	$k_1(25^o)$	$\Delta G_u^{\ddagger}(25^o)$	$\Delta H^{\ddagger}$	$\Delta S_u^{\ddagger}(25^o)$	$[F]_{total}$	Number of Shots (points) in the Arrhenius Analysis
	$M^{-1}sec^{-1}$	kcal/mole	kcal/mole	e.u./mole	M	
RF	4.8×10^7	4.5 ± 0.1	7.8 ± 0.1	11.0 ± 0.3	$5.9 \rightarrow 12.6 \times 10^{-7}$	35
LF	1.50×10^8	3.9 ± 0.3	6.3 ± 0.2	8 ± 1	5.8×10^{-7}	16
LC	2.5×10^8	3.6 ± 0.5	8 ± 2	15 ± 7	7.0×10^{-7}	6
10 EtOHF	9.7×10^7	4.1 ± 0.3	7.4 ± 0.4	11 ± 1	8.9×10^{-7}	7
TARF*	4.9×10^7	4.4 ± 0.1	4.4 ± 0.8	0 ± 3	1.75×10^{-6}	4
FMN*	8.1×10^6	5.4 ± 0.1	5.0 ± 0.6	-2 ± 2	1.75×10^{-6}	4
3 MeLF	1.75×10^8	3.7 ± 0.2	5.4 ± 0.2	6 ± 1	8.9×10^{-7}	8
3 BzLF	1.65×10^8	3.9 ± 0.4	6.1 ± 0.7	7 ± 2	5.0×10^{-7}	8
3 OAc^-LF	3.8×10^7	4.6 ± 0.4	7.2 ± 0.5	9 ± 2	5.0×10^{-7}	9

3,4 dihydroRF**	3.3×10^7	4.7 ± 0.4	7.7 ± 0.4	10 ± 1	2.0×10^{-6}	8
deazaRF	8.9×10^7	4.2 ± 0.3	5.9 ± 0.4	6 ± 1	2.0×10^{-6}	8
isoLF	1.65×10^8	3.8 ± 0.3	7.7 ± 0.3	12 ± 1	5.0×10^{-7}	9
8 NorLF	1.15×10^8	4.0 ± 0.2	6.2 ± 0.7	7 ± 2	5.0×10^{-7}	5
10 MeIA	1.20×10^8	4.0 ± 0.4	6.0 ± 0.3	7 ± 1	5.1×10^{-7}	11
7 ClLF	1.65×10^8	3.8 ± 0.2	6.7 ± 0.4	10 ± 1	5.0×10^{-7}	5
8 ClLF	1.45×10^8	3.9 ± 0.2	6.6 ± 0.3	9 ± 1	5.0×10^{-7}	5
7,8 diClLF	1.50×10^8	3.9 ± 0.2	6.9 ± 0.2	10 ± 1	5.0×10^{-7}	8
3 Me, 8α MorphLF	5×10^7	5 ± 1	---	---	5.0×10^{-7}	2
1,3 diMeA	1.5×10^8	3.9 ± 0.5	---	---	2.0×10^{-6}	2

* The Arrhenius plots in these cases consisted of data points at only two temperatures.

** The values for 3,4 dihydroRF are subject to some uncertainty as a result of the apparent contamination of this analog with RF.

changes in the values of ΔH^{+} and ΔS^{+} between the negatively charged and uncharged analogs are in opposite directions for the two pairs.

The introduction of a methyl or even a benzyl residue at position 3 has little effect on the rate constant, but some effect on the activation energies.

The rate constants for the analogs altered in the 5, 6, and 7 positions show little difference from the rate constant for LF. With the exception of the ΔH and ΔS_u^{+} values for isoLF, the activation energies for any analog within this group are quite similar to the values for any other.

Attachment of the morpholino residue at position 8α decreases the rate constant for binding about a factor of 3, as seen by comparison of the data for 3 Me, 8α Morph LF and 3 MeLF.

Comparing the data for 3 MeLF, 10 MeIA, and 1,3 diMeA indicates that the shift of a methyl residue from position 10 to position 1 has little effect on the rate of binding of the analog to apoRBP.

Relaxation Studies on Flavin Analog Binding to ApoRBP

Of concern in this section is the number of steps in the binding sequence. The hypothesis is that if a value of k_{-1} for the binding of a given analog to apoRBP can be determined by an independent method and shown equal to k_1/K_a, then any additional step(s) in the reaction (e.g. Equation (3)) must satisfy the relation $k_{2\ldots}/k_{-2\ldots} = 1$ or $\Delta G_{2\ldots} = 0$. If it can also be demonstrated that $\Delta G_{2\ldots} = 0$ at different temperatures, then $\Delta H_{2\ldots} = 0$ and $\Delta S_{2\ldots} = 0$. Any additional

step is thus of little consequence to binding and the reversible binding of flavin analogs by apoRBP will have been shown to be adequately described by a one-step mechanism.

Relaxation techniques provide an independent method of measuring reaction rate constants. In these techniques information can sometimes be extracted about the number of steps in the reaction and about the various rate constants.

Specifically consider the binding system of Equation (1). After defining the quantity $[\delta F] = [F] - [F]_e$, the displacement at any time of the concentration from its final equilibrium value, it is easily shown (91, also see Appendix D) that

$$[\delta F] = [\delta F]_o \, e^{-\tau t}$$

where $[\delta F]_o$ is the maximum displacement of the quantity [F] and

$$[\tau]^{-1} = k_1([A]_e + [F]_e) + k_{-1} \qquad \text{Equation 13}$$

Thus the binding system of Equation (1) produces a relaxation process described by a single exponential constant, τ, and the plot of $(\tau)^{-1}$ against $[A]_e + [F]_e$, where these are final equilibrium values, yields k_1 as slope and k_{-1} as y-intercept. By contrast, multistep reactions, in theory, yield relaxation kinetics characterized by one τ value for each step - but these τ values must differ by about an order of magnitude to be experimentally differentiated (92). Multistep reactions also yield plots of τ^{-1} against $[A]_e + [F]_e$ which have slope and intercept values with dependencies on k_1 and k_{-1} altered from those of single step reactions (92).

Relaxation studies were conducted with several analog-apoRBP complexes to see if 1) the kinetics were described by a single exponential constant and 2) if the values of k_{-1} obtained at different temperatures were equal to the calculated k_1/K_a values for the several complexes at the different temperatures.

Relaxation reactions associated with flavin binding to apoRBP can be observed when holoprotein solutions are rapidly diluted with an equal volume of buffer in the stopped-flow fluorimeter*. The following argument demonstrates that dilution perturbs the equilibrium of this system. Let the superscript B indicate concentrations before mixing. Before mixing, $K_a = \dfrac{[H]_e^B}{[F]_e^B \times [A]_e^B}$. Immediately after dilution, $\dfrac{\frac{1}{2}[H]_e^B}{\frac{1}{2}[F]_e \times \frac{1}{2}[A]_e^B} \neq K_a$, that is, the system is no longer at equilibrium. Two factors combine to make the dilution method an attractive one for studying the relaxation kinetics of the analog-apoRBP system. 1) The expected dissociation rate constants, k_{-1}, are all less than 100 sec^{-1}, thus the second term in Equation (13) will not cause the relaxation process to be completed within the dead time of the instrument. 2) Analogs with maximum absorbance at wavelengths greater than 400 nm have enough fluorescence intensity in the stopped-flow fluorimeter

---

* Appendix D shows that this mixing ratio does not violate the condition that $[\delta F]$ be small relative to $[F]_e$, this condition being necessary to obtain Equation (13).

that sufficiently low concentrations of complex can be used in order to reduce the first term in Equation (13) to a value < 100 sec^{-1}.

In order that these experiments be conclusive, some care must be taken in their design. The object of this section of the thesis concerns the measurement of k_{-1}, not just the measurement of many different τ values. Thus the after-mixing values of $[A]_e$ and $[F]_e$ must be selected to maximize the information about k_{-1} contained in the τ values. Ideally one would like to perform the studies such that $k_{-1} >> k_1([A]_e + [F]_e)$ throughout the concentration range studied. Thus τ^{-1} plotted against $[A]_e + [F]_e$ would approach a horizontal line and the magnitude of the y-intercept (k_{-1}) would be easy to discern. In the present study this would require the use of free flavin concentrations too dilute to be observable in the stopped-flow fluorimeter. On the other hand, at much higher concentrations of $[A]_e + [F]_e$ such that $k_{-1} << k_1([A]_e + [F]_e) < 200\ sec^{-1}$ the experimental relaxation traces would have vastly improved signal-to-noise, yet would contain little useful information about k_{-1}. In the latter case, the plot of τ^{-1} against $[A]_e + [F]_e$ would have considerable slope and a y-intercept not significantly different from zero (e.g., Figure 46A). Slight data scatter, common in relaxation plots, would make the value of k_{-1} uncertain. Appendix D shows that a suitable compromise is to use a series of solutions of the complex which, when diluted, include a solution at a concentration near the K_d value of the complex. From the foregoing one concludes that, for the RBP system, values of k_{-1}

will be difficult to measure by means of relaxation studies for the binding of analogs with any one of the following properties: 1) a k_{-1} value > 100 sec^{-1}, 2) a K_d value < 10^{-7} M, or 3) a long wavelength maximum at wavelengths below 400 nm.

Relaxation experiments were conducted using apoRBP complexes with five analogs. The analogs were selected to give a wide range in 1) the values of K_d, 2) the values of k_{-1}, and 3) the chemical modifications of the "flavin" moiety. It is reasonable to expect that any deviation from one-step reversible binding will be manifested by relaxation studies of one of these widely different flavin analogs.

For each analog, relaxation studies were performed at two or more temperatures in the range 10-40°C. To improve signal-to-noise quality, from 5 to 15 shots were accumulated with the CAT. To determine the value of τ for a given shot, an average line was drawn through the readout trace and the logarithm of the arbitrary values of the points on this line were plotted as a function of time. Representative examples of traces and the semilogarithmic plots from them are shown in Figure 45. The traces with a high degree of signal-to-noise quality were found to be accurately described by a single exponential for more than two half lives.

The plots of τ^{-1} against $[A]_e + [F]_e$ for the five analog-apoRBP complexes are given in Figure 46A, B, C, D, and E. The agreement between the observed values of τ and the values expected for one-step reversible binding are seen to be good with apparently one exception.

Legend to Figure 45

The three traces in Figure 45 show the increases in fluorescence observed when solutions of analog-apoRBP complexes are diluted with an equal volume of buffer. The traces are selected to represent the signal-to-noise quality of the relaxation experiments. Each trace represents the average of several (from 3-12) shots accumulated in the CAT. Approximately 10% of all the traces had S/N quality poorer than that shown in trace A, while 10% had S/N quality better than that shown in trace C. The S/N quality of trace B represents a mean quality. The plots to the right of each trace are semilogarithmic plots of the curve fitted by hand to the recorded data.

Trace A shows the relaxation when a solution of 8 NorLF-apoRBP is diluted to 2.4×10^{-7} M at 25°.

Trace B shows the relaxation when a solution of LF-apoRBP is diluted to 8.0×10^{-8} M at 19.8°C.

Trace C shows the relaxation when a solution of FMN-apoRBP is diluted to 2.0×10^{-6} M at 15°C.

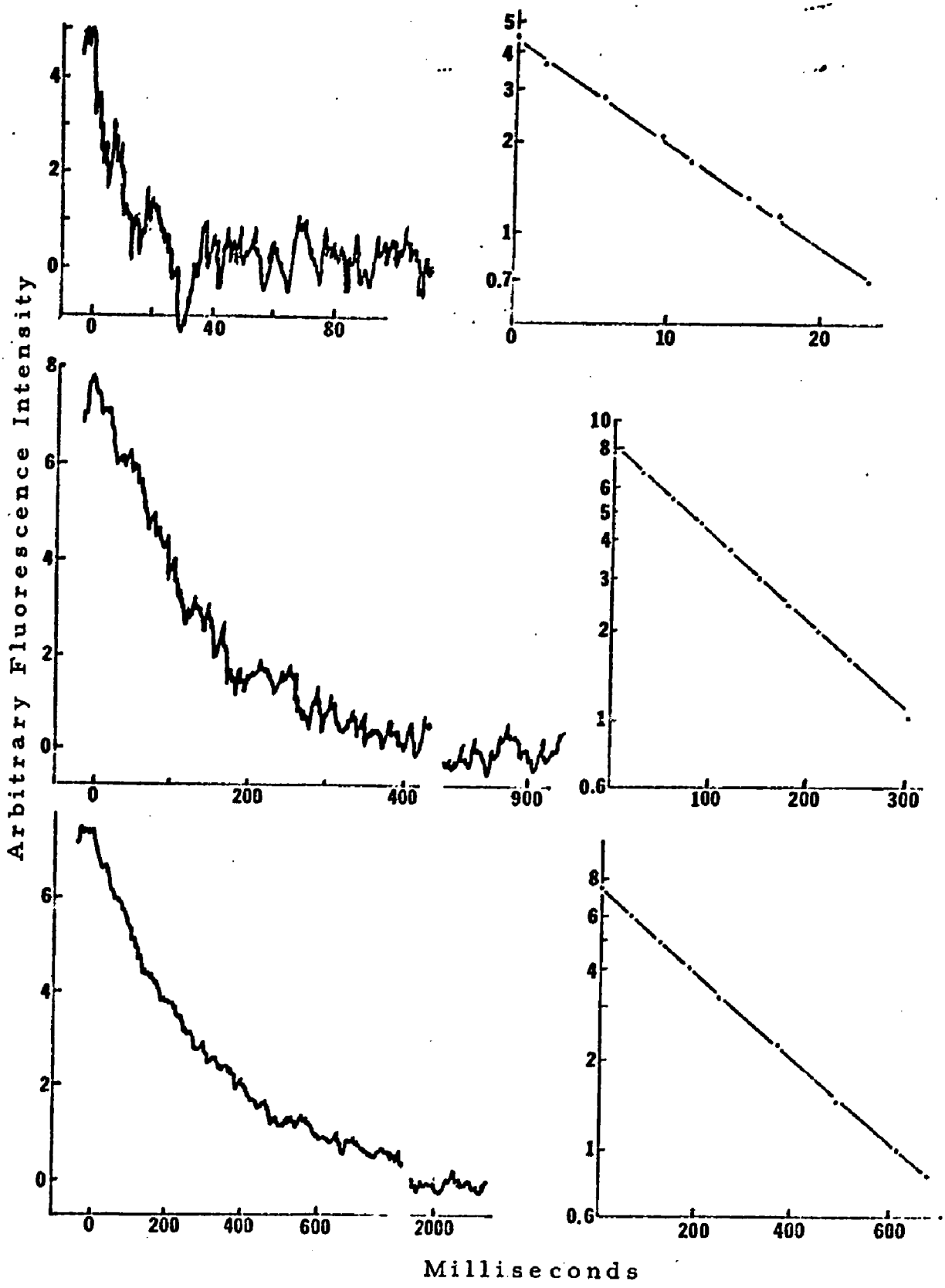

Figure 45. Representative Examples of Relaxation Traces for Dilution Experiments with Analog-ApoRBP Complexes.

Legend to Figure 46

The plots in Figure 46A, B, C, D, and E show the results of the dilution relaxation experiments for five analog-apoRBP complexes at different temperatures. The values for $2[F]_e = [A]_e + [F]_e$ were determined from Equation B1 in Appendix B. The value of K_d used in Equation B1 was the value at the appropriate temperature determined from the appropriate van't Hoff plot. Each data point represents an observed relaxation time. The lines are drawn with slopes equal to the values of k_1 at the appropriate temperature on the Arrhenius plots and with intercepts equal to the values of k_1/K_a taken at the appropriate temperatures on the Arrhenius and van't Hoff plots.

Figure	Complex	Temperature	Observed Intercept	Calculated $k_{-1} = k_1/K_a$
		(^oC)	(sec^{-1})	(sec^{-1})
46A	RF-apoRBP	30.2	0.1	0.15
		19.9	-0.05	0.03
		10.2	0.0	0.005
46B	LF-apoRBP	40	76.	51.
		30	33.	27.
		15	3.0	1.7
46C	8 NorLF-apoRBP	25	60.	55.
		15	13.	16.5
46D	3 OAc^-LF-apoRBP	25	13.	16.7
		15	4.2	4.9
46E	FMN-apoRBP	25	4.	10.5
		15	1.1	2.8

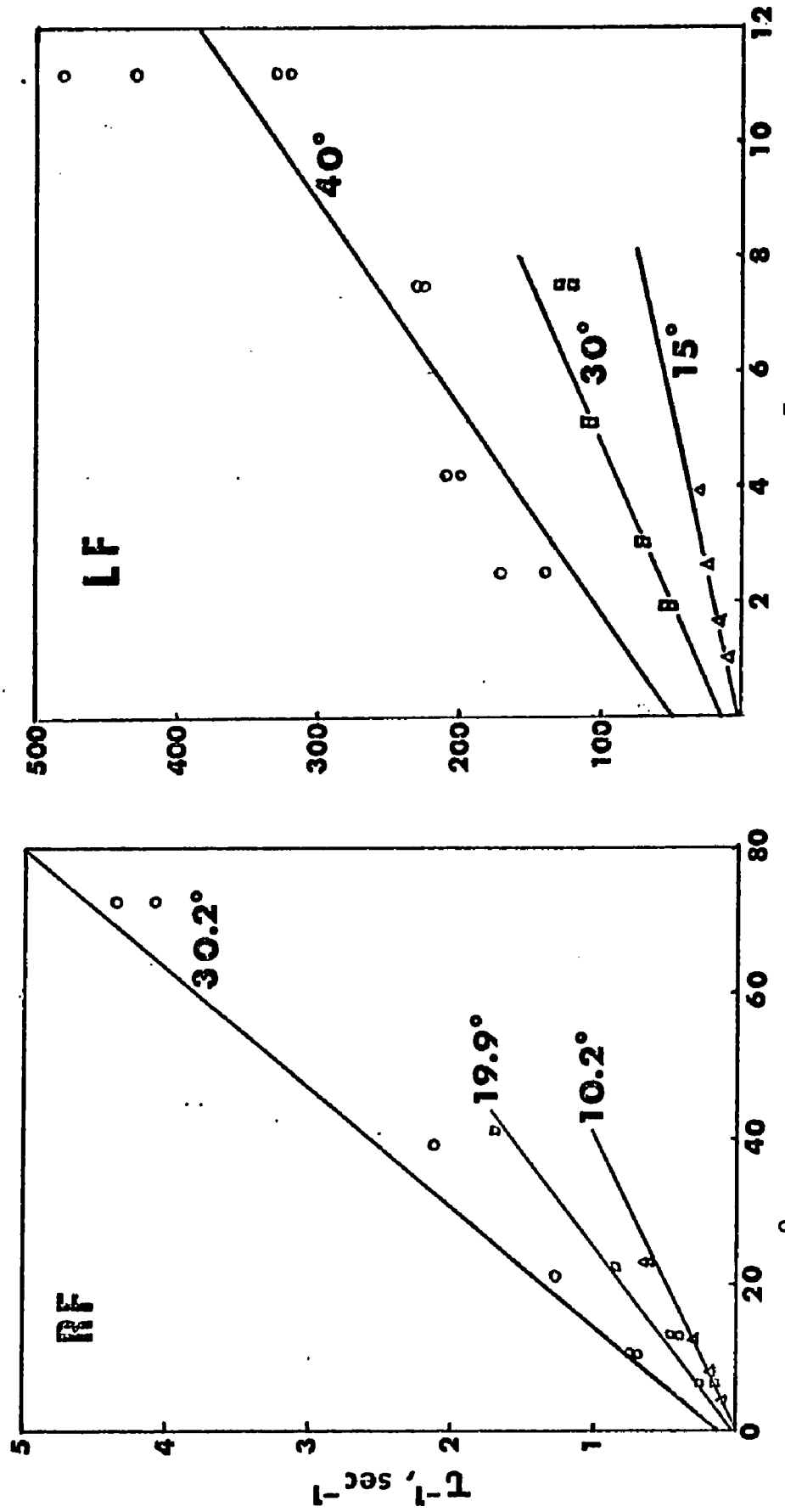

Figure 46A, B. Relaxation Analyses for the Binding of RF and LF to ApoRBP.

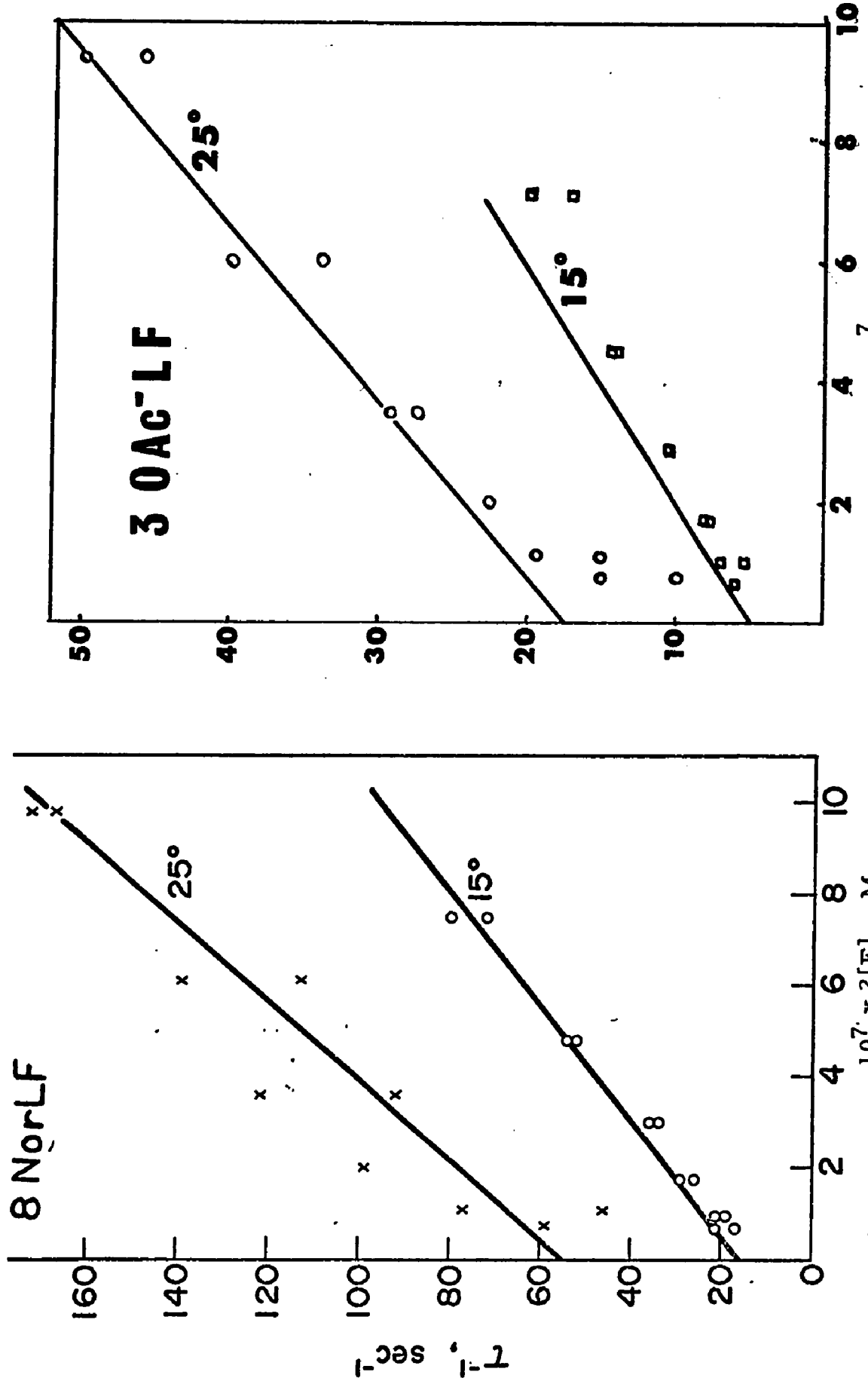

Figure 46C, D. Relaxation Analyses for the Binding of 8 NorLF and 3 OAc^-LF to ApoRBP.

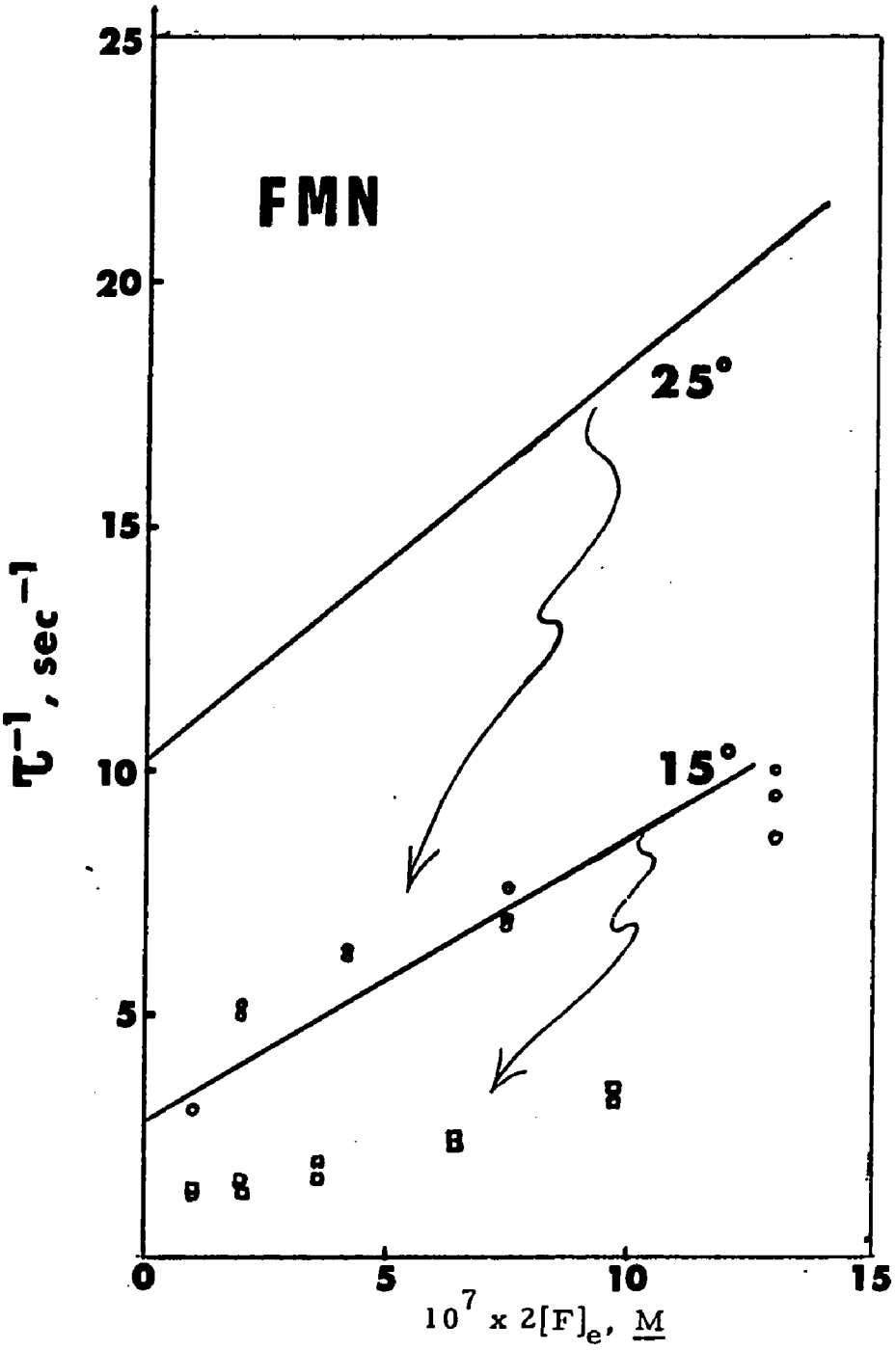

Figure 46E. Relaxation Analysis for the Binding of FMN to ApoRBP.

In the case of FMN, the plots yield y-intercepts (k_{-1} values) less than one half the values of k_1/K_a. In addition, agreement between the observed k_{-1} values and those calculated from k_1/K_a for RF binding cannot be verified from these experiments because of the very low value of K_d for RF binding. Adequate signal-to-noise quality is not available at the dilute concentrations required to obtain useful information about the value of k_{-1} for RF binding from these relaxation studies.

The scatter in the data in some of the plots in Figure 46 may warrant future reexamination of these relaxation analyses. However, it seems clear that the binding of those analogs which differ only slightly from LF can be adequately described by a one-step reversible reaction. On this basis, the equilibrium energies in Table X and the activation energies in Table XII can be used to obtain the activation energies for the dissociation of these analogs from RBP. These energies are given in Table XIII.

TABLE XIII

Activation Energies for the Reverse Reaction Step in the Binding of Some Flavin Analogs by ApoRBP

These are the values calculated from the data for the equilibrium constants and second order rate constants under the assumption that binding is a one-step reversible reaction.

Flavin	$k_{-1}(25^{\circ})$	$\Delta G^{\ddagger}_{-1}(25^{\circ})$	$\Delta H^{\ddagger}_{-1}$	$\Delta S^{\ddagger}_{-1}(25^{\circ})$
	sec^{-1}	kcal/mole	kcal/mole	e.u./mole
RF*	0.061	19.2	28.1	30
LF	7.0	16.3	23.6	25
LC	23	15.6	~25	~33
10 EtOHF*,**	2.8	16.8	26.1	31
TARF*,**	92	14.6	24.7	34
FMN*,**	11	15.8	25.1	31
3 MeLF	8.8	16.1	20.0	13
3 BzLF	1.57	17.2	23.3	20
3 OAc^{-}LF	17	15.7	22.0	22
3,4 dihydroRF*,***	0.9	17.4	23.9	22
deaza RF*	0.52	17.9	24.8	30
isoLF	13.6	15.9	23.1	23
8 NorLF	55	15.0	20.6	18
10 MeIA	44	15.2	21.0	20
7 ClLF	3.4	16.7	24.8	28
8 ClLF	11.8	16.0	22.8	23
7,8 diClLF	6.2	16.4	22.8	22
3 Me, 8α MorphLF	250	14.7	---	--
1,3 diMe A	6	16.4	---	--

* The binding of these analogs may not be adequately described by a one-step reversible reaction.

** These values are subject to additional uncertainty because of the two temperature Arrhenius analyses.

*** The values for 3,4 dihydroRF are subject to uncertainty as a result of the apparent contamination of this analog with RF.

CHAPTER 5

DISCUSSION

The Leghorn white RBP preparation used in the studies presented in this thesis is > 95% homogeneous by disc gel electrophoresis at pH 9 and by SDS gel electrophoresis at pH 7.0. A slight heterogeneity is found when RBP is subjected to disc gel electrophoresis at pH 6 and to gel isoelectric focusing. Both fractions seen in the electrofocused sample contain bound flavin. The RBP preparation is therefore homogeneous with respect to size but contains a slight charge heterogeneity.

As determined by the method of gel isoelectric focusing, the protein has a pI value of 4.5, a value slightly higher than found previously (39). By the method of SDS gel electrophoresis, the protein molecular weight is about 30,000 Daltons, a value in close agreement with published values (37, 39, 40).

No evidence is found to support the conclusion of Clagett and coworkers (40, 41, 66, 67) that Leghorn RBP is composed of subunits (24,000 and 8,000 Daltons) connected by disulfide bonds. This is concluded because the RBP sample reduced with 2-mercaptoethanol (a treatment which should have reduced all disulfide bonds) migrates by SDS gel

electrophoresis as a homogeneous protein of 30,000 Daltons. The absence of stainable material migrating with mobility greater than this peak indicates the absence of polypeptides with molecular weight less than 30,000 Daltons.

The apoprotein is easily produced and is homogeneous with respect to binding, as tested by two criteria. 1) The Scatchard analysis for RF binding shows that the interaction obeys a unique K_a value over wide ranges in both the fraction of flavin complexed and the fraction of apoprotein complexed. 2) ApoRBP fractions separated by chromatography on SE Sephadex (a method which is likely to separate the differently charged RBP molecules seen on electrophoresis at pH 6) show identical behavior in regard to the binding of LF.

The stoichiometry of binding is strictly one mole of flavin per mole of protein. The evidences for this assertion are 1) the weight of protein required to quench the fluorescence of one mole of flavin agrees with the molecular weight of the protein determined by physical methods and 2) the maximum amount of RF-apoRBP complex (as determined by the CD intensity at 458 nm) is formed when the mole fraction of each component is 0.5. These methods show that the apoRBP molecule has only one RF binding site with $K_a > 10^3 \ \underline{M}^{-1}$.

The protein does not contain stainable lipid, but does contain about 9 moles of sugar residues per mole of protein - a value consistent with that previously found (37, 40). RBP lacks the ability to form

a sulfite adduct, indicating it is not an oxidase-type flavoprotein (77). RBP also lacked the ability to mediate cytochrome c reduction by TPNH in the presence of ferredoxin.

The importance of using pure analogs in the studies presented in this thesis can not be over emphasized. A technique for affinity chromatography of flavin samples on G 50 Sephadex is found to achieve a separation of the flavins from some impurities but this technique is not able to separate different flavin analogs. In addition, some of the analogs (e.g. 3,4 dihydroRF; 3 Me, 8 α MorphLF) are found to contain impurities when subsequently analyzed by TLC. Accordingly, the binding studies for these analogs may warrant reexamination using samples further purified by preparative TLC or an equivalent method.

The most important conclusion reached from the stoichiometric binding titrations of the analogs is that one mole of apoRBP binds one mole of the analog. This is demonstrated by the agreement of the long wavelength analog absorptivities (Table VIII) both with one another and with published values (93).

As it has been in other flavin binding studies, the technique of flavin fluorescence quenching proves very useful to the study of the interaction of flavin analogs with apoRBP. The equilibrium constants for the analog-apoRBP complexes studied in this thesis range in value from $\sim 10^9$ $\underline{M}^{-1}$ to $< 10^4$ $\underline{M}^{-1}$, a fairly wide range, but of intermediate values in regard to the binding to other apoflavoproteins of their

natural flavin prosthetic groups. For example, FMN binds to apoOYE (9) and to P. elsdenii apoflavodoxin (26) with greater affinity, while FAD binds to apoDAAO with a K_a value about 5×10^6 M^{-1} (19) and to lipoamide apodehydrogenase with a K_a value about 3×10^5 M^{-1} (21)(this is a surprisingly low value), values toward the lower end of the range covered by analog binding to apoRBP.

Although the list of equilibrium energies in Table X contains the results for binding many different flavin analogs to apoRBP, the major conclusion is that no small modification in the flavin structure produces a change in the value of ΔG_u, ΔH, or $T\Delta S_u$ greater than a few kcal/mole. None of the deletions or alterations prevented binding - thus none of the altered groups on the flavin nucleus is absolutely essential to the interaction of flavins with this apoprotein. This result is contrasted by the observations for several other flavoproteins that a single interaction can have decisive control over the binding process. Thus P. elsdenii apoflavodoxin appears not to bind flavin analogs which have other than a single phosphate group on the terminal end of the riboflavin side-chain (26); A. vinelandii apoflavodoxin (Shethna apoprotein) binds FMN, 3 MeFMN, and RF, but not 3 MeRF (28), and apoOYE binds FMN with affinity more than a million times greater than it binds RF (9).

Although the differences in energy changes in Table X are small in comparing the results for the binding of one analog with another, several correlations can be drawn in regard to the functional

groups on the isoalloxazine ring which contribute favorably to the interaction between flavins and apoRBP:

1) The results for the binding of 10 EtOHF and RF in comparison to those for LF indicate that hydroxyl groups attached to a side chain in the N(10) position contribute favorably to the interaction. RF binds with a free energy change more negative by 2.5 kcal/mole than is observed for the binding of LC. The results of Rhodes et al. (39) for the binding of GalF and LyxF to apoRBP in comparison to LF binding indicate that other sugar residues attached to N(10) also contribute favorably to the interaction. However, the binding affinity for GalF and LyxF is smaller than for RF showing the importance of the stereospecificity of the hydroxyl groups.

2) Comparing the results for 1,3 diMeA with those for 10 MeIA may indicate that the introduction of a methyl residue in position 1 produces a free energy change more favorable to the interaction by about 1 kcal/mole. This assumes that one can use the results for LC and LF to show that the absence of a methyl residue in position 10 makes little difference to the free energy change and the results for 3 MeLF and LF to show that inclusion of a methyl residue in position 3 makes little difference to the free energy change.

3) The results for analogs with and without reduced C(4) = O groups shows that an intact carbonyl in this position may contribute between 1 and 2 kcal/mole to the total interaction free energy change.

4) The results for deazaRF and RF show that the nitrogen in position 5 contributes 1 kcal/mole to the interaction.

5) The results for 8 NorLF in comparison to those for LF indicate that a methyl residue attached to position 8 contributes more than 1 kcal/mole to the total free energy change.

6) Comparing the results for 10 MeIA with those for 8 NorLF shows no further difference in the free energy change accrues from the replacement of the methyl residue in position 7 by a hydrogen. However, the results for isoLF in comparison to those for 8 NorLF show that the introduction of a methyl residue in position 5 produces a more favorable free energy change on binding.

The preceding list shows the flavin functional groups and ring positions examined which do appear favorable to the interaction with apoRBP as judged by differences in free energy change on binding. To the extent one is justified in summing the differences, a total value for these individual interactions can be found. By this method almost half (6-7 kcal/mole) of the free energy change when RF binds to apoRBP (ΔG_u = -14.7 kcal/mole) is accounted for by the interactions with the functional groups at positions 4, 5, 8, and 10. The total change in free energy, enthalpy, or entropy which accompanies the binding of flavins to apoRBP appears largely to be composed of small contributions resulting from interactions at many positions of the flavin molecule, a result of some importance with regard to biological specificity.

The validity of the bookkeeping method by which differences in free energy changes are summed is somewhat in question as seen by comparison of the results for the binding to apoRBP of two pairs of analogs: A) LF and 10 MeIA, and B) 1, 3 diMeA and 1, 3, 7, 8 tetMeA. The structural difference between pairs A and B is the same, yet the difference in free energy changes for the binding of the analogs within the pairs is not the same, by about 1 kcal/mole. Rhodes et al. (39) studied the relative binding of RF, 3 MeRF, LF, and 3 MeLF to apoRBP - another set of analogs by which the summability of the differences in free energy changes can be examined. Their data, reproduced in Table V, show the difference between the relative binding of RF and 3 MeRF is greater than that observed between LF and 3 MeLF. One concludes that small differences observed in free energy changes may not, in fact, be summable. Future studies should examine this point in more detail.

The greatest differences in free energy change in Table X are seen to occur for the binding of those analogs to which relatively large, bulky substituents are attached. It is important to note, however, that in no case did a residue added to the flavin structure prevent binding of the analog by apoRBP. This indicates the protein moieties comprising the site do not place severe steric limitations on the size of the flavin, i.e. that the site can accomodate larger flavin analogs. The results for TARF (and for FMN and FAD, although the negative charge on the phosphate groups in these analogs probably contributes unfavorably to

the interaction) gives indication of a limitation in the amount of "space" available in the protein region around the flavin side chain. A steric limitation may also exist in the region around position 8 α , as indicated by the more positive change in free energy of binding for 3 Me, 8 α MorphLF and 8 α histLF. (That the latter is a zwitterion may contribute to its less favorable free energy change.)

It is interesting to note that, for the "bulky" analogs where the binding data are available, an unfavorable entropic contribution to the interaction results in the observed decrease in free energy.

Some regions of the binding site appear more accomodating to "bulky" residues attached to the flavin and indicate a lower degree of steric restriction. Thus, a benzyl residue at position 3 actually favors the interaction slightly. Although the binding of 3 BzLF is entropically less favorable than the binding of 3 MeLF (a consistent but less dramatic example of the concurrence of "bulk" with an unfavorable Δ S value), a more favorable enthalpy change results in the slightly more favorable free energy change.

As is often found, these studies merely indicate the need for further experiments, in this case to delineate the relative importance of size and of chemical nature in regard to the effects of these "bulky" residues. However, the approach of attaching large substituents at various positions on the flavin nucleus appears fruitful.

The results of the equilibrium binding of flavin analogs to apoRBP are summarized in terms of the diagram in Figure 47. The

differences among the values of ΔG_u in Table X say little about the binding site in three dimensions, that is, the interactions responsible for the observed effects may be directed from above, below, or in the plane of the isoalloxazine ring. Accordingly, the symbols given below depict the position but not the orientation of the effect:  = an interaction accounting for a free energy contribution more favorable (negative) by 1 kcal/mole,  = a site which can interact with a methyl residue at this position on the flavin nucleus to yield a free energy contribution more negative by about 1 kcal/mole,  = a region of relative steric limitation,  = a region out of the plane of the flavin which can interact favorably with an aromatic group and = uncharted territory.

Figure 47. A Diagram of the Flavin Binding Site on ApoRBP.

In comparison of the equilibrium energies for many pairs of analogs, it is often noted that two analogs have the same ΔG_u value as the result of considerably different ΔH and ΔS_u values. This is an example of entropy-enthalpy compensation (94). In order to have strict entropy-enthalpy compensation, ΔG_u must remain unchanged for a series of analogs, and it is clear that this is not the case for flavin binding to apoRBP. Nevertheless, an entropy-enthalpy compensation plot is given in Figure 48 summarizing all the data for analog binding to apoRBP. While the points representing the results for the different analogs are scattered, a trend is evident from lower left to upper right. The extent to which this indicates the involvement of water (as has been suggested for compensation in general (95)) in the binding process is uncertain.

The study of the pH dependence of RF binding to apoRBP shows a plateau region between pH 6 and pH 9 over which the value of K_a is nearly the same. The value of K_a decreases rapidly toward lower pH values in a curve very similar to the one for the pH dependence of specific flavin binding capacity as shown by Farrell et al. (37). A decrease in K_a value is also seen at values above pH 9. (This region was not studied by Farrell et al. (37).) Increasing the ionic strength of holoRBP solutions produces a decrease in K_a value at low pH values, but apparently not at neutral pH values.

The flavin analog complexes with apoRBP have optical and CD spectra characteristic of many flavoproteins. Namely, the optical

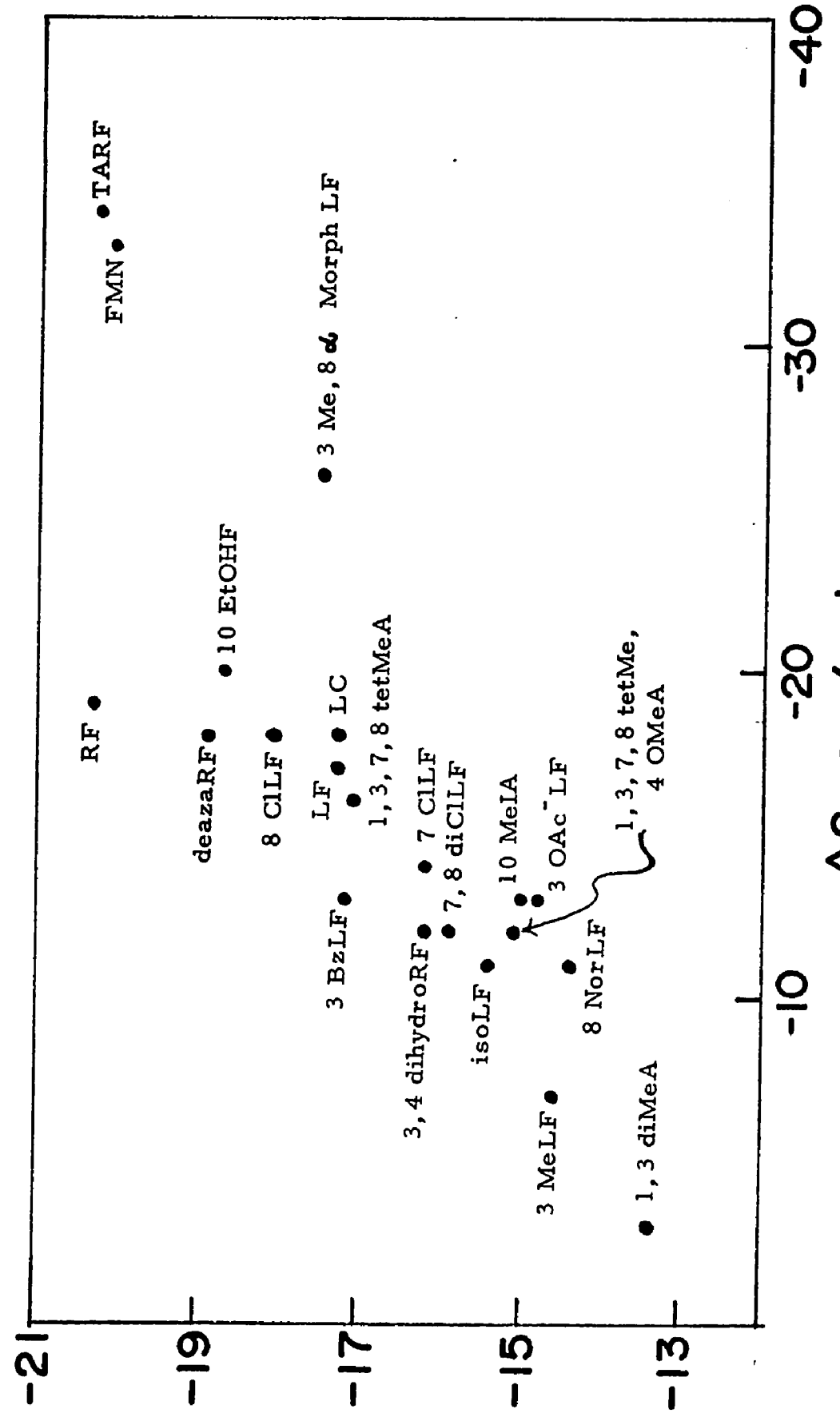

Figure 48. Entropy-Enthalpy Compensation Plot for the Binding of Flavin Analogs by ApoRBP.

spectra of the complexes generally show hypochromism of the flavin bands, resolution of the 450 nm free flavin peak, and long wavelength tailing toward the red. The CD intensity corresponding to the electronic transitions in the flavin is greatly increased on binding and the long wavelength CD peak corresponds in position to the long wavelength optical absorptivity peak. (The CD peak at 340 nm observed for many analog-apoRBP complexes does not correspond in position to the prominent optical peak in this region (370 nm).

On the basis of several spectral deviations, however, the apoRBP complexes with one group of analogs could be distinguished from the complexes with the other analogs. When complexed to apoRBP, the analogs lacking a methyl residue on position 8, namely 10 MeIA, 8 NorLF, and isoLF differed from other analogs in the following ways: 1) the complexes with these three analogs lacked a definite shoulder in their optical spectra near 480 nm, 2) the complexes lacked definite shoulders in their CD spectra near 480 nm, and 3) the intensity of the 340 nm CD peak for these complexes was considerably reduced from that observed for the complexes with other analogs having a methyl residue in position N(10).

Few studies are available for direct comparison. However, some examples exist which are consistent with these observations. FMN and isoFMN free in aqueous solution are both similar in showing little structure in the long wavelength peaks of their optical absorptivity spectra. However, as shown by Mayhew (26,27), considerable

resolution of the FMN peak at 450 nm occurs on binding to the apoflavodoxin from P. elsdenii. This is radically contrasted by the behavior for the complex of isoFMN with this apoprotein, which shows no more resolution in the long wavelength peak for the complex than for the free flavin - although considerable red shift and hypochromism are evident. The optical spectra for the complexes of FMN and isoFMN with the apoflavodoxin from A. vinelandii are consistent but less dramatic in this regard. The optical spectrum of the complex of this apoprotein with isoFMN apparently has a shoulder near 480 nm (96), but the absorptivity of this shoulder is considerably smaller than the absorptivity for the shoulder at 480 nm seen for the complex of A. vinelandii apoflavodoxin with FMN (96, 97).

One study is not consistent with the foregoing observations. The CD spectra for the FMN and isoFMN complexes with the apoflavodoxin from A. vinelandii are similar and show positive dichroism peaks near 475 nm of about the same absorptivity value ($3\ \underline{M}^{-1}\,cm^{-1}$) (96).

To what extent other apoflavoprotein complexes with this group of analogs will show diminished resolution at 480 nm, altered CD spectra, or other spectral differences remains to be investigated.

The spectra for LF and 8 NorLF behave similarly near 480 nm in dioxane, toluene, and the 1 : 1 mixture of these two solvents (98). This indicates that the observed spectral differences between the complexes with hydrogens and with methyl residues on position 8 results from more than a change in polarity as the molecules pass

from the environment of the aqueous solvent to the environment of the binding site.

Although little change is seen in the optical absorptivity spectra for the complexes of apoRBP with each of the following sequence of analogs: LF, 10 EtOHF, RF, and TARF, a significant and monotonic increase in the CD intensity at 450 nm occurs for the complexes with successive analogs in that sequence. These observations are consistent with the previous observations of Edmondson and Tollin (97) that the relative intensity in the 450 nm region is sensitive to the presence of side chain hydroxyls (they were comparing the results for the apoflavodoxin binding of RF and of FMN with their corresponding deoxy analogs). However, one must not conclude that the increase in CD intensity at 450 nm is necessarily a direct result of an increase in "through space"* interaction between the centers of chirality on the N(10) residue and the isoalloxazine ring. Clearly 10 EtOHF lacks a center of chirality, yet has a CD intensity at 458 nm closer to the value for the complex with RF than to the value for the complex with LF. Thus one hydroxyl residue on an optically inactive two carbon residue attached to the N(10) position could account for the majority of the difference between the intensities for LF and RF at 458 nm. In this regard the CD intensity at 458 nm for the complex of 10 ethylflavin with apoRBP might prove to be a helpful future study.

---

* "Through space" is a term used by Scola-Nagelschneider and Hemmerich (99) to indicate a direction other than in the plane of the isoalloxazine ring.

The considerably larger CD intensity seen for the complex with TARF indicates that the esterified residues may further promote the interactions responsible for the increase in CD intensity for analogs with a ribose attached to position N(10). The data for TARF indicate this increase is not a unique property of hydroxyl groups located on the N(10) residue.

The CD spectra for the complexes of apoRBP with the analogs in the sequence LF, 10 EtOHF, RF show another prominent feature. The CD intensity at 340 nm for the complex with 10 EtOHF is substantially decreased from the intensity for the complex with LF. However, little difference exists for the intensities at 340 nm between the complexes with 10 EtOHF and RF. This is consistent with the conclusion of Scola-Nagelschneider and Hemmerich (99) that the transition responsible for the 370 nm peak is influenced by the electron density at position N(10) and is therefore "susceptible to a 'through chain' interaction with the 2' center of the N(10)-side chain." A future study with other N(10) analogs (e.g. N(10)-ethylflavin, N(10)-3' hydroxypropylflavin, etc.) is indicated.

On the basis of the far ultraviolet mean residue ellipticity for holoRBP in comparison with that for both model polypeptides and egg white lysozyme, the alpha helical content of holoRBP is estimated to be about 25-30%.

The small difference in the far ultraviolet CD spectra between apoRBP and holoRBP suggests that binding causes relatively minor

changes in the overall conformation of the protein. The magnitude of this difference in far ultraviolet CD intensity is considerably smaller for RBP than that observed for several other flavoproteins (glucose oxidase (88), the flavodoxins from four bacteria (88), and lipoamide dehydrogenase (89)). Moreover, the difference shown in Figure 41 is considerably smaller than that reported by Phillips (40) for Leghorn egg white RBP. Because the far ultraviolet CD intensity for free RF is hidden below the linewidth indicating zero dichroism in Figure 41, the arithmetic sum of the CD intensities for free RF and apoRBP in this region does not equal the CD intensity for the holoprotein as asserted by Phillips (40).

Although the difference between the CD intensities of apoRBP minus holoRBP in the region from 210 to 240 nm is small relative to the peak intensity at 208 nm, the maximum difference is about 100 $\underline{M}^{-1}cm^{-1}$. This is five times larger than the largest near ultraviolet CD peak for the holoprotein and ten times larger than the largest visible CD peak. Thus, it is likely that the difference in CD intensity between apoRBP and holoRBP in the 210 to 240 nm region does not result purely from asymmetry induced in the flavin or aromatic chromophores of the protein. It is more likely to result from a small perturbation of some part(s) of the peptide chain. Although conjectures advanced on the basis of far ultraviolet CD spectra are often hazardous, erroneous, or highly oversimplified, the difference in CD intensity between apoRBP and holoRBP in this region could be

accounted for by a slight change in the beta content of the protein. On the basis of the studies by Chen et al. (86) of five proteins, an average spectrum was computed for the beta form. This spectrum shows positive dichroism at 230 nm and negative dichroism at 220 nm with a change in sign at 224 nm. In comparison, the CD spectra for apoRBP and holoRBP show an isosbestic point near 225 nm. The magnitude of the difference between apo and holoRBP corresponds to about 10% of the value calculated for pure beta structure. Thus one speculative explanation for the difference between the two RBP spectra would be an increase in beta structure corresponding to 10% of the RBP residues when RF binds. From the relative size of the CD intensities for pure beta and for pure helical forms calculated by Chen et al. (86), a much smaller change in alpha helix content (corresponding to about 3% of the total residues) could account for the magnitude of the change but not the wavelength of the observed effect. Clearly, however, quite small changes in protein conformation can account for the total change in the far ultraviolet CD intensity which accompanies binding.

The quenching of flavin fluorescence by apoRBP monitors a fast binding process which is strictly second order for all the analogs studied. This is demonstrated by the agreement among the k_1 values for RF binding under widely different relative concentrations of flavin and apoprotein. It is demonstrated for the other analogs (which have association rate constants too fast to be studied under pseudo first order conditions) by the adherence at all temperatures studied of the

kinetic trace to the trace expected for a single-step, reversible, second order binding process.

The values of the second order rate constants found for the binding of flavin analogs to apoRBP range from 8×10^6 to about 3×10^8 $\underline{M}^{-1}sec^{-1}$. These values are somewhat large, but by no means the largest observed for the binding of prosthetic groups to their apoproteins or for the binding of substrates to enzymes (100), however, they are the largest second order values thus far reported for the binding of flavins to apoflavoproteins.

The presence of a ribose moiety on position N(10) of the analog decreases the association rate constant by about a factor of 2-4, while the presence of a negative charge on the analog decreases this rate by a factor of 4-6. The latter observation is consistent with the effects of electrostatic repulsion since the protein bears a net negative charge at pH 7.00. Other modifications in the flavin structure have relatively small effect on the value of the second order rate constant - even the presence of a morpholino residue at position 8α . These observations correlate with the equilibrium and CD binding data to indicate that the site is readily available for interaction and is probably close to or on the surface of the molecule.

For the most part, the activation energies for the association of flavins to apoRBP vary only slightly from one analog to the next. The only activation energies in Table XII which are significantly different from the others are the activation energies for the binding of

FMN and TARF. And for these analogs the decrease in enthalpy of activation is almost entirely compensated by a decrease in the entropy of activation.

Most of the flavin analogs bind to apoRBP with values for the activation free energy, enthalpy, and $T\Delta S^{+}$ of 4, 7, and -3 kcal/mole, respectively. The value for the activation enthalpy compares well with the value for FMN binding to the apoflavodoxin from P. elsdenii (7.7 kcal/mole (26,27)). However, FMN binds to apoflavodoxin with an activation free energy about 9 kcal/mole and an activation entropy of 2 kcal/mole, values significantly different from those for analog binding to apoRBP. From studies of FMN binding to apoOYE, Theorell and Nygaard (8) found values for the activation free energy, enthalpy, and $T\Delta S^{+}$ of 7, 12, and -5 kcal/mole, respectively. These values are also significantly different from the results for analog binding to apoOYE.

The compensation plot for the activation enthalpies and entropies of flavin analog binding to apoRBP is shown in Figure 49. One might expect a higher degree of strict compensation for the activation energies than for the equilibrium energies because the differences in the activation free energies in Table XII are much smaller in absolute magnitude than the differences in the free energy changes in Table X. However, the relative differences are comparable in both cases and as a result, the compensation plot for the activation energies also

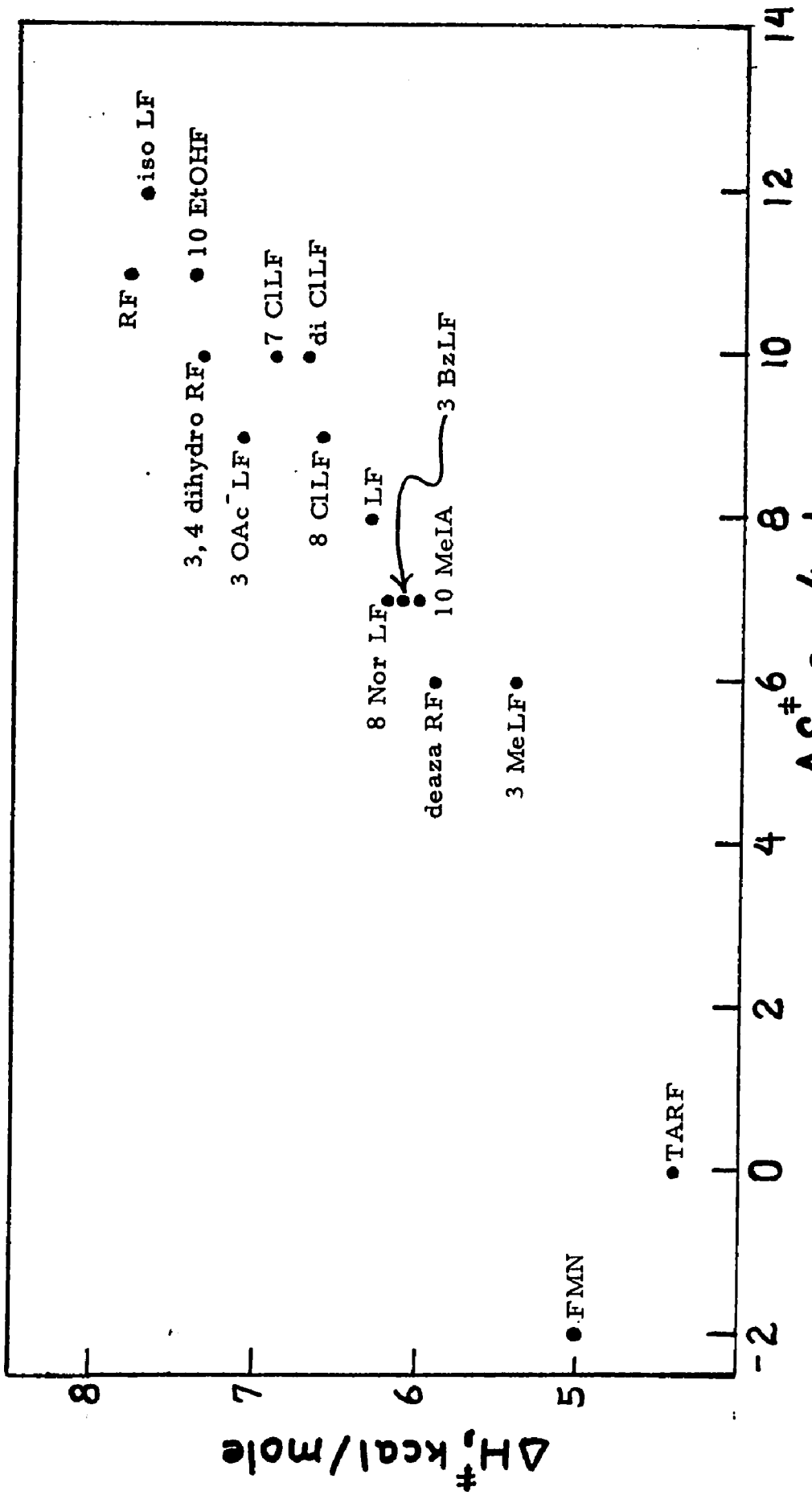

Figure 49. Compensation Plot of Activation Enthalpy Against Activation Entropy for the Binding of Flavin Analogs by ApoRBP.

shows scatter in the data points. Nevertheless, a trend toward compensation is also evident for the activation enthalpies and entropies.

The relaxation studies on the binding of several flavin analogs by apoRBP demonstrate that the binding process for many analogs can be adequately described by the single step equilibrium of Equation (1). For a variety of analog-apoRBP complexes at several temperatures, a rapid change in the concentration of the complex induces a relaxation process which is described by a single exponential having a value expected on the basis of a single step equilibrium. Of the five analog-apoRBP complexes studies, only the relaxation processes for the FMN-apoRBP complex are shown not to be adequately described by Equation (1). It must be added, however, that the relaxation studies on the RF-apoRBP complex are indefinite because of experimental limitations (the large value of K_a). The discrepancy for the FMN studies is unknown but is not necessarily related to the negative charge on the flavin since the observed relaxation behavior for the 3 OAc^-LF-apoRBP complexes agrees well with that expected for single step binding.

The conclusion that binding of widely different analogs is adequately described by a single step process justifies calculating the value of k_{-1} from k_1/K_a in other cases. Calculation of the activation energies for the dissociation process from the results of the equilibrium and association studies also becomes legitimate. This allows the completion of the thermodynamic description for the binding of these flavin analogs by apoRBP.

Small differences in the values of k_1 for analog binding coupled with large differences in the K_a values has a consequence in the relation between K_a and k_{-1} for a single-step equilibrium. This may be considered by taking the logarithm of both sides of the equation $K_a = k_1/k_{-1}$:

$$\log K_a = \log k_1 - \log k_{-1}.$$

If the value of k_1 is invariant, then a plot of log K_a against log k_{-1} is linear with slope of -1. Figure 50 examines such a plot for the binding of all flavin analogs by apoRBP at 25°. The values for log K_a and log k_{-1} cover almost four decades, yet the points fall close to a line with slope -1. To a considerable degree the strength of the interaction, K_a, depends on the rate of dissociation, k_{-1}, of the complex. This result is consistent with a similar observation made by Nygaard and Theorell (9) for the binding of RF, FMN, and FAD to apoOYE.

Very important aspects of the binding of flavins to apoRBP which remain to be investigated are the interactions of portions of the isoalloxazine nucleus with the protein. Of interest in this regard are the soluble members of these classes of analogs (and their resemblance to the flavin structure in Figure 1): 1) pyrimidines (right hand six membered ring), 2) purines (to some extent the two right hand rings), 3) pteridines (the two right hand rings), 4) pyrazines (the middle ring), 5) quinoxalines (the left two rings), etc. These studies might be approached either by competitive binding experiments as delineated in Appendix A, Part III, or by direct methods as described in this thesis.

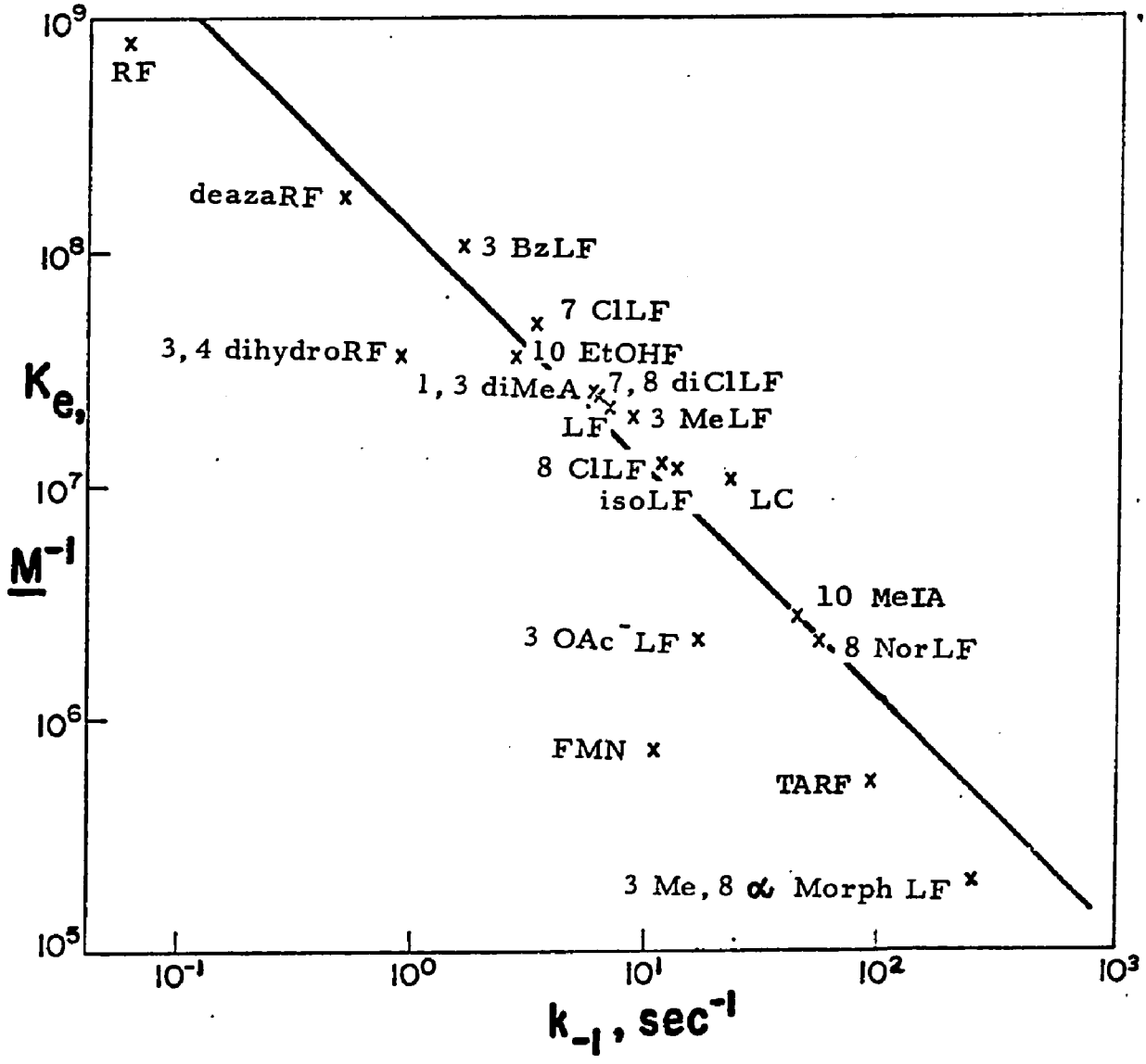

Figure 50. Plot of Log K_a Against Log k_{-1} for Flavin Binding to ApoRBP.

The trend shows the strength of the interaction is determined by the dissociation rate.

Several properties characterize RBP as a dehydrogenase flavoprotein. It is hoped that the studies presented as well as proposed in this thesis will be useful in understanding the interactions which define the specificity of this class of flavoproteins.

REFERENCES

1. Slater, E. C., ed., Flavins and Flavoproteins, Biochim. Biophys. Acta Library Volume 8, Elsevier Publishing Co., New York, 1966.

2. Yagi, K., ed., Flavins and Flavoproteins, Proceedings of the 2nd Conference, University Park Press, Baltimore, Maryland, 1968.

3. Kamin, H., ed., Flavins and Flavoproteins, Third International Symposium, University Park Press, Baltimore, Maryland, 1971.

4. Kenney, W. C., W. H. Walker, E. B. Kearney, R. Seng, and T. P. Singer, Z. Fur Naturforsch. 27b: 1069, 1972.

5. Eyring, H., J. Chem. Phys. 3: 107, 1935; Chem. Rev. 17: 65, 1935.

6. Moore, W. J., Physical Chemistry, Fourth Edition, Prentice-Hall, Inc., Englewood Cliffs, N.J., 1972.

7. Theorell, H. and A. P. Nygaard, Acta Chem. Scand. 8: 877, 1954.

8. Theorell, H. and A. P. Nygaard, Acta Chem. Scand. 8: 1649, 1954.

9. Nygaard, A. P. and H. Theorell, Acta Chem. Scand. 9: 1587, 1955.

10. Warburg, O. and W. Christian, Biochem. Z. 298: 150, 368, 1938.

11. Ehrenberg, A., Acta Chem. Scand. 11: 1257, 1957.

12. Theorell, H. and A. Akeson, Arch. Biochem. Biophys. 65: 439, 1956.

13. Theorell, H., K. Yagi, G. D. Ludwig, and F. Egami, Nature 180: 922, 1957.

14. Strittmatter, P., J. Biol. Chem. 236: 2329, 1961.

15. Strittmatter, P., J. Biol. Chem. 242: 4630, 1967.

16. Walaas, E. and O. Walaas, Acta Chem. Scand. 10: 122, 1956.

17. Chassy, B. M. and D. B. McCormick, Biochim. Biophys. Acta 110: 91, 1965.

18. Dixon, M. and K. Kleppe, Biochim. Biophys. Acta 96: 357, 1965.

19. Massey, V. and B. Curti, J. Biol. Chem. 241: 3417, 1966.

20. Massey, V. and H. Ganther, Biochem. 4: 1161, 1965.

21. Kalse, J. F. and C. Veeger, Biochim. Biophys. Acta 159: 244, 1968.

22. Visser, J., D. B. McCormick, and C. Veeger, Biochim. Biophys. Acta 159: 257, 1968.

23. Visser, J. and C. Veeger, Biochim. Biophys. Acta 206: 224, 1970.

24. Swoboda, B. E. P., Biochim. Biophys. Acta 175: 365, 1969.

25. Swoboda, B. E. P., Biochim. Biophys. Acta 175: 380, 1969.

26. Mayhew, S., Biochim. Biophys. Acta 235: 289, 1971.

27. Mayhew, S., in Flavins and Flavoproteins, Third International Symposium, H. Kamen, ed., University Park Press, Baltimore, Maryland, 1971, p. 185.

28. Edmondson, D. E. and G. Tollin, Biochem. 10: 124, 1971.

29. Scatchard, G., Ann. N.Y. Acad. Sci. 51: 660, 1949.

30. Edsall, J. T. and J. Wyman, Biophysical Chemistry, Volume I, Academic Press, Inc., New York, 1958, p. 610 ff.

31. Lowry, O. H., N. J. Rosebrough, A. L. Farr, and R. J. Randall, J. Biol. Chem. 193: 265, 1951.

32. Hinkson, J. W., Biochem. 7: 2666, 1968.

33. Barman, B. G. and G. Tollin, Biochem. 11: 4746, 1972.

34. Massey, V., Biochem. J. 53: 72, 1953.

35. Rhodes, M. B., P. R. Azari, and R. E. Feeney, J. Biol. Chem. 230: 399, 1958.

36. Winter, W. P., E. G. Buss, C. O. Clagett, and R. V. Boucher, Comp. Biochem. Physiol. 22: 892, 1967.

37. Farrell, H. M., Jr., M. F. Mallette, E. G. Buss, and C. O. Clagett, Biochim. Biophys. Acta 194: 433, 1969.

38. Farrell, H. M., E. G. Buss, and C. O. Clagett, Intern. J. Biochem. 1: 157, 1970.

39. Rhodes, M. B., N. Bennett, and R. E. Feeney, J. Biol. Chem. 234: 2054, 1959.

40. Phillips, J. W., Ph. D. Thesis, Pennsylvania State University, 1969.

41. Cotner, R. C. and C. O. Clagett, Fed. Proc. 31: 851Abs., 1972.

42. Nishikimi, M. and K. Yagi, J. Biochem. (Japan) 66: 427, 1969.

43. Means, G. E. and R. E. Feeney, Chemical Modification of Proteins, Holden-Day, Inc., San Francisco, 1971, p. 12.

44. Ostrowski, W., Z. Zak, and A. Krawczyk, Acta Biochim. Polon. 15: 241, 1968.

45. Zak, Z. and W. Ostrowski, Acta Biochim. Polon. 10: 427, 1963.

46. Ostrowski, W. and A. Kzawczyk, Acta Chem. Scand. 17: S241, 1963.

47. Zak, Z., L. E. G. Eriksson, R. Rigler, C. Zalenski, and A. Ehrenberg, "Interaction between protein and flavin in the riboflavin binding protein from egg yolk," presented at the Fourth Conference on Flavins and Flavoproteins, Konstanz, Germany, 1972.

48. Palmer, G. and L. Casola, unpublished results, 1968.

49. Palmer, G., F. Muller, and V. Massey, Flavins and Flavoproteins, Third International Symposium, H. Kamin, ed., University Park Press, Baltimore, 1971, p. 123.

50. Massey, V. and G. Palmer, Biochem. 5: 3181, 1966.

51. Ballou, D. P., University of Michigan, Ph. D. Thesis, 1971.

52. EMI Photomultiplier Tubes, Manual #20M/6-671/PMT Issue I, Whittaker Corporation, Plainview, N.Y., 11803.

53. Udenfriend, S., Fluorescence Assay in Biology and Medicine, Volume II, Academic Press, New York, 1969, p. 603.

54. Pi, W.-H. and S.-H. Lam, Principles of Fluid Mechanics, Addison-Wesley Publishing Co., Inc., Reading, Massachusetts, 1964.

55. Roughton, F. J. W. and B. Chance, in Technique of Organic Chemistry, A. Weissberger, E. S. Lewis, and S. L. Friess, eds., Vol. 8, Part II, Wiley (Interscience), New York, 1963.

56. Davis, B. J., Ann. N.Y. Acad. Sci. 121: 404, 1964.

57. Chrambach, A. and D. Rodbard, Science 172: 440, 1971.

58. Shapiro, A. L., E. Vinuela, and J. V. Maisel, Jr., Biochem. Biophys. Res. Comm. 28: 815, 1967.

59. Weber, K., J. R. Pringle, and M. Osborn, in Methods in Enzymology, Vol. XXVI, C. H. W. Hirs and S. N. Timasheff, eds., Academic Press, New York, 1972, p. 3.

60. Weber, K. and M. Osborn, J. Biol. Chem. 244: 4406, 1969.

61. Dale G. and A. L. Latner, The Lancet 1968: 847, 1968.

62. Percival, L. H., G. G. Dunckley, and H. D. Purves, Aust. J. Exp. Biol. Med. Sci. 48: 171, 1970.

63. Muller, F., personal communication.

64. Massey, V. and B. E. P. Swoboda, Biochem. Z. 338: 474, 1963.

65. Urry, D. W. and J. W. Pettegrew, J. Am. Chem. Soc. 89: 5276, 1967.

66. Phillips, J. W., M. F. Mallette, C. O. Clagett, Fed. Proc. 28: 888, 1969.

67. Clagett, C. O., Fed. Proc. 30: 127, 1971.

68. Deranlau, D. A., J. Am. Chem. Soc. 91: 4044, 1969.

69. Beinert, H., in The Enzymes, Vol. 2, Pt. A, P. D. Boyer, H. Lardy, and K. Myrback, eds., Academic Press, New York, 1960, p. 339.

70. Palmer, G. and M. Hunter, unpublished results.

71. Job, P., Ann. Chim. Phys. 9: 113, 1928.

72. Heslop, R. B., Numerical Aspects of Inorganic Chemistry, Elsevier Publishing Co., Ltd., New York, 1970.

73. Dubois, M., K. A. Gilles, J. K. Hamilton, P. A. Rebers, and F. Smith, Anal. Chem. 28: 350, 1956.

74. Warren, L., J. Biol. Chem. 234: 1971, 1959.

75. Feeney, R. E., M. B. Rhodes, and J. S. Anderson, J. Biol. Chem. 235: 2633, 1960.

76. Sargent, J. R., Methods in Zone Electrophoresis, British Drug Houses, Ltd., Dorset, England, 1965.

77. Massey, V., F. Muller, R. Feldberg, M. Schuman, P. A. Sullivan, L. G. Howell, S. G. Mayhew, R. G. Matthews, and G. P. Foust, J. Biol. Chem. 244: 3999, 1969.

78. Foust, G. P., S. G. Mayhew, and V. Massey, J. Biol. Chem. 244: 964, 1969.

79. Massey, V., H. Komai, G. Palmer, G. B. Elion, in Vitamins and Hormones, Vol. 28, Academic Press, New York, 1970, p. 505.

80. Weber, G., in Molecular Biophysics, B. Pullman and M. Weissbluth, eds., Academic Press, New York, 1965, p. 369.

81. Biochemists' Handbook, C. Long, ed., Van Nostrand Co., Inc., Princeton, N.J., 1961, p. 44.

82. Kauzmann, W., in Advances in Protein Chemistry, Vol. 14, C. B. Anfinsen, M. L. Ansen, K. Bailey, and J. T. Edsall, eds., Academic Press, New York, 1959, p. 1.

83. Palmer, G. and V. Massey, in Biological Oxidations, T. P. Singer, ed., Interscience Publishers, New York, 1968, p. 263.

84. Moffit, W. and A. Moscowitz, J. Chem. Phys. 30: 648, 1959.

85. Beychok, S., in Biological Macromolecules, Vol. 1, G. D. Fasman, ed., Marcel Dekker, Inc., New York, 1967, p. 293.

86. Chen, Y.-H., J. T. Yand, and H. M. Martinez, Biochem. 11: 4120, 1972.

87. Canfield, R. E. and A. K. Liu, J. Biol. Chem. 240: 1997, 1965.

88. D'Anna, J. A. and G. Tollin, Biochem. 11: 1073, 1972.

89. Veeger, C., H. Voetberg, J. Visser, G. E. J. Staal, and J. F. Koster, in Flavins and Flavoproteins, Third International Symposium, H. Kamin, ed., University Park Press, Baltimore, Maryland, 1971, p. 261.

90. Blake, C. C. F., D. F. Koenig, G. A. Mair, A. C. T. North, C. D. Philips, and V. R. Sarma, Nature (London) 206: 757, 1965.

91. Laidler, K. J., Chemical Kinetics, McGraw-Hill Book Co., New York, 1965.

92. Czerlinski, G. H., Chemical Relaxation, Marcel Dekker Inc., New York, 1966.

93. Dudley, K. H., A. Ehrenberg, P. Hemmerich, and F. Muller, Helv. Chim. Acta 47: 1354, 1964.

94. Leffler, J. and E. Grunwald, Rates and Equilibria of Organic Reactions, John Wiley and Sons, New York, 1963.

95. Lumry, R., in Electron and Coupled Energy Transfer in Biological Systems, T. E. King and M. Klingenberg, eds., Marcel Dekker, Inc., New York, 1971; Lumry, R. and S. Rajender, Biopolymer 9: 1125, 1970.

96. Edmondson, D. E., University of Arizona, Ph. D. Thesis, 1970.

97. Edmondson, D. E. and G. Tollin, Biochem. 10: 113, 1971.

98. Ghisla, S., personal communication.

99. Scola-Nagelschneider, G. and P. Hemmerich, Z. fur Naturforsch 27b: 1044, 1972.

100. Mahler, H. R. and E. H. Cordes, Biological Chemistry, Harper & Row, Publishers, New York, 1966, p. 275.

APPENDIX A

COMPETITIVE BINDING

Part I. Some Amplifications on the Equations of Edsall and Wyman (30)

This appendix describes a method which permits the measurement of the equilibrium constant for the binding of a compound to apoRBP if the compound competitively inhibits the binding flavin-apo-RBP interaction and if the concentrations of the unbound compound and unbound flavin can be simultaneously determined.

For a solution containing apoRBP, (A), flavin, (F), and a compound (C) which competes with the falvin for the same site on the protein the equilibria and equilibrium constants are :

$$A + F \rightleftarrows AF \; ; \; K_a^F = \frac{[AF]}{[A][F]}$$

$$A + C \rightleftarrows AC \; ; \; K_a^C = \frac{[AC]}{[A][C]}$$

The conservation equations are:

$$[A]_{total} = [A] + [AF] + [AC]$$

$$[F]_{total} = [F] + [AF]$$

$$[C]_{total} = [C] + [AC]$$

The fraction, $\bar{\nu}_F$, of the total apoprotein sites which are occupied by F is

$$\bar{\nu}_F = \frac{[AF]}{[A] + [AF] + [AC]} \qquad \text{Equation A1}$$

From the equilibrium equations, $[AF] = K_a^F = [A] \times [F]$ and $[AC] = K_a^C = [A] \times [C]$. Substituting these into Equation (A1) and dividing both numerator and denominator by $K_a^F = [A][F]$ yields:

$$\bar{\nu}_F = \frac{1}{1 + \frac{1}{[F]K_a^F} + \frac{K_a^C[C]}{K_a^F[F]}} \qquad \text{Equation A2}$$

For competition experiments in which the condition $[F] >> K_d^F$ is satisfied, the second term in the denominator of Equation (A2) approaches zero. This allows a rearrangement to give Equation (A3):

$$\frac{K_a^C}{K_a^F} = \frac{[F]}{[C]}\left(\frac{1 - \bar{\nu}_F}{\bar{\nu}_F}\right) \qquad \text{Equation A3}$$

Thus the previous determination of K_a^F and the measurement of [F], [C], and $\bar{\nu}_F$ from competition experiments yield K_a^C.

Part II. Competitive Binding In Regard to the Work of Rhodes et al.(39)

In the competitive binding experiments of Rhodes et al. (39), 10 ug of RF + 60 ug of analog + 1 mg apoRBP were dissolved in 3 ml of 0.025 M sodium phosphate buffer, pH 7.0, and dialyzed against 22 ml of buffer. Had the same experiment been conducted in the absence of analog, essentially all the RF would have been in the bag because the number of moles of apoRBP was in a small excess over the total moles of RF and $[A]_{total} \sim 10^5 K_d^{RF}$. The concentration of unoccupied sites would have been nearly zero because the excess was small. In

the presence of analog, to a good approximation each molecule of analog which bound, did so at the expense of an RF molecule. The free RF molecules distributed throughout the 25 ml, giving at equilibrium [AC] x 3 ml = [RF] x 25 ml = total mmoles of RF displaced. Inside the bag, $[A]_{total} = [AF] + [AC]$, since [A] = 0. Thus

$$\frac{1 - \bar{\nu}_F}{\bar{\nu}_F} = \frac{1 - \frac{[AF]}{[A]_{total}}}{\frac{[AF]}{[A]_{total}}} = \frac{[AC]}{[AF]} = \frac{\text{total moles RF displaced 3/ml}}{\text{total moles RF bound/3 ml}}$$

Substitution of this result into Equation (A3) yields Equation (A4), an equation which appears similar to but actually differs considerably from the one used by Rhodes et al. (39) (see p. 43).

$$\frac{K_a^C}{K_a^F} = \text{Relative Binding} = \frac{\text{total amount RF displaced}}{\text{total amount RF bound}} \times \frac{[RF]}{[\text{Analog}]}$$

Equation A4

Whereas the ratio $\frac{\text{total umoles RF}}{\text{total umoles analog}}$ appears in their equation, the ratio of the concentrations of the free species, $\frac{[RF]}{[\text{Analog}]}$, appears in Equation (A4).

Part III. Competitive Binding in Regard to Further Studies with RBP

Competitive binding should provide an extremely powerful means to study the binding by apoRBP of compounds which are analogs to a portion of the isoalloxazine ring. As mentioned in the Discussion section, compounds of interest in this regard include the water soluble members of classes: pyrimidines, purines, pteridines, pyrazines, quinoxalines, etc. The competitive binding technique is especially

useful for these compounds because they lack absorptivity at wavelengths > 300 nm. The aim of the experiments would be to displace LF, RF, or other suitable flavins from apoRBP by addition of a sufficient amount of test analog. The extent of the reaction could be followed at wavelengths > 300 nm by monitoring the amount of flavin displaced (using fluorescence), the amount of complex remaining (using CD absorbance), or the relative amounts of free flavin and complex (using optical absorbance).

A good protocol for the experiments would be to add aliquots of a concentrated stock solution of the test compound to a cuvette containing equimolar concentrations of apoRBP and flavin, for example, $[\text{apoRBP}]_{\text{total}} = [\text{LF}]_{\text{total}} \gtrsim 10^{-5}$ M. In relation to the equations developed in Part I of this appendix, these concentrations would satisfy the condition $[F] \gtrsim 20\ K_d$ at temperatures below 25° when > 10% of the LF had been displaced, and therefore make the second term in the denominator of equation (A2) approach zero. The greater the percentage of LF displaced, the closer $\frac{K_d^{LF}}{[LF]}$ would approach zero at any given temperature. Also, $[A] \sim 0$ under the conditions $[A]_{\text{total}} = [F]_{\text{total}} >>> K_d^F$. Therefore each molecule of C which bound would stoichiometrically displace a molecule of F and the following identities would result:

$$[A]_{\text{total}} = [AC] + [AF]$$

$$[AC] = [F]$$

$$[C] = [C]_{\text{total}} - [AC] = [C]_{\text{total}} - [F] \ .$$

Therefore, $\frac{1 - \bar{\nu}_F}{\bar{\nu}_F} = \frac{[F]}{[F]_{total} - [F]}$.

Substitution of these results into Equation (A3) yields:

$$K_a^C = K_a^F \times \frac{[F]}{[C]_{total} - [F]} \times \frac{[F]}{[F]_{total} - [F]} \quad \text{Equation A5}$$

This is an equation in only one variable, [F], and is designed to be used in fluorescence experiments. Similar equations could be developed for CD and optical absorbance experiments. Note that in the special case when half of the flavin is displaced, Equation (A5) reduces to:

$$K_a^C = K_a^F \times \frac{\frac{1}{2}[F]_{total}}{[C]_{total} - \frac{1}{2}[F]_{total}} .$$

APPENDIX B

SOME CONSIDERATIONS ON THE EQUATION FOR SIMPLE BINDING

Equation (11) (page 149) can be rearranged to give Equation (B1) which solves for $[F]$ in terms of $[F]_T$, $[A]_T$, and K_d. The positive square root is chosen in this case because negative values of $[F]$ are impossible.

$$[F] = \tfrac{1}{2}\left\{-(K_d+[A]_T-[F]_T) + \sqrt{(K_d+[A]_T-[F]_T)^2 + 4[F]_TK_d}\right\}$$

Equation (B1)

Expressed in units of K_d, Table BI lists values of $[F]$ for various values of $[F]_T$ and $[A]_T$.

Conditions a - e are those used to give the different percentages of quenching in the titrations used to obtain values of K_d.

Condition i shows that in order to produce 99% of all possible complexes when flavin and apoprotein concentrations are equal, the total reactant concentrations must be 10^4 times the value of K_d. Thus in order to perform a stoichiometric binding titration which is linear over the entire (99%) range of quenching, the initial flavin concentration must be $\gtrsim 10^4K_d$.

TABLE BI

Concentrations of $[F]$ For Various Concentrations of $[F]_T$ and $[A]_T$

$[F]_{Total}$ in units of K_d	$[A]_{Total}$ in units of K_d	$[F]$ in units of K_d	$[F]/[F]_T$ x 100%	Condition label
2	0.31	.20	10%	a
2	1.02	.60	30%	b
2	2.0	1.0	50%	c
2	3.7	1.4	70%	d
2	10.8	1.8	10%	e
20	20	4.0	20%	f
100	100	9.5	10%	g
1000	1000	31.	3%	h
10^4	10^4	100.	1%	i
100	200	0.98	1%	j
50	100	0.96	1.9%	k

However, condition i shows that 99% of all possible complexes are formed when one reagent has a total concentration of 200 K_d and the other has a concentration $\lesssim$ 100 K_d. Therefore titrating a flavin solution with $[F]_{total}$ = 200 K_d will produce a stoichiometric binding titration which covers the initial 50% of the quenching range. Condition k shows that the titration is nearly stoichiometric ($\gtrsim$ 98% of all possible complexes) for the initial 50% of quenching when $[F]_{total}$ = 100 K_d.

Condition h is very close to the condition at equivalence in Figure 30 (page 132), since $[A]_T = [RF]_T$ = 1.25×10^{-6} M and K_d (25°) 1.25×10^{-9} M. The deviation from linearity of the points near equivalence in Figure 30 can be seen to correspond very closely to the concentrations of free flavin expected on equilibrium basis.

APPENDIX C

CONSIDERATIONS ON APOPROTEIN BINDING HETEROGENEITY

Two types of heterogeneity are considered. The first concerns some of the results expected when each apoprotein molecule contains one site but the apoprotein population contains molecules with different binding affinities. The second considers some ramifications of a secondary set of sites which have lesser affinity for flavin than the primary sites.

Some Scatchard Plots for Flavin Binding to a Heterogeneous Apoflavoprotein Sample

For purposes of this discussion, the total apoprotein population is considered to consist of a 50-50 mixture of apoprotein molecules with different flavin binding affinity. Half of the apoprotein molecules have an intrinsic dissociation constant K_d', (the single prine (') population), and half have an intrinsic dissociation constant K_d'', (the double prime (") population). The final equilibrium is established which satisfies the two equilibria:

$$F + A' \underset{K_d'}{\rightleftharpoons} H' \qquad \text{Equation (C1)}$$

$$F + A'' \underset{K_d''}{\rightleftharpoons} H'' \qquad \text{Equation (C2)}$$

At equilibrium, $[F]_{total}$ is distributed over free flavin and both bound species:

$$[F]_T = [F] + [H]' + [H]''$$

The total apoprotein population consists of the two types of both free and bound species:

$$[A]_T = [A_T]' + [A_T]''$$

$$[A_T]' = [A]' + [H]'$$

$$[A_T]'' = [A]'' + [H]''$$

The concentration of free flavin at equilibrium must simultaneously satisfy Equation (B1) of Appendix B for the two populations (' and ").

$$[F]' = \tfrac{1}{2}\left\{ -(K_d' + [A_T]' - [F_T]') + \sqrt{(K_d' + [A_T]' - [F_T]')^2 + 4[F_T]' K_d'} \right\} \qquad \text{Equation (C3)}$$

$$F'' = \tfrac{1}{2}\left\{ -(K_d'' + [A_T]'' - [F_T]'') + \sqrt{(K_d'' + [A_T]'' - [F_T]'')^2 + 4[F_T]'' K_d''} \right\} \qquad \text{Equation (C4)}$$

It is of utmost importance to realize that $[F_T]' \neq [F_T]''$. The total concentration of flavin molecules participating in Equilibrium (C1) does not include the concentration of flavin molecules bound to the double prime apoprotein molecules. Also, the total concentration of flavin molecules participating in Equilibrium (C2) does not include the

concentration of flavin molecules bound to the single prime apoprotein molecules.

$$[F_T]' = [F_T] - [H]''$$
$$[F_T]'' = [F_T] - [H]'$$

Two examples of Scatchard analyses are considered in which the quantities K_d', K_d'', and $[F_T]$ are set (do not vary) and $[A_T]$ varies for the different points plotted. In each example the quantities

$$[F],\ [A]',\ [A]'',\ [H]',\ \text{and}\ [H]''$$

are determined by successive approximation using Equations (C3) and (C4) until $[F]' = [F]''$.

The Scatchard analysis in Table CI and Figure C1 is calculated under the condition

$$[F_T] = 10\ K_d'' = 100\ K_d'$$

The plot in Figure C1 shows definite curvature under these conditions, but has an x-intercept value near 1.

The Scatchard analysis in Table CII and Figure C2 is calculated under the condition

$$[F_T] = 10\ K_d' = 0.01\ K_d'' .$$

Under this condition only about half of the apoprotein mole- (i.e. those with sites of binding constant K_d') will bind any significant amount of flavin. Thus this condition approximates the condition when the value of $[A_T]$ used in Scatchard analyses is twice as large as the actual concentration of binding sites. The plot in Figure C2 is quite

TABLE CI

Some Evaluations of the Reactant Concentrations When the Apoprotein Is a 50-50 Mixture of Molecules With Binding Sites of K_d' and K_d'' And $[F_T] = 10\,K_d'' = 100\,K_d'$. All Concentrations Are in Units of K_d''.

Point Label in Figure C1	$[A_T]$	$[A_T]'$	$[A_T]''$	$[F_T]$	$[H]'$	$[H]''$	$[A]'$	$[A]''$	$[F]$	$\alpha = \frac{[H]' + [H]''}{[A_T]}$	$\alpha/[F]$
a	5	2.5	2.5	10	2.45	2.09	0.05	0.41	5.46	0.91	0.166
b	10	5	5	10	4.76	3.29	0.24	1.71	1.95	0.805	0.413
c	20	10	10	10	7.46	2.25	2.54	7.75	0.29	0.485	1.67
d	50	25	25	10	8.69	1.26	16.1	23.7	0.053	0.199	3.74
e	100	50	50	10	8.91	1.07	41.1	48.9	0.022	0.100	4.62

TABLE CII

Some Evaluations of the Reactant Concentrations When the Apoprotein Is a 50-50 Mixture and $[F_T] = 10\ K_d' = 0.01\ K_d''$.

All Concentrations Are in Units of K_d'.

Point Label in Figure C2	$[A_T]$	$[A_T]'$	$[A_T]''$	$[F_T]$	$[H]'$	$[H]''$	$[A]'$	$[A]''$	$[F]$	$\alpha = \frac{[H]' + [H]''}{[A_T]}$	$\alpha / [F]$
a	1	0.5	0.5	10	0.45	0	0.05	0.50	9.55	.453	.047
b	5	2.5	2.5	10	2.22	.001	0.28	2.50	7.88	.440	.057
c	10	5	5	10	4.258	.005	0.742	4.995	5.7	.425	.075
d	20	10	10	10	7.30		2.70	9.99	2.7	.365	.135
e	50	25	25	10	9.39	.01	15.61	24.99	0.60	.188	.313

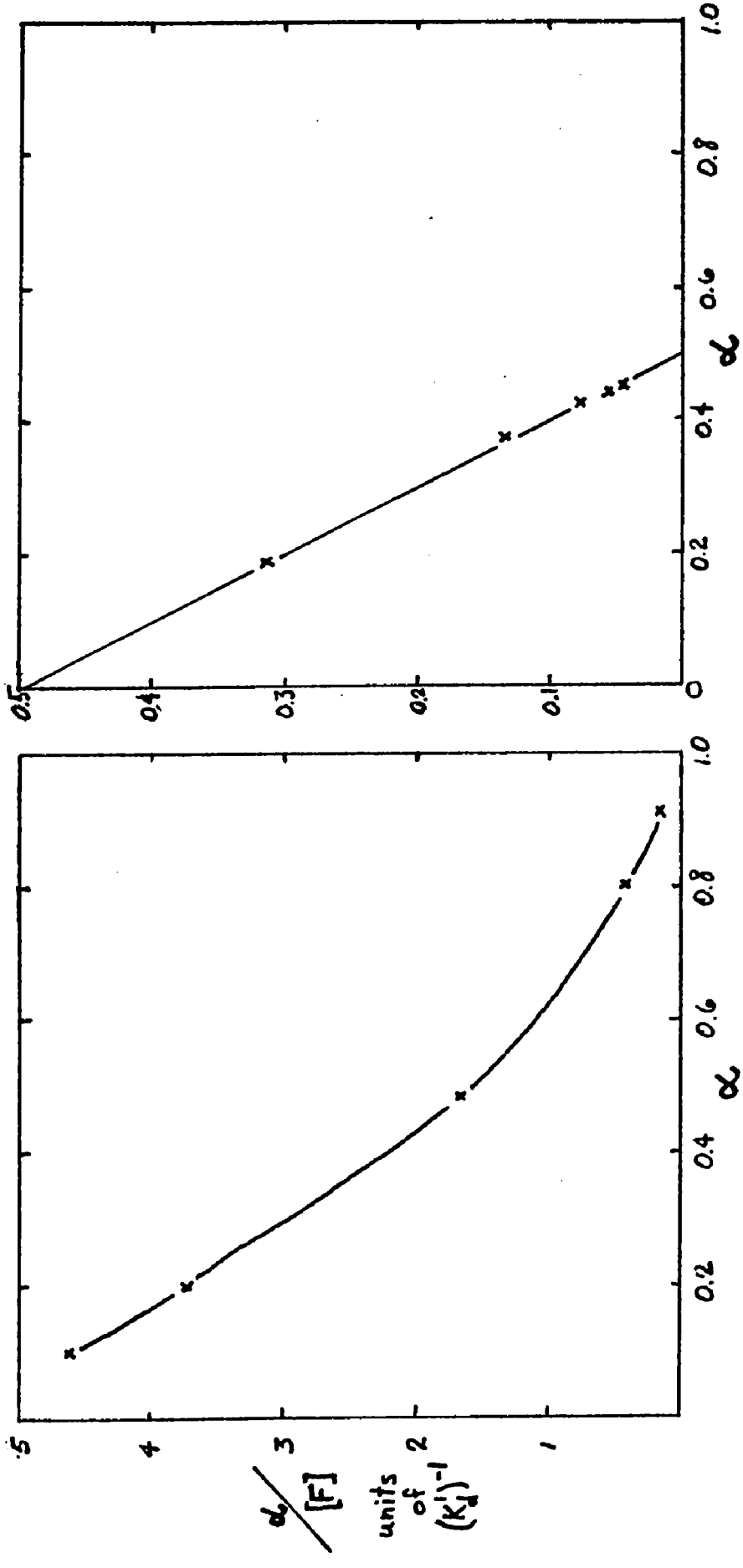

Figure C1.

Figure C2.

Scatchard Plots for Binding to Apoprotein Populations Composed 50% of Molecules with Affinity K'_d and 50% of molecules with Affinity K''_d. The condition in Figure C1 is $[F_t] = 10K'_d = 100K''_d$. The condition in Figure C2 is $[F_t] = 10K'_d = 0.01K'_d$.

linear and the value of the slope is equal to the value of $-K_a$ for the apoprotein molecules with stronger flavin binding affinities. Not that the plot has an x-intercept near 0.5.

How Secondary Apoprotein Binding Sites Would Affect The Stoichiometric Titrations (Figures 30,34) and Job Analysis (Figure 31)

The statement on page 135 that secondary binding sites with K_a values $> 10^5$ $\underline{M}^{-1}$ would produce > 2% deviation from stoichiometric quenching plots under the condition $[RF]_{total} \sim 10^{-6}$ $\underline{M}$ is rationalized as follows:

When $[A_T] = 10^{-7}$, $[RF]_{free} \sim 9 \times 10^{-7}$ $\underline{M}$. Sites which quench fluorescence must have a K_a value $> 10^5$ $\underline{M}^{-1}$ in order to reduce $[RF]_{free}$ below 8.8×10^{-7} $\underline{M}$--i.e. a change of 2% from that expected from one site.

Secondary Sites which bind flavin but do not quench flavin fluorescence would necessarily have to bind flavin with a K_a value within a few orders of magnitude of 10^9 $\underline{M}^{-1}$. Otherwise the higher affinity sites will partition the RF molecules from the lesser affinity sites--in similar fashion to the results for the Scatchard plot in Figure C2.

In the Job analysis of Figure 31, when the mole fraction of RF is 0.6, the concentration of complex (with the "primary" sites) is 4.8×10^{-5} $\underline{M}$, while [RF] "free" in solution is 2.4×10^{-5} $\underline{M}$. Secondary Sites with an intrinsic

K_d value of 10^{-3} M would bind about 5% of this free flavin and could produce an increase of 2% in the CD intensity observed if both sites had the same CD absorptivity for bound flavin. However, sites with an intrinsic K_d value of 10^{-4} M would produce about a 10% increase in Cd intensity assuming equal absorptivity. Under these assumptions the results in Figure 31 indicate the absence of sites with K_a values $> 10^3$ M^{-1}.

How a Small Percentage of Sites with Lower Affinity Affect the Calculated Value of $(K_d)_{average}$

The consequences are examined of an apoprotein population composed 90% of molecules with an intrinsic dissociation constant K_d' and 10% of molecules with an intrinsic dissociation constant K_d''. Using an iterative procedure similar to that in the first section of Appendix C, the reactant concentrations and values of $(K_d)_{average}$ are found for two concentrations of $[F_T] = [A_T]$ and are given in Table CIII.

The result shows that the farther $[F_T] = [A_T]$ is from the value of K_d, the more unduly $(K_d)_{average}$ is affected by the sites with lower affinity. This can have significant adverse effect on the value of ΔH calculated from van't + Hoff plots obtained when the same $[F_T]$ value is used at all temperatures.

TABLE CIII

Reactant Concentrations When the Apoprotein Has a 10% Heterogeneity With Dissociation Constant 10 Times Larger Than the Majority.
All Concentrations Are in Units of K_d'.

$[F_T]=[A_T]$	$[A_T]'$	$[A_T]''$	$[F_T]'$	$[F_T]''$	$[F]$	$[H]'$	$[H]''$	$[A]'$	$[A]''$	$(K_d)_{average}$
2	1.8	0.2	1.98	1.08	1.06	0.92	0.02	0.88	0.18	1.2
100	90	10	94.6	17.2	11.8	82.8	5.4	7.2	4.6	1.6

APPENDIX D

CONSIDERATIONS ON RELAXATION KINETICS OF FLAVIN BINDING TO APORBP

An expression for the relaxation trace expected when the equilibrium in Equation (1) (page 9) is perturbed can be derived from the differential rate equation for the reaction in Equation (1):

$$\frac{d[F]}{dt} = -k_1[A] \times [F] + k_{-1}[H]$$

Equation (D1)

The variables can be rewritten in terms of the final equilibrium concentrations of the reactants and their displacements from equilibrium:

$$\begin{aligned} [F] &= [F]_e + [\delta F] \\ [A] &= [A]_e + [\delta A] \\ [H] &= [H]_e + [\delta H] \end{aligned}$$

Equations (D2)

Substituting Equations D2 into Equation D1 yields:

$$\frac{d([F]_e + [\delta F])}{dt} = \frac{d[\delta F]}{dt} =$$

$$= \left\{-k_1[A]_e[F]_e + k_{-1}[H]_e\right\} - k_1([A]_e[\delta F] + [F]_e[\delta A]) - k_1[\delta A][\delta F] + k_{-1}[\delta H]$$

Equation (D3)

The term in brackets in Equation (D3) is identically equal to zero because of the equilibrium condition. The remaining terms can be rewritten (Equation (D4)) using the conservation equation:

$$[\delta F] = [\delta A] = -[\delta H] .$$

$$\frac{d[\delta F]}{dt} = -[\delta F]\left\{ k_1([A]_e+[F]_e)+k_{-1} \right\} + k_1 [\delta F]^2$$

Equation (D4)

For small values of $[\delta F]$, $[\delta F]^2$ approaches zero. Equation (D4) under this condition has a solution

$$[\delta F] = [\delta F]_o \, e^{-\tau t}$$

$$\text{where} \quad \frac{1}{\tau} = k_1([A]_e+[F]_e)+k_{-1}$$

Equation (D5)

Thus a plot of $\frac{1}{\tau}$ against the final equilibrium concentration of $([A]_e+[F]_e)$ yields k_1 as slope and k_{-1} as intercept.

In order to solve the differential Equation (D4), $[\delta F]_o$ must be shown to be small relative to the quantity $[A]_e+[F]_e$ under all the conditions used in the experiments where holoprotein solutions were diluted with an equal volume of buffer. For these experiments

$$[A]_e + [F]_e = 2[F]_e \qquad \text{and}$$

$$[\delta F]_o = \frac{[F]_e^B}{2} - [F]_e^A$$

where the superscript B signifies before and the superscript A signifies after the dilution.

Values of $[\delta F]_o$ and $[F]_e$ can be evaluated relative to $[F_T]$ in units of K_d by the use of Equation (B1) in Appendix B. Table DI examines the relative value of $[\delta F]_o$ and $2[F]_e$ for several final values of $[F_T]$. This tabulation indicates that the value of $[\delta F]_o$ is small with respect to the value of $2[F]_e$ for the final values of $[F_T]$ considered.

TABLE DI

Comparison of the Values of $[\delta F]_o$ and $[F]_e$ For Dilution Relaxation Experiments at Various Values of the Final $[F_T]$. The Values Are in Units of K_d and Are For the Experiments Where the Holoprotein is Diluted With an Equal volume of Buffer.

$[A_T]=[F_T]$	$[F]_e$	$[\delta F]$	$[\delta F]/2[F]_e$
0.1	0.092	.006	.03
0.5	0.366	.057	.08
1.0	0.618	.118	.09
2.5	1.16	.268	.11
5.0	1.79	.44	.12
10.0	2.70	.70	.13
100.0	9.51	2.68	.14
1000.0	31.1	9.02	.15

The last consideration in this appendix concerns the concentrations used in the relaxation experiments (e.g. Figure 46). The object of the relaxation experiments is to

evaluate k_{-1}. To achieve this object, the values of τ^{-1} in the relaxation plots must approach the value of k_{-1}. An approach which is "suitably" close is arbitrarily determined to be one in which at least one τ^{-1} value is less than or equal to one-half the value of k_{-1}. From Equation (D5), this means one dilution experiment in a given plot must satisfy the condition

$$k_{-1} = k_1([A]_e+[F]_e) = 2k_1[F]_e$$

Rewriting k_{-1} in terms of k_1, $[F_T]$, and $[F]_e$ using the equilibrium condition yields:

$$3[F]_e = 2[F_T] .$$

Using Equation (B1) in Appendix B the value of $[F_T]$ which satisfies this relationship is

$$[F_T] = \frac{3K_d}{4}$$

Thus at least one dilution experiment in each relaxation plot should be carried out to give a final concentration of holoprotein near the value of K_d.

APPENDIX E

COMPUTER PROGRAMS

Program K_d

This program is designed to determine the value of the dissociation constant at successive titration points in a fluorescence quenching titration according to Equation (11) (page 149). The program prompts for the concentrations of the stock solutions of apoprotein (CONAPO=?) and flavin analog (CONFLA=?). The values of these concentrations must be expressed in the e format (e.g. 2.76×10^{-5} M ≡ 2.76e-05). The program also prompts for the fluorescence signal resulting from buffer background (BACKGROUND=?), the microliter volume of stock flavin solution (VOLFLA=?) added to the 3 ml of buffer in the fluorescence cuvette, and the number of apoprotein additions (NUMBER OF ADDITIONS=?) which comprise the points in the titration. The program then prompts for the cumulative microliter volume of apoprotein (ENTER CUMULATIVE LAMBDA) at successive points. These should be entered as a string of numbers (e.g. 10.,20.,50.,100.,....). The program then prompts for the fluorescence readings after successive additions.

These should also be entered as a string of numbers. The program then prints the value of K_d as well as the concentrations of F , A , and H at each titration point. The program is terminated by entering the number 0. after the request CONAPO=? (The program listing commenses on the next page.)

```
#list dk1
>      1            DIMENSION LAMBDA(20),F(20),FREFLA(20),TOTFLA(20),BNDFLA(20),
>      2           1TOTAPO(20),FREAPO(20),KD(20),FNBAR(20)
>      3            REAL LAMBDA,KD
>      4         5  WRITE(6,10)
>      5        10  FORMAT(1H1,'CONAPO=?,0.=SIGNOFF')
>      6            READ(5,20)CONAPO
>      7        20  FORMAT(E12.3)
>      8            IF (CONAPO.EQ.0.)CALL EXIT
>      9            WRITE(6,30)
>     10        30  FORMAT('CONFLA=?')
>     11            READ(5,20)CONFLA
>     12            WRITE(6,40)
>     13        40  FORMAT('BACKGROUND=?')
>     14            READ(5,50)BACKR
>     15        50  FORMAT(F9.2)
>     16            WRITE(6,60)
>     17        60  FORMAT('FZERO=?')
>     18            READ(5,50)FZERO
>     19            WRITE(6,65)
>     20        65  FORMAT('VOLFLA=?(MICROLITRES)')
>     21            READ(5,50)VOLFLA
>     22            WRITE(6,70)
>     23        70  FORMAT('NUMBER OF ADDITIONS=?')
>     24            READ(5,80)FN
>     25        80  FORMAT(F5.1)
>     26            N=FN
>     27            WRITE(6,90)
>     28        90  FORMAT('ENTER CUMULATIVE LAMBDA')
>     29            READ(5,100)(LAMBDA(I),I=1,N)
>     30       100  FORMAT(19F6.1)
>     31            WRITE(6,110)
```

```
>     32       110  FORMAT('ENTER FLUORESCENCE READINGS')
>     33            READ(5,100)(F(I),I=1,N)
>     34            ALPHA=VOLFLA*CONFLA
>     35            BETA=3000.+VOLFLA
>     36            GAMMA=ALPHA/BETA
>     37            DO 200 I=1,N
>     38            FREFLA(I)=((F(I)-BACKR)*GAMMA)/(FZERO-BACKR)
>     39            TOTFLA(I)=ALPHA/(BETA+LAMBDA(I))
>     40            BNDFLA(I)=TOTFLA(I)-FREFLA(I)
>     41            TOTAPO(I)=(LAMBDA(I)*CONAPO)/(BETA+LAMBDA(I))
>     42            FREAPO(I)=TOTAPO(I)-BNDFLA(I)
>     43            FNBAR(I)=BNDFLA(I)/TOTFLA(I)
>     44       200  KD(I)=(FREFLA(I)*FREAPO(I))/BNDFLA(I)
>     45            WRITE(6,310)CONAPO
>     46       310  FORMAT(1H1,'CONAPO=',1PE10.3)
>     47            WRITE(6,320)CONFLA
>     48       320  FORMAT('CONFLA=',1PE10.3)
>     49            WRITE(6,330)BACKR
>     50       330  FORMAT('BACKGR=',F5.1)
>     51            WRITE(6,340)FZERO
>     52       340  FORMAT('FZERO=',F6.1)
>     53            WRITE(6,350)VOLFLA
>     54       350  FORMAT('VOLFLA='F5.1)
>     55            WRITE(6,360)
>     56       360  FORMAT(T8,'KD',T17,'LAMBDA',T28,'FLUOR',T39,'FREFLA'
>     57           1,T51,'BNDFLA',T63,'FREAPO',T73,'FNBAR=BF/TF')
>     58            WRITE(6,380)(KD(I),LAMBDA(I),F(I),FREFLA(I),BNDFLA(I),
>     59           1FREAPO(I),FNBAR(I),I=1,N)
>     60       380  FORMAT(1PE12.3,0PF10.2,F10.2,1PE12.3,E12.3,E12.3,0PF10.4)
>     61            GO TO 5
>     62        400 CALL EXIT
>     63            END
#END OF FILE
```

Program REVERSIBLE

This program solves for the second order rate constant k_1 for the reaction:

$$A + B \underset{k_{-1}}{\overset{k_1}{\rightleftharpoons}} Y$$

under the initial conditions $[A]_o = [B]_o \neq 0$; $[Y]_o = 0$. The purpose of the program is to obtain the best value of

$$k_1 t = \frac{[Y]_e}{[A]_o^2 - [Y]_e^2} \text{ lon } \frac{[Y]_e([A]_o^2 - [Y][Y]_e)}{[A]_o^2([Y]_e - [Y])} = F(Y)$$

which fits all the points on the reaction trace which have been selected by the user. The program first prompts for the equilibrium concentrations $[A]_e$ and $[Y]_e$ for the trace. These are to be entered under ####### headings. The program then prompts for the values of time and $[Y]$. The user lists as many data pairs as he wishes under the appropriate column headed by #######. The data set is terminated with $ENDFILE . The program prints successive approximations to the k_1 value and calculates 95% confidence limits on the k_1 value based on the Students' t-distribution. In conversational mode the program then asks the user if he wishes the iteration to continue: reply "YES" or "NO". The reply "NO" causes the program to print the values of

t, Y(t), residual Y(t), F(Y), and calculated F(Y). The program then prompts for a new data pair $[A]_e$ and $[Y]_e$. Entering $ENDFILE terminates the program. (The program listing starts on the next page.)

```
      DIMENSION V(40),Y(40),X(40),X2(40),XV(40),CALV(40),RES(40)          LSQ010
      DIMENSION BTAB(40)                                                  LSQ020
      DIMENSION DELTA(40)                                                **LSQ021
      INTEGER IN,YES                                                      LSQ030
      LOGICAL CON                                                         LSQ040
      REAL M,MXNB,MOLD                                                    LSQ050
      DATA     BTAB/12,706,4,303,3,182,2,776,2,571,2,447,2,365,2,306,     LSQ060
     $2.262,2.228,2,201,2.179,2,160,2,145,2,131,2,120,2,110,2,101,2,093,  LSQ070
     $2.086,2.080,2,074,2,069,2.064,2.060,2,056,2.052,2,048,2,045,2,042,  LSQ080
     $10*2,0/,YES/'Y'/,CON/.FALSE./                                       LSQ090
      WRITE(6,99)                                                         LSQ100
      CALL CREPLY(820)                                                    LSQ110
      CON=.TRUE.                                                          LSQ120
   20 WRITE(6,101)                                                       **LSQ130
      READ(5,200,END=999) AE,YE                                          **LSQ131
      A02=(AE+YE)**2                                                     **LSQ132
      C=YE/(A02-YE*YE)                                                   **LSQ133
      WRITE(6,100)                                                       **LSQ134
   30 N=1                                                                 LSQ140
      IC=1                                                                LSQ150
   40 READ(5,200,END=50) X(N),Y(N)                                       **LSQ160
      N=N+1                                                               LSQ170
      IF(N.LE.40) GO TO 40                                                LSQ180
   50 IF(N.EQ.1) STOP                                                     LSQ190
      N=N-1                                                               LSQ200
      NM1=N-1                                                             LSQ210
      FN=FLOAT(N)                                                         LSQ220
      SV=0.                                                               LSQ230
      SX=0.                                                               LSQ240
      SX2=0.                                                              LSQ250
      SXV=0.                                                              LSQ260
      DO 60 I=1,N                                                         LSQ270
      V(I)=C*ALOG( (A02-Y(I)*YE)/(YE-Y(I)) )                             **LSQ280
      SV=SV+V(I)                                                          LSQ290
      SX=SX+X(I)                                                          LSQ300
      X2(I)=X(I)*X(I)                                                     LSQ310
```

```
      SX2=SX2+X2(I)                                                    LSQ320
      XV(I)=X(I)*V(I)                                                  LSQ330
   60 SXV=SXV+XV(I)                                                    LSQ340
      M=(SX*SV-FN*SXV)/(SX*SX-FN*SX2)                                  LSQ350
      B=(SV-M*SX)/FN                                                   LSQ360
      WRITE(6,300) M,B                                                 LSQ370
   70 IC=IC+1                                                          LSQ380
      SWXV=0.                                                          LSQ390
      SW=0.                                                            LSQ400
      SWX=0.                                                           LSQ410
      SWV=0.                                                           LSQ420
      SWX2=0.                                                          LSQ430
      WZ2=0.                                                           LSQ440
      DO 80 I=1,N                                                      LSQ450
      MXNB=M*X(I)+B                                                    LSQ460
      CALV(I)=MXNB                                                     LSQ470
      EVC=EXP(CALV(I)/C)                                               **LSQ480
      CALCY=(A02-YE*EVC)/(YE-EVC)                                      **LSQ481
      RES(I)=Y(I)-CALCY                                                LSQ490
      T=V(I)-MXNB                                                      LSQ500
      W=(A02-Y(I)*YE)**2 * (YE-Y(I))**2 / (YE*YE)                      **LSQ510
      IF(I.EQ.1) GO TO 75                                              **LSQ511
      DELTA(I)=( V(I)-V(I-1) ) / ( X(I)-X(I-1) )                       **LSQ512
   75 CONTINUE                                                         **LSQ513
      WZ2=WZ2+W*T*T                                                    LSQ520
      SWXV=SWXV+XV(I)*W                                                LSQ530
      SW=SW+W                                                          LSQ540
      SWX=SWX+W*X(I)                                                   LSQ550
      SWV=SWV+W*V(I)                                                   LSQ560
   80 SWX2=SWX2+W*X2(I)                                                LSQ570
```

```
      MOLD=M
      FACT=SW*SWX2-SWX*SWX                                              LSQ580
      IF(FACT.EQ.0.,OR,SW.EQ.0.) GO TO 85                               LSQ590
      M=(SW*SWXV-SWX*SWV)/FACT                                          LSQ600
      B=(SWV-M*SWX)/SW                                                  LSQ610
      VARB=(WZ2*SW)/( FLOAT(N-2)*FACT )                                 LSQ620
      CONF=      BTAB(NM1)*SQRT( VARB/FLOAT(NM1) )                      LSQ630
      WRITE(6,310) M,B,CONF                                             LSQ640
      IF(ABS((MOLD-M)/M),GT,0.005,AND,IC,LT,10) GO TO 70                LSQ650
   85 IF(CON) GO TO 90                                                  LSQ660
      WRITE(6,400) (X(I),Y(I),RES(I),V(I),CALV(I),DELTA(I),I=1,N)       LSQ670
      GO TO 20                                                         **LSQ680
   90 WRITE(6,500)                                                      LSQ690
      READ(5,600) IN                                                    LSQ700
      IF(IN.EQ.YES) GO TO 70                                            LSQ710
      WRITE(6,400) (X(I),Y(I),RES(I),V(I),CALV(I),DELTA(I),I=1,N)       LSQ720
      GO TO 20                                                         **LSQ730
   99 FORMAT(' A + B <=> Y)      A0 = AE + YE',/,' F(Y) = YE/(A0**2-YE**2 LSQ740
     $) = LON( (A0**2-Y*YE)/(YE-Y) ) = M*X+B')
  101 FORMAT('0ENTER AE AND YE',/,' ########## ##########')
  100 FORMAT('1ENTER X  AND  Y(X)',/,' ########## ##########')          **LSQ751
  200 FORMAT(G10.0,1X,G10.0)                                            **LSQ760
  300 FORMAT('1    SLOPE',6X,'Y-INTERCEPT',6X,'+/-',/,6X,'(=M)',8X,'(=B)**LSQ770
     $',4X,'TO 95% CONFID',/,1P2E13.3)                                  LSQ780
  310 FORMAT(1P3E13.3)                                                  LSQ781
  400 FORMAT('0',/,7X,'X',11X,'Y(X)',6X,'RESIDUAL Y',6X,'F(Y)',4X,      LSQ790
     $'CALCULATED F(Y)',3X,'DELTA',/,(1P6E13.3))                       **LSQ800
  500 FORMAT(' CONTINUE ITERATION?')                                    **LSQ810
  600 FORMAT(A1)                                                        LSQ820
  999 STOP                                                              LSQ830
      END                                                               LSQ840
                                                                        LSQ850
```

Program LINEAR

This program performs a standard least squares analysis for the best straight line (y = mx + b) through the data set listed by the user. The program prompts for the values of x and y(x). These are to be listed under the appropriate ####### headings. The data set is terminated with $ENDFILE. The program then prints the slope (m), intercept (b), the 95% confidence limits on the slope, and the standard deviation of all the residuals (y - calculated y). The program then lists x, y, residual y, and calculated y, then prompts for a new data set x and y(x). Entering $ENDFILE terminates the program. (The program listing begins on the next page.)

```
      DIMENSION V(40),Y(40),X(40),X2(40),XV(40),CALV(40),RES(40)          LSQ010
      DIMENSION BTAB(40)                                                  LSQ020
      INTEGER IN,YES                                                      LSQ030
      LOGICAL CON                                                         LSQ040
      REAL M,MXNB,MOLD                                                    LSQ050
      DATA     BTAB/12,706,4,303,3,182,2,776,2,571,2,447,2,365,2,306,     LSQ060
     $2.262,2.228,2.201,2,179,2,160,2,145,2,131,2,120,2,110,2.101,2,093,  LSQ070
     $2.086,2.080,2,074,2,069,2,064,2.060,2,056,2,052,2,048,2,045,2,042,  LSQ080
     $10*2,0/,YES/'Y'/,CON/,FALSE,/                                       LSQ090
      WRITE(6,99)                                                         LSQ100
      CALL CREPLY(&20)                                                    LSQ110
      CON=.TRUE.                                                          LSQ120
   20 WRITE(6,100)                                                      **LSQ130
   30 N=1                                                                 LSQ140
      IC=1                                                                LSQ150
   40 READ(5,200,END=50) X(N),Y(N)                                      **LSQ160
      N=N+1                                                               LSQ170
      IF(N.LE.40) GO TO 40                                                LSQ180
   50 IF(N.EQ.1) STOP                                                     LSQ190
      N=N-1                                                               LSQ200
      NM1=N-1                                                             LSQ210
      FN=FLOAT(N)                                                         LSQ220
      SV=0.                                                               LSQ230
      SX=0.                                                               LSQ240
      SX2=0.                                                              LSQ250
      SXV=0.                                                              LSQ260
      DO 60 I=1,N                                                         LSQ270
      V(I)=Y(I)                                                        **LSQ280
      SV=SV+V(I)                                                          LSQ290
      SX=SX+X(I)                                                          LSQ300
      X2(I)=X(I)*X(I)                                                     LSQ310
      SX2=SX2+X2(I)                                                       LSQ320
      XV(I)=X(I)*V(I)                                                     LSQ330
   60 SXV=SXV+XV(I)                                                       LSQ340
      M=(SX*SV-FN*SXV)/(SX*SX-FN*SX2)                                     LSQ350
      B=(SV-M*SX)/FN                                                      LSQ360
```

```
C
   70 IC=IC+1                                                          **LSQ370
      SWXV=0.                                                            LSQ380
      SW=0.                                                              LSQ390
      SWX=0.                                                             LSQ400
      SWV=0.                                                             LSQ410
      SWX2=0.                                                            LSQ420
      WZ2=0.                                                             LSQ430
      DO 80 I=1,N                                                        LSQ440
      MXNB=M*X(I)+B                                                      LSQ450
      CALV(I)=MXNB                                                       LSQ460
      CALCY=MXNB                                                         LSQ470
      RES(I)=Y(I)-CALCY                                                 **LSQ480
      T=V(I)-MXNB                                                        LSQ490
      W=1.Y=MXNB                                                         LSQ500
      WZ2=WZ2+W*T*T                                                     **LSQ510
      SWXV=SWXV+XV(I)*W                                                  LSQ520
      SW=SW+W                                                            LSQ530
      SWX=SWX+W*X(I)                                                     LSQ540
      SWV=SWV+W*V(I)                                                     LSQ550
   80 SWX2=SWX2+W*X2(I)                                                  LSQ560
      MOLD=M                                                             LSQ570
      FACT=SW*SWX2-SWX*SWX                                               LSQ580
      IF(FACT.EQ.0.,OR.SW.EQ.0.) GO TO 85                                LSQ590
      M=(SW*SWXV-SWX*SWV)/FACT                                           LSQ600
      B=(SWV-M*SWX)/SW                                                   LSQ610
      VARB=(WZ2*SW)/( FLOAT(N-2)*FACT )                                  LSQ620
      CONF=      BTAB(NM1)*SQRT( VARB/FLOAT(NM1) )                       LSQ630
      WRITE(6,300) M,B,CONF,VARB,FACT                                    LSQ640
      IF(ABS((MOLD-M)/M).GT.0.005.AND.IC.LT.10) GO TO 70                **LSQ650
                                                                         LSQ660
```

```
 85 IF(CON) GO TO 90                                                    LSQ670
    WRITE(6,400) (X(I),Y(I),RES(I),V(I),CALV(I),I=1,N)                  LSQ680
    GO TO 20                                                            LSQ690
 90 WRITE(6,500)                                                        LSQ700
    READ(5,600) IN                                                      LSQ710
    IF(IN.EQ.YES) GO TO 70                                              LSQ720
    WRITE(6,400) (X(I),Y(I),RES(I),V(I),CALV(I),I=1,N)                  LSQ730
    GO TO 20                                                            LSQ740
 99 FORMAT(' Y=M*X+B')                                                  **LSQ750
100 FORMAT('1ENTER X  AND  Y(X)',/,' ########## ##########')            **LSQ760
200 FORMAT(G10.0,1X,G10.0)                                              **LSQ770
300 FORMAT('    SLOPE         INTERCEPT      */=          S.D,         **LSQ780
   *   S**2',/,5E14.3)                                                  **LSQ790
400 FORMAT('0',/,7X,'X',11X,'Y(X)',6X,'RESIDUAL Y',                     **LSQ800
   $'CALCULATED 1/Y',/,(1P4E13.3))                                      **LSQ810
500 FORMAT(' CONTINUE ITERATION?')                                      LSQ820
600 FORMAT(A1)                                                          LSQ830
999 STOP                                                                LSQ840
    END                                                                 LSQ850
```